Modulation of lipid mediator biosynthesis by *Tripterygium wilfordii* Glycosides and its bioactive compound celastrol in human macrophages

Dissertation

in Partial Fulfilment of the Requirements for the Degree of

"doctor rerum naturalium" (Dr. rer. nat.)

Submitted to the Council of the Faculty of Biological Sciences

of Friedrich Schiller University Jena

by Kehong Zhang

Master of Science in Biology and Master of Marine Science

born on August 6th, 1992 in Zhejiang, China

1st Reviewer: Prof. Dr. Oliver Werz, Friedrich-Schiller-Universität Jena
2nd Reviewer: Prof. Dr. Xinchun Chen, Universität Shenzhen
3rd Reviewer: Prof. Dr. Robert Fürst, Goethe-Universität Frankfurt
Date of submission: April 5th, 2022
Date of defense: September 28th, 2022
Dissertation, Friedrich-Schiller-Universität Jena, [2022]

Table of contents

List of Figures **V**

Abbreviations **VII**

Summary **XI**

Zusammenfassung **XV**

1 Introduction **1**

1.1 Lipid mediators in inflammation 1

1.1.1 Eicosanoids 3

1.1.1.1 Prostanoids 4

1.1.1.2 Leukotrienes 4

1.1.2 Specialized pro-resolving mediators (SPM) 5

1.1.2.1 AA-derived SPM 5

1.1.2.2 DHA-derived SPM 7

1.1.2.3 EPA-derived SPM 7

1.1.2.4 n-3 DPA-derived SPM 8

1.2 Cells of innate immunity 8

1.2.1 Monocytes 8

1.2.2 Macrophages 10

1.2.2.1 M1 Macrophages 12

1.2.2.2 M2 Macrophages 12

1.2.3 Neutrophils 12

1.2.4 Other immune-relevant cells 13

1.3 *Tripterygium wilfordii* Hook F 13

1.3.1 Chemical constituents and tablet development 13

1.3.2 Pharmacological activities 15

1.3.2.1 Anti-inflammatory properties 15

1.3.2.2 Anti-arthritic activities 15

1.3.2.3 Other activities 16

1.3.3 Toxicity 16

1.4 Celastrol 16

1.4.1 Chemical properties 16

1.4.2 Pharmacological activities 17

1.4.2.1 Anti-inflammatory properties . . . 17
1.4.2.2 Anti-arthritic activities . . . 18
1.4.2.3 Other activities . . . 19
1.4.3 Toxicity . . . 19

2 Aim of thesis **21**

3 Manuscripts **23**
3.1 Manuscript I . . . 24
3.2 Manuscript II . . . 47
3.3 Manuscript III . . . 63

4 Discussion **101**
4.1 Inhibition of *Tripterygium wilfordii* glycosides in human macrophages . . . 101
4.2 Inhibition of celastrol in polarized human macrophages . . . 104
4.3 Inhibition of celastrol during human macrophages polarization . . . 107

5 References **111**

6 Appendices **133**
6.1 Acknowledgements . . . 133
6.2 List of publications . . . 135
6.3 Author contribution statement . . . 136
6.4 Eigenständigkeitserklärung . . . 137

List of Figures

1.1 Lipid mediators in the inflammatory response. 2
1.2 The eicosanoid biosynthetic pathways from arachidonic acid and eicosapentaenoic acid. 3
1.3 The biosynthetic pathways of specialized pro-resolving mediators. 6
1.4 Immuno-related properties of bioactive lipid mediators. 9
1.5 Human macrophage polarization. 11
1.6 Representative chemical constituents isolated from *Tripterygium wilfordii* root extract and their corresponding biological activities. 14
1.7 The structure of celastrol. 17

4.1 Schematics of *Tripterygium wilfordii* glycosides on lipid mediator network in human macrophages. 104
4.2 Manipulation of lipid mediator biosynthesis by short-time exposure of celastrol in polarized human macrophages. 107
4.3 Proposed mechanism of celastrol inhibition in affecting COX-2 pathways during M1 macrophages polarization. 109

Abbreviations

AA	arachidonic acid
ACR	American College of Rheumatology
AD	Alzheimer's disease
AIA	adjuvant-induced arthritis
AKBA	3-O-acetyl-11-keto-β-boswellic acid
AP-1	activator protein-1
Arg-1	arginase-1
BCS	biopharmaceutics classification system
Ca^{2+}	calcium ion
CAM	cellular adhesion molecule
CB2	cannabinoid receptor type 2
CCL	chemokine (C-C motif) ligand
CCR	C-C chemokine receptor
CD	cluster of differentiation OR Crohn's disease
CIA	collagen-induced arthritis
COX	cyclooxygenase
Coxibs	selective COX-2 inhibitors
cPGES	cytosolic PGE_2 synthase
CS	celastrol (3-hydroxy-9β,13α-dimethyl-2-oxo-24,25,26-trinoroleana-1(10),3,5,7-tetraen-29-oic acid)
CX3CR	C-X3-C Motif Chemokine Receptor
CYP	cytochrome P450 monooxygenase
Cys-LT	cysteinyl-leukotrienes
Cys-SPM	cysteinyl-specialized pro-resolving mediators
DC	dendritic cells
DHA	docosahexaenoic acid
DMARD	disease-modifying anti-rheumatic drug
DSS	dextran sulfate sodium
EEQ	epoxyeicosatetraenoic acids
EET	epoxyeicosatrienoic acids
EPA	eicosapentaenoic acid

ER	endoplasmic reticulum
ERK	extracellular signal-regulated kinase
FcγR	Fc gamma receptor
FcεR	Fc epsilon receptor
FLAP	5-lipoxygenase-activating protein
GM-CSF	granulocyte/macrophage colony-stimulating factor
GPCRs	G-protein coupled receptors
hERG	human ether-a-go-go-related gene
HETE	hydroxyeicosatetraenoic acid
H(p)ETE	hydro(peroxy)eicosatetraenoic acid
HpDHA	hydroperoxydocosahexaenoic acid
H-PGDS	hematopoietic PGD_2 synthase
HSP	heat shock protein
IBD	inflammatory bowel disease
ICAM	intracellular adhesion molecule
IFNγ	interferon γ
IL	interleukin
iNOS	inducible nitric oxide synthase
IκB	inhibitor of nuclear factor of kappa light polypeptide gene enhancer in B-cells
IKK	IκB kinase
JNK	c-Jun N-terminal kinase
Kir	rectifying potassium
LLDT-8	(5*R*)-5-hydroxytriptolide
LM	lipid mediators
LOX	lipoxygenase
L-PGDS	lipocalin type PGDS
LPS	lipopolysaccharide
LTA_4H	leukotriene A_4 hydrolase
LTB_4	leukotriene B_4
LT	leukotrienes
LXA_4	lipoxin A_4
LX	lipoxins
MAPK	mitogen-activated protein kinase
MaR	maresins
MDM	monocyte-derived macrophage
MHC	major histocompatibility complex
MMP	matrix metalloproteinases
mPGES	microsomal PGE_2 synthase
mTOR	mammalian target of rapamycin
NADPH	nicotinamide adenine dinucleotide phosphate
NPD1	neuroprotectin D1
NF-κB	nuclear factor kappa-light-chain-enhancer of activated B cells
NLRP3	NOD-like receptor protein 3 inflammasome

NSAID	non-steroidal anti-inflammatory drugs
PD	protectins
PG	prostaglandins
PGE_2	prostaglandin E_2
PGFS	PGF synthase
PGIS	PGI synthase or prostacyclin
PI3K/Akt	phosphoinositide 3-kinase/protein kinase B
PMNL	polymorphonuclear leukocytes
PUFA	polyunsaturated fatty acids
RA	rheumatoid arthritis
RASFs	RA synovial fibroblasts
Rv	resolvins
SACM	*Staphylococcus aureus*-conditioned medium
SDS-PAGE	sodium dodecyl sulfate-polyacrylamide gel electrophoresis
sPLA2IIA	secretory phospholipase A2 group IIA
SPM	specialized pro-resolving mediators
STAT	signal transducer and activator of transcription
T4	tripchlorolide
TGF-β	transforming growth factor beta
Th-1/2	T-helper type 1/2
TNF	tumor necrosis factor
TP	triptolide
TRAF	TNF receptor associated factor
TWG/TGT	TwHF glycosides tablet
TwHF	*Tripterygium wilfordii* Hook F
TXAS	TXA synthase
TX	thromboxanes
UC	ulcerative colitis
UPLC-MS/MS	ultra-performance liquid chromatography–tandem mass spectrometry
VCAM	vascular cellular adhesion molecule

Summary

Inflammation is a self-defensive process and is responsible for the pathogenesis of diseases of altered homeostasis [1]. Innate immune cells like human polymorphonuclear leukocytes (PMNL) and primary human macrophages carry out important roles in the immune system, including the production of large amounts of soluble mediators. Among these mediators, cytokines, chemokines, and endogenous bioactive lipids – including pro-inflammatory eicosanoids and specialized pro-resolving mediators (SPM) – perform critical functions during the onset, progression, and resolution of inflammation. Pro-inflammatory eicosanoids such as leukotrienes (LT) and prostaglandins (PG) magnify acute inflammation, and their overexpression leads to several chronic diseases including rheumatoid arthritis, atherosclerosis, diabetes, and cancer [2,3]. Similar to the onset of inflammation, resolution of inflammation is an active process as well, orchestrated by the anti-inflammatory and pro-resolving properties of SPM [4,5].

Tripterygium wilfordii Hook F (TwHF), a herb used in traditional Chinese medicine, has been widely reported to be therapeutically efficacious in the treatment of rheumatoid arthritis [6]. The approved TwHF glycosides tablets, named TWG, are among the most commonly used TwHF formulations used by RA patients and biomedical researchers [7]. Among its many constituents, celastrol (CS) is an active triterpene derived from TwHF that has been used to treat chronic inflammation, arthritis, and other diseases [8,9]. These diseases are characterized by aberrant production of lipid mediators (LM), biomolecules produced from polyunsaturated fatty acids primarily by the enzymatic action of cyclooxygenases (COX) and lipoxygenases (LOX) as part of a complex network controlling inflammatory and immunological responses. Both TWG and CS show promising biological activity, however, their role in the modulation of the biosynthesis of inflammation-related lipid mediators, especially in human macrophages, remained unknown. This thesis provides a more comprehensive understanding of TwHF and natural products in general as a constructive reference for future studies of TWG and CS in the field of the resolution of inflammation.

First, in-depth LM signature profiles by TWG treatment in human monocyte-derived macrophage (MDM) phenotypes was generated using ultra-performance liquid chromatography coupled to tandem mass spectrometry. In exotoxin-challenged pro-inflammatory M1-MDM, TWG (30 μg/mL) effectively inhibited the production of 5-LOX products. Similarly, TWG (10 μg/mL) showed an inhibitory effect of 5-LOX products in agonist-activated PMNL. Additionally, TWG directly inhibited 5-LOX in a cell-free assay with IC_{50} value of

2.9 µg/mL. In cell-based assays, TWG surprisingly and prominently inhibited the production of thromboxane in M1-MDM while other prostaglandins were inversely affected. TWG was therefore characterized further in a non-cellular setting and showed no inhibitory effect on thromboxane synthase. Interestingly, in anti-inflammatory M2-MDM, TWG induced massive formation of SPM and SPM precursors without activating COX or 5-LOX. At lower concentrations, TWG (1 µg/mL) inhibited the production of pro-inflammatory 5-LOX products during MDM polarization towards M1 or M2 subtypes. Furthermore, TWG induced a strong reduction in COX-derived LM and their associated biosynthetic enzymes, pro-inflammatory cytokines, and M1 phenotypic markers during MDM polarization. To summarize, TWG exhibited beneficial effects against RA via inhibition of pro-inflammatory LM but stimulation of SPM which may comprise a novel pharmacological strategy for treatment of RA.

Next, the effects of the natural product CS on LM modulation during the short-term treatment of polarized MDM was investigated. CS (1 µM) potently inhibits the formation of 5-LOX-derived pro-inflammatory LT in both activated PMNL and M1-MDM. In a cell-free environment, CS was further shown to directly and selectively inhibit the activity of 5-LOX with an IC_{50} of 0.19-0.49 µM. Of interest, in M2-MDM, CS remarkably induced the generation of 12-/15-LOX-derived LM including the SPM resolvin D5. CS triggered the subcellular distribution of soluble 15-LOX-1, but not of 5-LOX. In parallel, elevation of intracellular Ca^{2+} influx was not induced by CS. Furthermore, in zymosan-induced peritonitis mice, CS (10 mg/kg) pretreatment significantly lowered LT biosynthesis but increased pro-resolving 12-/15-LOX-derived LM and SPM. Conclusively, CS facilitates the switch from LT biosynthesis to the formation of SPM in vitro and in vivo and thus has a great potential for the prevention and treatment of inflammatory diseases.

Finally, we evaluated the long-term effects of CS with a low concentration (0.2 µM) on LM profiles after manipulating the polarization of MDM towards M1- and M2-like phenotypes. During M1-MDM polarization, CS significantly reduced gene and enzyme expression of COX-2 and microsomal PGE_2 synthase (mPGES-1), as well as M1 surface markers. Additionally, CS suppressed the phosphorylation of nuclear factor $\varkappa$B (nuclear factor kappa-light-chain-enhancer of activated B cells, NF-$\varkappa$B) and p38 mitogen-activated protein kinase (MAPK). During M2-MDM polarization, CS decreased the capacity to generate large amounts of almost all LM including pro-inflammatory eicosanoids and pro-resolving SPM but did not affect the release of fatty acid substrates. Collectively, the data further illustrated that long-term treatment of CS affects LOX activity not only favorably in M1-MDM but may also have some deleterious effects such as impairing the production of SPM in M2-MDM. Therefore, a broad assessment of this natural product's pharmacological profile should be addressed in the future and considered for the treatment of inflammatory disorders.

Together, this thesis revealed that TWG and CS differentially regulate the biosynthetic pathways of inflammation-related LM in human macrophages. TWG promoted an LM class switch from pro-inflammatory eicosanoids towards pro-resolving SPM in polarized MDM

without affecting the capacity to generate SPM during M2-MDM polarization. In short-term experiments, CS showed a LM profile similar to TWG, but with a focus on strongly reduced 5-LOX activity in vitro and in vivo. For long-term incubations, CS mainly suppressed COX-derived LMs and related biosynthetic enzymes by inhibiting phosphorylation of NF-$\varkappa$B and p38 MAPK during M1-MDM polarization, but had only limited effects on the generation of beneficial SPM during M2-MDM polarization.

Zusammenfassung

Unter dem Begriff „Entzündung“ versteht man in der Humanmedizin eine Abwehrreaktion des Körpers mit dem Zweck, homöostatische Bedingungen wieder herzustellen [1]. Hierbei spielen Immunzellen des angeborenen Immunsystems wie polymorphkernige Leukozyten (engl.: polymorphonuclear leukocytes, PMNL) oder primäre Makrophagen eine Schlüsselrolle, da sie unter anderem als Produzenten löslicher Mediatoren die Initiierung, die Aufrechterhaltung, aber auch die aktive Auflösung entzündlicher Prozesse steuern. Zu diesen Mediatoren gehören Zytokine, Chemokine und bioaktive Lipide, welche zusätzlich in pro-inflammatorische Eicosanoide und spezialisierte pro-resolvierende Mediatoren (specialized pro-resolving mediators, SPM) untergliedert werden können. Zu den pro-inflammatorischen Eicosanoiden gehören Leukotriene (LT) und Prostaglandine (PG), welche im Rahmen einer akuten Entzündung durch Lipoxygenasen (LOX) und Cyclooxygenasen (COX) produziert werden, deren Dysregulation jedoch auch in chronisch-entzündlichen Krankheiten wie rheumatoider Arthritis (RA), Atherosklerose, Diabetes oder Krebs eine wichtige Rolle spielen [2,3]. Umgekehrt werden bei der Auflösung einer Entzündung vermehrt SPM produziert, welche bereits in geringen Konzentrationen anti-zündliche (passive) und Entzündungs-auflösende (aktive) Effekte zeitigen [4,5].

In der RA-Behandlung hat sich Wilfords Dreiflügelfrucht (*Tripterygium wilfordii* Hook F, TwHF), eine in der traditionellen chinesischen Medizin etablierte Arzneipflanze, als erfolgversprechend erwiesen [6]. Hierbei finden am häufigsten das tablettierte Pflanzenextrakt (TwHF-Glycoside, TWG) oder Celastrol (CS), einer seiner Inhaltstoffe, Anwendung [7-9]. Sowohl TWG als auch CS sind aufgrund ihrer vielversprechenden biologischen Aktivität Gegenstand intensiver Forschungsbemühen, jedoch war der Effekt auf die Biosynthese entzündungsrelevanter Lipidmediatoren in menschlichen Makrophagen bisher unbekannt. Dessen Aufklärung ist der Gegenstand dieser Arbeit, mit dem Ziel ein umfassenderes Verständnis der Wirkungsweise von TwHF sowie von Naturstoffen allgemein beizutragen, welches konstruktive Hinweise für künftige Studien zu TWG und CS im Bereich der Entzündungsbekämpfung liefern wird.

Zunächst wurde ein detailliertes LM-Profil in menschlichen, von Monozyten abgeleiteten Makrophagen (monocyte-derived macrophages, MDM) angefertigt, welches mit Hilfe von Ultra-Performance-Flüssigkeitschromatographie und Tandem-Massenspektrometrie aufgenommen wurde. In MDM des pro-inflammatorischen Subtyps M1, die durch Exotoxine zur Lipidmediatorsynthese angeregt wurden, hemmte TWG (30 µg/mL) effektiv die Produktion

von 5-LOX-Produkten. In ähnlicher Weise zeigte TWG (10 µg/mL) eine hemmende Wirkung auf 5-LOX-Produkte in agonistisch aktivierten PMNL. Darüber hinaus zeigte TWG eine direkte Hemmung von 5-LOX im zellfreien Assay mit einem IC_{50}-Wert von 2,9 µg/mL. Überraschenderweise hemmte TWG die Produktion von Thromboxan in M1-MDM deutlich, während andere Prostaglandine entgegengesetzt beeinflusst wurden. TWG wurde in einer nicht-zellulären Umgebung näher charakterisiert, zeigte jedoch keine hemmende Wirkung auf das Enzym Thromboxan-Synthase. Interessanterweise induzierte TWG in entzündungshemmenden M2-MDM eine massive Bildung von SPM und SPM-Vorläufern, ohne COX oder 5-LOX zu aktivieren. TWG (1 µg/mL) hemmte die Produktion von pro-inflammatorischen 5-LOX-Produkten auch während der Polarisation von MDM zu M1- oder M2-Subtypen. Darüber hinaus bewirkte TWG eine starke Verringerung von COX-abgeleiteten LM und den damit verbundenen biosynthetischen Enzymen, pro-inflammatorischen Zytokinen und M1-Phänotypmarkern während der MDM-Polarisierung. Zusammenfassend ist die Hemmung von pro-inflammatorischen LM bei gleichzeitiger Stimulierung anti-zündlicher SPM durch TWG als heilungsfördernd bei der Therapie der RA einzustufen und tragen dazu bei, die Wirksamkeit von TwHF besser zu verstehen.

Als nächstes wurde die Rolle des Naturprodukts CS bei der kurzfristigen Behandlung von polarisierten MDM untersucht. CS (1 µM) hemmte die von 5-LOX gebildeten proinflammatorischen LT sowohl in aktivierten PMNL als auch in M1-MDM. In einer zellfreien Umgebung hemmte CS außerdem direkt und selektiv die Aktivität von 5-LOX mit einer effektiven IC_{50} von 0,19 - 0,49 µM. Interessanterweise induzierte CS in M2-MDM in bemerkenswerter Weise die Bildung von 12-/15-LOX-abgeleiteten LM einschließlich des SPM Resolvin D5. CS löste die subzelluläre Translokation von löslichem 15-LOX-1, nicht aber von 5-LOX aus, und induzierte auch nicht den intrazellulären Einstrom von Ca^{2+}. In Mäusen mit Zymosan-induzierter Peritonitis führte die Vorbehandlung mit CS (10mg/kg) zu einer signifikanten Verringerung der LT-Biosynthese, gleichzeitig aber auch zu einem Anstieg der pro-resolvierenden 12-/15-LOX-abgeleiteten LM-Produkte und SPM. Daraus lässt sich schließen, dass CS die Umstellung von der LT-Biosynthese auf die Bildung von SPM in vitro und in vivo erleichtert und somit ein großes Potenzial für die Prävention und Behandlung chronisch-entzündlicher Krankheiten hat.

Schließlich wurden die langfristigen Auswirkungen von CS in einer niedrigen Konzentration (0,2 µM) auf das LM-Profil während Polarisierung zu M1- und M2-ähnlichen MDM untersucht. Während der M1-MDM-Polarisierung reduzierte CS signifikant die Gen- und Enzymexpression von COX-2 und mikrosomaler PGE_2-Synthase (mPGES-1) sowie wichtiger M1-Oberflächenmarker. Darüber hinaus unterdrückte CS die Phosphorylierung des Nuklearfaktors $\varkappa$B (nuclear factor kappa-light-chain-enhancer of activated B cells, NF-$\varkappa$B) und der mitogen-aktivierten Proteinkinase (MAPK) p38. Während der M2-MDM-Polarisierung verringerte CS die Fähigkeit, große Mengen fast aller LM zu erzeugen, einschließlich pro-inflammatorischer Eicosanoide und entzündungsauflösender SPM, hatte aber keine Auswirkungen auf die Freisetzung von Fettsäuresubstraten. Insgesamt zeigen diese Daten, dass

eine Langzeitbehandlung mit CS nicht nur therapeutisch als positiv zu bewertende Effekte auf M1-MDM bewirkt (Inhibition von 5-LOX), sondern auch negative Auswirkungen haben kann, wie die Beeinträchtigung der Produktion von SPM in M2-MDM, welche in der umfassenden Bewertung des pharmakologischen Profils dieses Naturprodukts für die Behandlung von Entzündungskrankheiten zu beachten ist.

Zusammenfassend konnte in dieser Dissertation gezeigt werden, dass TWG und CS die Biosynthesewege von entzündungsbezogenen Lipidmediatoren in menschlichen Makrophagen unterschiedlich regulieren. TWG förderte einen LM-Klassenwechsel von pro-inflammatorischen LM hin zu entzündungsauflösenden SPM in polarisierten MDMs, ohne die Fähigkeit, SPM während der M2-MDM-Polarisierung zu erzeugen, zu beeinträchtigen. In Kurzzeitexperimenten zeigte CS ein ähnliches LM-Profil wie TWG, jedoch mit dem Schwerpunkt einer stark reduzierten 5-LOX-Aktivität in vitro und in vivo. Bei Langzeitinkubationen unterdrückte CS hauptsächlich COX-abgeleitete LM und verwandte biosynthetische Enzyme, wahrscheinlich durch Hemmung der Phosphorylierung von NF-$\varkappa$B und p38 MAPK im Zuge der M1-MDM-Polarisierung, während SPM-steigernde Effekte im Rahmen der M2-MDM-Polarisierung nur schwach ausgeprägt waren.

1 Introduction

1.1 Lipid mediators in inflammation

Inflammation is a physiological and protective response against microbial pathogens or injury, whereas para-inflammation targeting tissue stress or malfunction seems to be responsible for chronic inflammatory conditions [1]. Acute inflammation usually occurs immediately after injury and includes two stages: an initial pro-inflammatory reaction to eliminate invaders, followed by a resolution phase which is essential to regain homeostasis [10]. Nowadays, it is widely accepted and appreciated that resolution is an active and complex process launched at an early stage of inflammation [10]. However, failed resolution of acute inflammation is associated with the emergence of chronic inflammation that occurs with persistent infection. If this persists with no recovery, tissue damage and fibrosis may arise even with a worse sign of different diseases [5,10].

The emerging area of inflammation research promises novel anti-inflammatory therapeutics, in particular, endogenous biochemicals (e.g. cytokines, chemokines, and lipid mediators (LM)) generated by different immune cells (e.g. macrophages, neutrophils) which contribute to counter-regulating inflammation and promoting resolution [4]. Small molecule inhibitors may be able to switch off acute inflammation by altering endogenous mediators, and involved mechanisms may open up new pathways for the resolution of inflammation [11].

LM play a crucial role in the inflammatory process, in particular, prostaglandin E2 (PGE_2) was found to trigger LM class switch from pro-inflammatory leukotriene B_4 (LTB_4), a 5-lipoxygenase (5-LOX) product, to pro-resolving lipoxin A_4 (LXA_4), a 15-lipoxygenase (15-LOX) product to stop PMNL infiltration and promote resolution [12]. Pre-resolving therapeutic approaches are increasingly being considered rather than anti-inflammatory strategies, the former actively promote resolution emerging with endogenous specialized pro-resolving mediators (SPM), while the latter function as antagonists limiting the duration of the inflammatory response [13-15]. Overall, there is wishful thinking to reduce the pro-inflammatory LM to prevent excess inflammation, and simultaneously enhance the production of pro-resolving SPM to restore a healthy state. To understand more knowledge of LM in inflammation it is required to shed light on the potential implications of drug development, targeting to stimulate endogenous pro-resolving mediators or direct administration of agonists of resolution in inflammation-based diseases.

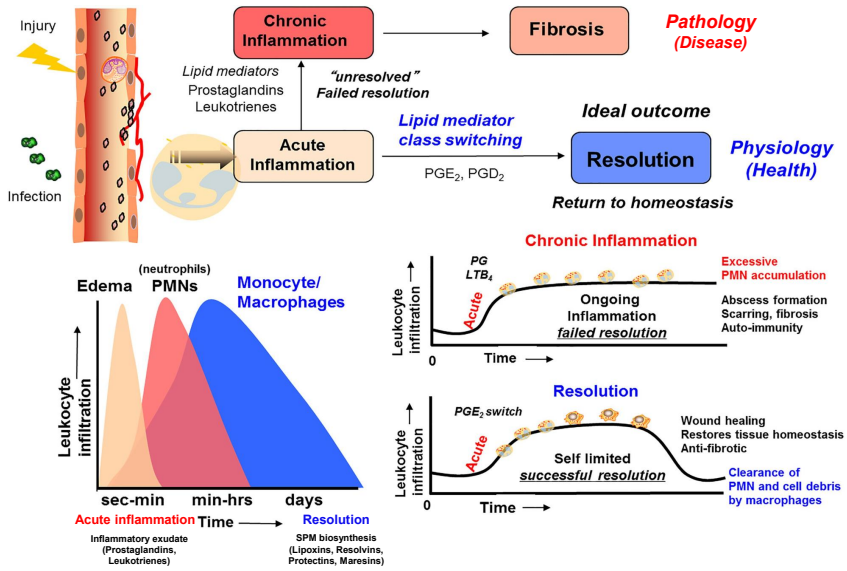

Figure 1.1: Lipid mediators in the inflammatory response. Tissue barrier break, injury or microbial invasion initiate the vascular response and leukocytes start to traffic to the site of injury. The prostaglandins (PG) and leukotrienes (LT) as endogenous lipid mediators (LM) stimulate the migration of neutrophils to the inflamed sites leading to acute inflammation. LM class switching from eicosanoids to lipoxins (LX) takes place in an active way to contribute to the resolution as one of the consequences in the excessive pro-inflammatory responses, and homeostasis is restored - 'health state' as an ideal outcome in the end with the help of specialized pro-resolving mediators (SPM). Failed resolution causes chronic inflammation to appear with redundant pro-inflammatory mediators, which further leads to persistent infection - 'disease state'. Figure modified from Hansen et al [16].

1.1.1 Eicosanoids

Eicosanoids mainly include PG, LT, and thromboxanes (TX) in the initial steps that are necessary for immune cell activation and pro-inflammatory messenger synthesis [17]. Arachidonic acid (AA)-derived eicosanoids are the most abundant 2-series PG and 4-series LT in inflammation; while eicosapentaenoic acid (EPA) as an alternative eicosanoid substrate produced 3-series PG and 5-series LT in favor of the whole biosynthesis pathway, mainly involving the COX, the cytochrome P450 monooxygenase (CYP) and the LOX pathways [18].

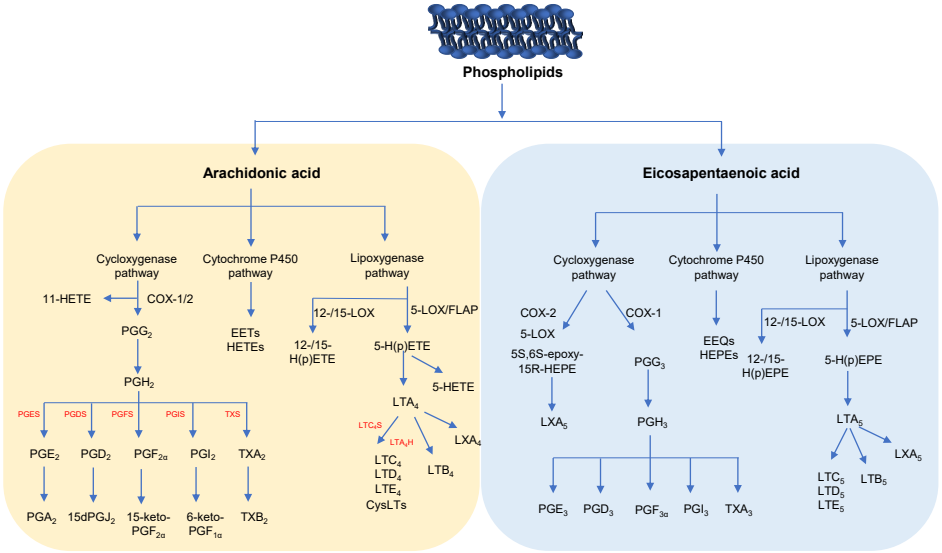

Figure 1.2: The eicosanoid biosynthetic pathways from arachidonic acid (AA) and eicosapentaenoic acid (EPA). Phospholipid-derived AA and EPA are metabolized to eicosanoids by three major pathways: the cyclooxygenase (COX), the cytochrome P450 monooxygenase (CYP) and the lipoxygenase (LOX) pathways. COX pathways produce prostaglandins (PG) and thromboxanes (TX) by specific synthases. P450 metabolizes AA into epoxyeicosatrienoic acids (EET) and hydroxyeicosatetraenoic acids (HETE), and EPA into epoxyeicosatetraenoic acids (EEQ) and hydroxyeicosapentaenoic acids (HEPE). LOX pathways mainly convert substrates into leukotrienes (LT) and HETE. Distinct biosynthetic enzymes involved in the formation of specific eicosanoid are indicated in red color.

1.1.1.1 Prostanoids

PG actions were identified in the 1930s which gave rise to modern ideas in lipid pharmacology, and also brightened many outstanding issues related to anti-inflammatory pharmacology, hemostatic disorders, and reproductive physiology [19]. PG formation initially requires two steps: 1) the conversion of AA yields PGG_2 through cyclooxygenase reaction; 2) PPG_2 conversion to highly unstable PGH_2 via peroxidase reaction. Then, PGH_2 is immediately metabolized to different PG through specific prostaglandins synthases: the hematopoietic PGD_2 synthase (H-PGDS) and lipocalin type (L-PGDS) form PGD_2; the cytosolic PGE_2 synthase (c)PGES and the microsomal (m)PGES-1/-2 produce PGE_2; the PGF synthase (PGFS) generates $PGF_{2\alpha}$; the PGI synthase (PGIS) forms PGI_2 (also named prostacyclin); the TXA synthase (TXAS) makes TXA_2 [20,21].

PG formation from AA to PGH_2 proceeds via the bifunctional cyclooxygenase-1 (COX-1) and cyclooxygenase-2 (COX-2) [22]. COX-1 is constitutively expressed in most cells, while COX-2 often is inducible and emerged as the more important cyclooxygenase in the context of inflammation [22,23]. COX-2-selective inhibitors, called "Coxibs" were developed as promising anti-inflammatory therapeutics with reduced gastrointestinal side effects, which have the same beneficial effects as the traditional or nonselective nonsteroidal anti-inflammatory drugs (NSAID) [24]. However, selective inhibition on COX-2 is not the only beneficial mechanism involved in gastrointestinal toxicity. Coxibs, on the other hand, can create cardiovascular safety issues [25,26]. As a result, there is a need to develop new anti-inflammatory drugs to alleviate dysregulated inflammation diseases in the aspects of the initial and resolving stage of inflammation.

1.1.1.2 Leukotrienes

LT generated by the 5-LOX, their biosynthesis and actions are crucial in the regulation of innate immunity and inflammation [27]. 5-LOX is mainly expressed in various leukocytes such as neutrophils, eosinophils, monocytes, macrophages, mast cells, dendritic cells, and B-lymphocytes [28]. AA is oxygenated by 5-LOX coupled with 5-LOX-activating protein (FLAP) to yield 5-hydroperoxy-eicosatetraenoic acid (5-HpETE) that is then reduced to 5-hydroxyeicosatetraenoic acid (5-HETE) or further converted into an unstable intermediate, leukotriene A_4 (LTA_4). LTA_4 can further form LTB_4 via the soluble enzyme LTA_4 hydrolase (LTA_4H) or is converted by the nuclear membrane-bound glutathione-S-transferase by insertion of the tripeptide glutathione into LTA_4 to form LTC_4 which is further metabolized to LTD_4 and afterward LTE_4, these three isoforms are called cysteinyl-LT (Cys-LT, "slow-reacting substance of anaphylaxis"). Moreover, LXA_4 can be generated from LTA_4 [29]. AA also can be metabolized to 15-HpETE through 15-LOX, and then be reduced to 15-HETE and further converted by 5-LOX into a 5,6-epoxyeicosatrienoic acid, which is the precursor of both LXA_4 and LXB_4. Epimers of LXA_4 and LXB_4 can also be produced in the presence

of aspirin and referred to as aspirin-triggered LX. 12-LOX usually is expressed in platelets that also can form LXA_4 from LTA_4 [29,30].

5-LOX translocates from either the nucleus (in macrophages) or cytosol (in neutrophils) to the nuclear envelope in response to cell activation, and this process is dependent on FLAP [31]. Cys-LT and the dihydroxy-LT (LTB_4) are generated by a series of enzymes/proteins constituting the LT synthetic pathway or 5-LO pathway. Their function is mediated by interacting with multiple receptors that are well characterized such as Cys-LT receptors 1 and 2, BLT1 and 2 [32]. Overall, LT, as a family of potent eicosanoid lipid mediators, play an important role in several diseases processes such as inflammation, neuronal disorder, tumors and are most notably observed in allergic conditions like asthma [33-36]. Zileuton is clinically applicable as anti-asthmatic drug by inhibiting 5-LOX, and many studies are currently targeting FLAP for modulating 5-LOX [37,38].

1.1.2 Specialized pro-resolving mediators (SPM)

The treatment of inflammation has recently been proposed not only to be restricted to the use of inhibitors or antagonists of acute inflammation but to exploit potential inducers or agonists of resolution of inflammation. In other words, emphasis has shifted from just inhibition of inflammation to fostering the termination and resolution of inflammation. Therefore, the concept of anti-inflammation and pro-resolution are not completely equivalent [13].

Diverse chemical mediators biosynthesized during the acute cascade later on serve either as antagonists or agonists, which means they can both inhibit the inflammatory cascade and actively regulate the restoration of homeostasis. An emerging family of SPM including lipoxins (LX), resolvins (Rv), and protectins (PD), function as agonists that actively promote resolution. This novel discovery helps to open more possibilities for drug development through stimulating endogenous pro-resolving mediators and revealing their involved signaling pathways [13]. The essential ω3-PUFAs (n-3 polyunsaturated fatty acids, i.e. EPA and DHA) were found to be the main substrates for SPM biosynthesis, but also have other critical biological functions. However, EPA and DHA must be absorbed within the diet and are not de novo biosynthesized [39]. AA-derived LX and n-3 DPA-derived SPM are also potential immunoresolvents [40,41]. Besides, cell-type-specific and receptor-dependent actions, SPM may provide a new window for treatment of inflammation-based diseases.

1.1.2.1 AA-derived SPM

AA-derived LX belonging to the leukotriene branch, are usually catalyzed by 5-/12-/15-LOX, and 15-HETE is the monohydroxylated precursor of these mediators. Two main members of LX are LXA_4 and LXB_4, and epi-LX are aspirin-triggered [29,40]. The impairment of the

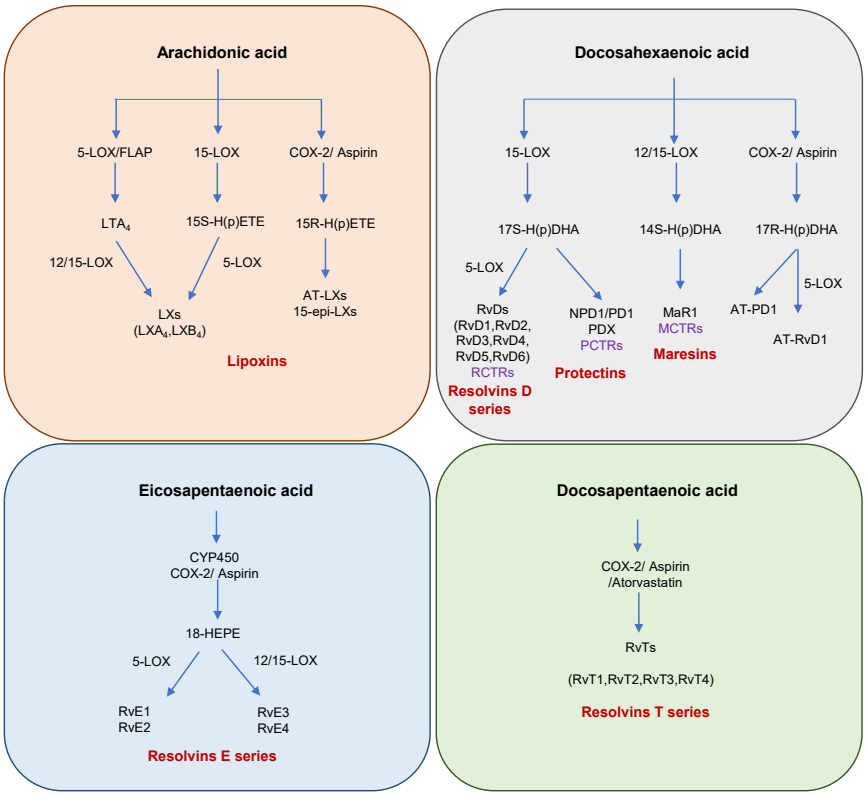

Figure 1.3: The biosynthetic pathways of specialized pro-resolving mediators (SPM). Fatty acid substrates (AA, EPA, DHA and DPA) are converted to different series of SPM including lipoxins (LX), D/E/T-series resolvins (RvDs, RvEs, RvTs), protectins (PD), and maresins (MaR).

production of LXA_4 and LXB_4 are associated with chronic inflammatory diseases, including asthma [42,43].

LX have been proved to exert beneficial actions on inflammation and resolution [29]. For instance, transgenic rabbits overexpressing 15-LOX type 1 ameliorates inflammation via increased production of LXA_4 [44]. Similarly, administration of exogenously plant 15-LOX to mice as well as 15-LOX expressed during infection by *Toxoplasma gondii* with AA generated endogenous LXA_4, which limited acute inflammation and dampened host immune responses [45]. LX suppress the biosynthesis of pro-inflammatory cytokines, activate NF-$\varkappa$B, and are actively involved in homeostasis restoration associated with macrophages [46]. LX also stimulate macrophage efferocytosis (phagocytosis of apoptotic neutrophils and debris) [47]. Moreover, 5-LOX-derived LXA_4 enhances the ability to block *Mycobacterium tuberculosis* infection, thus inhibitors of LXA_4 biosynthesis are crucial for bacterial clearance [48]. LX also show neuroprotective activities with low levels in the brain and cerebrospinal fluid from Alzheimer's disease (AD) patients [49-51].

1.1.2.2 DHA-derived SPM

Maresins (MaR) were first discovered from human macrophages and exhibit pronounced anti-inflammatory effects as biosynthesized bioactive products from DHA [52]. MaR biosynthesis is mediated by 12-/15-LOXs, which generate MaR1 and MaR2 [53,54]. MaR1 was found to reduce psoriasis-like inflammation and UVB irradiation damage [55,56], accelerate planaria regeneration [57], and improve functional neurological recovery after spinal cord injury [58], as well as attenuate neuroinflammation in perioperative neurocognitive disorders in mice [59].

Resolvins (Rv), a family of bioactive 17-hydroxy-containing di- and tri-hydroxy-docosanoids, were found in mice and human tissues and are involved in the resolution of inflammation [60]. Resolvins of D-series (RvDs) are made from DHA by 5-LOX and 15-LOX in humans, via 12-/15-LOX and 5-LOX in mice, and recently six subtypes of RvDs (RvD1, RvD2, RvD3, RvD4, RvD5, RvD6) have been found and synthesized from the intermediate product 17S-hydroperoxy-DHA; RvD epimers are aspirin triggered, called AT-RvDs made from 17R-hydroperoxy-DHA [61]. RvDs generally regulate cytokine biosynthesis and inhibit acute inflammation, and stimulate the polarization of the pro-inflammatory M1-like phenotype towards the resolving M2-like phenotype [62,63]. RvD1 and its G-protein coupled receptors (GPCRs) are considered as potential therapeutic agents and targets, respectively, for inflammation-related human pathologies [64].

Protectins (PD) are also biosynthesized from DHA by various human cells, murine exudates, and brain cells, mediated by 15-LOXs [65]. Protectin 1 (PD1, or neuroprotectin D1 (NPD1)), as the key member of the PDs family, shows powerful anti-inflammatory properties, and enhances the efferocytosis of apoptotic neutrophils, and displays potent neuroprotective actions in the brain, retina, and central nervous system [66,67]. The aspirin-triggered epimer 17R-NPD1 shares the action of NPD1 in controlling neutrophils, enhancing macrophage functions, and attenuating experimental stroke [68,69].

Cysteinyl-SPM (Cys-SPM) based on DHA backbone include three series of peptide-lipid conjugated SPM: maresin conjugates in tissue regeneration (MCTRs), protectin conjugates in tissue regeneration (PCTRs), and resolvin conjugates in tissue regeneration (RCTRs), showing classic pro-resolving function and tissue regenerative ability [70,71].

1.1.2.3 EPA-derived SPM

Resolvins of E-series (RvEs) are derived from EPA, including RvE1, RvE2, RvE3, and RvE4 [72]. RvE1 was reported to be produced in endothelial cells upon treatment with aspirin that acetylated COX-2 that then converts EPA into 18-HEPE. Further metabolism of 18-HEPE by activated leukocytes yields RvE1 [73]. RvE1 reduced neuroinflammation in a murine model of AD and promoted intestinal epithelial wound healing in colitis [74,75]. RvE2 stimulated host-protective actions mediated by leukocyte GPCRs in murine peritonitis

[74,76]. RvE3 attenuated lipopolysaccharide (LPS) induced depression-like behavior in mice and allergic airway inflammation via interleukin (IL) 23-IL17A pathway [77-79]. RvE4, recently identified in M2-macrophages in a hypoxic environment, stimulated efferocytosis of apoptotic neutrophils and senescent erythrocytes, and reduced mouse hemorrhagic exudates better than aspirin [72]. Collectively, RvEs exert potent host-protective actions in target cells and tissues.

1.1.2.4 n-3 DPA-derived SPM

Besides the above-mentioned substrates, n-3 DPA is also converted to SPM including MaRn-3 DPA, RvDn-3 DPA, and PDn-3 DPA, as well as 13-series resolvins (RvTs) [80,81]. They show similar beneficial actions of EPA- and DHA-derived SPM in regulating the innate immune response, controlling cardiovascular disease and arthritis, as well as promoting resolution [82-84]. Systemic treatment with PD1 n-3 DPA or RvD5 n-3 DPA protected against colitis and intestinal inflammation in mice [85]. Moreover, PD1 n-3 DPA promotes the resolution of neuroinflammation and arrests epileptogenesis [86].

1.2 Cells of innate immunity

Innate immune cells include monocytes, macrophages, neutrophils, dendritic cells and others, which serve as a first-line defense against invading pathogens and regulate tissue homeostasis [87].

1.2.1 *Monocytes*

Monocytes mainly circulate in peripheral blood, spleen, and bone marrow, which not only have poor proliferative capacity and heterogeneity but also are critical effectors of innate immune response [88-90]. Inflammation and immune stimuli increase the recruitment of monocytes to peripheral sites, which subsequently develop and differentiate into macrophages and dendritic cells (DC) [91]. All of them contribute to host defense and tissue homeostasis [92]. Moreover, monocytes are not just precursors for macrophages or DC but also are regarded as mononuclear phagocytes with their own functions and roles [93].

Blood monocytes are typically comprised of three cell populations and distinguished by surface receptor expression: 1) the 'classical' inflammatory monocytes (defined as $Ly6C^{hi}$ in mouse and (cluster of differentiation) $CD14^{++}CD16^{+}$ in humans), comprising 85% of blood monocytes and exhibiting high C-C chemokine receptor type (CCR)2 and intermediating C-X3-C Motif Chemokine Receptor (CX3CR)1 expression; 2) the non-classical patrolling monocytes ($Ly6C^{low}$ in mouse, $CD14^{+}$ $CD16^{++}$ in humans), showing low CCR2 and high

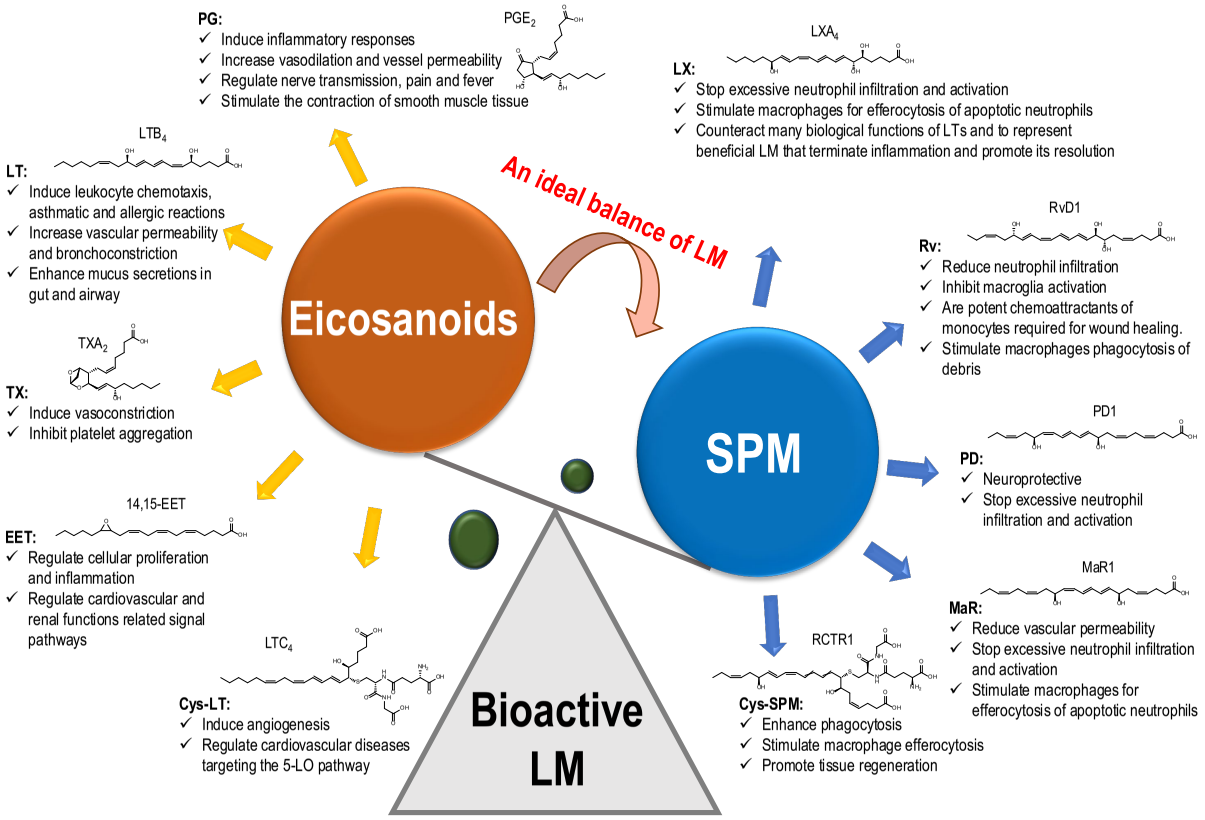

Figure 1.4: Immuno-related properties of bioactive lipid mediators. Two main classes of lipid mediators - eicosanoids and pro-resolving lipid mediators are potent bioactive compounds in the initiation and resolution of inflammation in response to extracellular stimuli. Their balance/disbalance lead to homeostasis or to the pathogenesis of chronic disorders. Eicosanoids include prostaglandins (PG), leukotrienes (LT), thromboxanes (TX), epoxyeicosatrienoic acids (EET) and cysteinyl-LT (Cys-LT), exerting excessive pro-inflammatory actions such as increased vasodilation and vessel permeability. Specialized pro-resolving mediators (SPM) include lipoxins (LX), resolvins (Rv), protectins (PD), maresins (MaR) and cysteinyl-SPM (Cys-SPM), showing dual anti-inflammatory pro-resolving actions including reduction of neutrophils infiltration, enhanced phagocytosis, and stimulated macrophage efferocytosis as well as promoted tissue regeneration.

CX3CR1 expression; 3) the intermediate monocytes, as a transition from classical to non-classical monocytes [94-96].

Human peripheral blood monocytes were initially identified by CD14 with respect to LPS recognition. CD16, known as Fc gamma receptor (FcγR) III, together with CD14 characterize monocytes as two subsets of $CD14^{+}CD16^{-}$ and $CD14^{+}CD16^{+}$ cells [94]. The latter ones express higher amounts of major histocompatibility complex (MHC) class II molecules and CD32 (also known as FcγRII) and express CCR5 [97]. Both subsets can differentiate into DC in response to granulocyte/macrophage colony-stimulating factor (GM-CSF) and IL-4 [98]. Furthermore, one more monocyte subset was found by the expression of CD14, CD16, and CD64 (also known as FcγRI) and showed combined characteristics of monocytes and DC. In particular, $CD14^{+}CD16^{+}CD64^{+}$ cells produce numerous cytokines such as tumor necrosis factor (TNF) and IL-6 and also show higher phagocytic activity in comparison with $CD14^{+}CD16^{-}CD64^{+}$ or $CD14^{+}CD16^{+}CD64^{-}$ [99].

Murine monocytes subtypes were identified by expression of CX3CR1, CCR2, CD62L (also known as L-selectin) [100]. $CX3CR1^{hi}$ mouse monocytes appeared to preferentially migrate into noninflamed sites compared with $CX3CR1^{low}$ monocytes [95]. The Geissmann's group characterized Ly6C (known as part of the epitope of GPI-linked myeloid differentiation marker like Gr-1) as an additional marker [95]. $Ly6C^{hi}$ monocytes mature in the circulation and are the precursor for $Ly6C^{low}$ monocytes, and have the capacity to migrate into sites of peripheral inflammation [100]. Evidence indicated that $CCR2^{+}CD62L^{+}CX3CR1^{low}$ $Ly6C^{+}$ mouse monocytes may correspond to $CD14^{hi}CD16^{-}$ (classic) human monocytes, mainly expressing $CCR2^{+}CX3CR1^{low}$; and $CCR2^{-}CD62L^{-}CX3CR1^{hi}Ly6C^{-}$ mouse monocytes correspond to $CD14^{+}CD16^{+}CD64^{-}$ human monocytes, mainly expressing $CX3CR1^{hi}$, which is of great importance for a better understanding of human monocyte heterogeneity and biology by studying systems for monocyte subsets in mice [101].

1.2.2 Macrophages

Tissue-resident macrophages are generally considered to be derived from circulating monocytes, while adult macrophages are also generated from bone marrow-resident hematopoietic stem cells, all of which show a critical role in tissue homeostasis during inflammation [102,103]. Distinct phenotypes and physiological activities of inflammatory-monocyte-derived macrophages have received much attention by many researchers, which may apply to studies of human biology [101]. The two major functional phenotypes are classically activated M1 macrophages and alternatively M2 macrophages which react differently to pathogenic bacteria and pharmacologic inhibitors, generating discrete LM profiles that differentiate inflammatory into pro-resolving behaviors in these cells [70,104,105].

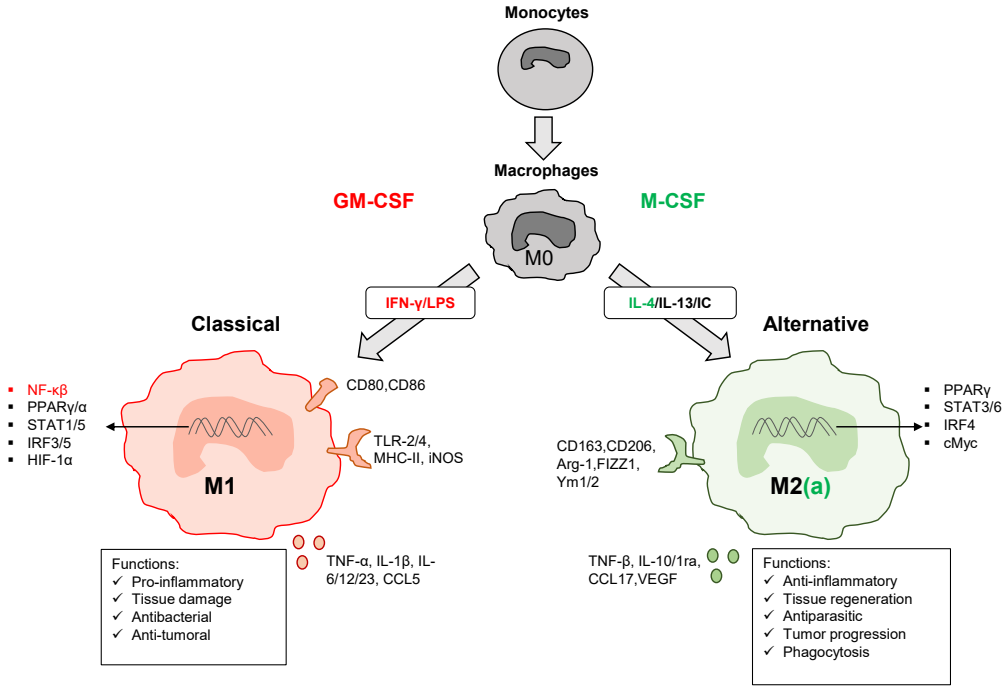

Figure 1.5: Human macrophage polarization. Classical activated (M1) macrophages (stimulated by LPS and IFN-γ) and alternative activated (M2) macrophages (M2a, stimulated by IL-4) display distinct roles with different surface marker expression, secreted cytokines release and biological functions related gene expression. LPS, lipopolysaccharides; IFN-γ, interferon-gamma; NF-κB, nuclear factor κB; PPAR, peroxisome proliferator-activated receptors; STAT, signal transducer and activator of transcription; IRF, interferon regulatory factor; HIF, hypoxia inducible factor; TLR, Toll-like receptor; MHC, major histocompatibility complex; iNOS, inducible nitric oxide synthase; TNF-α, tumor necrosis factor alpha; IL, interleukin; CCL, chemokine (C-C motif) ligand; IC: interferon consensus; cMyc, cellular Myc; Arg-1, arginase 1; FIZZ1, resistin-like α; Ym1, chitinase 3-like gene; TGF-β, transforming growth factor beta; VEGF, vascular endothelial growth factor.

1.2.2.1 M1 Macrophages

The classically activated, pro-inflammatory M1-like macrophages are associated with high bactericidal ability, phagocytic and cytotoxic capabilities, and responsible for the production of pro-inflammatory cytokines (e.g. IL-6, IL-12, IL-1β, and TNF-α) and chemokines (e.g., chemokine (C-C motif) ligand (CCL)2, CCL5) as well as tissue remodeling enzymes (matrix metalloproteinases (MMP)-3 and MMP-12) [105,106]. They are characterized by their expression of MHC-II, CD14, CD80/CD86, and CD38, as well as inducible nitric oxide synthase (iNOS) [105]. The pathogenesis of non-allergic asthma is connected to M1 macrophages, whereas allergic asthma is dominated by M2 [107]. LM metabololipidomics in M1 macrophages usually reveal higher levels of eicosanoids including PG and LT [108]. The uptake of apoptotic cells by M1 cells resulted in a reduction in LT, such as LTB_4 and LTB_5, as well as an increase in SPM production [108].

1.2.2.2 M2 Macrophages

The alternatively activated, anti-inflammatory M2-like macrophages are associated with wound healing, clearance of dead cells and tissues, and resolution of inflammation [109]. They express the cell surface markers CD36, CD206, and CD163 [110]. Compared to M1 macrophages, the M2 phenotype is more complex, and at least four subtypes of pro-reparative M2 macrophages are thought to exist, namely, M2a, M2b, M2c, and M2d, which are categorized based on markers and functions [105,111], but not all appear to play a role in wound healing [112]. However, it is still unclear how these different M2 phenotypes are developed. Of interest, M2a macrophages, which are linked to Th2-polarized allergic inflammation in the lungs, can be obtained by polarization with IL-4 and/or IL-13, and produce a lot of IL-10, transforming growth factor beta (TGF-β) and inflammatory chemokines like CCL17, CCL18, CCL22, and CCL24 [113,114].

There is evidence that the shift from M1 to M2 is critical for a fast repair process of diabetic wounds, while in contrast, impaired switching ability to M2 phenotypes are related to poor angiogenesis, decreased collagen deposition, and delayed wound closure [115]. Likewise, the inhibitor GW2580 was used to block the switch to M2 macrophages by impairing the macrophage-colony stimulating factor (M-CSF-1) signaling cascade, which leads to persistent inflammation and increased M1 macrophages in the wound [116]. Importantly, M2 macrophages produce more pro-resolving LM such as SPM rather than M1 cells, which further favors termination of the acute inflammatory process [108].

1.2.3 Neutrophils

Neutrophils also known as polymorphonuclear leukocytes (PMNL), are the most abundant leukocyte type in human blood and immune effector cells for antimicrobial responses,

which are critical in host defense and maintenance of tissue homeostasis [117]. During neutrophils' extravasation in response to microbial infection, they need to penetrate the blood vessel wall and several sub-steps are involved such as margination, rolling, firm adhesion, transmigration to the injured site, and phagocytosis in the end [118]. Besides, neutrophils express enzymes that potently synthesize bioactive lipids derived from fatty acids and also have been found as a major producer of key pro-inflammatory lipid mediators such as LT and PG, and they possess the capacity to generate SPM [5]. The traditional dogma of neutrophils is considered to act alone to kill the invasive pathogens but has been currently challenged by multiple experimental evidence that neutrophils and their products, in fact, interact with other leukocytes and regulate both innate and adaptive immunity [119,120]. Overall, to better understand how the plastic neutrophils participate in the process of inflammation-based diseases, how they coordinate other cells to operate an appropriate immune response, together with their produced pro-inflammatory and pro-resolving LM upon stimulation may provide new therapeutic approaches in the future.

1.2.4 Other immune-relevant cells

Apart from the above-mentioned cells, there are many other immune cells including DC, mast cells, natural killer cells, basophil, eosinophil that are also critical for immediate responses to fight pathogens. DC originate from the bone marrow and migrate to lymphoid tissues, and distinct subsets have significant phenotypic heterogeneity and functional plasticity [121]. Mast cells are hematopoietic cells and can produce various bioactive products with further responses to many biological processes [122]. Natural killer cells as large granular lymphocytes show anti-tumor and anti-inflammatory functions [123]. Basophil and eosinophil, like neutrophils, are bone marrow-derived granulocytes and are also recruited and activated in the inflamed site [124]. However, they show different functional effects in contrast to neutrophils, but nevertheless, research on these granulocytes is important [124].

1.3 *Tripterygium wilfordii* Hook F

1.3.1 Chemical constituents and tablet development

Extracts of the root of the Chinese herb *Tripterygium wilfordii* Hook F (TwHF), also known in China as "lei gong teng" or "thunder god vine", have been extensively reported and widely used as remedies to treat a variety of inflammatory and autoimmune diseases, including rheumatoid arthritis (RA), muscle and skeletal injury, and skin diseases for several centuries [125,126]. TwHF has been documented to contain more than 100 components, including diterpenes, triterpenes, glycosides, and alkaloids, and 95% of them are terpenoids [127,128]. Two primary active components – the triterpenoid celastrol (CS) and the diterpenoid

***Tripterygium wilfordii* Hook F**

Classes	Chemical constituents	Biological activities
Diterpenes	Triptolide, tripdiolide, triptonide	Anti-inflammatory, anti-cancer, immuno-suppressive, anti-depressive
Triterpenes	Celastrol, Pristimerin, WilforlideA	Anti-inflammatory, anti-rheumatic, anti-cancer, antioxidative
Sesquiterpenes	Tripterygiumines, Triptersinines	Immunosuppressive, anti-inflammatory, neuroprotective, antiviral, and insecticidal activities
Alkaloids	Wilforine, wilfordine, Celabazine, celacinnine, celafurine, and celallocinnine	Anti-inflammatory, antiviral, immunosuppressive, and insecticidal activities
Flavonoids	Tripteryols A-C	Anti-inflammatory, antiproliferative, anti-malarial activities
Lignans	Wilforine A-D	Anti-inflammatory, anti-cancer, antioxidative
Glycosides	Tripterycoside A-C, glucose	Anti-rheumatic, anti-grave ophthalmopathy, anti-diabetic nephropathy
Organic acid	3-oxo-olean-9,3-acetoxy oleanolic acid, tricosanoic acid, stearic acid, and palmitic acid	Anti-inflammatory and anti-cancer
Anthraquinones	1,8-Diphydroxy-4-hydrxymethylanthraquinone, emodin	Anti-inflammatory, neuroprotective, antioxidative, and antifertility
Coumarin	L-epicatechin, fraxetin	Neuroprotective, antifertility activities

Figure 1.6: Representative chemical constituents isolated from *Tripterygium wilfordii* root extract and their corresponding biological activities. Figure adjusted from Zhang et al [6].

triptolide (TP) – account for many pharmacologic activities and immunosuppressive effects of TwHF [9].

In the initial stage, patients were treated with the decoction of TwHF which is a crude water extract method. Two new preparations of the extraction procedure (ethanol/ethyl acetate and chloroform-methanol/T2 extract) were developed in China in the 1970s [129]. Better therapeutic effects and fewer side effects promote the development of usage and clinical trials of TwHF [130,131]. As the representative agents of TwHF, *Tripterygium wilfordii* Glycoside Tablets (TWG, also named TGT) and *Tripterygium wilfordii* Tablets (TWT) were included as Class A drugs in the 2019 edition of Medicine Catalogue for National Basic Medical Insurance, Injury Insurance, and Maternity Insurance [132]. TwHF is a potential source for novel drugs against rheumatoid arthritis, but its impact on the immune system, pharmacological activities and toxic effects need to be explored and may provide a more scientific way for wider use in clinical treatment.

1.3.2 Pharmacological activities

1.3.2.1 Anti-inflammatory properties

Impact on pro-inflammatory lipid mediators In the exudate of TwHF extracts-treated animals, the numbers of white blood cells including neutrophils were significantly reduced, along with lower concentration of PGE_2, nitrite and TNF [133]. TwHF selectively suppresses the expression of COX-2 in inflamed tissues/organs while it did not decrease the expression of COX-1 in non-inflamed tissues/organs. As a result, PGE_2 generation in the inflamed/injured tissue or organ is specifically inhibited by TwHF [133,134]. Aside from suppressing COX-2, TwHF was also found to disrupt the transcription of the iNOS gene, and to inhibit the synthesis of MMP-3 and MMP-13 by impairing activator protein-1 (AP-1) and NF-$\varkappa$B binding activities [135].

Impact on pro-inflammatory genes and cytokines TwHF extracts mainly decreased the expression of pro-inflammatory genes such as IL-2, iNOS, TNF-α, COX-2 and interferon-gamma (IFN-ɣ) in immune cells from human and collagen-induced arthritis (CIA) rat model [136]. In addition, TwHF extracts suppressed the production of pro-inflammatory cytokines like TNF-α, IL-2/-6/-7, and IFN-ɣ by T cells and macrophages in response to antigen [137].

Impact on adhesion molecules TwHF extracts also inhibited the secretion and expression of vascular cellular adhesion molecule (VCAM)-1 and intracellular adhesion molecule (ICAM)-1 in human neutrophils, synovial fibroblasts, and endothelial cells [138].

Impact on the NF-$\varkappa$B signaling pathway Both in vivo and in vitro studies with TwHF extract revealed anti-inflammatory and immunosuppressant activity in RA models [6]. TwHF extracts suppressed the inflammatory response by inhibiting the NF-$\varkappa$B signaling pathway and regulated a variety of cytokines, such as the T-helper type 1 or 2 (Th1/Th2) cytokine expression profile [139,140]. In addition, NF-$\varkappa$B activates the transcription of genes for iNOS and COX-2 and this was reported to be inhibited by TwHF extracts and TP [135]. Together, these results indicate that the anti-inflammatory effect of TwHF extracts may be conferred through regulating some or all of the steps of NF-$\varkappa$B activation, including phosphorylation, ubiquitination, degradation of nuclear factor of kappa light polypeptide gene enhancer in B-cells inhibitor, alpha (I$\varkappa$Bα), nuclear translocation, and DNA binding of NF-$\varkappa$B [141].

1.3.2.2 Anti-arthritic activities

Some systematic reviews and meta-analyses concluded that TwHF-based therapy is beneficial in the treatment of RA and has better clinical efficacy than existing conventional

synthetic disease-modifying anti-rheumatic drugs (DMARD) [142-144]. Similarly, a two-stage clinical trial revealed that American College of Rheumatology (ACR) 20 and 50 responses were significantly higher in the TwHF monotherapy group compared to the methotrexate-sulfasalazine combined therapy group [145]. TwHF extracts effectively suppressed the proliferation of T and B cells and triggered apoptosis of T cells, which may be the major reason for the therapy of inflammatory or autoimmune diseases [146,147].

1.3.2.3 Other activities

TwHF extracts, as multiple pharmacological targets, show plenty of activities such as immune modulation, antitumor, antifertility and anti-HIV effects [136,148,149].

1.3.3 Toxicity

There have also been numerous reports of TwHF's negative consequences related to toxicity, which must be taken into account [150]. The major side effects of TwHF that have been reported include gastrointestinal tract disturbances like diarrhea, leukopenia, loss of appetite, skin rash and pigmentation, malfunction of the reproductive system [127,151,152]. However, adverse reactions of TwHF can stop spontaneously or with dose adjustment, or with integrative therapies, of note, age, gender and the cumulative amount of drug taken probably being the most relevant determinants [153]. In addition, modern research has steadily progressed from the study of raw materials to the study of single compounds such as CS and TP, focusing mostly on the identification of active components, their structural alterations, and the creation of new derivatives with high efficiency but low toxicity [9]. As a result, further clinical trials with longer follow-up periods are needed in the future to validate clinical effectiveness of TwHF and even its bioactive compounds in the treatment of RA.

1.4 Celastrol

1.4.1 Chemical properties

Celastrol (3-hydroxy-9β,13α-dimethyl-2-oxo-24,25,26-trinoroleana-1(10),3,5,7-tetraen-29-oic acid) is a pentacyclic triterpenoid, extracted from the roots of *Tripterygium wilfordii*, and has been studied extensively for its anti-inflammatory and anticancer properties [154,155]. In the fields of organic, biochemistry, and medicinal chemistry, CS has received considerable interest due to its unique chemical structure and potential therapeutic effects [156].

Regarding the interesting therapeutic effects of CS, the market demand of wild plants of TwHF and other members of the Celastraceae family, where CS is present, increased acutely [157,158]. Therefore, to reduce the pressure for agriculture production of plants and also

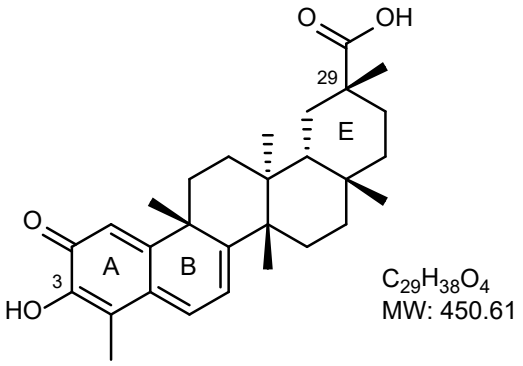

Figure 1.7: The structure of celastrol. The quinone methyl of the A/B rings, the hydroxyl at C-3 position, and the carboxyl group at 29-position were found to be the main pharmacodynamic groups and were addressed in view of structure-modifications, structure-activity relationships, and pharmacology and toxicology.

to investigate more chemistry and biology of CS, the chemical synthesis of CS started to be at a state-of-the-art method due to its high yields, low cost, sustainability, and other advantages [159]. Many chemists put strong efforts in the synthesis and luckily that the total synthesis of this molecule was realized for the first time in 2015 [160].

However, the toxic effect, poor water solubility, and low oral bioavailability of CS limited its clinical applications and further referred to be classified as a biopharmaceutics classification system (BCS) class IV drug [161]. To improve its cytotoxic properties, several studies have revealed that the substitution of the C29 carboxylic group in the E ring and/or the conversions in A/B rings seems to be a great choice [162-164].

1.4.2 Pharmacological activities

1.4.2.1 Anti-inflammatory properties

CS has been well studied in various cells and mouse models of inflammation-related diseases such as ulcerative colitis (UC), allergic asthma, skin fibrosis, and LPS-induced inflammation [165].

Inflammatory bowel disease (IBD) primarily comprises Crohn's disease (CD) and UC, usually known as a nonspecific chronic inflammatory bowel disease. In a dextran sulfate sodium (DSS)-induced UC mouse model, CS was observed to relieve inflammation symptoms and colon injury, which is associated with decreased colonic neutrophil infiltration (myeloperoxidase), inhibition of the NOD-like receptor protein 3 (NLRP3) inflammasome, suppression of the IL-23/IL-17 pathway but stimulation of colonic IL-10 and TNF-α release, and intestinal homeostasis through lowering CD98 upregulation [154]. In an IL-10 knockout mouse model, CS was found to alleviate colitis by induction of intestinal autophagy

via suppression of the phosphatidylinositol-3-kinase/protein kinase B and the mammalian target of rapamycin (PI3K/Akt/mTOR) signaling pathway [166]. Another human CD study showed that CS decreased the secretion of pro-inflammatory cytokines such as IL-1β, IL-6, IL-8, and TNF-α [167]. Interestingly, a lipidomics study revealed that CS treatment significantly alleviated DSS-induced colitis in mice via upregulation of a key enzyme named stearoyl-coenzyme A desaturase 1 [168].

The prevalence of allergic disorders such as atopic dermatitis, asthma, and rhinitis, which are caused by an inappropriate reactivity to antigens, is also a common chronic inflammatory disease [169]. In an allergic asthma mouse model, CS exerted antiallergic effects via MAPK/NF-κB pathway in inflammatory cells and the inhibition of immunoglobulin Fc epsilon receptor I (FcεRI) signaling [170,171]. Cannabinoid receptor type 2 (CB2) was found to show antifibrotic effects in dermal fibrosis [172]. CB2 pathway-related studies revealed that CS reduces inflammation and alleviated dermal fibrosis and renal fibrosis [173,174]. CS also exerts its anti-inflammatory effects through the modulation of a variety of inflammation mediators induced by LPS [175]. In vivo and in vitro studies showed that CS alleviated LPS-induced inflammation by reduction of NO, PGE_2, TNF-α, and IL-6 through inhibiting the activation of NF-κB and AP-1, as well as reduction of IL-1β and suppression of the NLRP3 inflammasome [176,177].

In 2016, Joshi et al first reported that CS relieves inflammation by modulation of the AA pathway by inhibition of secretory phospholipase A2 group IIA (sPLA2IIA), 5-LOX, and COX-2 [178]. Aside from inflammatory mediators and cytokines, CS shows its anti-inflammatory effects via nuclear receptor 77 and TNF receptor associated factor (TRAF)2 interaction and induction of mitochondrial ubiquitination and autophagy [179].

1.4.2.2 Anti-arthritic activities

The clinical efficacy of CS for treating RA has been well-documented, but its mechanism of action remains unclear. RA synovial fibroblasts (RASFs) are important effector cells in the pathogenesis of RA, making them a potential therapeutic target in the therapy of RA [180]. CS inhibits RA-fibroblast-like synovial cells proliferation by inducing DNA damage, cell cycle arrest, and apoptosis in vitro, which might provide proof for its application in RA treatment [181]. CS was reported to be able to mobilize cytosolic calcium (Ca^{2+}) and mapped the target genes of the Ca^{2+} signaling network in RASFs [182]. A further study illustrated that Ca^{2+} signaling causes cell death and is effectively involved in CS treatment of RA [183]. In a rat model of adjuvant-induced arthritis (AIA), CS appears to decrease inflammation and limit synovial immune cell infiltration and proliferation [184]. Another CIA rat model also indicated CS alleviates arthritis by downregulation of inflammatory cytokine (TNF-α, IL-1β, IL-6, and IFN-γ) and oxidative stress [185].

1.4.2.3 Other activities

Besides anti-inflammatory features, CS has a wide spectrum of other pharmacological properties, including anti-obesity and anti-cancer, as well as neuroprotective and antiviral properties. For instance, CS showed anti-obesity effects by increasing the activity of antioxidant enzymes but suppressing nicotinamide adenine dinucleotide phosphate (NADPH) oxidase activity as well as regulating signal transducer and activator of transcription 3-dependent leptin signaling and inhibition of endoplasmic reticulum (ER) stress [187,188]. CS also showed a wide range of anticancer activities mainly through inhibition of heat shock protein (HSP)90, suppression of angiogenesis, induction of apoptosis, and impairment of DNA damage repair [189-193]. CS treatment showed effectively improved memory, learning, and psychomotor activities tests in AD [194]. CS showed antiviral properties against HIV, SARS-CoV, Dengue virus via different mechanisms [195-197]. Considering that CS constitutes a strong drug candidate for the therapy of multiple human diseases, further efforts to reveal its underlying molecular mechanisms of action and pharmacological activity are urgently required.

1.4.3 Toxicity

Despite the wide range of activities offered, one reason for the limited clinical application of CS is toxicity including cardiotoxicity, hepatotoxicity, reproductive toxicity, and hematological toxicity [164]. The efficient inhibitory activity of CS (200 nmol/L) on rectifying potassium (Kir)2.1 and human ether-a-go-go-related gene (hERG) potassium channels, as well as the effective reduction of cell surface channel density highlight the drug's cardiotoxicity [198]. In addition, CS showed its antifertility effects in spermatogenic cells by reduction of Ca^{2+} and inhibition of sperm acrosome reaction initiated by progesterone [199]. In the adult murine hematopoietic system, CS was found to specifically impair the development of B cells and erythrocytes in all tested organs, suggesting it might be a modulator in the hematopoietic system [200].

To reduce the cytotoxicity of CS, combination therapy and nanotechnology-based CS formulations came up to be useful approaches. As an example, CS and the histone deacetylase inhibitor suberoylanilide hydroxamic acid were coupled to activate the NF-$\varkappa$B and E-cadherin signaling pathways concurrently, effectively inhibiting the development of human cancer cells in vitro and in vivo [201]. CS-albumin nanoparticles decreased the accumulation of free CS in off-target organs and tissues, which effectively lowering its systemic toxicity [202].

Nevertheless, CS has a strong potential as therapeutics for inflammatory-based diseases, multiple pharmacological properties of CS may outweigh its toxicological drawbacks, as a result, more trials need to be conducted to get a clear insight into the safety profile and to determine the optimum dosage of this compound.

2 Aim of thesis

Chronic inflammation and autoimmune diseases are a consequence of failure to resolve inflammation. Resolution of inflammation is connected to a temporal LM class switch, stopping the production of pro-inflammatory eicosanoids (PG and LT) and starting the biosynthesis of SPM. TwHF extracts from the roots of the traditional Chinese herb and its predominant active natural ingredient CS have been shown to possess significant anti-inflammatory and immunosuppressive properties and thus are widely used for the treatment of various diseases such as RA, IBD, psoriasis, and kidney disease. TWG, a stable glycoside tablet made from TwHF, has been approved for the routine treatment of CD, UC, and RA. However, the toxicity and side effects limited their wider clinical application, and the mechanisms underlying the pharmacological functions of TwHF remain unclear. Previous studies demonstrated that TwHF and CS target cytokine release and the NF-$\varkappa$B signaling pathway. However, how TWG and CS regulate functions of innate immune cells with respect to inflammation-mediated LM is incompletely understood. Therefore, this thesis aimed at investigating the role of TWG and CS in the modulation of LM biosynthesis in polarized human macrophages and during M1 and M2 macrophages polarization.

Specific objectives:

1. Explore the role of TWG on LM biosynthetic pathways in human macrophages (**manuscript I**).
2. Determine the impact of CS on the 5-LOX activity, allosteric site, and subcellular localization (**manuscript II**).
3. Explore the role of CS on the LM class switch in vitro and in vivo (**manuscript II**).
4. Explore the role of CS on LM biosynthetic pathways during human macrophages polarization (**manuscript III**).
5. Study the impact of CS on gene and enzyme expression of COX-2 as well as related signaling pathways (**manuscript III**).

3 Manuscripts

Manuscript I

K. Zhang*, S. Pace*, P. M. Jordan, L. K. Peltner, A. Weber, D. Fischer, R. K. Hofstetter, X. Chen, O. Werz. Beneficial Modulation of Lipid Mediator Biosynthesis in Innate Immune Cells by Antirheumatic *Tripterygium wilfordii* Glycosides (2021). *Biomolecules* 11(5):746

Manuscript II

S. Pace*, **K. Zhang***, P. M. Jordan, R. Bilancia, W. Wang, F. Börner, R. K. Hofstetter, M. Potenza, C. Kretzer, J. Gerstmeier, D. Fischer, S. Lorkowski, N C. Gilbert, M. E. Newcomer, A. Rossic, X. Chen, O. Werz. Anti-inflammatory celastrol promotes a switch from leukotriene biosynthesis to formation of specialized pro-resolving lipid mediators (2021). *Pharmacological Research* (167)

Manuscript III

K. Zhang, P. M. Jordan, S. Pace, R. K. Hofstetter, M. Werner, X. Chen, O. Werz. Modulation of inflammation-related lipid mediator pathways by celastrol during human macrophage polarization (2022). *Journal of Inflammation Research*, in press

3.1 Manuscript I

Beneficial Modulation of Lipid Mediator Biosynthesis in Innate Immune Cells by Antirheumatic *Tripterygium wilfordii* Glycosides

Kehong Zhang*, Simona Pace*, Paul M. Jordan, Lukas K. Peltner, Alexander Weber, Dagmar Fischer, Robert K. Hofstetter, Xinchun Chen, Oliver Werz (2021)

Biomolecules 11 (2021) 746

In this study, we examined LM modulation in human monocyte-derived macrophage (MDM) phenotypes by TWG, a traditional Chinese medicine applied against RA, by LM metabololipidomics using ultra-performance liquid chromatography-tandem mass spectrometry (UPLC-MS/MS). LM are generated primarily by COX and LOX enzymes in complex networks and govern inflammation and immunological responses which are highly associated with RA. The results revealed that TWG (30 µg/mL) potently suppressed the agonist-induced formation of 5-LOX products in inflammatory M1-MDM, which was further confirmed by a similar inhibitory effect in human PMNL and traced back to direct inhibition of 5-LOX (IC_{50} = 2.9 µg/mL). TWG effectively inhibited the production of thromboxane in M1-MDM while not inhibiting other prostanoids or COX enzymes. Interestingly, TWG (30 µg/mL) caused a significant increase in the synthesis of SPM and related 12/15-LOX-derived SPM precursors without activating COX or 5-LOX in anti-inflammatory M2-MDM. In addition, TWG (1 µg/mL) inhibited the production of pro-inflammatory 5-LOX and COX products, cytokines, and M1 phenotypic markers during MDM polarization. Taken together, TWG's antirheumatic activities may be due, at least in part, to inhibition of pro-inflammatory LM production but stimulation of SPM formation.

Contribution (70%): Cell culture and performance of blood cell isolation, determination of cell viability, determination of 5-LOX/COX-1/COX-2/mPGES-1 activity in cell-free assays, determination of TXAS activity, cell samples preparation for flow cytometry, *Staphylococcus aureus*-conditioned medium (SACM) preparation, sodium dodecyl sulfate-polyacrylamide gel electrophoresis (SDS-PAGE) and Western blot, determination of LM formation by UPLC-MS/MS, analysis of data and preparation of graphs, statistical analysis, writing of the manuscript.

Manuscript I

Titel des Manuskriptes: Beneficial Modulation of Lipid Mediator Biosynthesis in Innate Immune Cells by Antirheumatic *Tripterygium wilfordii* Glycosides

Autoren: Kehong Zhang*, Simona Pace*, Paul M. Jordan, Lukas K. Peltner, Alexander Weber, Dagmar Fischer, Robert K. Hofstetter, Xinchun Chen, Oliver Werz

Bibliographische Informationen Published

Der Kandidat / Die Kandidatin ist (bitte ankreuzen)

☐Erstautor/-in, ☒Ko-Erstautor/-in, ☐ Korresp. Autor/-in, ☐ Koautor/-in.

Anteile (in %) der Autoren / der Autorinnen an der Publikation (anzugeben ab 20%)

Autor/-in	**Konzeptionell**	**Datenanalyse**	**Experimentell**	**Verfassen des Manuskriptes**	**Bereitstellung von Material**
Kehong Zhang	20%	70%	70%	20%	20%
Oliver Werz	60%			70%	30%
Others	20%	30%	30%		50%
Total	100%	100%	100%	100%	100%

biomolecules

MDPI

Article

Beneficial Modulation of Lipid Mediator Biosynthesis in Innate Immune Cells by Antirheumatic *Tripterygium wilfordii* Glycosides

Kehong Zhang [1,2,†], Simona Pace [1,†], Paul M. Jordan [1], Lukas K. Peltner [1], Alexander Weber [3], Dagmar Fischer [3], Robert K. Hofstetter [1], Xinchun Chen [2] and Oliver Werz [1,*]

[1] Department of Pharmaceutical/Medicinal Chemistry, Institute of Pharmacy, Friedrich-Schiller-University, Philosophenweg 14, D-07743 Jena, Germany; kehong.zhang@uni-jena.de (K.Z.); simona.pace@uni-jena.de (S.P.); paul.jordan@uni-jena.de (P.M.J.); lukas.klaus.peltner@uni-jena.de (L.K.P.); robert.klaus.hofstetter@uni-jena.de (R.K.H.)

[2] Guangdong Provincial Key Laboratory of Regional Immunity and Diseases, Department of Pathogen Biology, Shenzhen University School of Medicine, Shenzhen 518000, China; chenxinchun@szu.edu.cn

[3] Department of Chemistry and Pharmacy, Pharmaceutical Technology, Friedrich-Alexander-Universität Erlangen-Nürnberg, Cauerstrasse 4, 91058 Erlangen, Germany; alexander.christian.weber@fau.de (A.W.); dagmar.fischer@fau.de (D.F.)

* Correspondence: oliver.werz@uni-jena.de; Tel.: +49-3641-949801; Fax: +49-364-194-9802

† Authors contributed equally to this work.

check for updates

Citation: Zhang, K.; Pace, S.; Jordan, P.M.; Peltner, L.K.; Weber, A.; Fischer, D.; Hofstetter, R.K.; Chen, X.; Werz, O. Beneficial Modulation of Lipid Mediator Biosynthesis in Innate Immune Cells by Antirheumatic *Tripterygium wilfordii* Glycosides. *Biomolecules* **2021**, *11*, 746. https://doi.org/10.3390/biom11050746

Academic Editors: George Kokotos and Sasanka Ramanadham

Received: 14 April 2021
Accepted: 10 May 2021
Published: 17 May 2021

Publisher's Note: MDPI stays neutral with regard to jurisdictional claims in published maps and institutional affiliations.

Abstract: *Tripterygium wilfordii* glycosides (TWG) is a traditional Chinese medicine with effectiveness against rheumatoid arthritis (RA), supported by numerous clinical trials. Lipid mediators (LM) are biomolecules produced from polyunsaturated fatty acids mainly by cyclooxygenases (COX) and lipoxygenases (LOX) in complex networks which regulate inflammation and immune responses and are strongly linked to RA. The mechanism by which TWG affects LM networks in RA treatment remains elusive. Employing LM metabololipidomics using ultra-performance liquid chromatography-tandem mass spectrometry revealed striking modulation of LM pathways by TWG in human monocyte-derived macrophage (MDM) phenotypes. In inflammatory M1-MDM, TWG (30 µg/mL) potently suppressed agonist-induced formation of 5-LOX products which was confirmed in human PMNL and traced back to direct inhibition of 5-LOX (IC_{50} = 2.9 µg/mL). TWG also efficiently blocked thromboxane formation in M1-MDM without inhibiting other prostanoids and COX enzymes. Importantly, in anti-inflammatory M2-MDM, TWG (30 µg/mL) induced pronounced formation of specialized pro-resolving mediators (SPM) and related 12/15-LOX-derived SPM precursors, without COX and 5-LOX activation. During MDM polarization, TWG (1 µg/mL) decreased the capacity to generate pro-inflammatory 5-LOX and COX products, cytokines and markers for M1 phenotypes. Together, suppression of pro-inflammatory LM but SPM induction may contribute to the antirheumatic properties of TWG.

Keywords: *Tripterygium wilfordii* glycosides; lipoxygenase; cyclooxygenase; inflammation; specialized pro-resolving mediators

1. Introduction

Lipid mediators (LM) encompass oxygenated polyunsaturated fatty acids (PUFA) which are involved in maintenance of normal hemostasis but also display significant roles in host defense as well as in pain, fever and in inflammation and its resolution [1–3]. They are mainly derived from arachidonic acid (AA), eicosapentaenoic acid (EPA) and docosahexaenoic acid (DHA) that are liberated from membrane phospholipids by phospholipases (PL)A_2 upon cell stimulation [4,5]. Cyclooxygenases (COX)-1/2, six lipoxygenases (LOX) in humans, and CYP enzymes convert these free PUFA towards a broad spectrum of

LM that act via specific receptors (mainly G protein-coupled receptors (GPCRs)). The most prominent LM related to inflammation are categorized into (i) the pro-inflammatory COX-derived prostaglandins (PGs) and 5-LOX-derived leukotrienes (LTs) [1,2,6] and (ii) the anti-inflammatory so-called specialized pro-resolving mediators (SPM) that are produced by multiple LOXs, COX-2 or CYP enzymes, with 15-LOX-1 as key enzyme [3,7,8]. SPM are potent endogenous immunoresolvents with beneficial functions in host defense, pain, organ protection, and tissue remodeling, possessing strong therapeutic potential for treatment of a multitude of inflammatory pathologies [9].

Rheumatoid arthritis (RA) is a chronic systemic autoimmune inflammatory disorder of the joints that results in bone and cartilage destruction [10], characterized by the production of eicosanoids, cytokines, adhesion molecules, and lymphocyte and macrophage infiltration in the synovium [11]. Current RA treatment options include disease-modifying anti-rheumatic drugs (DMARDs), corticosteroids, monoclonal antibodies and non-steroidal anti-inflammatory drugs (NSAIDs) [12], but there is still an unmet clinical need for novel RA treatments, ameliorating existing strategies. NSAIDs are the most widely used agents for symptomatic RA treatment which mainly act by blocking COX enzymes and thus the formation of pro-inflammatory PGs that contribute to the progressive destruction of cartilage and bone [13]. However, NSAIDs exert severe side effects and toxicity due to inhibition of PGs which hampers their clinical use [14]. In this respect, harnessing of SPM to promote resolution of inflammation is a new and alternative approach for the treatment of RA [15].

Tripterygium wilfordii Hook F (TwHF) is a traditional Chinese medicine made from the root of the plant that exhibits anti-inflammatory and immune-modulatory activities [16]. Among different TwHF preparations, *Tripterygium wilfordii* glycosides (TWG) tablets are the most widely clinically used form. A large number of clinical trials reported on the effectiveness and safety of TWG in RA [16–18], which was recently documented by a meta-analysis of 40 randomized controlled trials [19]. Some of these trials have even indicated that TWG may achieve better effectiveness than DMARDs monotherapy in patients with RA [20], but multi-organ toxicity and diverse side-effects of TWG have been reported [21]. The anti-rheumatic efficacy of TWG is based on immunosuppression, anti-inflammation, anti-angiogenesis, and bone and cartilage protection activities, due to reduced expression of proinflammatory cytokines and PGs, adhesion molecules and matrix metalloproteinases by macrophages, lymphocytes, synovial fibroblasts and chondrocytes [21,22], but the precise mechanisms of action are still obscure and await more detailed explorations. Triptolide and celastrol are the predominant constituents of TWG, accounting for the pharmacological features as well as for the reported toxicity [23]. Previous studies showed that TWG interferes with PGE_2 biosynthesis by blocking the expression of COX-2 in a variety of cells [24,25], but how TWG impacts the complex LM networks and whether or not TWG affects SPM formation and LOX activities has not been addressed yet. We recently reported that celastrol is a direct 5-LOX inhibitor and promotes SPM biosynthesis [26]. Here we show that TWG significantly modulates the activity and the expression of various LM-biosynthetic enzymes leading to beneficial LM profiles supporting the anti-rheumatic properties of this remedy.

2. Materials and Methods

2.1. Materials

Tripterygium glycosides tablets (TWG, lei gong teng duogan pian, 10 mg/tablet, Approval number Z31020415) were obtained from Shanghai Fudan Fuhua Pharmaceutical Co., Ltd. (Shanghai, China). Zileuton (10006967), indomethacin (70270) and MK886 (21753), were supplied from Biomol GmbH (Hamburg, Germany); dexamethasone (CAS number 50-02-2) and ozagrel hydrochloride hydrate (CAS Number 78712-43-3) were purchased from Sigma-Aldrich (Steinheim, Germany).

Solvents for reversed phase-high performance liquid chromatography (RP-HPLC) of 5-LOX products were obtained from Merck (Darmstadt, Germany). Ultrapure wa-

ter was produced by a Sartorius Arium 611 UV water purification system (Göttingen, Germany). Deuterated and non-deuterated LM standards for ultra-performance liquid chromatography-tandem mass spectrometry (UPLC-MS-MS) were purchased from Cayman Chemicals (Ann Arbor, MI, USA). All other chemicals and reagents were obtained from Sigma-Aldrich (Munich, Germany), unless stated otherwise.

2.2. High-Performance Liquid Chromatography (HPLC) Analysis of TWG and Celastrol

For analysis of TWG and celastrol determination we applied a gradient-based C18-reversed phase high-performance liquid chromatography (RP-HPLC) using an Agilent 1260 Infinity II system equipped with a diode-array-detection system (all Agilent Technologies Inc., Santa Clara, CA, USA) and a Xterra® RP18 5 µm (4.6 mm × 250 mm) column (Waters Corporation, Milford, MA, USA). Detection was performed at 421 nm. The software OpenLAB CDS Rev. C.01.07 (Agilent Technologies) was used for method control and analysis. As mobile phase A acetonitrile (HPLC grade) and as mobile phase B 1% phosphoric acid in ultrapure water (both Carl Roth GmbH + Co. KG, Karlsruhe, Germany) were used. Each run was conducted with an injection volume of 50 µL. Elution was performed with 1 mL/min at 38 °C using the following gradient: 0–3 min 58A:42B, 3–8 min 58A:42B → 95A:5B, 8–13 min 95A:5B, 13–15 min 95A:5B → 58A:42B, 15–18 min 58A:42B. A calibration curve was established with celastrol (abcr GmbH, Karlsruhe, Germany) as reference substance in a concentration range from 0.5 to 250 µg/mL. Correlation coefficient displayed linearity with a value of 0.99997. The limit of detection (LOD) was 231.5 ng/mL, and the limit of quantification (LOQ) 241.7 ng/mL. One tablet containing 10 mg TWG was grinded, 1.5 mL acetonitrile were added and treated by ultrasonication. After centrifugation at 14,500 rpm for 5 min, the supernatant was analyzed by RP-HPLC. The amount of celastrol in the tablets containing 10 mg of TWG was determined at 15.8 µg or 0.158% based on the amount of extract, respectively. A representative chromatogram of TWG including detection of celastrol is shown in Supplementary Figure S1.

2.3. Isolation of Cells from Human Blood

For cell isolation, leukocyte concentrates from freshly withdrawn blood (16 IU heparin/mL blood) from healthy adult volunteers were obtained from the Department of Transfusion Medicine at the University Hospital of Jena, Germany. The experimental protocols were approved by the local ethical committee and were performed in accordance with guidelines and regulations; informed consent was obtained. Peripheral blood mononuclear cells (PBMC) were separated using dextran sedimentation, followed by centrifugation on lymphocyte separation medium (C-44010, Promocell, Heidelberg, Germany). PBMC were seeded in RPMI 1640 (Thermo Fisher Scientific, Schwerte, Germany) containing 10% (v/v) heat-inactivated fetal calf serum (FCS), 100 U/mL penicillin, and 100 mg/mL streptomycin in cell culture flasks (Greiner Bio-one, Frickenhausen, Germany) for 1.5 h at 37 °C and 5% CO_2 for adherence of monocytes. Differentiation of monocytes to macrophages and polarization towards M1-monocyte-derived macrophages (MDM) and M2-MDM was performed as recently described [27]. Briefly, $M0_{GM\text{-}CSF}$ and $M0_{M\text{-}CSF}$ were generated by incubating monocytes with 20 ng/mL GM-CSF or M-CSF (Cell Guidance Systems Ltd., Cambridge, UK), respectively, for 6 days in RPMI 1640 supplemented with 10% FCS, 2 mmol/L L-glutamine and 100 U/mL penicillin-streptomycin. Then, 100 ng/mL LPS and 20 ng/mL IFNγ (Peprotech, Hamburg, Germany) were added to $M0_{GM\text{-}CSF}$ for 48 h to obtain M1-MDM, while 20 ng/mL IL-4 (Peprotech) were added to $M0_{M\text{-}CSF}$ for 48 h to obtain M2-MDM. To obtain polymorphonuclear leukocytes (PMNL), contaminating erythrocytes of pelleted PMNL after the density centrifugation step were removed by hypotonic lysis using water. PMNL were washed twice in ice-cold PBS and finally resuspended in PBS pH 7.4 containing 1 mg/mL glucose and then incubated as described below for the analysis of 5-LOX product formation. Platelet-rich plasma was obtained from the supernatants after density gradient centrifugation, mixed with PBS pH 5.9 (3:2 v/v), centrifuged (2100× g, 15 min, room temperature), and the pelleted platelets were resuspended in PBS

pH 5.9/0.9% NaCl (1:1, *v*/*v*). Washed platelets were finally resuspended in PBS pH 7.4 and 1 mM $CaCl_2$.

2.4. Determination of LM Formation in Human MDM

M2-MDM (2×10^6/mL) were incubated with vehicle (0.1% DMSO) and TWG (3, 30 µg/mL) in PBS containing 1 mM $CaCl_2$ for 180 min at 37 °C. The reaction was stopped by transferring supernatants (1 mL) into 2 mL ice-cold MeOH. In another set of experiments, with the scope to elucidate the effect of TWG on challenged M1-MDM, cells (2×10^6/mL) were pre-treated with TWG (3, 30 µg/mL) in PBS containing 1 mM $CaCl_2$ for 15 min prior to stimulation with 1% *Staphylococcus aureus* 6850 wt-conditioned medium (SACM) for another 90 min. Cultivation of *S. aureus* and preparation of SACM was performed as previously described [28]. The vehicle group received 0.1% DMSO. The reaction was stopped by transferring supernatants (1 mL) into 2 mL ice-cold MeOH.

To assess long-term effects of TWG on LM formation during macrophage polarization, $M0_{GM\text{-}CSF}$ as well as $M0_{M\text{-}CSF}$ (2×10^6/mL) were pre-treated with TGW (1 µg/mL) for 15 min before the addition of LPS and IFNγ (for M1-MDM) or IL-4 (for M2-MDM) for subsequent 48 h polarization. Afterwards, 1% SACM was added to cells in PBS containing 1 mM $CaCl_2$ for 90 min to induce LM biosynthesis. The reaction was stopped by transferring supernatants (1 mL) into 2 mL ice-cold MeOH. After addition of the deuterated LM standards (200 nM d8-5S-HETE, d4-LTB_4, d5-LXA_4, d5-RvD2, d4-PGE_2 and 10 µM d8-AA; Cayman Chemical/Biomol GmbH, Hamburg, Germany), samples were processed for LM analysis using UPLC-MS-MS as described below.

2.5. Lipid Mediator Metabololipidomics by UPLC-MS-MS

Samples obtained from incubated MDM were kept at −20 °C for at least 60 min to allow protein precipitation. After centrifugation (1200× *g*, 4 °C, 10 min), acidified H_2O (8 mL, final pH = 3.5) was added and samples were subjected to solid phase cartridges (Sep-Pak® Vac 6cc 500 mg/6 mL C18; Waters, Milford, MA, USA). The columns had been equilibrated with 6 mL methanol and 2 mL H_2O before sample loading. After washing with 6 mL H_2O and then with 6 mL *n*-hexane, LM were eluted with 6 mL methyl formate. The samples were brought to dryness using an evaporation system (TurboVap LV, Biotage, Uppsala, Sweden) and resuspended in 100 µL methanol/water (50/50, *v*/*v*) for UPLC-MS-MS analysis. LM were analyzed with an Acquity™ UPLC system (Waters, Milford, MA, USA) and a QTRAP 5500 Mass Spectrometer (ABSciex, Darmstadt, Germany) equipped with a Turbo V™ Source and electrospray ionization. LM were eluted using an ACQUITY UPLC® BEH C18 column (1.7 µm, 2.1 mm × 100 mm; Waters, Eschborn, Germany) at 50 °C with a flow rate of 0.3 mL/min and a mobile phase consisting of methanol-water-acetic acid of 42:58:0.01 (*v*/*v*/*v*) that was ramped to 86:14:0.01 (*v*/*v*/*v*) over 12.5 min and then to 98:2:0.01 (*v*/*v*/*v*) for 3 min [29]. The QTRAP 5500 was operated in negative ionization mode using scheduled multiple reaction monitoring (MRM) coupled with information-dependent acquisition. The scheduled MRM window was 60 s, optimized LM parameters were adopted [29], and the curtain gas pressure was set to 35 psi. The retention time and at least six diagnostic ions for each LM were confirmed by means of an external standard (Cayman Chemical/Biomol GmbH, Hamburg, Germany). Quantification was achieved by calibration curves for each LM. Linear calibration curves were obtained for each LM and gave r^2 values of 0.998 or higher. Additionally, the limit of detection for each targeted LM was determined [29].

2.6. Determination of 5-LOX Activity in a Cell-Free Assay

Human recombinant 5-LOX was expressed in *E. coli* BL21 (DE3) transformed with pT3–5LO plasmid and purified by affinity chromatography on an ATP-agarose column as described previously [30]. Briefly, *E. coli* was lysed in 50 mM triethanolamine/HCl, pH 8.0, 5 mM EDTA, 60 µg/mL soybean trypsin inhibitor, 1 mM phenylmethanesulphonyl fluoride, 1 mM dithiothreitol and 1 mg/mL lysozyme and then sonified (3 × 15 s). The homogenate

was then centrifuged at 40,000× *g* for 20 min at 4 °C. 5-LOX in the supernatant was partially purified by affinity chromatography on an ATP-agarose column (Sigma–Aldrich, Munich, Germany). Semi-purified 5-LOX was diluted in PBS containing EDTA (1 mM) and ATP (1 mM) and immediately used for 5-LOX activity assays.

Purified 5-LOX (0.5 µg) in PBS pH 7.4 containing EDTA (1 mM) and ATP (1 mM) was pre-incubated with vehicle (DMSO 0.1%), TWG (0.1, 0.3, 1, 3, 10 µg/mL) or zileuton (3 µM) for 15 min at 4 °C. Then, samples were pre-warmed for 30 s at 37 °C, and 2 mM $CaCl_2$ plus 20 µM AA were added to start 5-LOX product formation. The reaction was stopped after 10 min by addition of one volume of ice-cold methanol, and the formed metabolites were analyzed by RP-HPLC. For the extraction of 5-LOX products, 200 ng of internal PGB_1 standard was added to each sample and samples were centrifuged at 2000 rpm for 10 min. 5-LOX products were purified by solid phase extraction. After elution with 300 µL methanol, samples were analyzed for all-trans isomers of LTB_4 and 5-H(p)ETE by RP-HPLC using a C-18 Radial-PAK column (Waters, Eschborn, Germany) as previously reported [31].

2.7. Determination of 5-LOX Activity in Human PMNL

Freshly isolated PMNL (5×10^6) were pre-incubated with vehicle (DMSO, 0.1%), TWG (0.1, 0.3, 1, 3, 10 µg/mL), or zileuton (3 µM) for 10 min at 4 °C. Then, 2.5 µM A23187 was added together with 20 µM AA for another 10 min at 37 °C in order to induce 5-LOX product formation. The reaction was stopped by adding 1 mL of ice-cold MeOH to the cell suspension on ice. For the extraction of 5-LOX products (all-trans isomers of LTB_4, LTB_4 and 5-H(p)ETE), 200 ng of internal PGB_1 standard was added, samples were centrifuged at 2000× *g* for 10 min, and solid phase extraction and analysis by RP-HPLC was performed as described above.

2.8. Determination of Cell Viability by MTT Assay

Freshly isolated human $M0_{GM\text{-}CSF}$ or $M0_{M\text{-}CSF}$ (2×10^5/mL) in a 96-well plate were pre-incubated with 0.1% vehicle (DMSO), TWG (1, 3, 10, 30 µg/mL) or 1% Triton X-100 for 15 min, then LPS and IFNγ or IL-4 (for M1 and M2 polarization, respectively) were added for 48 h at 37 °C and 5% CO_2. For short term treatment, polarized M1-MDM and M2-MDM were incubated with 0.1% vehicle (DMSO) or TWG (1, 3, 10, 30 µg/mL) or 1% Triton X-100 for 3 h. Then, calcein-AM and 3-(4,5-dimethylthiazol-2-yl)-2,5-diphenyltetrazolium bromide (MTT, 5 mg/mL, 20 µL; Sigma-Aldrich, Munich, Germany) solution were added in darkness for 2–3 h at 37 °C and 5% CO_2. The formazan product was solubilized with sodium dodecyl sulfate (SDS, 10% in 20 mM HCl), and absorbance was measured at 570 nm using a Multiskan Spectrum microplate reader (Thermo Fisher Scientific, Schwerte, Germany).

2.9. Determination of COX-1 and -2 Activity

For determination of COX activities, purified ovine COX-1 (Cayman Chemicals; 50 units) or human recombinant COX-2 (Cayman Chemicals; 20 units) were diluted in Tris buffer (100 mM, pH 8) supplemented with glutathione (5 mM), EDTA (100 µM) and hemoglobin (5 µM). After pre-incubation with TWG, vehicle (0.1% DMSO) or indomethacin (IND, 10 µM) for 5 min at RT, the samples were pre-warmed for 30 s at 37 °C, and the reactions were started by addition of 5 µM AA (COX-1) or 2 µM AA (COX-2). After 5 min at 37 °C the reactions were stopped by addition of one volume of ice-cold methanol. Formation of COX-derived 12(*S*)-hydroxy-5-*cis*-8,10-*trans*-heptadecatrienoic acid (12-HHT) was analyzed by RP-HPLC on a Nova-Pak C18 Radial-Pak Column (4 µm, 5 × 100 mm, Waters) as described [31].

2.10. Determination of mPGES-1 Activity in a Cell-Free Assay

Microsomes of A549 cells stimulated by IL-1β (2 ng/mL for 48 h) were used as source for microsomal prostaglandin E_2 synthase (mPGES)-1, as described elsewhere [32]. In brief, A549 cells were incubated with ice-cold homogenization buffer (0.1 M potassium phos-

phate buffer pH 7.4, 1 mM phenylmethanesulphonyl fluoride, 60 µg/mL soybean trypsin inhibitor, 1 µg/mL leupeptin, 2.5 mM glutathione and 250 mM sucrose). After sonication, the lysate was first centrifuged at 10,000× *g* for 10 min, and then at 174,000× *g* for 1 h at 4 °C. The pelleted microsomal fraction was then resuspended into 1 mL of homogenization buffer and diluted in a potassium phosphate buffer (0.1 M, pH 7.4) containing 2.5 mM glutathione. Afterwards, TWG, vehicle (0.1% DMSO), or the positive control MK886 (10 µM) were added for 15 min on ice in 100 µL incubation volume. The reaction was started after addition of PGH_2 (20 µM) and stopped after 1 min at 4 °C using 100 µL of a stop solution (40 mM $FeCl_3$, 80 mM citric acid, and 10 µM of 11β-PGE_2 as internal standard). PGE_2 and 11β-PGE_2 were extracted by solid phase extraction using acetonitrile as eluent and quantified by RP-HPLC.

2.11. Determination of Thromboxane A Synthase Activity

Thromboxane A synthase (TXAS) activity was determined in lysates of human platelets. Freshly isolated cells were resuspended in ice-cold PBS pH 7.4 containing 1 mM EDTA (1×10^8 cells/mL) and sonicated (4 × 10 s) on ice. The reaction was initiated by the addition of 20 µM PGH_2 for 1 min at 4 °C in cell homogenates (1 mL) after pre-incubation with TWG (1 and 10 µg/mL), vehicle (0.1% DMSO) or the positive control ozagrel (OZA, 50 µM) for 15 min at 4 °C and terminated by the addition of ice-cold MeOH (2 mL). Then, samples were processed as described for LM metabololipidomics analysis and formed TXB_2 was determined by UPLC-MS-MS, as reported above.

2.12. SDS-PAGE and Western Blot

$M0_{GM\text{-}CSF}$ and $M0_{M\text{-}CSF}$ MDM were treated with vehicle (DMSO), 1 µg/mL TWG or 100 nM dexamethasone for 15 min prior to addition of polarizing agents for 48 h at 37 °C and 5% CO_2 and then lysed, as described previously [28]. Then, lysates were centrifuged (15,000 rpm, 5 min, 4 °C), cell supernatants were collected, and their protein concentration determined by DC-protein assay kit (Bio-Rad Laboratories GmbH, Munich, Germany). After addition of 4×SDS loading buffer (50 mM Tris-HCl, pH 6.8, 2% (*w*/*v*) SDS, 10% (*v*/*v*) glycerol, 1% (*v*/*v*) β-mercaptoethanol, 12.5 mM EDTA, 0.02% (*w*/*v*) bromophenol blue) to the lysates, samples were heated at 95 °C for 5 min. Equal aliquots were separated on 8% (for $cPLA_2\alpha$ and COX-2), 10% (for 5-LOX, 15-LOX-1), 16% (for COX-1, mPGES-1) SDS-PAGE gels and then blotted onto nitrocellulose membranes (Amersham Protran Supported 0.45 µm nitrocellulose, GE Healthcare, Freiburg, Germany). The membranes were incubated with the following primary antibodies: rabbit polyclonal anti-$cPLA_2\alpha$,1:1000 (2832S; Cell Signaling Technology); rabbit polyclonal anti-5-LOX, 1:1000 (to a peptide corresponding to the C-terminal 12 amino acids of 5-LOX: CSPDRIPNSVAI; kindly provided by Dr. M. E. Newcomer, Louisiana State University, Baton Rouge, LA, USA); mouse monoclonal anti-15-LOX-1, 1:500 (ab119774; Abcam, Cambridge, UK); rabbit polyclonal anti-COX-1, 1:1000 (4841S; Cell Signaling Technology); rabbit monoclonal anti-COX-2, 1:1000 (12282S; Cell Signaling Technology); rabbit polyclonal anti-mPGES-1, 1:5000 (kindly provided by Dr. Per-Johan Jakobsson, Karolinska Institute, Stockholm, Sweden); mouse monoclonal anti-β-actin, 1:1000 (3700S; Cell Signaling). Immunoreactive bands were stained with IRDye 800CW Goat anti-Mouse IgG (H + L), 1:10,000 (926-32210, LI-COR Biosciences, Lincoln, NE), IRDye 800CW Goat anti-Rabbit IgG (H + L), 1:15,000 (926 32211, LI-COR Biosciences) and/or IRDye 680LT Goat anti-Mouse IgG (H + L), 1:40,000 (926-68020, LI-COR Biosciences), and visualized by an Odyssey infrared imager (LI-COR Biosciences, Lincoln, NE, USA). Data from densitometric analysis were background corrected.

2.13. Determination of Cytokine Levels

$M0_{M\text{-}CSF}$ macrophages were treated with TWG (1 µg/mL), 100 nM dexamethasone or vehicle (0.1% DMSO) and stimulated with 100 ng/mL LPS for 20 h. For measurement of extracellular cytokine levels, supernatants were collected by centrifugation (2000× *g*,

4 °C, 10 min). The cytokines IL-1β and TNF-α were analyzed by in-house–made ELISA kits (R&D Systems, Bio-Techne, Abingdon, UK).

2.14. Flow Cytometry

$M0_{M\text{-}CSF}$ MDM were treated with TWG (1 μg/mL) or vehicle (0.1% DMSO) for 48 h. Then, cells were stained in PBS pH 7.4 containing 0.5% BSA, 2 mM EDTA and 0.1% sodium azide by Zombie Aqua™ Fixable Viability Kit (Biolegend, San Diego, CA, USA) for 5 min at 4 °C to determine cell viability. Non-specific antibody binding was blocked by using mouse serum (10 min at 4 °C) prior to staining by the following fluorochrome-labelled antibodies (20 min, 4 °C): FITC anti-human CD14 (clone M5E2, #555397, BD Bioscience, San Jose, CA, USA), APC-H7 anti-human CD80 (clone L307.4, #561134, BD Bioscience), PE-Cy7 anti-human CD54 (clone HA58, #353115, Biolegend, Koblenz, Germany), PE anti-human CD163 (clone GHI/61, #556018, BD Biosciences, Heidelberg, Germany), APC anti-human CD206 (clone 19.2, #550889, BD Bioscience) to determine M1 and M2 surface marker expression using LSRFortessa™ cell analyzer (BD Bioscience), and data were analyzed using FlowJo X Software (BD Bioscience).

2.15. Statistical Analysis

Results are expressed as mean + S.E.M. of each independent experiment, where *n* represents the indicated numbers from separate donors performed on different days. Statistical analysis and graphs were made by using GraphPad Prism 8 software (San Diego, CA, USA). Paired *t*-test was used to analyze experiments for comparison of two groups; while for multiple comparisons, ANOVA with Bonferroni or Dunnett multiple comparison tests were applied as indicated. A p-value ≤ 0.05 is a criterion for statistical significance.

3. Results

3.1. TWG Modulates LM Formation in Activated Pro-Inflammatory Macrophages

Human MDM were polarized with IFNγ and LPS for 48 h towards a pro-inflammatory M1-like phenotype and preincubated with TWG (3 or 30 μg/mL, as low or high dose) for 15 min prior to activation with SACM [28] to induce LM biosynthesis. LM profile signatures in the medium were analyzed by UPLC-MS-MS after 90 min of these M1-MDM incubations, and revealed substantial amounts of COX- and 5-LOX-derived LM, with only minor formation of 12/15-LOX products (Table 1), as reported before [27,28]. Analysis of the cell viability by MTT assay revealed no detrimental effects of TWG within 180 min up to 30 μg/mL (Figure 1A). TWG at the high dose of 30 μg/mL potently suppressed formation of all 5-LOX products (LTB_4, t-LTB_4, 5-HETE, 5-HEPE and 7-HDHA) with minor efficiency at the low dose of 3 μg/mL (Table 1, Figure 1B,D). The sum of COX-derived products was not altered by TWG, however, PGE_2 and PGD_2 were elevated but formation of TXB_2 was strongly diminished (Table 1, Figure 1B,C), suggesting that conversion of the COX product PGH_2 by terminal prostanoid synthases is differentially affected by TWG. Of interest, TWG suppressed generation of 12-LOX products (i.e., 14-HDHA, 12-HETE and 12-HEPE) and RvD5, while 15-LOX products (i.e., 17-HDHA, 15-HETE and 15-HEPE) were rather elevated (Table 1), at least at 30 μg/mL TWG. The release of PUFA as LM substrates was not markedly affected by TWG.

Table 1. Heatmap of LM produced by pro-inflammatory human M1-MDM and effects of Table 1. MDM were pre-treated for 15 min with 3 or 30 µg/mL TWG or 0.1% DMSO as vehicle. Then, cells were stimulated with 1% *S. aureus*-conditioned medium (SACM) for 90 min. LM were analyzed by UPLC-MS/MS in the supernatants of cells. Data are means ± S.E.M., $n = 3$.

							0 1 80				
LM	**Vehicle**			**TWG, 3 µg/mL**			**%**	**TWG, 30 µg/mL**			**%**
PGE_2	7899	±	1734	10,047	±	1975	**127**	14,612	±	2939	**185**
PGD_2	132	±	28	300	±	82	**226**	651	±	33	**492**
$PGF_{2\alpha}$	517	±	78	410	±	56	**79**	917	±	109	**177**
TXB_2	9799	±	2114	3474	±	636	**35**	517	±	119	**5**
11-HETE	859	±	215	560	±	119	**65**	1265	±	323	**147**
11-HEPE	37	±	7	26	±	2	**69**	54	±	12	**145**
5-HETE	5643	±	3000	2825	±	1677	**50**	492	±	364	**9**
5-HEPE	534	±	269	214	±	97	**40**	46	±	27	**9**
t-LTB_4	717	±	413	587	±	405	**82**	84	±	69	**12**
LTB_4	1488	±	467	1577	±	572	**106**	322	±	237	**22**
7-HDHA	55	±	11	21	±	6	**38**	9	±	2	**16**
17-HDHA	79	±	14	72	±	12	**91**	96	±	11	**122**
15-HETE	821	±	156	630	±	101	**77**	1649	±	392	**201**
15-HEPE	13	±	2	11	±	1	**86**	26	±	1	**202**
14-HDHA	14	±	4	12	±	4	**87**	10	±	3	**73**
12-HETE	75	±	22	49	±	26	**66**	56	±	29	**74**
12-HEPE	8	±	2	5	±	2	**65**	5	±	2	**69**
RvD5	3	±	0	2	±	0	**65**	1	±	0	**39**
AA	35,272	±	6967	40,740	±	7838	**116**	40,043	±	7620	**114**
EPA	4272	±	659	5274	±	685	**123**	4669	±	575	**109**
DHA	25,373	±	4809	27,362	±	6445	**108**	24,547	±	3921	**97**

3.2. TWG Selectively Inhibits 5-LOX among LM-Biosynthetic Enzymes

Intrigued by the significant and differential modulation of certain LM by TWG in activated MDM, we assessed the effects of TWG on enzymatic activities of isolated LM-biosynthetic enzymes in cell-free assays. TWG concentration-dependently inhibited the activity of human recombinant 5-LOX with IC_{50} of 2.9 µg/mL (Figure 2A,B). COX-1 activity was not inhibited, and COX-2 activity was moderately suppressed at 10 µg/mL TWG, the highest concentrations tested (Figure 2A). Surprisingly, TXAS was not affected despite efficient suppression of TXB_2 formation in MDM (see Figure 1C), but mPGES-1 activity was reduced by 44% at 10 µg/mL TWG (Figure 2A). To explore 5-LOX inhibition we also assessed the effects of TWG in a robust and well-recognized cell-based assay, that is, A23187-activated human PMNL. Again, TWG concentration-dependently inhibited 5-LOX activity (Figure 2C), like in MDM.

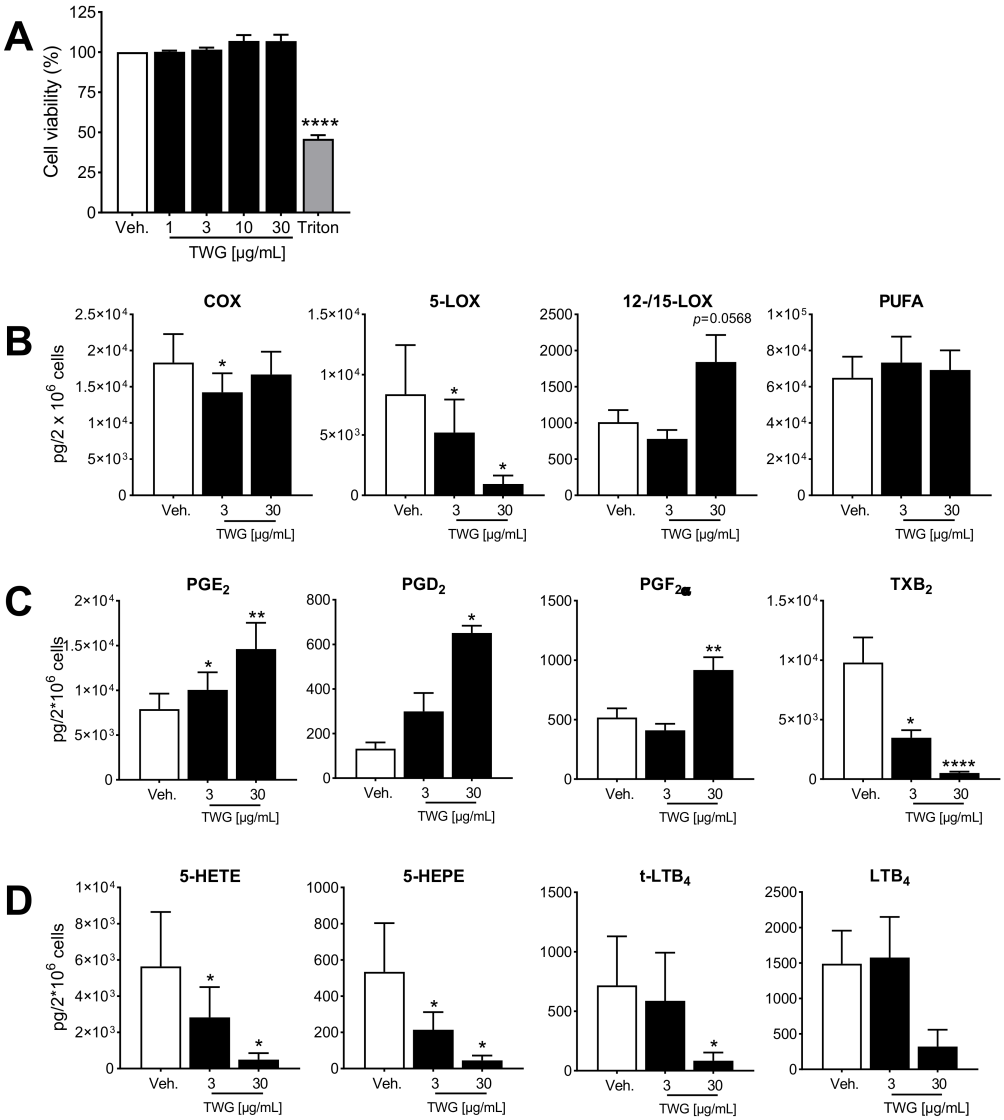

Figure 1. Effects of TWG on cell viability and LM modulation in human M1-MDM. (**A**) M1-MDM were treated with TWG at the indicated concentrations, 1% triton X-100, or 0.1% DMSO as vehicle for 3 h. Then, cell viability was assessed by MTT assay. Values are means + S.E.M., $n = 3$, expressed as percentage of vehicle control (=100%); **** $p < 0.0001$ TWG vs. control group, one-way ANOVA for multiple comparisons with Bonferroni's correction. (**B**–**D**) M1-MDM were pre-treated with 3 and 30 µg/mL TWG or 0.1% DMSO as vehicle for 15 min and then stimulated with 1% *S. aureus*-conditioned medium (SACM) for 90 min. Produced LM were analyzed by UPLC-MS-MS in the supernatants. (**B**) The sum of COX products, 5-LOX products, 12/15-LOX products, and PUFA are expressed as pg/2 $\times$ 10^6 cells of TWG-treated and vehicle-treated cells. (**C**,**D**) Individual members of COX products (**C**) and of 5-LOX products (**D**). Data are means $\pm$ S.E.M., $n = 3$ and were log-transformed for statistical analysis, * $p < 0.05$, ** $p < 0.01$, **** $p < 0.0001$, TWG vs. control group, one-way ANOVA and Dunnett's multiple comparisons test.

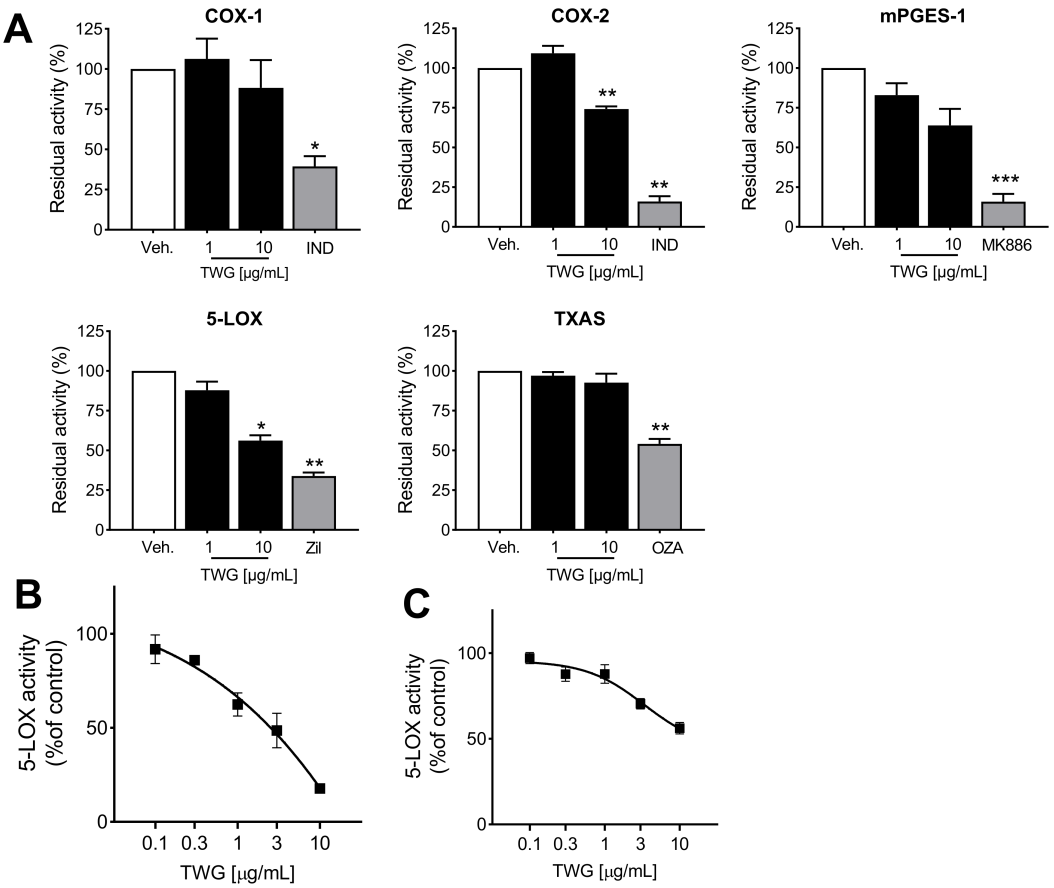

Figure 2. TWG selectively inhibits 5-LOX. (**A**) Effect of 1 and 10 µg/mL TWG on the residual activities of isolated ovine COX-1, human recombinant COX-2 and 5-LOX, mPGES-1 in microsomes from A549 cells, and TXAS in homogenates of human platelets. Data are expressed as percentage of vehicle (=100%) and given as means ± S.E.M., $n = 3$ (for COX-1/2, 5-LOX) or $n = 4$ (for mPGES1, TXAs). Indomethacin (IND) 10 µM, MK886 10 µM, and zileuton 3 µM were used as positive controls. * $p < 0.05$, ** $p < 0.01$, *** $p < 0.001$, TWG vs. control group, one-way ANOVA and Dunnett's multiple comparisons test. (**B**,**C**) Concentration response curves of TWG for inhibition of (**B**) isolated human recombinant 5-LOX incubated with 20 µM AA, and (**C**) 5-LO in human intact PMNL stimulated with 2.5 µM A23187 plus 20 µM AA. Data are means + S.E.M., $n = 3$.

3.3. TWG Induces the Formation of SPM and 12/15-LOX Products in Anti-Inflammatory Macrophages

Novel recent pharmacological approaches for treatment of chronic and excessive inflammatory disorders favor the formation of SPM, besides blocking pro-inflammatory PGs and LTs [8,33]. We employed the use of anti-inflammatory M2-MDM polarized with IL-4 that possess high capacities for SPM production due to substantial expression of 15-LOX-1, with moderate formation of PGs and LTs [27]. Like for M1-MDM, cell viability analysis by MTT assay showed no detrimental effects by TWG up to 30 µg/mL within 180 min for M2-MDM (Figure 3A). Intriguingly, exposure of M2-MDM to TWG at 30 µg/mL caused a massive formation of the SPMs PDX, RvD5 and MaR2 along with substantial formation of their monohydroxylated precursors 17-HDHA and 14-HDHA as well as other 12/15-LOX products with minor effects at 3 µg/mL TWG (Table 2, Figure 3B,C). The very low amounts of 5-LOX products in M2-MDM were not diminished by TWG (Table 2,

Figure 3B). COX products were much less efficiently elevated by TWG as compared to SPM (Figure 3C), again with differential effects depending on the individual prostanoids: PGD_2 was most potently elevated while TXB_2 was not altered (Table 2). Together, these data indicate that TWG suppresses pro-inflammatory 5-LOX products in M1- but elevates inflammation-resolving SPM and 12/15-LOX products in M2-MDM.

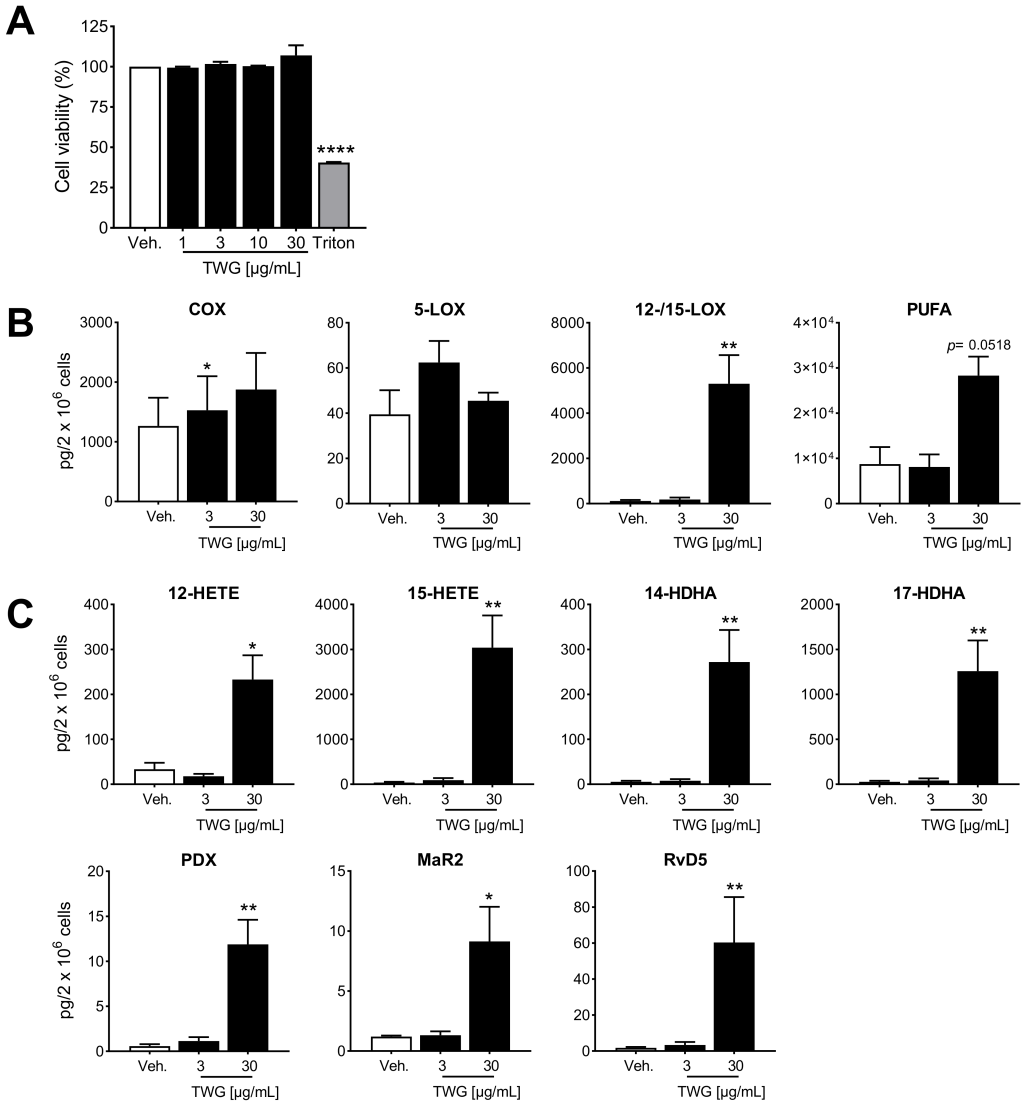

Figure 3. TWG induces LM production in anti-inflammatory human M2-MDM. (**A**) M2-MDM were treated with TWG at the indicated concentrations, 1% triton X-100, or 0.1% DMSO as vehicle for 3 h. Then, cell viability was assessed by MTT assay. Values are means + S.E.M., $n = 3$, expressed as percentage of vehicle control (=100%); **** $p < 0.0001$, TWG vs. control group, one-way ANOVA for multiple comparisons with Bonferroni's correction. (**B**,**C**) M2-MDM were treated with 3 or 30 µg/mL TWG or with 0.1% DMSO as vehicle for 180 min and LM from cells supernatants were analyzed by UPLC-MS/MS. (**B**) The sum of COX products, 5-LOX products, 12/15-LOX products and PUFA are expressed as pg/2 × 10^6 cells of TWG-treated and vehicle-treated cells. (**C**) Individual members of 12/15-LOX products, expressed as pg/2 × 10^6 cells of TWG-treated and vehicle-treated cells. Data are means + S.E.M., $n = 5$ and were log-transformed for statistical analysis, * $p < 0.05$, ** $p < 0.01$, TWG vs. control group, one-way ANOVA and Dunnett's multiple comparisons test.

Table 2. Heatmap of LM produced by anti-inflammatory human M2-MDM and effects of TWG. M2-MDM were treated for 180 min with 3 or 30 µg/mL TWG or 0.1% DMSO as vehicle. Then, formed LM released into the medium were extracted and analyzed by UPLC-MS/MS. Data are means ± S.E.M., $n = 5$.

							0 1 80				
LM	**Vehicle**			**TWG, 3 µg/mL**			**Fold**	**TWG, 30 µg/mL**			**Fold**
PGE_2	34	±	7	46	±	9	**1.4**	121	±	28	**3.6**
PGD_2	9	±	3	35	±	2	**3.7**	217	±	52	**22.8**
$PGF_{2\alpha}$	41	±	16	61	±	21	**1.5**	131	±	21	**3.2**
TXB_2	1181	±	454	1386	±	546	**1.2**	1409	±	632	**1.2**
11-HETE	5	±	2	6	±	2	**1.2**	44	±	10	**8.5**
11-HEPE	3	±	1	2	±	1	**0.8**	9	±	1	**3.4**
5-HETE	25	±	8	46	±	11	**1.8**	30	±	2	**1.2**
5-HEPE	5	±	1	7	±	1	**1.3**	5	±	1	**1.0**
t-LTB_4	6	±	2	6	±	2	**1.0**	6	±	0	**1.0**
LTB_4	3	±	1	4	±	1	**1.1**	5	±	1	**1.5**
7-HDHA	12	±	2	13	±	3	**1.1**	18	±	3	**1.5**
17-HDHA	27	±	11	43	±	23	**1.6**	1259	±	340	**46.3**
15-HETE	38	±	15	92	±	44	**2.4**	3039	±	716	**78.9**
15-HEPE	10	±	3	20	±	10	**2.1**	431	±	92	**45.0**
14-HDHA	6	±	2	8	±	4	**1.4**	272	±	71	**49.2**
12-HETE	33	±	14	18	±	5	**0.5**	233	±	54	**7.0**
12-HEPE	4	±	1	4	±	2	**1.0**	70	±	15	**18.3**
PDX	1	±	0	1	±	0	**2.0**	12	±	3	**20.5**
RvD5	2	±	1	3	±	2	**2.1**	60	±	25	**38.3**
MaR2	1	±	0	1	±	0	**1.1**	9	±	3	**7.6**
AA	4155	±	1678	4330	±	1388	**1.0**	15,991	±	1863	**3.8**
EPA	680	±	297	546	±	189	**0.8**	3148	±	245	**4.6**
DHA	3926	±	1814	3232	±	1294	**0.8**	9167	±	2329	**2.3**

3.4. TWG Modulates the Expression of LM-Biosynthetic Enzymes in Macrophages during Polarization

Next, we investigated if TWG may also affect LM biosynthetic pathways during polarization of the MDM with consequence for LM-producing capacities of the cells. MDM were pre-treated with TWG for 15 min, polarized for 48 h towards M1-MDM using IFNγ plus LPS or towards M2-MDM using IL-4, harvested, and then activated with SACM to elicit LM production. Analysis by MTT assay showed that during 48 h exposure to TWG, both M1- and M2-MDM were susceptible to TWG ≥ 3 µg/mL with loss of viability (Figure 4A), and thus we applied lower TWG concentrations of only 1 µg/mL. As shown in Table 3 and Figure 4B, 5-LOX and COX products formed by M1-MDM were significantly impaired when cells had been pre-treated with TWG, and also 15-LOX products were diminished, while 12-LOX products remained elevated; release of PUFA was not markedly altered. In M2-MDM, a significant but moderate reduction of 5-LOX products was observed without significant alterations of other LM (Table 3, Figure 4C).

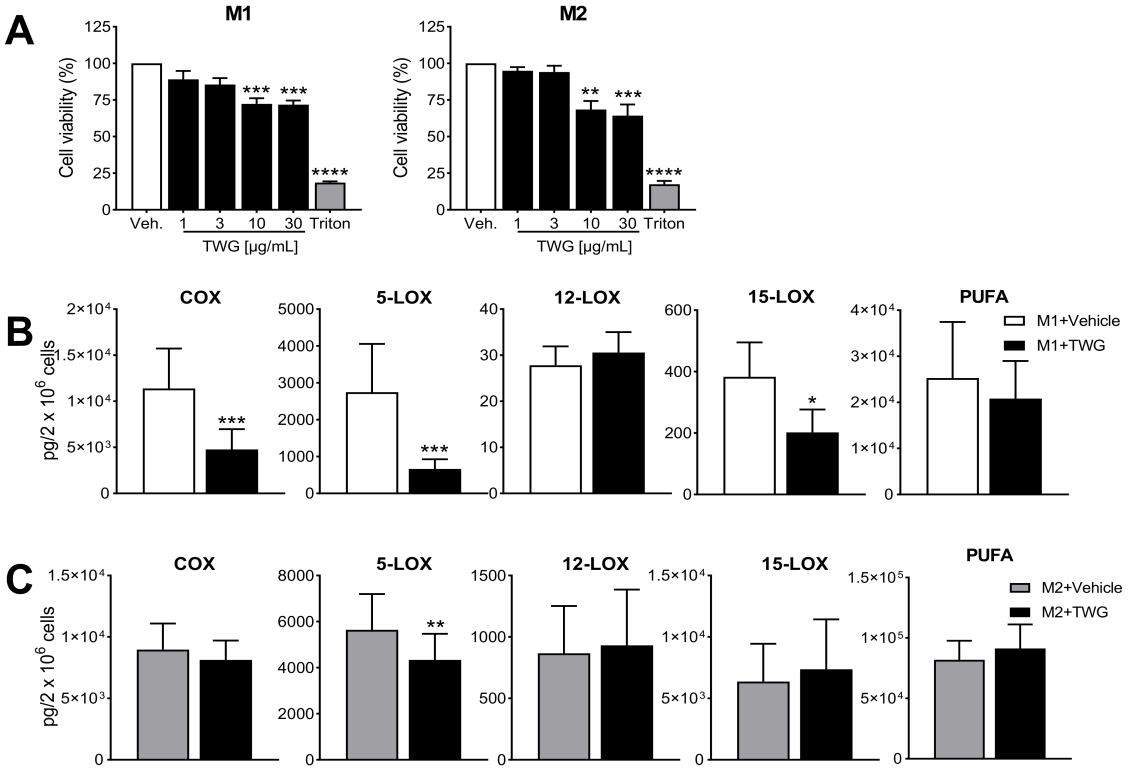

Figure 4. Effects of TWG on cell viability and LM pathway modulation during polarization of human M1- and M2-MDM. Human monocytes were differentiated towards M0 macrophages using GM-CSF or M-CSF for 6 days. These $M0_{GM\text{-}CSF}$ and $M0_{M\text{-}CSF}$ were pretreated for 15 min with test compounds or vehicle and then polarized for 48 h towards M1-MDM using LPS plus IFNγ or towards M2-MDM using IL-4, respectively. (**A**) TWG at the indicated concentrations, 10% triton X-100 or 0.1% DMSO as vehicle were added as test compounds and after 48 h polarization, cell viability was assessed by MTT assay. Data are means + S.E.M., $n = 3$ (both M1-MDM and M2-MDM), expressed as percentage of vehicle control (=100%); * $p < 0.05$, ** $p < 0.01$, *** $p < 0.001$, **** $p < 0.0001$, TWG vs. control group, one-way ANOVA for multiple comparisons with Bonferroni's correction. (**B**,**C**) TWG (1 µg/mL) or 0.1% DMSO as vehicle was added. After 48 h polarization, M1-MDM (**B**) and M2-MDM (**C**) were incubated with 1% *S. aureus*-conditioned medium (SACM) for 90 min. Produced LM were analyzed by UPLC-MS-MS in the supernatants. The sum of COX products, 5-LOX products, 12/15-LOX products and PUFA are expressed as pg/2 × 10^6 cells of TWG-treated and vehicle-treated cells. Data are means + S.E.M., $n = 5$ (both M1-MDM and M2-MDM). Data were log-transformed for statistical analysis, * $p < 0.05$, ** $p < 0.01$, *** $p < 0.001$, TWG vs. control group, paired *t*-test.

We then assessed if TWG affects the amounts of LM-biosynthetic enzymes during polarization; dexamethasone (DEX, 100 nM) was used as reference drug. Western blot analysis with M1-MDM showed no significant changes of $cPLA_2$, 5-LOX, COX-1 and COX-2 protein amounts by TWG, but mPGES-1 was significantly reduced; DEX suppressed COX-2 protein levels as expected without affecting other enzymes addressed (Figure 5A,B). In M2-MDM, TWG impaired the amounts of 5-LOX protein (yet no statistical significance was reached) without affecting 15-LOX-1 levels, while DEX caused the opposite: it slightly decreased the protein amounts of 15-LOX-1 without affecting those of 5-LOX (Figure 5C,D).

Biomolecules **2021**, *11*, 746

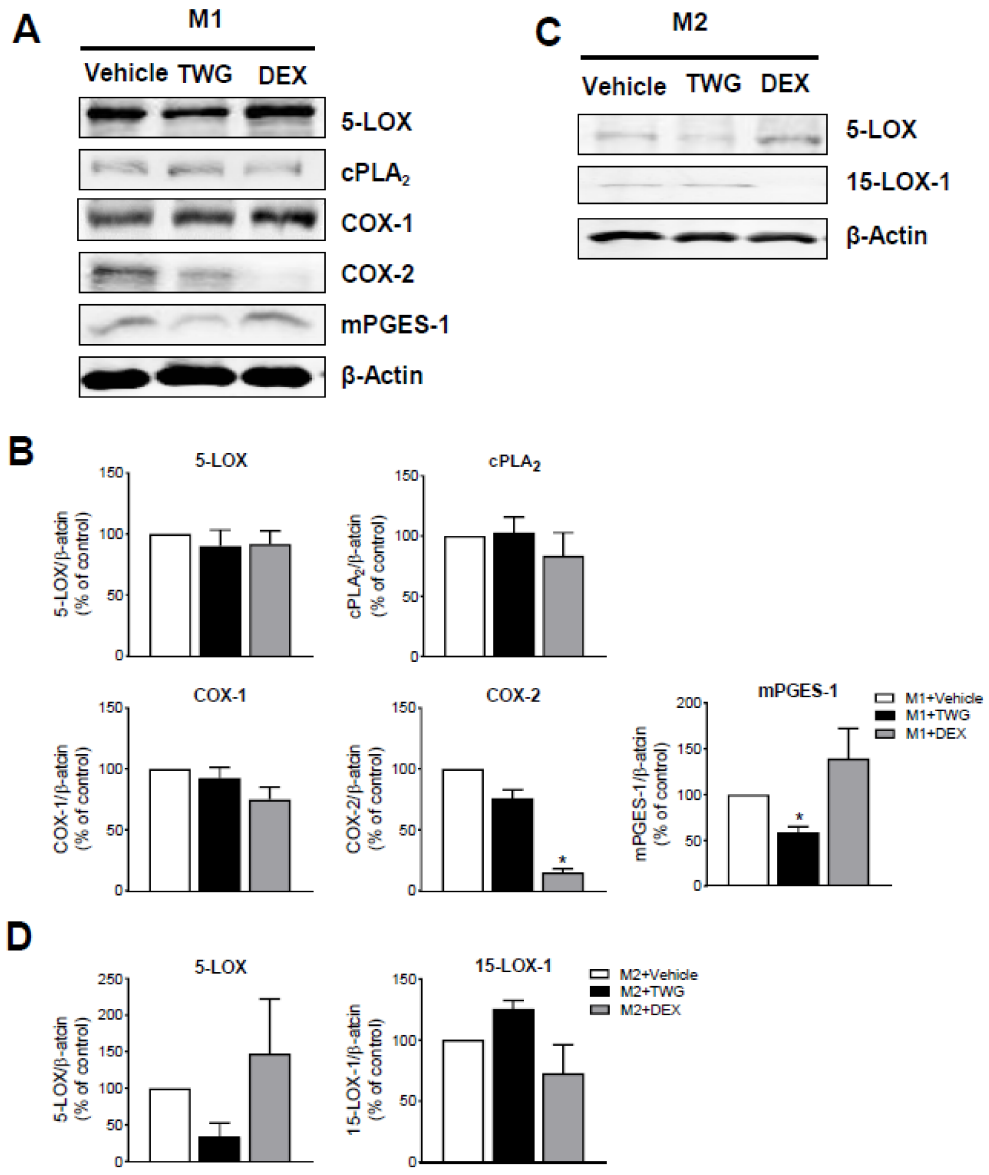

Figure 5. Effects of TWG on LM-biosynthetic enzyme expression during polarization of human M1- and M2-MDM. Human monocytes were differentiated towards M0 macrophages using GM-CSF or M-CSF for 6 days. These $M0_{GM\text{-}CSF}$ and $M0_{M\text{-}CSF}$ were pretreated for 15 min with 1 µg/mL TWG, 100 nM dexamethasone (DEX) or 0.1% DMSO as vehicle and then polarized for 48 h towards M1-MDM using LPS plus IFNγ or towards M2-MDM using IL-4, respectively. (**A**–**D**) Protein expression in lysates of M1-MDM (**A**,**B**) and M2-MDM (**C**,**D**) were analyzed by Western blotting. For densitometric analysis (**B**,**D**), 5-LOX, $cPLA_2$, COX-1, COX-2 and mPGES-1 proteins were normalized to β-actin; exemplary results (**A**,**C**) are shown as means + S.E.M. from $n = 3$ separate donors (both M1-MDM and M2-MDM). Values shown are percentages of DMSO controls (=100%). Densitometric ratios were used for statistical analysis, * $p < 0.05$, TWG vs. control group, one-way ANOVA and Dunnett's multiple comparisons test.

Table 3. Heatmap of LM produced by human M1- and M2-MDM and effects of TWG. $M0_{GM\text{-}CSF}$ and $M0_{M\text{-}CSF}$ MDM were pre-treated with 1 μg/mL TWG or 0.1% DMSO as vehicle for 15 min prior to polarization toward M1- or M2-MDM for 48 h by the addition of LPS/IFNγ (M1-MDM, left) and IL-4 (M2-MDM, right), respectively. Cells in PBS plus 1 mM $CaCl_2$ were then stimulated with 1% SACM for 90 min. LM from cells released into the supernatants were extracted and analyzed by UPLC-MS/MS. Data are means ± S.E.M., n = 5 (both M1-MDM and M2-MDM); n.d., not detectable.

							0·100·130								0·100·130
LM (M1)	**Vehicle**			**TWG**			**%**	**LM (M2)**	**Vehicle**			**TWG**			**%**
PGE_2	5670	±	2179	1961	±	986	**35**	PGE_2	650	±	123	774	±	158	**119**
PGD_2	90	±	30	39	±	14	**43**	PGD_2	85	±	19	107	±	26	**126**
$PGF_{2\alpha}$	303	±	81	155	±	51	**51**	$PGF_{2\alpha}$	238	±	70	259	±	93	**109**
TXB_2	5326	±	2078	2622	±	1158	**49**	TXB_2	7994	±	2012	6988	±	1382	**87**
11-HETE	288	±	116	107	±	49	**37**	11-HETE	279	±	54	288	±	63	**103**
11-HEPE	17	±	4	8	±	3	**48**	11-HEPE	24	±	5	27	±	8	**113**
5-HETE	1346	±	635	353	±	134	**26**	5-HETE	3886	±	1074	3008	±	805	**77**
5-HEPE	142	±	67	42	±	14	**29**	5-HEPE	483	±	153	411	±	130	**85**
$t\text{-}LTB_4$	378	±	204	74	±	34	**20**	$t\text{-}LTB_4$	310	±	74	222	±	36	**72**
LTB_4	880	±	406	194	±	81	**22**	LTB_4	967	±	301	695	±	199	**72**
7-HDHA	30	±	10	14	±	3	**47**	7-HDHA	59	±	10	44	±	7	**74**
17-HDHA	56	±	12	45	±	16	**81**	17-HDHA	792	±	205	802	±	266	**101**
15-HETE	319	±	99	150	±	58	**47**	15-HETE	5070	±	2588	5922	±	3409	**117**
15-HEPE	9	±	1	7	±	2	**75**	15-HEPE	510	±	282	642	±	397	**126**
14-HDHA	7	±	2	9	±	3	**128**	14-HDHA	211	±	79	214	±	77	**101**
12-HETE	18	±	2	18	±	2	**102**	12-HETE	560	±	259	606	±	314	**108**
12-HEPE	3	±	0	3	±	1	**114**	12-HEPE	96	±	49	112	±	63	**117**
PDX		n.d.			n.d.		-	PDX	2	±	1	2	±	1	**83**
RvD5		n.d.			n.d.		-	RvD5	25	±	8	19	±	7	**73**
AA	12,388	±	6118	9969	±	4046	**80**	AA	51,707	±	10,270	57,824	±	12,417	**112**
EPA	1926	±	674	1499	±	343	**78**	EPA	11,310	±	2601	13,841	±	3753	**122**
DHA	10,974	±	5412	9362	±	3783	**85**	DHA	18,926	±	3274	19,709	±	3947	**104**

3.5. TWG Suppresses Pro-Inflammatory Cytokines and Impacts Macrophage Polarization

Since TWG suppressed pro-inflammatory COX and 5-LOX pathways during polarization of M1-MDM, we studied if also pro-inflammatory cytokines are affected by TWG. In fact, TWG (1 μg/mL) blocked release of TNF-α and IL-1β in $M0_{M\text{-}CSF}$ MDM, similar as the reference drug DEX (Figure 6A). Finally, we investigated if TWG may affect macrophage polarization by assessing CD54 and CD80 as M1 markers and CD163 and CD206 as markers for M2 macrophages [27]. In agreement with the impaired capacities to generate pro-inflammatory LM (i.e., COX/5-LOX products) and cytokines (TNF-α and IL-1β) but increasing anti-inflammatory SPM, the markers for M1-MDM, i.e., CD54 and CD80 were significantly decreased but those for M2 (CD163, CD206) were slightly increased (Figure 6B). Together, TWG apparently impairs polarization of pro-inflammatory macrophages, characterized by suppression of pro-inflammatory cytokines and LM in M1, while promoting inflammation-resolving SPM in M2 macrophages.

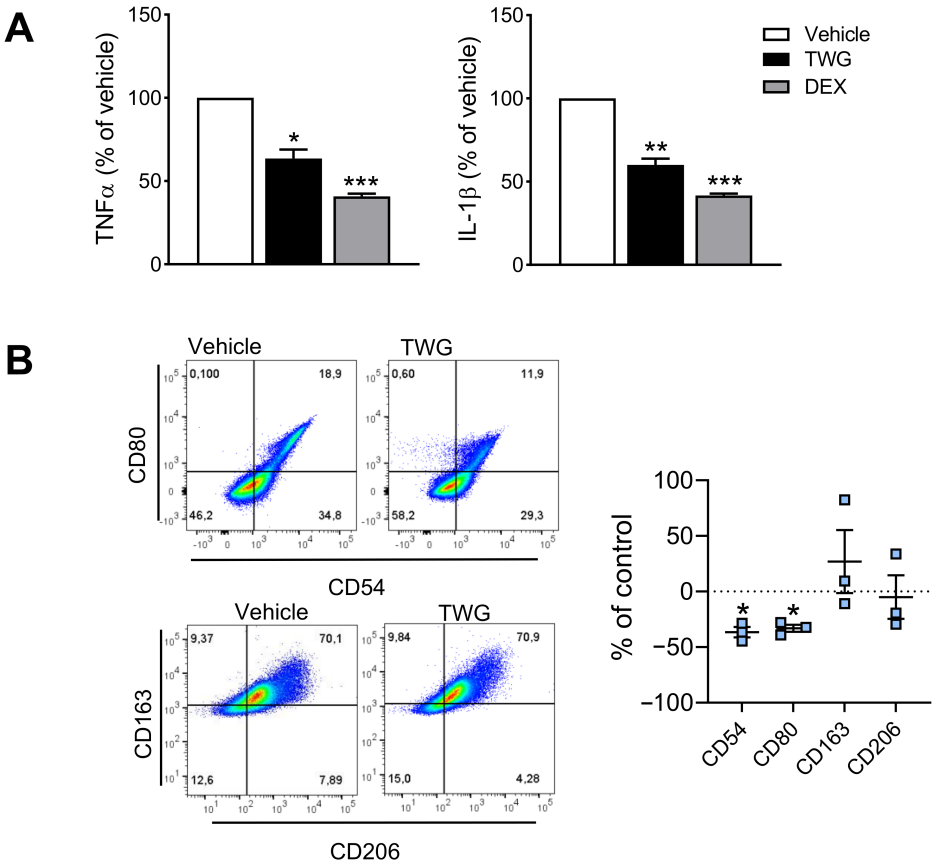

Figure 6. Effects of TWG on cytokine release and macrophage surface marker expression. Human monocytes were differentiated towards M0 macrophages using M-CSF for 6 days. (**A**) The $M0_{M\text{-}CSF}$ were then treated with 1 μg/mL TWG, 100 nM dexamethasone (DEX) or 0.1% DMSO as vehicle. After 20 h of stimulation with 100 ng/mL LPS, TNFα and IL-1β in the cell supernatants were analyzed by ELISA (presented as 100% of vehicle). Data are means + S.E.M., $n = 4$ separate experiments. Absolute values (shown in pg/10^6 cells) were log-transformed for statistical analysis, * $p < 0.05$, ** $p < 0.01$, *** $p < 0.001$, TWG vs. control group, one-way ANOVA and Dunnett's multiple comparisons test. (**B**) The $M0_{M\text{-}CSF}$ were then treated with 1 μg/mL TWG or 0.1% DMSO as vehicle. After 48 h, expression of the surface markers CD54 and CD80 (M1-like) as well as CD163 and CD206 (M2-like) among living $CD14^+$ cells was analyzed by flow cytometry; shown are representative pseudocolor dot plots of M1-like and M2-like surface markers. Mean fluorescence intensity (MFI) of each marker was determined. The change of the MFI from TWG-treated macrophages against the MFI of DMSO-treated cells (control) was calculated and given in % of control in scatter dot plots as single values and means ± S.E.M., $n = 3$. Statistics are calculated with raw data (MFI), * $p < 0.05$ TWG vs. control group, ratio paired *t*-test.

4. Discussion

Employing a comprehensive LM metabololipidomics approach we show here that TWG beneficially modulates the biosynthesis of LM networks in various innate immune cells, that is, suppressing the formation of pro-inflammatory 5-LOX products and thromboxane in M1-MDM and PMNL, but elevating the levels of inflammation-resolving SPM in anti-inflammatory M2-MDM. Our results suggest multiple points of attack of TWG in the LM networks, such as direct inhibition of 5-LOX activity and blocking 5-LOX expression, reducing the expression and activity of mPGES-1, and intriguingly, induction of the activation of 12/15-LOXs. Since these bioactions of TWG occurred at fairly low effective

concentrations (i.e., 1–30 μg/mL) that might be of pharmacological relevance, our data suggest that such beneficial switch from pro-inflammatory to pro-resolving LM production in innate immune cells may contribute to the anti-rheumatic features of TWG documented in numerous clinical trials of RA [16,18,19,21]. Future studies on how TWG modulates LM production in co-culture system that more closely recapitulate RA pathology such as human RA synovial fibroblasts or synovial cell lines with macrophages may sustain the direct link with RA.

Modulation of LM networks in innate immune cells by TWG has not been reported yet, to the best of our knowledge. Only one study was published that demonstrated suppression of PGE_2 formation due to inhibition of COX-2 expression [24]. Therefore, modulation of cellular LOX activities and thus LT and SPM formation by TWG are novel findings. We confirmed PGE_2 suppression using pro-inflammatory human M1-MDM that acquire substantial amounts of COX-2 protein during polarization [27]. When TWG was present during M1-MDM polarization, the cells showed reduced capacities to generate PGE_2, but also other COX-derived prostanoids such as PGD_2, $PGF_2\alpha$ and TXB_2 upon subsequent stimulation. Interestingly, we discovered that besides interference with COX-2, TWG also inhibited the induction of mPGES-1 protein and slightly impaired its enzymatic activity, which may sustain the reduced PGE_2 formation by TWG. Among the three PGE_2 synthases, mPGES-1 is an inducible isoform and strongly linked to inflammatory diseases [34], including RA [35].

While long-term treatment of M1-MDM with TWG clearly impaired formation of all COX-derived products possibly due to COX-2 suppression, short term exposure of these cells to TWG selectively blocked formation of only TXB_2, suggesting an inhibitory effect on the biosynthetic branch from PGH_2 towards TXA_2 [36] potentially by acting on TXAS. Surprisingly, TWG however failed to inhibit TXAS in a cell-free assay, excluding direct interaction of TWG with the enzyme. It is reasonable that TXAS inhibition requires the intracellular environment, for example to convert the responsible bioactive ingredient(s) into the active form, a phenomenon well-known for naturally occurring quinones (like celastrol), which act as potent inhibitors of 5-LOX as reduced hydroquinones [37].

Our study reveals 5-LOX as a direct target of TWG by using cell-free assays and inhibition of 5-LOX products in M1-MDM and in PMNL; 5-LOX and its products, especially LTB_4, have been implicated in RA as well [6,11], playing essential roles in the induction of pain and bone damage [38]. Also, 5-LOX was strongly expressed in lining and sublining macrophages, neutrophils and mast cells of RA synovial biopsies which was suppressed by glucocorticoid treatment [39]. Results of several studies underline the crucial role for LTB_4 and its receptor BLT1 in the pathogenesis of inflammatory arthritis [40]. Therefore, the potent impairment of LT formation in pro-inflammatory M1-MDM and PMNL due to 5-LOX inhibition may reasonably contribute to amelioration of RA by TWG treatment. This is also supported by our recent finding that the pentacyclic triterpenoid quinone methide celastrol, as major bioactive TWG constituent [23], potently inhibits 5-LOX in cell-free and cell-based assays at 0.1 to 1 μM [26]. Our RP-HPLC analysis and calculation revealed a celastrol content of 0.158% in TWG, implying that at the IC_{50} of 2.9 μg/mL TWG for 5-LOX, 0.0044 μg/mL or ~0.1 μM celastrol is present, which fits to the reported IC_{50} of 0.19 μM for celastrol under the same 5-LOX assay conditions [26].

Although our results are in favor of beneficial properties of TWG for treatment of RA, the well-known toxicity of TWG observed in clinical trials is still a concern [18,19]. We have carefully considered the issue of potential cytotoxicity and thus avoided the use of high concentrations of TWG, i.e., $\leq$30 μg/mL in short-term and 1 μg/mL in long-term incubations, along with exclusion of cytotoxic effects under the experimental conditions that we employed.

We suggest that promoting a switch from pro-inflammatory LTs and PGs towards inflammation-resolving SPM by smart manipulation of LM networks using TWG might a beneficial strategy for RA treatment. In contrast to LTs and PGs that initialize and maintain persistent and excessive inflammation-promoting various inflammatory pathologies [1,2],

the SPM are anti-inflammatory immunoresolvents and promote the resolution of inflammation leading to tissue repair and return to homeostasis [3,9,41]. Recent studies indicated that RA may arise from a decreased ability of the immune response to engage resolution programs that terminate inflammation and prevent chronicity [15]. Experimental models of delayed or non-resolving joint inflammation showed that SPM, i.e., RvD3, were downregulated [42]. In arthritic patients, synovial levels of RvE2 correlated with decreased joint pain [43]. Recently, SPM levels in peripheral blood of RA patients were linked with both DMARD responsiveness and disease pathotype [44] and strategies to increase SPM production have been shown to be connected with decreased joint inflammation and promotion of joint protection [45]. Intriguingly, exposure of M2-MDM to 30 µg/mL TWG caused massive induction of 12-/15-LOX product formation including the biosynthesis of SPM. Note that in contrast to reduced capacities of MDM to generate COX and 5-LOX products upon long-term treatment with TWG, the remedy did not impair the ability to form 12/15-LOX-derived LM. How such potent 12-/15-LOX activation is induced by TWG remains to be investigated but might be again caused by celastrol that induced SPM formation in M2-MDM at 1 µM [26], the calculated celastrol concentration present in 30 µg/mL TWG.

Besides celastrol, other bioactive ingredient(s) contained in TWG might be responsible for the observed actions on LM pathways, especially related to the suppression of the expression of the LM biosynthetic enzymes COX-2, mPGES-1 and 5-LOX. The diterpenoid triepoxide triptolide is another major constituent of TwHF with glucocorticoid-like properties that mediates many of the pharmacological actions and the anti-rheumatic activity of TWG [23]. Studies on celastrol and triptolide with focus on modulation of expression of LM pathways under long-term conditions are currently ongoing in our laboratory.

Taken together, TWG causes beneficial modulation of LM biosynthesis in prime innate immune cells by suppressing pro-inflammatory PG and LT pathways via multiple points of attack and by promoting SPM formation. In view of the well-established detrimental impact of PG and LT in RA pathology on one hand and the beneficial features of SPM on the other, our findings may help to explain the ameliorating effects of TWG in RA treatment and encourage future evaluation of the efficacy and safety of such remedies.

Supplementary Materials: The following are available online at https://www.mdpi.com/article/10.3390/biom11050746/s1: Supplementary Figure S1: Chromatograms of the RP-HPLC analysis of TWG and determination of celastrol.

Author Contributions: Conceptualization, S.P., D.F., X.C. and O.W., methodology, K.Z., P.M.J., R.K.H., L.K.P., and A.W.; investigation, K.Z., P.M.J., R.K.H., L.K.P., and A.W.; writing—original draft preparation, O.W.; writing—review and editing, O.W., S.P., and D.F. All authors have read and agreed to the published version of the manuscript.

Funding: This research was funded by the Deutsche Forschungsgemeinschaft (DFG, German Research Foundation)—project-ID 316213987—SFB 1278 PolyTarget (project C02) and—project-ID 239748522—SFB 1127 ChemBioSys (project A04), and by the Free State of Thuringia and the European Social Fund (2019 FGR 0095).

Institutional Review Board Statement: Not applicable.

Informed Consent Statement: Not applicable.

Data Availability Statement: The data presented in this study are available on reasonable request from the corresponding author. The data are not publicly available due to privacy.

Acknowledgments: The authors thank Petra Wiecha, Katrin Fischer, Alrun Schumann and Heidi Traber for expert technical assistance.

Conflicts of Interest: The authors declare no conflict of interest.

References

1. Calder, P.C. Eicosanoids. *Essays Biochem.* **2020**, *64*, 423–441. [CrossRef] [PubMed]
2. Funk, C.D. Prostaglandins and Leukotrienes: Advances in Eicosanoid Biology. *Science* **2001**, *294*, 1871–1875. [CrossRef] [PubMed]
3. Serhan, C.N. Pro-resolving lipid mediators are leads for resolution physiology. *Nature* **2014**, *510*, 92–101. [CrossRef] [PubMed]

4. Calder, P.C. Polyunsaturated fatty acids and inflammation. *Prostaglandins Leukot. Essent. Fat. Acids* **2006**, *75*, 197–202. [CrossRef]
5. Dennis, E.A.; Norris, P.C. Eicosanoid storm in infection and inflammation. *Nat. Rev. Immunol.* **2015**, *15*, 511–523. [CrossRef]
6. Rådmark, O.; Werz, O.; Steinhilber, D.; Samuelsson, B. 5-Lipoxygenase, a key enzyme for leukotriene biosynthesis in health and disease. *Biochim. Biophys. Acta Mol. Cell Biol. Lipids* **2015**, *1851*, 331–339. [CrossRef]
7. Bannenberg, G.; Serhan, C.N. Specialized pro-resolving lipid mediators in the inflammatory response: An update. *Biochim. Biophys. Acta Mol. Cell Biol. Lipids* **2010**, *1801*, 1260–1273. [CrossRef]
8. Chiang, N.; Serhan, C.N. Specialized pro-resolving mediator network: An update on production and actions. *Essays Biochem.* **2020**, *64*, 443–462. [CrossRef]
9. Serhan, C.N.; Levy, B.D. Resolvins in inflammation: Emergence of the pro-resolving superfamily of mediators. *J. Clin. Investig.* **2018**, *128*, 2657–2669. [CrossRef]
10. Scott, D.L.; Wolfe, F.; Huizinga, T.W. Rheumatoid arthritis. *Lancet* **2010**, *376*, 1094–1108. [CrossRef]
11. Hoxha, M. A systematic review on the role of eicosanoid pathways in rheumatoid arthritis. *Adv. Med. Sci.* **2018**, *63*, 22–29. [CrossRef]
12. Aletaha, D.; Smolen, J.S. Diagnosis and Management of Rheumatoid Arthritis: A Review. *JAMA* **2018**, *320*, 1360–1372. [CrossRef]
13. Crofford, L.J. Use of NSAIDs in treating patients with arthritis. *Arthritis Res. Ther.* **2013**, *15*, 1–10. [CrossRef]
14. Rainsford, K. Anti-Inflammatory Drugs in the 21st Century. *Alzheimer's Disease* **2007**, *42*, 3–27. [CrossRef]
15. Perretti, M.; Cooper, D.; Dalli, J.; Norling, L.V. Immune resolution mechanisms in inflammatory arthritis. *Nat. Rev. Rheumatol.* **2017**, *13*, 87–99. [CrossRef]
16. Wang, J.; Chen, N.; Fang, L.; Feng, Z.; Li, G.; Mucelli, A.; Zhang, X.; Zhou, X. A Systematic Review about the Efficacy and Safety of Tripterygium wilfordii Hook.f. Preparations Used for the Management of Rheumatoid Arthritis. *Evid. Based Complement. Alternat. Med.* **2018**, *2018*, 1567463.
17. Goldbach-Mansky, R.; Wilson, M.; Fleischmann, R.; Olsen, N.; Silverfield, J.; Kempf, P.; Kivitz, A.; Sherrer, Y.; Pucino, F.; Csako, G.; et al. Comparison of Tripterygium wilfordii Hook F versus sulfasalazine in the treatment of rheumatoid arthritis: A randomized trial. *Ann. Intern. Med.* **2009**, *151*, 229–240. [CrossRef]
18. Zhou, Y.-Y.; Xia, X.; Peng, W.-K.; Wang, Q.-H.; Peng, J.-H.; Li, Y.-L.; Wu, J.-X.; Zhang, J.-Y.; Zhao, Y.; Chen, X.-M.; et al. The Effectiveness and Safety of Tripterygium wilfordii Hook. F Extracts in Rheumatoid Arthritis: A Systematic Review and Meta-Analysis. *Front. Pharmacol.* **2018**, *9*, 356. [CrossRef]
19. Zheng, W.; Mei, Y.; Chen, C.; Cai, L.; Chen, H. The effectiveness and safety of Tripterygium wilfordii glycosides combined with disease-modifying anti-rheumatic drugs in the treatment of rheumatoid arthritis: A systematic review and meta-analysis of 40 randomized controlled trials. *Phytother. Res.* **2020**. [CrossRef]
20. Lv, Q.-W.; Zhang, W.; Shi, Q.; Zheng, W.-J.; Li, X.; Chen, H.; Wu, Q.-J.; Jiang, W.-L.; Li, H.-B.; Gong, L.; et al. Comparison of Tripterygium wilfordii Hook F with methotrexate in the treatment of active rheumatoid arthritis (TRIFRA): A randomised, controlled clinical trial. *Ann. Rheum. Dis.* **2015**, *74*, 1078–1086. [CrossRef]
21. Zhang, Y.; Mao, X.; Li, W.; Chen, W.; Wang, X.; Ma, Z.; Lin, N. Tripterygium wilfordii: An inspiring resource for rheumatoid arthritis treatment. *Med. Res. Rev.* **2021**, *41*, 1337–1374. [CrossRef] [PubMed]
22. Tang, Y.; Liu, Q.; Feng, Y.; Zhang, Y.; Xu, Z.; Wen, C.; Zhang, Y. Tripterygium Ingredients for Pathogenicity Cells in Rheumatoid Arthritis. *Front Pharmacol.* **2020**, *11*, 583171. [CrossRef] [PubMed]
23. Chen, S.-R.; Dai, Y.; Zhao, J.; Lin, L.; Wang, Y.; Wang, Y. A Mechanistic Overview of Triptolide and Celastrol, Natural Products from Tripterygium wilfordii Hook F. *Front. Pharmacol.* **2018**, *9*, 104. [CrossRef] [PubMed]
24. Tao, X.; Schulze-Koops, H.; Ma, L.; Cai, J.; Mao, Y.; Lipsky, P.E. Effects of Tripterygium wilfordii hook F extracts on induction of cyclooxygenase 2 activity and prostaglandin E2 production. *Arthritis Rheum.* **1998**, *41*, 130–138. [CrossRef]
25. Maekawa, K.; Yoshikawa, N.; Du, J.; Nishida, S.; Kitasato, H.; Okamoto, K.; Tanaka, H.; Mizushima, Y.; Kawai, S. The molecular mechanism of inhibition of interleukin-1beta-induced cyclooxygenase-2 expression in human synovial cells by Trip-terygium wilfordii Hook F extract. *Inflamm. Res.* **1999**, *48*, 575–581. [CrossRef]
26. Pace, S.; Zhang, K.; Jordan, P.M.; Bilancia, R.; Wang, W.; Börner, F.; Hofstetter, R.K.; Potenza, M.; Kretzer, C.; Gerstmeier, J.; et al. Anti-inflammatory celastrol promotes a switch from leukotriene biosynthesis to formation of specialized pro-resolving lipid mediators. *Pharmacol. Res.* **2021**, *167*, 105556. [CrossRef]
27. Werz, O.; Gerstmeier, J.; Libreros, S.; De La Rosa, X.; Werner, M.; Norris, P.C.; Chiang, N.; Serhan, C.N. Human macrophages differentially produce specific resolvin or leukotriene signals that depend on bacterial pathogenicity. *Nat. Commun.* **2018**, *9*, 1–12. [CrossRef]
28. Jordan, P.M.; Gerstmeier, J.; Pace, S.; Bilancia, R.; Rao, Z.; Borner, F.; Miek, L.; Gutierrez-Gutierrez, O.; Arakandy, V.; Rossi, A.; et al. Staphylococcus aureus-Derived al-pha-Hemolysin Evokes Generation of Specialized Pro-resolving Mediators Promoting Inflammation Resolution. *Cell Rep.* **2020**, *33*, 108247. [CrossRef]
29. Werner, M.; Jordan, P.M.; Romp, E.; Czapka, A.; Rao, Z.; Kretzer, C.; Koeberle, A.; Garscha, U.; Pace, S.; Claesson, H.; et al. Targeting biosynthetic networks of the proinflammatory and proresolving lipid metabolome. *FASEB J.* **2019**, *33*, 6140–6153. [CrossRef]
30. Fischer, L.; Szellas, D.; Radmark, O.; Steinhilber, D.; Werz, O. Phosphorylation- and stimulus-dependent inhibition of cellular 5-lipoxygenase activity by nonredox-type inhibitors. *FASEB J.* **2003**, *17*, 949–951. [CrossRef]

31. Albert, D.; Zundorf, I.; Dingermann, T.; Muller, W.E.; Steinhilber, D.; Werz, O. Hyperforin is a dual inhibitor of cyclooxy-genase-1 and 5-lipoxygenase. *Biochem. Pharmacol.* **2002**, *64*, 1767–1775. [CrossRef]
32. Koeberle, A.; Siemoneit, U.; Bühring, U.; Northoff, H.; Laufer, S.; Albrecht, W.; Werz, O. Licofelone Suppresses Prostaglandin E2 Formation by Interference with the Inducible Microsomal Prostaglandin E2 Synthase-1. *J. Pharmacol. Exp. Ther.* **2008**, *326*, 975–982. [CrossRef]
33. Gerstmeier, J.; Kretzer, C.; Di Micco, S.; Miek, L.; Butschek, H.; Cantone, V.; Bilancia, R.; Rizza, R.; Troisi, F.; Cardullo, N.; et al. Novel benzoxanthene lignans that favorably modulate lipid mediator biosynthesis: A promising pharmacological strategy for anti-inflammatory therapy. *Biochem. Pharmacol.* **2019**, *165*, 263–274. [CrossRef]
34. Koeberle, A.; Werz, O. Perspective of microsomal prostaglandin E2 synthase-1 as drug target in inflammation-related disorders. *Biochem Pharmacol* **2015**, *98*, 1–15. [CrossRef]
35. Kojima, F.; Matnani, R.G.; Kawai, S.; Ushikubi, F.; Crofford, L.J. Potential roles of microsomal prostaglandin E synthase-1 in rheumatoid arthritis. *Inflamm. Regen.* **2011**, *31*, 157–166. [CrossRef]
36. Nakahata, N. Thromboxane A2: Physiology/pathophysiology, cellular signal transduction and pharmacology. *Pharmacol. Ther.* **2008**, *118*, 18–35. [CrossRef]
37. Schaible, A.M.; Filosa, R.; Temml, V.; Krauth, V.; Matteis, M.; Peduto, A.; Bruno, F.; Luderer, S.; Roviezzo, F.; Di Mola, A.; et al. Elucidation of the molecular mechanism and the efficacy in vivo of a novel 1,4-benzoquinone that inhibits 5-lipoxygenase. *Br. J. Pharmacol.* **2014**, *171*, 2399–2412. [CrossRef]
38. Zheng, L.-X.; Li, K.-X.; Hong, F.-F.; Yang, S.-L. Pain and bone damage in rheumatoid arthritis: Role of leukotriene B4. *Clin. Exp. Rheumatol.* **2019**, *37*, 872–878.
39. Gheorghe, K.R.; Korotkova, M.; Catrina, A.I.; Backman, L.; af Klint, E.; Claesson, H.E.; Radmark, O.; Jakobsson, P.J. Ex-pression of 5-lipoxygenase and 15-lipoxygenase in rheumatoid arthritis synovium and effects of intraarticular glucocorticoids. *Arthritis Res. Ther.* **2009**, *11*, R83. [CrossRef]
40. Miyabe, Y.; Miyabe, C.; Luster, A.D. LTB 4 and BLT1 in inflammatory arthritis. *Semin. Immunol.* **2017**, *33*, 52–57. [CrossRef]
41. Serhan, C.N.; Gupta, S.K.; Perretti, M.; Godson, C.; Brennan, E.; Li, Y.; Soehnlein, O.; Shimizu, T.; Werz, O.; Chiurchiu, V.; et al. The Atlas of Inflammation Resolution (AIR). *Mol. Aspects Med.* **2020**, *74*, 100894. [CrossRef] [PubMed]
42. Arnardottir, H.H.; Dalli, J.; Norling, L.V.; Colas, R.A.; Perretti, M.; Serhan, C.N. Resolvin D3 Is Dysregulated in Arthritis and Reduces Arthritic Inflammation. *J. Immunol.* **2016**, *197*, 2362–2368. [CrossRef] [PubMed]
43. Barden, A.E.; Moghaddami, M.; Mas, E.; Phillips, M.; Cleland, L.G.; Mori, T.A. Specialised pro-resolving mediators of inflammation in inflammatory arthritis. *Prostaglandins Leukot Essent Fatty Acids* **2016**, *107*, 24–29. [CrossRef] [PubMed]
44. Gomez, E.A.; Colas, R.A.; Souza, P.R.; Hands, R.; Lewis, M.J.; Bessant, C.; Pitzalis, C.; Dalli, J. Blood pro-resolving mediators are linked with synovial pathology and are predictive of DMARD responsiveness in rheumatoid arthritis. *Nat. Commun.* **2020**, *11*, 1–13. [CrossRef]
45. Norling, L.V.; Headland, S.E.; Dalli, J.; Arnardottir, H.H.; Haworth, O.; Jones, H.R.; Irimia, D.; Serhan, C.N.; Perretti, M. Proresolving and cartilage-protective actions of resolvin D1 in inflammatory arthritis. *JCI Insight* **2016**, *1*, 85922. [CrossRef]

Supplementary Figure S1

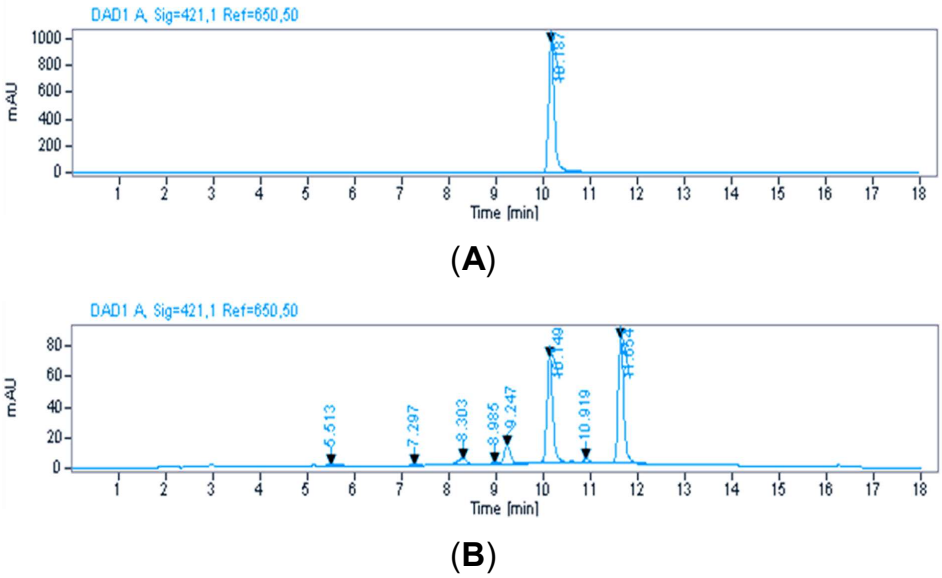

Figure S1 RP-HPLC Chromatograms of TWG and determination of celastrol

Chromatogram of celastrol reference substance (**A**) and of TWG (**B**) at 421 nm VIS detection. Under optimized conditions retention times of 10.168 ± 0.02 min for celastrol could be realized.

3.2 Manuscript II

Anti-inflammatory celastrol promotes a switch from leukotriene biosynthesis to formation of specialized pro-resolving lipid mediators

Simona Pace*, Kehong Zhang*, Paul M. Jordan, Rossella Bilancia, Wenfei Wang, Friedemann Börner, Robert K. Hofstetter, Marianna Potenza, Christian Kretzer, Jana Gerstmeier, Dagmar Fischer, Stefan Lorkowski, Nathaniel C. Gilbert, Marcia E. Newcomer, Antonietta Rossi, Xinchun Chen, Oliver Werz (2021)

Pharmacological Research 167 (2021) 105556

CS isolated from TwHF effectively reduces inflammation and has therapeutic potential for inflammatory disorders. However, the molecular mechanisms underlying the anti-inflammatory and inflammation-resolving features of CS are still unknown. Here, we found CS potently inhibits cellular formation of the 5-LOX-derived pro-inflammatory LM and simultaneously showed a direct inhibition of 5-LOX (IC_{50} = 0.19-0.49 μM). Short time exposed activated human PMNL and M1-MDM, as well as resting M2-MDM with CS were analyzed by UPLC-MS/MS. In the former two pro-inflammatory cell settings, CS (1 μM) potently suppressed 5-LOX-derived products without impairing the formation of products of 12-/15-LOXs as well as fatty acid substrate release. In human M2-MDM, CS remarkably induced the generation of 12-/15-LOX-derived LM including the SPM resolvin D5. Importantly, CS showed a strong reduction of LT formation and meanwhile promoted the production of 12-/15-LOX-derived LM and SPM in a zymosan-induced mouse model. Conclusively, CS promotes a switch from LT biosynthesis to the formation of SPM in vitro and in vivo, which may underlie the anti-inflammatory and inflammation-resolving properties of CS, offering an interesting pharmacological strategy for the treatment of inflammatory diseases.

Contribution (45%): Cell culture and performance of blood cell isolation, determination of cell viability, determination of COX-1/COX-2 activity in cell-free assays, determination of TXAS activity, 5-LOX activity in isolated enzyme and PMNL homogenates, competitive assay and wash out experiments, *E. coli* culture and SACM preparation, determination of LM formation by UPLC-MS/MS, analysis of data and preparation of graphs, statistical analysis, writing of the manuscript.

Manuscript II

Titel des Manuskriptes: Anti-inflammatory celastrol promotes a switch from leukotriene biosynthesis to formation of specialized pro-resolving lipid mediators

Autoren: Simona Pace*, Kehong Zhang*, Paul M. Jordan, Rossella Bilancia, Wenfei Wang, Friedemann Börner, Robert K. Hofstetter, Marianna Potenza, Christian Kretzer, Jana Gerstmeier, Dagmar Fischer, Stefan Lorkowski, Nathaniel C. Gilbert, Marcia E. Newcomer, Antonietta Rossi, Xinchun Chen, Oliver Werz

Bibliographische Informationen Published

Der Kandidat / Die Kandidatin ist (bitte ankreuzen)

☐ Erstautor/-in, ☒ Ko-Erstautor/-in, ☐ Korresp. Autor/-in, ☐ Koautor/-in.

Anteile (in %) der Autoren / der Autorinnen an der Publikation (anzugeben ab 20%)

Autor/-in	Konzeptionell	Datenanalyse	Experimentell	Verfassen des Manuskriptes	Bereitstellung von Material
Kehong Zhang	20%	50%	40%	20%	20%
Simona Pace	40%	20%	20%	40%	20%
Oliver Werz	40%			30%	
Others		30%	40%		60%
Total	100%	100%	100%	100%	100%

Pharmacological Research 167 (2021) 105556

Contents lists available at ScienceDirect

Pharmacological Research

journal homepage: www.elsevier.com/locate/yphrs

Anti-inflammatory celastrol promotes a switch from leukotriene biosynthesis to formation of specialized pro-resolving lipid mediators

Simona Pace [a,1], Kehong Zhang [a,b,1], Paul M. Jordan [a], Rossella Bilancia [a,c], Wenfei Wang [a,b], Friedemann Börner [a], Robert K. Hofstetter [a], Marianna Potenza [a,d], Christian Kretzer [a], Jana Gerstmeier [a], Dagmar Fischer [e], Stefan Lorkowski [f,h], Nathaniel C. Gilbert [g], Marcia E. Newcomer [g], Antonietta Rossi [c], Xinchun Chen [b,*], Oliver Werz [a,*]

[a] Department of Pharmaceutical/Medicinal Chemistry, Institute of Pharmacy, Friedrich Schiller University, Philosophenweg 14, D-07743 Jena, Germany
[b] Guangdong Provincial Key Laboratory of Regional Immunity and Diseases, Department of Pathogen Biology, Shenzhen University School of Medicine, Shenzhen 518000, China
[c] Department of Pharmacy, School of Medicine and Surgery, University of Naples Federico II, Via D. Montesano 49, I-80131 Naples, Italy
[d] Department of Pharmacy, University of Salerno, Via Giovanni Paolo II, 132, I-84084 Fisciano, Italy
[e] Department of Chemistry and Pharmacy, Pharmaceutical Technology, Friedrich-Alexander-Universität Erlangen-Nürnberg, Cauerstrasse 4, 91058 Erlangen, Germany
[f] Department of Nutritional Biochemistry and Physiology, Institute of Nutritional Sciences, Friedrich Schiller University, Dornburger Str. 25, 07743 Jena, Germany
[g] Department of Biological Sciences, Louisiana State University, Baton Rouge, LA, USA
[h] Competence Cluster for Nutrition and Cardiovascular Health (nutriCARD) Halle-Jena-Leipzig, Germany

ARTICLE INFO

Keywords:
Celastrol
Specialized pro-resolving mediators
5-lipoxygenase
Leukotriene
Inflammation

Chemical compounds studied in this article:
arachidonic acid (PubChem CID: 444899)
celastrol (PubChem CID: 122724)
celecoxib (PubChem CID: 2662)
dimethyl sulfoxide (PubChem CID: 679)
indomethacin (PubChem CID: 3715)
MK886 (PubChem CID: 3651377)
resolvin D5 (PubChem CID: 16061139)
zileuton (PubChem CID: 60490)
zymosan (PubChem CID: 64689)

ABSTRACT

The pentacyclic triterpenoid quinone methide celastrol (CS) from *Tripterygium wilfordii* Hook. F. effectively ameliorates inflammation with potential as therapeutics for inflammatory diseases. However, the molecular mechanisms underlying the anti-inflammatory and inflammation-resolving features of CS are incompletely understood. Here we demonstrate that CS potently inhibits the activity of human 5-lipoxygenase (5-LOX), the key enzyme in pro-inflammatory leukotriene (LT) formation, in cell-free assays with $IC_{50} = 0.19–0.49$ μM. Employing metabololipidomics using ultra-performance liquid chromatography coupled to tandem mass spectrometry in activated human polymorphonuclear leukocytes or M1 macrophages we found that CS (1 μM) potently suppresses 5-LOX-derived products without impairing the formation of lipid mediators (LM) formed by 12-/15-LOXs as well as fatty acid substrate release. Intriguingly, CS induced the generation of 12-/15-LOX-derived LM including the specialized pro-resolving mediator (SPM) resolvin D5 in human M2 macrophages. Finally, intraperitoneal pre-treatment of mice with 10 mg/kg CS strongly impaired zymosan-induced LT formation and simultaneously elevated the levels of SPM and related 12-/15-LOX-derived LM in peritoneal exudates, spleen and plasma in vivo. Conclusively, CS promotes a switch from LT biosynthesis to formation of SPM which may underlie the anti-inflammatory and inflammation-resolving effects of CS, representing an interesting pharmacological strategy for intervention with inflammatory disorders.

Abbreviations: AA, arachidonic acid; 5-HpETE, 5-hydro(pero)xy-eicosatetraenoic acid; 12-HHT, 12(S)-hydroxy-5-cis-8,10-trans-heptadecatrienoic acid; COX, cyclooxygenase; DHA, docosahexaenoic acid; EPA, eicosapentaenoic acid; FCS, fetal calf serum; IFN, interferon; IL, interleukin; LM, lipid mediator; LOX, lipoxygenase; LPS, lipopolysaccharide; LT, leukotriene; mPGES-1, microsomal prostaglandin E2 synthase 1; MDM, monocyte-derived macrophages; PBMC, peripheral blood mononuclear cells; PG, prostaglandin; PMNL, polymorphonuclear leukocytes; RP, reversed phase; SACM, *Staphylococcus aureus*-conditioned medium; SPE, solid phase extraction; SPM, specialized pro-resolving mediator; TwHF, *Tripterygium wilfordii Hook. F.*; TX, thromboxane; TXAS, thromboxane A synthase; UPLC-MS-MS, ultra-performance liquid chromatography coupled to tandem mass spectrometry.

* Corresponding authors.
E-mail addresses: simona.pace@uni-jena.de (S. Pace), kehong.zhang@uni-jena.de (K. Zhang), paul.jordan@uni-jena.de (P.M. Jordan), rossella.bilancia@unina.it (R. Bilancia), wenfei.wang@uni-jena.de (W. Wang), robert.klaus.hofstetter@uni-jena.de (R.K. Hofstetter), mpontenza@unisa.it (M. Potenza), Christian.kretzer@uni-jena.de (C. Kretzer), jana.gerstmeier@uni-jena.de (J. Gerstmeier), dagmar.fischer@fau.de (D. Fischer), stefan.lorkowski@uni-jena.de (S. Lorkowski), ngilbert@lsu.edu (N.C. Gilbert), newcomer@lsu.edu (M.E. Newcomer), antrossi@unina.it (A. Rossi), chenxinchun@szu.edu.cn (X. Chen), oliver.werz@uni-jena.de (O. Werz).
[1] Authors contributed equally.

https://doi.org/10.1016/j.phrs.2021.105556
Received 8 December 2020; Received in revised form 2 March 2021; Accepted 10 March 2021
Available online 31 March 2021

1. Introduction

Inflammation is a physiological protective event that occurs in the body in order to eliminate harmful agents, to repair damaged tissue, and to promote the return to homeostasis [1]. As persistent and uncontrolled inflammation can lead to chronic inflammatory disorders [2], coordinated orchestration of the inflammation process from the onset to the resolution phase is of major importance. Bioactive lipid mediators (LM) derived from the enzymatic conversion of free polyunsaturated fatty acids (i.e., arachidonic acid (AA), eicosapentaenoic acid (EPA) and docosahexaenoic acid (DHA)) by lipoxygenases (LOXs) and cyclooxygenases (COXs)) play key roles in the regulation of inflammation [3,4]. These LM are commonly divided into pro-inflammatory eicosanoids (prostaglandins (PGs), thromboxanes (TX) and leukotrienes (LTs)) that exacerbate inflammation and are mediators of pain, swelling, edema formation and smooth muscle cell contractions [5], and into specialized pro-resolving mediators (SPM) including lipoxins (LX), maresins (MaR), protectins (PD), and resolvins (Rv)) that actively promote termination of the inflammatory reaction and tissue repair [3,6].

For LT production, 5-LOX converts AA that is liberated from membrane phospholipids by the cytosolic phospholipase A_2 ($cPLA_2$) in a two-step reaction, yielding first 5-hydroperoxyeicosatetraenoic acid (5-HpETE) and then the epoxide LTA_4 [7]. Subsequently, LTA_4 can be hydrolyzed into LTB_4 by LTA_4 hydrolase or conjugated with glutathione to yield LTC_4 by LTC_4 synthase; the consecutive cleavage of the glutathione residue yields LTD_4 and then LTE_4 [7]. In the cell, translocation of 5-LOX to the nuclear envelope and interaction with the 5-LOX-activating protein (FLAP) is necessary to access AA as substrate for conversion to LTA_4 [7,8]. For PG formation, AA is transformed by COX-1/2 enzymes into PGH_2 [5]. This unstable intermediate is substrate for different isomerases that catalyze the formation of the bioactive prostanoids PGE_2, PGD_2, $PGF_{2\alpha}$, PGI_2 or TXA_2 [9]. For SPM biosynthesis AA, EPA and DHA are metabolized by the concerted action of the different LOXs (5-/12-/15-LOX) or CYP enzymes, which first results in mono-hydroxylated precursors (i.e., 7-/14-/17-HDHA, 12-/15-HETE or 18-HEPE) and subsequently in SPM by further introduction of hydroxy groups [3].

A common strategy to intervene with inflammation is the utilization of anti-inflammatory drugs that suppress the formation of pro-inflammatory mediators, namely non-steroidal anti-inflammatory drugs (NSAID) to inhibit COXs as well as the use of glucocorticoids. An alternative and more effective approach to counteract inflammation might be to suppress the formation of pro-inflammatory mediators and simultaneously increase the production of inflammation-resolving SPM in order to accelerate the return to homeostasis and minimize the development of side effects often evident with NSAID or glucocorticoid therapies that can block resolution of inflammation and act as immunosuppressants [4,10,11].

We here investigated how the natural compound celastrol (CS) from *Tripterygium wilfordii* Hook. F. (TwHF), also known as Thunder God Vine, affects inflammation by modulating the biosynthesis of LM. Extracts of TwHF have been largely used in Traditional Chinese Medicine for ameliorating symptoms of rheumatoid arthritis, and its efficacy against inflammatory and immune disorders is well documented [12]. Among the various bioactive ingredients isolated from TwHF extracts, CS has been intensively investigated for its anti-inflammatory and antioxidant properties [13,14]. Several reports showed that CS is able to ameliorate inflammation by acting through HSP90 or by reducing the production of interleukin (IL)-1β and IL-18 as well as by suppressing the NPL3 inflammasome [12–15], but the effect of CS on LM formation in inflammation remains still poorly explored. Hence, we here employed in vitro and in vivo models of inflammation with different stimuli in order to elucidate the ability of CS to modulate the biosynthesis of LM with crucial roles in inflammation.

2. Materials and methods

2.1. Materials

Solvents for reversed phase-high performance liquid chromatography (RP-HPLC) were obtained from Merck (Darmstadt, Germany). Ultrapure water was produced by a Sartorius Arium 611 UV water purification system (Göttingen, Germany). Celastrol (item number 70950), zileuton (10006967), celecoxib (10008672), arachidonic acid (90010), indomethacin (70270), Resolvin (10007280), and MK886 (21753) were supplied from Biomol GmbH (Hamburg, Germany). Zymosan A (Z4250) was purchased from Merck (Munich, Germany). Deuterated and non-deuterated LM standards for ultra-performance liquid chromatography-tandem mass spectrometry (UPLC-MS-MS) were purchased from Cayman Chemicals (Ann Arbor, MI).

2.2. Isolation of cells from human blood

Human leukocyte concentrates obtained from freshly withdrawn blood (16 I.E. heparin/mL blood by healthy adult volunteers) were provided by the Department of Transfusion Medicine at the University Hospital of Jena, Germany. The procedures were approved by the local ethical committee and were performed in accordance with the guidelines and regulations, an informed consent was obtained. As described elsewhere [16], human polymorphonuclear leukocytes (PMNL) and peripheral blood mononuclear cells (PBMC) were separated by a two-step procedure: i) sedimentation by dextran, and ii) density gradient centrifugation on lymphocyte separation medium (C-44010, Promocell, Heidelberg, Germany). Platelet-rich plasma was obtained from the supernatants after density gradient centrifugation, mixed with phosphate-buffered saline (PBS) pH 5.9 (3:2 v/v), centrifuged (2100×*g*, 15 min, room temperature), and the pelleted platelets were resuspended in PBS pH 5.9/0.9% NaCl (1:1, v/v). Washed platelets were finally resuspended in PBS pH 7.4 and 1 mM $CaCl_2$. For obtaining monocytes, PBMC were collected from the intermediate fraction after the gradient centrifugation and seeded in RPMI medium containing 5% heat-inactivated fetal calf serum (FCS), 2 mM *L*-glutamine, 100 U/mL penicillin and 100 µg/mL streptomycin in culture flasks (Greiner Bio-one, Nuertingen, Germany) for 1.5 h (37 °C, 5% CO_2). Adherent monocytes were then collected by scraping and resuspended in PBS. PMNL were isolated from the pelleted fraction after hypotonic lysis of erythrocytes [16].

2.3. Monocyte-derived macrophages (MDM): differentiation, polarization and incubation

In order to differentiate monocytes into macrophages, freshly isolated monocytes were kept at 37 °C in RPMI medium (supplemented with 10% FCS, 2 mM *L*-glutamine, 100 U/mL penicillin and 100 µg/mL streptomycin) containing 20 ng/mL GM-CSF or M-CSF (Peprotech, Hamburg, Germany) for 6 days. Polarization towards a M1 phenotype was obtained by stimulation of GM-CSF-treated macrophages ($M0_{GM\text{-}CSF}$) with 100 ng/mL lipopolysaccharide (LPS) and 20 ng/mL interferon (IFN)-γ (Peprotech, Hamburg, Germany) for 48 h, while M2 macrophages were obtained by addition of 20 ng/mL IL-4 to M-CSF-treated macrophages ($M0_{M\text{-}CSF}$) (Peprotech, Hamburg, Germany), as described [17]. Adherent M1 MDM (2×10^6 /mL) were pre-treated with CS (0.1 or 1 µM), MK886 (0.3 µM), celecoxib (5 µM) or vehicle (DMSO, 0.1%) for 15 min. Afterwards, 1% *Staphylococcus aureus* 6850 wt-conditioned medium (SACM) was added for 90 min at 37 °C in order to induce LM formation [18]. The group "vehicle (-)" was left untreated. The reaction was stopped by transferring supernatants (1 mL) containing released LM into 2 mL ice-cold MeOH. In another set of experiments, adherent M1 and M2 MDM were treated with CS (1 µM) with or without a mixture of EPA and DHA (3 µg/mL) for 180 min at 37 °C in order to induce LM formation. The group termed "DMSO" received only DMSO (0.1%) for

180 min, and the group "SACM" received 1% SACM plus 0.1% DMSO for 180 min. The reaction was stopped by transferring supernatants (1 mL) into 2 mL ice-cold MeOH. Experiments showed that the fraction of released LM clearly dominate (approx. 80–90%) the fraction of those remaining inside the cells. After addition of the deuterated LM standards (200 nM d8–5S-HETE, d4-LTB_4, d5-LXA_4, d5-RvD2, d4-PGE_2 and 10 μM d8-AA; Cayman Chemical/Biomol GmbH, Hamburg, Germany), samples were processed for LM analysis using UPLC-MS-MS as described below.

2.4. PMNL stimulation for lipid mediator formation

Immediately after isolation, PMNL were resuspended in PBS containing 1 mg/mL glucose and 1 mM $CaCl_2$ at a density of 5×10^6/mL. Cells were pre-treated with CS (0.1 and 1 μM) at 37 °C for 15 min. Then, LM biosynthesis was induced by the addition of *E. coli* (serotype O6:K2:H1, ratio 1:50). After 90 min, the reaction was stopped by the addition of 1 mL of ice-cold MeOH. The group "Vehicle (-)" was left untreated. After centrifugation of samples (1200×*g*, 5 min, 4 °C), the cell supernatants (2 mL) were transferred to new glass vials containing 1 mL of ice-cold MeOH and deuterated LM standards (200 nM d8–5S-HETE, d4-LTB_4, d5-LXA_4, d5-RvD2, d4-PGE_2 and 10 μM d8-AA; Cayman Chemical/Biomol GmbH, Hamburg, Germany), and the samples were processed for LM analysis using UPLC-MS-MS as described below.

2.5. Metabololipidomics analysis of lipid mediators

Samples obtained from incubated MDM and PMNL (see 2.3. and 2.4.) were kept at −20 °C for 60 min to allow protein precipitation. After centrifugation (1200×*g*, 4 °C, 10 min) acidified H_2O (8 mL) was added (final pH = 3.5) and samples were subjected to solid phase cartridges (Sep-Pak® Vac 6cc 500 mg/6 mL C18; Waters, Milford, MA) that had been equilibrated with 6 mL methanol and 2 mL H_2O before samples were loaded onto columns. After washing with 6 mL H_2O and then with 6 mL *n*-hexane, LM were eluted with 6 mL methyl formate. The samples were brought to dryness using an evaporation system (TurboVap LV, Biotage, Uppsala, Sweden) and resuspended in 100 μL methanol/water (50/50, v/v) for UPLC-MS-MS analysis. LM were analyzed with an Acquity™ UPLC system (Waters, Milford, MA, USA) and a QTRAP 5500 Mass Spectrometer (ABSciex, Darmstadt, Germany) equipped with a Turbo V™ Source and electrospray ionization. LM were eluted using an ACQUITY UPLC® BEH C18 column (1.7 μm, 2.1× 100 mm; Waters, Eschborn, Germany) at 50 °C with a flow rate of 0.3 mL/min and a mobile phase consisting of methanol-water-acetic acid of 42:58:0.01 (v/v/v) that was ramped to 86:14:0.01 (v/v/v) over 12.5 min and then to 98:2:0.01 (v/v/v) for 3 min [4]. The QTRAP 5500 was operated in negative ionization mode using scheduled multiple reaction monitoring (MRM) coupled with information-dependent acquisition. The scheduled MRM window was 60 s, optimized LM parameters were adopted [4], and the curtain gas pressure was set to 35 psi. The retention time and at least six diagnostic ions for each LM were confirmed by means of an external standard (Cayman Chemical/Biomol GmbH, Hamburg, Germany). Quantification was achieved by calibration curves for each LM. Linear calibration curves were obtained for each LM and gave r^2 values of 0.998 or higher. Additionally, the limit of detection for each targeted LM was determined [4].

2.6. Determination of 5-LOX product formation in cell-free assays

5-LOX was expressed in *E. coli* BL21 (DE3) transformed with pT35-LO plasmid and purified by affinity chromatography on an ATP-agarose column as previously described [19] and immediately used for 5-LOX activity assays. 5-LOX (0.5 μg) in PBS pH 7.4 containing EDTA (1 mM) was pre-incubated with test compounds (0.01, 0.03, 0.1, 0.3, 1 μM CS or vehicle (0.1% DMSO) or 3 μM zileuton). After 15 min, samples were pre-warmed for 30 s at 37 °C, and 2 mM $CaCl_2$ plus 20 μM AA were added to start 5-LOX product formation. For the "substrate competitivity assay" different concentrations of AA (2.5 – 5 – 10 – 20–40 μM) were added to start product formation. For determining 5-LOX product formation in cell homogenates, PMNL (5×10^6) were resuspended in 1 mL PBS containing 1 mM EDTA for 5 min at 4 °C and sonicated (4 × 10 s, 4 °C). PMNL homogenates were incubated with test compounds for 15 min at 4 °C, pre-warmed for 30 s at 37 °C and the reaction was started by addition of 2 mM $CaCl_2$ plus 20 μM AA. After 10 min at 37 °C, an equal volume (1 mL) of ice-cold methanol was added and formed 5-LOX products (all-trans isomers of LTB_4, LTB_4 and 5-H(p)ETE) were extracted. Briefly, 500 μL acidified PBS and 200 ng of internal PGB_1 standard were added and solid phase extraction was performed [20]. After elution with methanol, samples were analyzed by RP-HPLC using a C-18 Radial-PAK column (Waters, Eschborn, Germany) as previously reported [20].

In order to evaluate whether inhibition of 5-LOX by CS is reversible, purified 5-LOX (0.5 μg) was pre-incubated with CS at 2 and 0.2 μM, where the sample with 2 μM CS was kept as is or 10-fold diluted to a final compound concentration of 0.2 μM on ice for 20 min. Then, 2 mM $CaCl_2$ plus 20 μM AA was added and samples were incubated at 37 °C. The reaction was terminated after 10 min and 5-LOX products were extracted and analyzed via RP-HPLC as described for intact PMNL.

2.7. Determination of microsomal prostaglandin E2 synthase-1 activity in a cell-free assay

The microsomal prostaglandin E_2 synthase (mPGES)-1 was obtained from microsomes of A549 cells that had been stimulated by IL-1β (2 ng/mL) over 48 h, as described elsewhere [21]. A549 cells were sonicated and the lysate was first centrifuged at 10,000×*g* for 10 min, and then at 174,000×*g* for 1 h at 4 °C. The pelleted microsomal fraction was then resuspended into 1 mL of homogenization buffer (0.1 M potassium phosphate buffer, pH 7.4, 1 mM phenylmethanesulfonyl fluoride, 60 μg/mL soybean trypsin inhibitor, 1 μg/mL leupeptin, 2.5 mM glutathione, and 250 mM sucrose). Microsomes were diluted in potassium phosphate buffer (0.1 M, pH 7.4) containing glutathione (2.5 mM) and placed into a 96-well plate (100 μL). Afterwards, CS (1 μM) or vehicle (0.1% DMSO) were added for 15 min on ice. The reaction was started after addition of PGH_2 (20 μM) and stopped after 1 min using 100 μL of a stop solution (40 mM $FeCl_3$, 80 mM citric acid, and 10 μM of 11β-PGE_2 as internal standard). PGE_2 and 11β-PGE_2 were extracted by solid phase extraction using acetonitrile as eluent, and PGE_2 formation was quantified by RP-HPLC, as previously described [22]. MK886 (10 μM) was used as positive control (residual mPGES-1 activity = 17.6 ± 1.5%).

2.8. Determination of COX-1 and COX-2 activities in cell-free assays

Inhibition of COX activity was assayed by using purified ovine COX-1 and recombinant human COX-2, respectively, as described [23]. Briefly, the enzymes were diluted in Tris buffer (100 mM, pH 8) supplemented with glutathione (5 mM), EDTA (100 μM) and hemoglobin (5 μM) to a final concentration of 50 U/mL (COX-1) or 20 U/mL (COX-2). After pre-incubation with test compounds or vehicle (0.1% DMSO) for 5 min at RT, the samples were pre-warmed for 30 s at 37 °C, and the reactions were started by addition of 5 μM AA (COX-1) or 2 μM AA (COX-2). After 5 min at 37 °C the reactions were stopped by addition of one volume of ice-cold methanol. Solid phase extraction was performed as described above (chapter 2.5.) after addition of 200 ng PGB_1 as internal standard, and COX product formation was determined by analysis of 12-hydroxyheptadecatrienoic acid (12-HHT) formation.

2.9. Determination of thromboxane synthase activity

Freshly isolated platelets were resuspended in ice-cold PBS pH 7.4 containing 1 mM EDTA (1.6×10^9 cells/mL) and sonicated (4 × 10 s) on ice. Platelet homogenates (1 mL) were pre-incubated with CS (1 μM) or vehicle for 15 min at 4 °C. The reaction was initiated by addition of 20

μM PGH_2 for 1 min at 4 °C and terminated by the addition of ice-cold MeOH (2 mL). Then, samples were processed as described below for LM analysis and thromboxane A synthase (TXAS) activity was determined by UPLC-MS-MS and evaluated as pg of TXB_2 formed.

2.10. Cell viability

Cell viability was evaluated in PMNL and $M0_{GM\text{-}CSF}$ MDM. Cells (2×10^6 cells/mL) were incubated with different concentrations of CS (0.1, 0.3, 1, 3, 10 μM) or with vehicle for 90 min (PMNL) or 180 min ($M0_{GM\text{-}CSF}$-MDM) at 37 °C. Cell viability was assessed by trypan blue staining using automated cell-counter (VI-CELLTM XR, Beckman Coulter).

2.11. Subcellular localization of 5-LOX and 15-LOX-1 by immunofluorescence microscopy

M0-MDM (0.8×10^6 cells) were seeded onto glass coverslips in a 12-well plate and polarized to M1 or M2 MDM for 48 h. Cells were washed and then stimulated in PBS containing 1 mM $CaCl_2$ and 0.5 mM $MgCl_2$ with 1 μM CS or vehicle (0.1% DMSO) or 1% SACM (as positive control [18]) for 180 min at 37 °C. Cells were then fixed using 4% paraformaldehyde solution. Acetone (3 min, 4 °C) and 0.25% triton X-100 (10 min, room temperature) were used for permeabilization before blocking with normal goat serum (10%, 50062Z, Thermo Fisher Scientific). Samples of M1 MDM were incubated with mouse monoclonal anti-5-LOX antibody, 1:100 (610694, BD Biosciences) and rabbit polyclonal anti-FLAP antibody, 5 μg/mL (ab85227, Abcam, Cambridge, UK Abcam) at 4 °C overnight. Samples of M2 MDM were incubated with mouse monoclonal anti-15-LOX-1 antibody, 1:100 (ab119774, Abcam, Cambridge, UK) and rabbit anti-5-LOX antibody, 1:100 (1550 AK6, provided by Dr. Olof Radmark, Karolinska Institutet, Stockholm, Sweden) overnight at 4 °C. 5-LOX, FLAP and 15-LOX-1 were stained with the fluorophore-labeled secondary antibodies; Alexa Fluor 488 goat anti-rabbit IgG (H + L), 1:500 (A11034, Thermo Fisher Scientific) and Alexa Fluor 555 goat anti-mouse IgG (H + L); 1:500 (A21424, Thermo Fisher Scientific). Nuclear DNA was stained with ProLong Gold Antifade Mountant with DAPI (15395816, Thermo Fisher Scientific). Samples were analyzed by a Zeiss Axiovert 200 M microscope, and a Plan Neofluar ×40/1.30 Oil (DIC III) objective (Carl Zeiss, Jena, Germany). An AxioCam MR camera (Carl Zeiss) was used for image acquisition.

2.12. Ca^{2+} assay

M2 MDM were pre-stained with 1 μM Fura-2/AM (Thermo Fisher Scientific) for 30 min at 37 °C in the dark. Cells were resuspended in modified Krebs-HEPES buffer (135 mM NaCl, 5 mM KCl, 1 mM $MgSO_4$ x $7H_2O$, 0.4 mM KH_2PO_4, 5.5 mM glucose, and 20 mM HEPES; pH 7.4) containing 0.1% BSA at a density of 1.25×10^6/mL. Then, 200 μL of the cell suspension was transferred into a 96-well plate. After 10 min, $CaCl_2$ was added to a final concentration of 1 mM. CS (1 μM), fMLP (1 μM) or vehicle (1% DMSO) were added by automated pipetting and the signal was monitored in a thermally (37 °C) controlled NOVOstar microplate reader (BMG Labtechnologies GmbH); emission at 510 nm, excitation at 340 nm (Ca^{2+}-bound Fura-2) and 380 nm (free Fura-2). After cell lysis with triton X-100 (1%), the maximal fluorescence signals were monitored (=100%) and after chelating Ca^{2+} with 20 mM EDTA, the minimal fluorescence signals (=0%) were recorded. $[Ca^{2+}]_i$ was calculated according to [24].

2.13. Docking of celastrol into Stable-5-LOX

CS was downloaded from pubchem and geometry restraints were checked in Phenix.elbow [25,26]. Stable-5-LOX with 3-*O*-acetyl-11-keto-β-boswellic acid (AKBA) in an allosteric site [27] was fetched from the Protein Data Bank (PDB; 6NCF, chain B). Preparation for docking was performed in Chimera; the solvent was deleted and hydrogen atoms and charges were added to the protein [28]. The Autodock Vina routine was performed through Chimera [29]. Restraints of 10 binding modes with the highest exhaustiveness and a maximum energy difference of 3 kcal/mol were utilized. Binding was performed using different target search volumes including options of the whole protein or focused searches in the binding cleft of AKBA, which is located between the membrane-binding and catalytic domains of Stable-5-LOX. The docking of CS to Stable-5-LOX was performed more than 5 times with different search volumes. For each docking routine, CS was placed in the AKBA allosteric site within the top three scores.

2.14. Animals

Adult (6–8 weeks) male CD1 mice (Charles River, Calco, Italy) were housed at the animal care facility of the Department of Pharmacy of the University of Naples "Federico II" and kept under controlled environment (i.e., temperature 21 ± 2 °C and humidity 60 ± 10%) and provided with normal chow and water ad libitum. Prior to experiments, mice were allowed to acclimate for 4 days and were subjected to 12 h light/dark schedule. Treatments were conducted during the light phase. The experimental procedures were approved by the Italian Ministry and carried out in accordance with the EU Directive 2010/63/EU and the Italian DL 26/2014 for animal experiments and in compliance with the ARRIVE guidelines and Basel declaration including the 3 R concept.

2.15. Zymosan-induced peritonitis in mice

Peritonitis in male mice was induced as described before [30]. Mice (n = 6/group) received intraperitoneally (i.p.) 10 mg/kg CS or the vehicle (2% DMSO in saline) in 0.5 mL saline/mouse 30 min prior to induction of peritonitis by injection of zymosan (1 mg/mouse in 0.5 mL saline, i.p.). After 2 h, mice were euthanized in a saturated CO_2-atmosphere and blood, spleen and peritoneal exudates were collected for further analysis. Peritoneal lavage was obtained by washing the peritoneal cavity with 3 mL ice-cold PBS and subsequent centrifugation (18, 000×*g*, 5 min, 4 °C). Blood (0.7–0.9 mL) was obtained by intracardiac puncture through the insertion of 1 mL syringe with a needle of 22 gauge (Carl Roth GmbH & Co. KG, Karlsruhe, Germany) using citrate as anticoagulant (3.8% (w/v)), immediately after killing mice with CO_2. Plasma was obtained by centrifugation of the blood at 800×*g* at 4 °C for 10 min. Spleens were weighted and approx. 30–40 mg were homogenized in ice-cold MeOH (20 μL/mg tissue). Cell-free supernatants of the exudates, plasma and spleens were immediately frozen and stored for the analysis of LM levels via UPLC-MS-MS as described below.

3. Statistical analysis

Data are shown as mean ± S.E.M. of the indicated number of independent experiments which is given in the figure legends for each and every figure panel. For animal experiments n = 6 mice in each group were examined. Statistical analysis and graphs were made by using Graphpad Prism 8 software. Paired *t*-test was used to analyze experiments with PMNL and macrophages, while unpaired *t*-test was used for animal experiments, and one-way ANOVA was used for the cytotoxicity assessment.

4. Results

4.1. Celastrol inhibits 5-LOX product formation in pro-inflammatory experimental cellular settings

Human PMNL are a major source for pro-inflammatory 5-LOX products in the body [8]. To investigate whether CS inhibits 5-LOX product formation, freshly isolated human PMNL were pre-treated with CS (0.1 or 1 μM) for 15 min and then challenged with pathogenic E. *coli* (O6:K2:H1 1:50, 90 min). Exposure of PMNL to *E. coli* induced

marked formation of 5-LOX [31] and 12-LOX products (analyzed by LM metabololipidomics using UPLC-MS-MS [4,17]) when compared to the unstimulated control group "vehicle (-)", while among the COX products, *E. coli* increased only TXB_2 formation (Fig. 1A). The marked formation of 12-HETE likely originates from platelets that express abundant 12-LOX and that contaminate PMNL preparations due to strong adherence, as reported by others before [32]. Pre-treatment of PMNL with 1 μM CS prior to *E. coli* challenge significantly inhibited 5-LOX product formation independently from the fatty acid substrates (i.e., LTs and 5-HETE from AA, 7-HDHA from DHA, and 5-HEPE from EPA; Fig. 1A and B). Of note, CS (0.1 and 1 μM) caused shunting towards the conversion of AA by COX resulting in increased PG formation (PGE_2, PGD_2, and $PGF_{2\alpha}$) while in contrast, CS markedly reduced the formation of TXB_2 (Fig. 1A). Moreover, CS (1 μM) increased formation of 12-LOX products (12-HETE, 12-HEPE and 14-HDHA; Fig. 1A and B). These data suggest that CS inhibits 5-LOX product formation and seemingly induces the biosynthesis of 12-LOX and COX products, except TXB_2.

Macrophages are key players in the innate immune response where the M1 phenotype acts as promoter of the inflammatory response by producing pro-inflammatory cytokines and eicosanoids [17,33]. Since exposure of M1 MDM to *S. aureus*-conditioned medium (SACM) causes substantial formation of a broad spectrum of pro-inflammatory LM [18], we used 1% SACM to stimulate human M1 MDM for 90 min to induce LM formation. Indeed, stimulation of M1 MDM with SACM generated LM derived from COX and 5-/12-/15-LOX and caused liberation of free fatty acid substrates (Fig. 1C), as found before [18]. Notably, the M1 MDM used in these experiments produced relatively high amounts of LTB_4 and 5-HETE even in the absence of a stimulus, although with marked variability between donors, suggesting that some M1 preparations were rich in 5-LOX/FLAP and/or became pre-activated prior stimulation. Pre-treatment of M1 MDM with 0.1 or 1 μM CS inhibited formation of 5-LOX products at both concentrations with more marked effects at 1 μM (Fig. 1C and D). It appeared that CS was somewhat more efficient to suppress 5-LO activity in PMNL (Fig. 1A and B) as compared to M1 (Fig. 1C and D). As noticed in PMNL, shunting phenomena of AA conversion by COX with consequent elevated PGs were evident also in M1 MDM with a trend in the upregulation of also 12- and 15-LOX product formation (Fig. 1C and D). The reference inhibitors MK886 (0.3 μM) and celecoxib (5 μM) reduced the formation of 5-LOX and COX products in M1 MDM, respectively, as expected (Supplementary Fig. 1). Cell viability assays using trypan blue staining revealed no immediate cytotoxic effects of CS at concentrations < 3 μM within 90 and 180 min

A

0 100 900

	LM	Vehicle (-)	*E. coli* (+) Vehicle (+)	CS 0.1 μM (+)	%	CS 1 μM (+)	%
COX	PGE_2	29.0 ± 3.6	36.8 ± 4.4	85.4 ± 12.1	232	329 ± 43.4	895
	PGD_2	7.5 ± 1.2	8.3 ± 1.2	12.4 ± 2.0	149	37.9 ± 5.8	457
	$PGF_{2\alpha}$	11.5 ± 1.0	13.6 ± 0.7	18.4 ± 1.5	135	40.1 ± 4.4	294
	TXB_2	1,304 ± 261	2,195 ± 265	1,499 ± 240	68	1,045 ± 148	48
5-LOX	5-HETE	15.0 ± 3.0	332 ± 85.9	316 ± 18.8	95	49.6 ± 5.3	15
	5-HEPE	2.5 ± 0.3	20.4 ± 3.2	26.6 ± 14.5	130	6.2 ± 2.2	30
	t-LTB_4	19.6 ± 2.8	45.8 ± 8.4	54.7 ± 11.6	120	22.3 ± 1.0	49
	LTB_4	20.4 ± 2.2	460 ± 82.7	487 ± 57.3	106	157 ± 28.4	34
	7-HDHA	7.1 ± 1.3	11.0 ± 1.3	8.3 ± 0.9	76	5.6 ± 0.2	51
12-/15-LOX	17-HDHA	36.7 ± 5.2	56.8 ± 7.1	42.9 ± 3.5	75	41.2 ± 2.2	73
	15-HETE	25.7 ± 6.7	44.4 ± 7.2	47.4 ± 3.9	107	40.6 ± 1.7	91
	15-HEPE	14.7 ± 1.9	21.1 ± 3.0	17.2 ± 2.2	81	14.3 ± 0.6	68
	14-HDHA	39.2 ± 3.3	168 ± 18.3	200 ± 40.3	119	241 ± 38.8	143
	12-HETE	851 ± 145	3,375 ± 570	3,494 ± 363	104	5,152 ± 459	153
	12-HEPE	31.7 ± 2.6	174 ± 24.5	206 ± 78.6	119	247 ± 75.7	142
Fatty Acids	AA	1,353 ± 71.7	2,136 ± 465	2,381 ± 464	111	2,482 ± 261	116
	EPA	117 ± 35.0	145 ± 35.2	172 ± 75.1	119	142 ± 36.3	98
	DHA	419 ± 39.4	469 ± 60.3	483 ± 47.3	103	432 ± 34.5	92

C

0 100 230

	LM	Vehicle (-)	SACM (+) Vehicle (+)	CS 0.1 μM (+)	%	CS 1 μM (+)	%
COX	PGE_2	1,025 ± 536	1,752 ± 638	2,031 ± 665	116	3,019 ± 1,067	172
	PGD_2	26.7 ± 13.8	47.4 ± 5.9	62.8 ± 1.8	133	109 ± 6.7	230
	$PGF_{2\alpha}$	51.8 ± 14.6	116 ± 29.8	130 ± 25.9	113	222 ± 50.6	192
	TXB_2	2,166 ± 801	7,567 ± 2,511	7,027 ± 2,449	93	5,695 ± 2,078	75
5-LOX	5-HETE	1,260 ± 1,052	11,828 ± 2,024	10,235 ± 1,456	87	8,249 ± 2,427	70
	5-HEPE	195 ± 170	1,726 ± 186	1,436 ± 251	83	1,048 ± 311	61
	t-LTB_4	248 ± 191	1,334 ± 250	922 ± 16.4	69	638 ± 109	48
	LTB_4	1,006 ± 851	3,238 ± 989	2,989 ± 927	92	2,610 ± 968	81
	7-HDHA	14.7 ± 7.5	156 ± 19.9	138 ± 18.0	89	82.7 ± 17.5	53
12-/15-LOX	17-HDHA	38.0 ± 10.7	435 ± 80.0	667 ± 119	153	725 ± 150	167
	15-HETE	93.2 ± 69.0	1268 ± 107	1,440 ± 93.4	114	1,687 ± 275	133
	15-HEPE	12.5 ± 3.5	86.2 ± 19.2	107 ± 22.1	124	130 ± 40.4	150
	14-HDHA	7.0 ± 2.9	82.8 ± 28.8	103 ± 42.5	125	112 ± 46.3	135
	12-HETE	23.0 ± 9.9	489 ± 290	594 ± 359	121	725 ± 468	148
	12-HEPE	3.8 ± 1.7	74.8 ± 44.0	93.2 ± 54.9	125	133 ± 94.0	178
Fatty Acids	AA	7,905 ± 2,355	72,351 ± 1,890	73,335 ± 4,546	101	71,972 ± 7,981	99
	EPA	1,321 ± 360	24,024 ± 2,435	25,081 ± 2,211	104	24,889 ± 3,634	104
	DHA	5,068 ± 1,157	55,999 ± 981	57,911 ± 3,747	103	55,161 ± 5,664	99

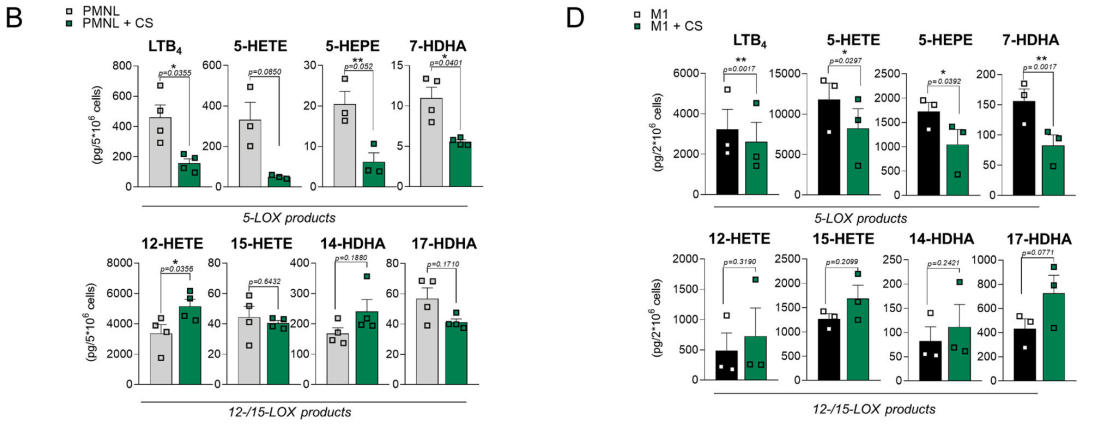

Fig. 1. Celastrol (CS) inhibits cellular formation of pro-inflammatory 5-LOX products. A) and B) Human PMNL were pre-incubated with CS (0.1 and 1 μM) for 15 min and then challenged with pathogenic *E. coli* (serotype O6:K2:H1, ratio 1:50) for 90 min. LM were analyzed by UPLC-MS/MS in the supernatants of cells. A) Heatmap of LM produced by PMNL and effects of 0.1 and 1 μM CS versus vehicle. B) Bar charts of prominent 5-LOX and 12-/15-LOX products (expressed as pg/5 × 10^6 cells) of CS-treated vs. vehicle-treated cells. C) and D) Human M1 MDM were pre-treated with CS (0.1 and 1 μM) for 15 min and cells were stimulated with 1% *S. aureus*-conditioned medium (SACM) for 90 min. C) Heatmap of LM produced by M1 MDM and effects of 0.1 and 1 μM CS versus vehicle. D) Bar charts of prominent 5-LOX and 12-/15-LOX products (expressed as pg/2 × 10^6 cells) of CS-treated vs. vehicle-treated cells. Data are means ± S.E.M. of single data points, n = 4 (for PMNL) or n = 3 (for M1 MDM) independent experiments; paired *t*-test, *p < 0.05; **p < 0.01 CS vs. control group.

in PMNL and MDM, respectively, excluding that CS suppresses 5-LOX product due loss of cellular integrity (Supplementary Fig. 2). Together, CS inhibits formation of pro-inflammatory LM produced by 5-LOX in two different experimental cellular settings, independent of the cell type and the stimulus.

4.2. Celastrol directly and selectively inhibits 5-LOX

Prompted by the finding that CS suppresses 5-LOX product formation in intact cells, we next aimed to investigate whether CS directly inhibits 5-LOX activity in a cell-free environment. Concentration-response studies showed that CS inhibits the activity of isolated human recombinant 5-LOX (IC_{50} = 0.19 μM, Fig. 2A) and of 5-LOX in PMNL homogenates (IC_{50} = 0.49 μM, Fig. 2B). The 5-LOX reference inhibitor zileuton (3 μM) inhibited recombinant 5-LOX and 5-LOX in PMNL homogenates down to a residual activity of 18% and 26%, respectively (Supplementary Fig. 3). Additionally, we screened CS (1 μM) for inhibition of other enzymes involved in pro-inflammatory LM biosynthesis. As shown in Table 1, CS failed to inhibit COX-1/2, mPGES-1 and TXAS. Together, the data suggest that among the enzymes within the pro-inflammatory LM pathways, CS selectively inhibits 5-LOX.

We next questioned if the inhibitory activity of CS on the recombinant 5-LOX enzyme is due to competition with AA as substrate and if 5-LOX inhibition is reversible. We thus conducted concentration-response studies with CS against isolated recombinant 5-LOX at various concentrations of AA (2.5 – 5 – 10 – 20 – 40 μM). Increasing concentrations of exogenous AA did not significantly alter the potency of CS, suggesting that CS does not compete with AA for inhibition of 5-LOX (Fig. 2C). Wash out experiments (10 times dilution of CS) indicated reversible 5-LOX inhibition as dilution of 2 μM CS to 0.2 μM reversed the strong suppression of 5-LOX activity (Fig. 2D).

We recently showed that the pentacyclic triterpenoid 3-*O*-acetyl-11-keto-β-boswellic acid (AKBA) from frankincense inhibits 5-LOX in a substrate concentration-independent manner via binding to an allosteric site [27]. We utilized AutoDock Vina [29] to ask whether CS might also dock into the recently solved structure of Stable-5-LOX bound to AKBA [27]. Docking was performed more than five times with different target search volumes, which included the entire Stable-5-LOX protein as well as volumes localized around the cleft between the membrane-binding and catalytic domains of 5-LOX. AutoDock Vina consistently placed CS

Table 1
Effect of CS on the activities of isolated enzymes.

Enzyme	Residual activity (%)	Positive control	Residual activity (%)
COX-1	118 ± 4.3[a]	IND	38.4 ± 7.5
COX-2	96.4 ± 5.3[a]	IND	35.3 ± 1.1
mPGES-1	100 ± 7.7[a]	MK886	17.6 ± 1.5
5-LOX	0.19[b]	Zileuton	18.5 ± 3.5
TXB synthase	93.7 ± 2.8[a]	–	–

[a] Residual activity at 1 μM CS (% of control).
[b] IC_{50} value in μM is given; data are means ± S.E.M., n = 3. Indomethacin (IND) 10 μM; MK886 10 μM; zileuton 3 μM.

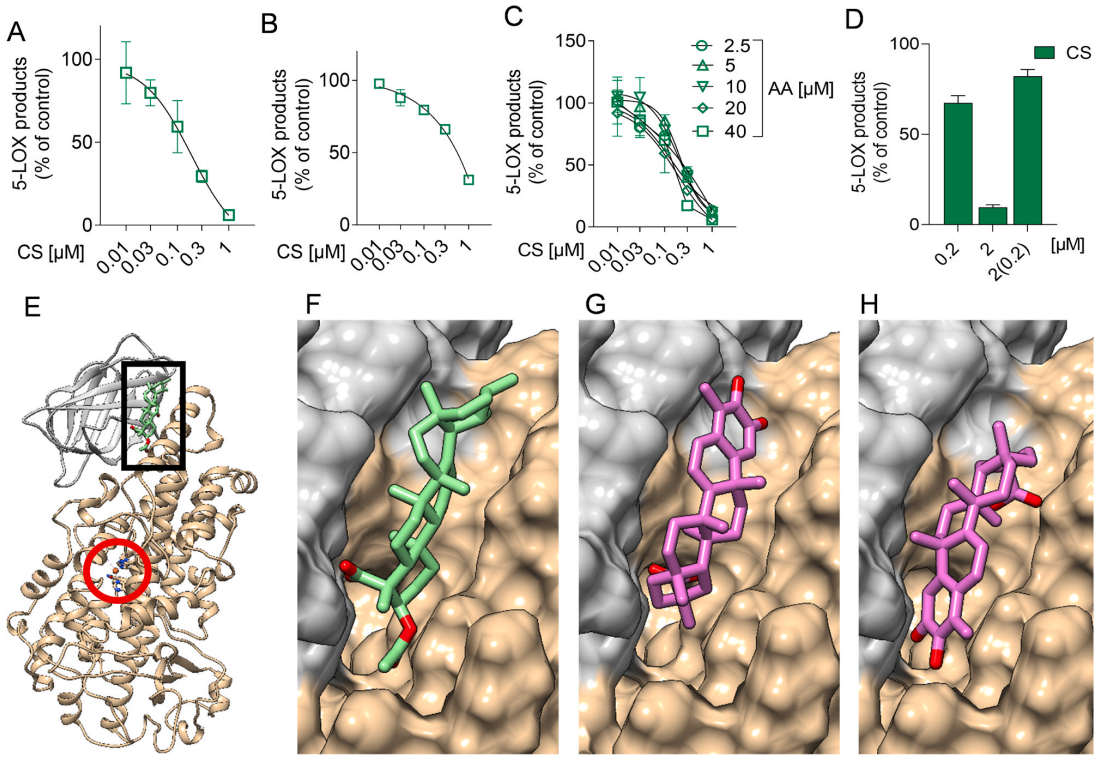

Fig. 2. Celastrol (CS) is a direct inhibitor of 5-LOX. Concentration-response curves of CS for inhibition of A) isolated human recombinant 5-LOX and B) 5-LOX in PMNL homogenates, and C) of isolated human recombinant 5-LOX at various concentrations of AA (2.5 – 5 – 10 – 20–40 μM). D) Wash-out experiment with isolated human recombinant 5-LOX and CS. Data are means ± S.E.M., n = 3 independent experiments and expressed as % residual activity versus uninhibited control (DMSO = 100%). E) Stable-5-LOX bound to AKBA is shown in cartoon with the membrane-binding domain as gray and catalytic domain as tan. Red circle highlights the active site and black box denotes the AKBA allosteric site. (F) AKBA in sticks (green carbons) is wedged between the two domains illustrated in surface rendering. (G/H) CS (purple, carbons) docked in the 5-LOX allosteric site in two different conformations.

in the interdomain allosteric site of AKBA. Burial of the hydrophobic triterpenoid appears to be the primary molecular driver of binding, and there are potential H-bond interactions with the carboxy, hydroxyl, and oxo group from CS with amino acids Arg 101, Arg 138, and His 130 of Stable-5-LOX from the different dockings. These amino acids also interact with AKBA. These results combine to suggest that disturbance of the cation-π and ionic interactions between the two domains by CS results in noncompetitive inhibition, as is the case for AKBA.

4.3. Celastrol induces formation of 12-/15-LOX products in M2 MDM

In contrast to PMNL and M1 macrophages with mainly pro-inflammatory phenotype, M2 macrophages are considered as pro-resolving subtypes with strong capacities to generate SPM involving 12-/15-LOX activities upon adequate challenge [17]. Since CS elevated 12-/15-LOX products in PMNL and in M1 MDM, it appeared possible that CS could evoke formation of SPM and their precursors in M2 MDM that strongly express 15-LOX-1 [17]. Therefore, M2 MDM were treated with CS (1 μM) for 180 min and LM in the supernatants were analyzed. The data presented in Fig. 3A show that CS, when compared to the vehicle control, inhibits 5-LOX product formation but strongly increases 12-/15-LOX products reaching a significant effect for the mono-hydroxylated precursor 17-HDHA and for the production of RvD5 (Fig. 3B). Interestingly, cells from donors showing the highest increase of RvD5 also showed the highest increase of 17-HDHA. When compared with bacterial exotoxins (present in SACM) that induced the formation of all LOX-derived products, the stimulatory effect of CS is confined only to 15-LOX being less pronounced vs. exotoxins (Supplementary Fig. 4A). In resting M1 MDM, exposure to 1 μM CS caused only moderate formation of 12-/15-LOX products (Supplementary Fig. 4B), most likely due to the fact that this phenotype expresses only modest levels of 15-LOX-1 [17].

Activation of LOX enzymes is tightly regulated by their subcellular localization and by intracellular Ca^{2+} levels [7,17]. Treatment of M2

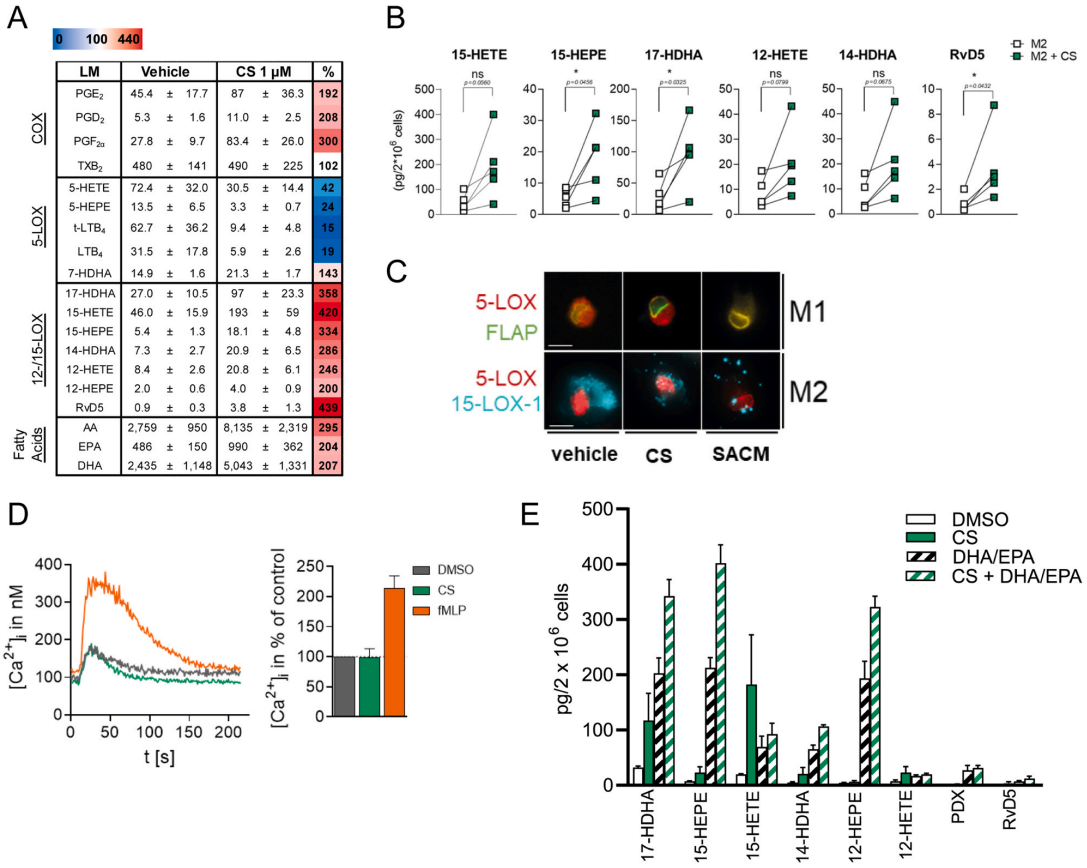

Fig. 3. Celastrol (CS) induces formation of 12-/15-LOX products in M2 MDM. A) and B) Human M2 MDM were exposed to CS (1 μM) for 180 min at 37 °C and formed LM were extracted from the supernatants and analyzed by UPLC-MS-MS. A) Changes in LM formation due to CS vs. vehicle control (=100%) are presented in a heatmap. Data expressed as pg/2 × 10^6 cells are means ± S.E.M., n = 5. B) Paired data of the 12-/15-LOX products as well as SPM (expressed as pg/2 x* 10^6 cells) are shown; paired *t*-test *p < 0.05. C) Subcellular redistribution of 5-LOX in M1 MDM and of 5-LOX and 15-LOX-1 in M2 MDM. The MDM were exposed to 1 μM CS, 1% of SACM (as positive control) or DMSO (0.1%, as vehicle) for 180 min at 37 °C. Cells were fixed, permeabilized, and incubated with antibodies against 5-LOX (red), FLAP (green), and 15-LOX-1 (cyan blue); scale bars = 10 μm. Results shown for one single cell are representative for approximately 100 individual cells analyzed in n = 3 independent experiments. D) Determination of $[Ca^{2+}]_i$. M2 MDM were pre-stained with Fura-2/AM (1 μM) for 30 min at 37 °C. Cells (1.25 × 10^6/mL) received 1 mM $CaCl_2$ prior to the measurement. CS (1 μM), fMLP (1 μM) or vehicle (1% DMSO) were added, and the signal was monitored in a NOVOstar microplate reader. Data are shown as a representative line plot of changes in $[Ca^{2+}]_i$ and as percentage of vehicle control during the first 40 s after injection, n = 3. E) Bar charts of LM formed in M2 MDM after treatment with DMSO (0.1%) or CS (1 μM) or mixture of DHA and EPA (3 μg/mL, each) or CS (1 μM) and DHA and EPA (3 μg/mL, each). Data are given as means ± SEM of n = 3 independent experiments.

MDM with 1 μM CS induced the subcellular redistribution of soluble 15-LOX-1 from the cytosol to subcellular membranous compartments (Fig. 3C), similar as observed for SACM but again less pronounced. In contrast, translocation of 5-LOX to the nuclear membrane for accessing FLAP is not induced by CS, neither in M2 nor in M1 MDM (Fig. 3C). Of note, the positive control SACM (1%) evoked marked redistribution of both 5-LOX and 15-LOX-1 (Fig. 3C).

Since elevation of the intracellular Ca^{2+} concentration ($[Ca^{2+}]_i$) is a prerequisite for 5-LOX/15-LOX-1 activation by the SACM and other stimuli (e.g. fMLP) that induce LM formation in M2 macrophages [17,18], we hypothesized that increasing $[Ca^{2+}]_i$ plays a role in CS-induced LM formation as well. For the measurement of $[Ca^{2+}]_i$, Fura-2/AM-stained M2 MDM were challenged with CS (1 μM) or the positive control fMLP (1 μM). As shown in Fig. 3D, CS did not alter the $[Ca^{2+}]_i$ versus vehicle, in contrast to fMLP that rapidly and strongly increased $[Ca^{2+}]_i$. Thus, CS activates 15-LOX-1 in M2 MDM resulting in the production of SPM without concomitant elevation of $[Ca^{2+}]_i$.

It appeared possible that induction of LM formation by CS is primarily due to elevation of the availability of free fatty acids as substrate. Therefore, we analyzed LM formation in M2 MDM treated with CS (1 μM) in the presence of a mixture of exogenously added DHA and EPA (3 μg/mL). Administration of the mixture of fatty acids alone induced the production of 12-/15-LOX products but co-treatment with CS markedly enhanced this effect (Fig. 3E). These data suggest that the marked formation of 12- and 15-LOX-derived products by CS is not simply due to enhancing fatty acid substrate supply, but instead CS promotes also the conversion of substrate by respective LOXs.

4.4. Celastrol suppresses LT formation but promotes SPM generation in vivo

In order to address whether CS is able to modulate LM formation in vivo in a model of acute inflammation, we made use of the zymosan-induced peritonitis in mice. Animals were pre-treated with vehicle (2% DMSO), CS (10 mg/kg) intraperitoneally (i.p.) 30 min before zymosan challenge (1 mg per mouse, i.p.). After 2 h mice were sacrificed, and LM were analyzed in the peritoneal exudates, in plasma as well as in the spleens (Fig. 4A). CS pre-treatment of the animals was able to switch the LM composition in the peritoneal exudates from pro-inflammatory 5-LOX products to the pro-resolving 12-/15-LOX-derived LM (Fig. 4B). Thus, CS significantly lowered LTB_4 and 5-HETE levels in the exudates, but significantly increased the mono-hydroxylated 12-/15-LOX products (i.e., 12-/15-HETE, 14-/17-HDHA, 12-/15-HEPE) and promoted the formation of resolvins (i.e., RvD1, RvD2, RvD3, and RvD4). Also, the levels of the SPM PD1, PDX and MaR1 were markedly increased by CS, although statistical significance was not reached (Fig. 4C). Analysis of spleens and plasma showed a similar pattern of LM profile modulation by CS, as there was a trend in the reduction of 5-LOX products with a concomitant increase of 12-/15-LOX-derived LM (Fig. 4D and E). Together, these data demonstrate that CS is able to suppress the biosynthesis of pro-inflammatory LT but elevates the formation of inflammation-resolving SPM in mice in vivo.

5. Discussion

Here we show that CS from TwHF modulates LM biosynthesis in vitro and in vivo. We found that 1) CS suppresses 5-LOX product formation in two different pro-inflammatory experimental cellular models, 2) CS is a direct inhibitor of 5-LOX without affecting related LM biosynthetic enzymes, 3) CS induces the formation of 12/15-LOX products including pro-resolving SPM in M2 MDM and that 4) in vivo, CS inhibits the formation of 5-LOX products but simultaneously increases the production of SPM during acute inflammation in mice. Such an impetus of the LM class switch from pro-inflammatory LTs to inflammation-resolving SPM by a natural product is of great interest for inflammation pharmacotherapy and offers an alternative strategy for intervention with inflammatory disorders over classical NSAIDs.

CS has been reported to be bioactive in a variety of inflammation-related in vivo models, for review see [13,14]. Thus, CS ameliorated joint inflammation as well as paw swelling in experimental models of arthritis [34,35], and in dextran sodium sulfate-induced colitis CS improved colon injury, PMNL infiltration and histological signs of damage at the intestinal level [36,37]. Both, experimental arthritis and colitis used as inflammatory disease models in these studies are typically related to aberrant LM biology, that is, elevated LT and reduced SPM [3,5,38,39]. Thus, shifting LM formation from LTs towards SPM may contribute to the reported beneficial anti-inflammatory effects of CS. Furthermore, in obese asthmatic mice, CS alleviated the airway hyperresponsiveness [40], which may be explained, at least in part, by suppressing formation of LTs that are potent bronchoconstrictors [41]. On the molecular level, the anti-inflammatory action of CS has been connected to inhibition of the NLRP3 inflammasome activation [42] and to the suppression of the PI3K/AKT/mTOR signaling [43] as well as to the blockade of NF-κB activation and the increase in IL-10 levels [37].

Manipulation of LM biosynthesis by CS is poorly explored and in particular modulation of SPM by CS has not been reported yet. SPM terminate and actively resolve inflammatory processes, limit tissue damage, promote wound healing and facilitate the return to homeostasis [3,6]. SPM cause cessation of neutrophil influx and activation, efferocytosis of apoptotic neutrophils and debris, bacterial killing, and clearance/phagocytosis of bacteria by macrophages [6]. Thus, SPM represent endogenous relievers of inflammation and recent evidence suggests that unresolved inflammation might be due to failure in the biosynthesis of appropriate amounts of SPM [44]. Therefore, that CS effectively enhances SPM formation is of great interest with respect to treatment of unresolved inflammation. In 2016, Joshi et al. first reported about modulation of the AA pathway by CS [45]. The authors found that CS inhibits the activity of human 5-LOX isolated from PMNL with an IC_{50} = 5 μM [45]. In our hands, CS was much more potent as it inhibited the activity of human recombinant 5-LOX and 5-LOX in homogenates of human PMNL with IC_{50} values of 0.19 and 0.49 μM, respectively. This discrepancy in the potency of CS might be explained by different experimental conditions: while we applied biologically relevant concentrations of substrate (2.5–40 μM AA), Joshi et al. assayed 5-LOX inhibition by CS at 150 μM AA [45]. Accordingly, also in intact PMNL and M1 MDM, CS displayed potent inhibitory activities on 5-LOX product formation at 1 μM, with higher efficiency in PMNL versus M1 MDM. Note that 5-LOX is mainly cytosolic in PMNL [8] but mainly nucleosolic in M1 MDM [17], so there might be a better accessibility of CS for 5-LOX in the cytosol of PMNL. Also, the amounts of formed 5-LOX products per 10^6 cells is much higher under these incubation conditions in M1 MDM vs. PMNL, indicating that 5-LOX catalytic activity might be superior in M1 MDM over PMNL, and allosteric inhibition of 5-LOX in M1 MDM by CS is thus less efficient compared to PMNL. We want to emphasize that in agreement with the literature [46,47] CS is cytotoxic in a variety of mammalian cells and also in our hands CS at concentrations > 3 μM caused detrimental effects on the viability of PMNL and MDM within a few hours of exposure.

Pro-inflammatory M1 and pro-resolving M2 macrophage phenotypes are associated with differential LM formation, that is, M1 macrophages produce dominantly PG and LT but barely SPM while the M2 subtype is a rich source for SPM generation [4,17]. CS effectively inhibited formation of LT and other 5-LOX products in M1 MDM. Given the balance and the co-existence of the M1 and M2 phenotypes in the body [33], we questioned if besides suppression of 5-LOX product formation CS treatment could result in increased SPM formation. It was shown that CS suppresses M1 polarization along with suppression of the M1 biomarkers IL-6, IL-1β, TNFα, iNOS and impaired activation of Nrf2 and HO-1 coupled to reduced ERK-1/2, p38 MAPK and JNK activation [48]. We employed M2 MDM and we found that CS induced the activation of 15-LOX-1, but not of 5-LOX, along with 15-LOX-derived product formation. This ability of CS to activate 15-LOX-1 for induction of SPM

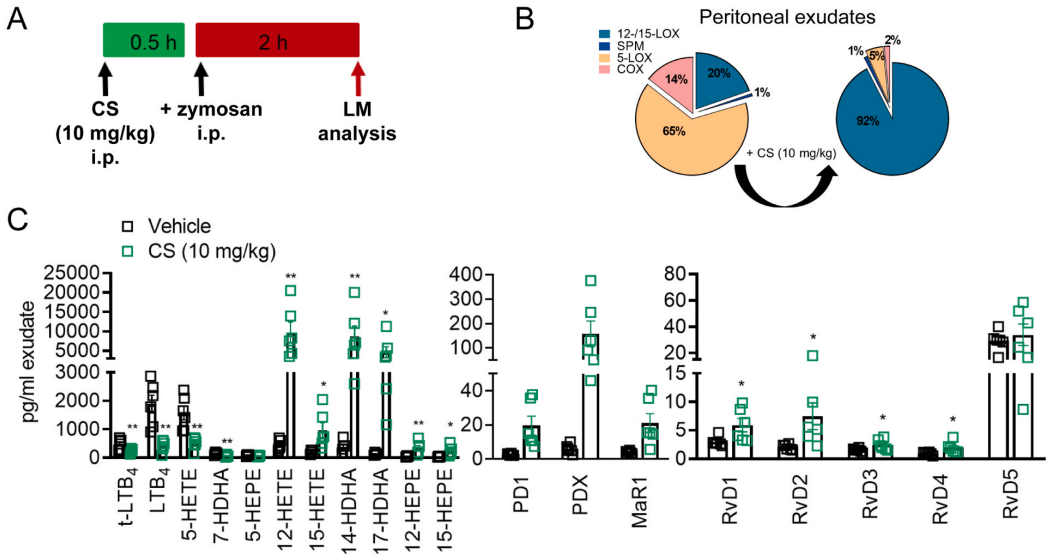

D

Spleen

60 100 170

	LM	Vehicle	CS 10 mg/kg	%
COX	PGE_2	11,017 ± 862	10,409 ± 315	94
	PGD_2	21,826 ± 962	21,375 ± 535	98
	$PGF_{2\alpha}$	3,524 ± 413	4,260 ± 345	121
	TXB_2	34,328 ± 3,288	36,474 ± 2,596	106
5-LOX	5-HETE	2,267 ± 390	2,153 ± 226	95
	5-HEPE	145 ± 16.8	139 ± 22.5	96
	$t\text{-}LTB_4$	390 ± 69.4	308 ± 40.7	79
	LTB_4	521 ± 127	341 ± 50.2	65
	7-HDHA	116 ± 13.0	114 ± 18.7	98
12-/15-LOX	17-HDHA	1,927 ± 204	2,105 ± 292	109
	15-HETE	16,210 ± 1,239	14,591 ± 1,720	90
	15-HEPE	412 ± 58.7	541 ± 62.8	131
	14-HDHA	20,758 ± 1,685	23,239 ± 4,047	112
	12-HETE	45,906 ± 2,644	53,369 ± 8,132	116
	12-HEPE	15,651 ± 2,182	17,537 ± 3,205	112
SPM	MaR1	22.3 ± 4.07	28.7 ± 5.71	129
	MaR2	73.9 ± 13.4	127 ± 22.1	171
	PD1	56.4 ± 6.7	76.0 ± 12.4	135
	PDX	32.5 ± 6.1	47.5 ± 7.4	146
	RvD2	2.5 ± 0.4	3.6 ± 0.5	145
	RvD4	6.5 ± 0.4	5.2 ± 0.4	80
	RvD5	13.1 ± 1.6	15.7 ± 2.8	120
Fatty Acids	AA	93,745 ± 7,337	94,019 ± 6,506	100
	EPA	18,661 ± 3,053	19,190 ± 1,650	103
	DHA	68,807 ± 3,871	67,634 ± 4,949	98

E

Plasma

80 100 240

	LM	Vehicle	CS 10 mg/kg	%
COX	PGE_2	593 ± 126	757 ± 122	128
	PGD_2	668 ± 109	785 ± 101	118
	$PGF_{2\alpha}$	168 ± 15.7	170 ± 22.9	101
	TXB_2	203 ± 20.7	233 ± 39.5	115
5-LOX	5-HETE	6,337 ± 1,473	6,218 ± 1,035	98
	5-HEPE	206 ± 14.7	191 ± 24.7	93
	$t\text{-}LTB_4$	108 ± 21.7	91.6 ± 12.1	85
	LTB_4	77.8 ± 20.3	63.2 ± 6.1	81
	7-HDHA	176 ± 36.9	212 ± 41.1	121
12-/15-LOX	17-HDHA	1,291 ± 222	1,906 ± 349	148
	15-HETE	4,093 ± 812	5,899 ± 1,174	144
	15-HEPE	61.6 ± 5.0	71.3 ± 6.3	116
	14-HDHA	7,876 ± 2,560	10,219 ± 1,301	130
	12-HETE	10,722 ± 2,711	15,886 ± 2,621	148
	12-HEPE	1,511 ± 394	1,875 ± 250	124
SPM	PD1	32.3 ± 11.7	77.5 ± 19.9	240
	PDX	8.8 ± 2.4	14.3 ± 2.9	162
	RvD2	18.3 ± 3.4	27.4 ± 4.1	150
	RvD4	328 ± 80.6	420 ± 63.3	128
	RvD5	8.2 ± 2.5	10.9 ± 1.7	132
Fatty Acids	AA	48,985 ± 1,645	60,172 ± 8,234	123
	EPA	16,164 ± 2,453	14,758 ± 2,828	91
	DHA	50,256 ± 548	60,321 ± 6,920	120

Fig. 4. Celastrol (CS) modulates LM formation in vivo. A) Experimental timeline of mouse peritonitis. Mice received CS (10 mg/kg) i.p. 30 min prior to induction of peritonitis by zymosan (1 mg/mouse, i.p.). After 2 h, animals were euthanized, and blood and spleen were collected as well as peritoneal exudates by lavage with 3 mL cold PBS. B) Pie charts of LM formed in the peritoneal cavity of vehicle group and CS-treated animals. Data are given as sum of LM formed by the different enzymes. C) Bar charts and single dot representing the 5-/12-/15-LOX products and SPMs in the different animals. D) and E) Absolute amounts of LM produced in spleen, presented as pg/mg tissue (D), and in plasma, presented as pg/mL (E), as well as respective heatmaps (% of vehicle group = 100%). Data are means ± S.E.M of n = 6 animals per group. Statistical analysis has been performed by unpaired *t*-test. *$p < 0.05$; *$p < 0.01$.

generation without evoking pro-inflammatory 5-LOX and COX products is intriguing and supports the potential as novel pharmacological strategy for intervention with inflammatory disorders. Such pharmacological profile of CS is in line with our previous report on synthetic small molecules that favorably modulated the agonist-induced LM profiles in MDM by inhibiting 5-LOX production and by enhancing SPM formation [4,11]. In this respect, CS may impact the phenotype of murine peritoneal macrophages during zymosan-induced peritonitis, due to the LM class switch from pro-inflammatory to pro-resolving LM, which will be subject in future studies using flow cytometry. The mechanisms underlying the ability of CS to induce pro-resolving mediators are still not completely elucidated. Recently, we showed that the pentacyclic triterpene acid AKBA binds at an allosteric site of 5-LOX between the C2-like and the catalytic domain which not only mediates inhibition of LT formation but also changes the enzyme's regiospecificity to convert AA to 12- and 15-LOX products [27]. Our docking experiments clearly support binding of CS at the same 5-LOX allosteric site as AKBA. Therefore, it is tempting to speculate that the pentacyclic triterpenoid CS may act in a similar fashion as the pentacyclic triterpene acid AKBA, but not only on 5-LOX but also on 15-LOX-1, thereby activating this enzyme. In fact, small molecules that activate 15-LOX via interaction with an allosteric site were recently reported, even though with a distinct chemical structure [49].

In conclusion, we identified 5-LOX as high affinity target for CS which is potently inhibited at submicromolar IC_{50} values in vitro and with high efficiency also in vivo. Interestingly, in M2 MDM, CS evoked the formation of 12-/15-LOX-derived LM with elevated production of SPM in the absence of any agonist, seemingly by activation of 15-LOX-1. Most intriguingly however, in an in vivo mouse model of acute inflammation CS promoted the LM class switch from pro-inflammatory LT to inflammation-resolving SPM. Our findings call for consideration of the application of small molecules such as CS in inflammatory diseases to "switch on" resolution of inflammation by promoting endogenous SPM formation.

Funding

This work was supported by the Deutsche Forschungsgemeinschaft (DFG, German Research Foundation) – project-ID 316213987 – SFB 1278 PolyTarget (projects A04, C02, Z01) and – project-ID 239748522 - SFB 1127 ChemBioSys (project A04), and by the Free State of Thuringia and the European Social Fund (2019 FGR 0095).

Author contributions

S.P. designed the study, performed animal experiments, analyzed data, prepared figures and wrote the manuscript. K.Z. and W.W. performed experiments with macrophages, PMNL, isolated enzymes, analyzed data and wrote the related method sections and prepared figures. P.M.J. performed and analyzed immunofluorescence experiments and wrote the related method section. R.B. performed animal experiments and isolated COX assay and wrote the related method section. M. P. performed mPGES-1 assays and wrote the related method section. F.B. performed Ca^{2+} imaging assays and wrote the related method section. C. K. analyzed LM in the peritoneal exudate, plasma and spleen. A.R. designed and performed animal experiments. D.F., J.G., R.K.H. and S.L. gave scientific advises and revised the manuscript. N.C.G. and M.E.N. performed the docking analysis and wrote parts of the manuscript. X.C. and O.W. conceived and designed the study. O.W. wrote the manuscript.

Declaration of Competing Interest

The authors declare that they have no known competing financial interests or personal relationships that could have appeared to influence the work reported in this paper.

Data availability

The data are available on request to the corresponding author.

Acknowledgments

We thank Katrin Fischer and Petra Wiecha for expert technical assistance.

Appendix A. Supporting information

Supplementary data associated with this article can be found in the online version at doi:10.1016/j.phrs.2021.105556.

References

[1] R. Medzhitov, Origin and physiological roles of inflammation, Nature 454 (2008) 428–435.
[2] I. Tabas, C.K. Glass, Anti-inflammatory therapy in chronic disease: challenges and opportunities, Science 339 (2013) 166–172.
[3] C.N. Serhan, Pro-resolving lipid mediators are leads for resolution physiology, Nature 510 (2014) 92–101.
[4] M. Werner, P.M. Jordan, E. Romp, A. Czapka, Z. Rao, C. Kretzer, A. Koeberle, U. Garscha, S. Pace, H.E. Claesson, C.N. Serhan, O. Werz, J. Gerstmeier, Targeting biosynthetic networks of the proinflammatory and proresolving lipid metabolome, FASEB J. 33 (2019) 6140–6153.
[5] C.D. Funk, Prostaglandins and leukotrienes: advances in eicosanoid biology, Science 294 (2001) 1871–1875.
[6] C.N. Serhan, B.D. Levy, Resolvins in inflammation: emergence of the pro-resolving superfamily of mediators, J. Clin. Investig. 128 (2018) 2657–2669.
[7] O. Radmark, O. Werz, D. Steinhilber, B. Samuelsson, 5-Lipoxygenase, a key enzyme for leukotriene biosynthesis in health and disease, Biochim. Biophys. Acta 2015 (1851) 331–339.
[8] J. Gerstmeier, C. Weinigel, S. Rummler, O. Radmark, O. Werz, U. Garscha, Time-resolved in situ assembly of the leukotriene-synthetic 5-lipoxygenase/5-lipoxygenase-activating protein complex in blood leukocytes, FASEB J. 30 (2016) 276–285.
[9] W.L. Smith, Y. Urade, P.J. Jakobsson, Enzymes of the cyclooxygenase pathways of prostanoid biosynthesis, Chem. Rev. 111 (2011) 5821–5865.
[10] K.D. Rainsford, Profile and mechanisms of gastrointestinal and other side effects of nonsteroidal anti-inflammatory drugs (NSAIDs), Am. J. Med. 107 (1999) 27–35 (27S–35S; discussion 35S–36S).
[11] J. Gerstmeier, C. Kretzer, S. Di Micco, L. Miek, H. Butschek, V. Cantone, R. Bilancia, R. Rizza, F. Troisi, N. Cardullo, C. Tringali, A. Ialenti, A. Rossi, G. Bifulco, O. Werz, S. Pace, Novel benzoxanthene lignans that favorably modulate lipid mediator biosynthesis: a promising pharmacological strategy for anti-inflammatory therapy, Biochem. Pharm. 165 (2019) 263–274.
[12] S.R. Chen, Y. Dai, J. Zhao, L. Lin, Y. Wang, Y. Wang, A. Mechanistic, A mechanistic overview of triptolide and celastrol, natural products from Tripterygium wilfordii Hook F, Front. Pharm. 9 (2018) 104.
[13] R. Cascao, J.E. Fonseca, L.F. Moita, Celastrol: a spectrum of treatment opportunities in chronic diseases, Front. Med. 4 (2017) 69.
[14] S.W. Ng, Y. Chan, D.K. Chellappan, T. Madheswaran, F. Zeeshan, Y.L. Chan, T. Collet, G. Gupta, B.G. Oliver, P. Wark, N. Hansbro, A. Hsu, P.M. Hansbro, K. Dua, J. Panneerselvam, Molecular modulators of celastrol as the keystones for its diverse pharmacological activities, Biomed. Pharm. 109 (2019) 1785–1792.
[15] X. Chen, B. Zhang, J. Li, M. Feng, Y. Zhang, W. Yao, C. Zhang, L. Wan, Celastrol attenuates incision-induced inflammation and pain associated with inhibition of the NF-kappaB signalling pathway via SARM, Life Sci. 205 (2018) 136–144.
[16] S. Pace, C. Pergola, F. Dehm, A. Rossi, J. Gerstmeier, F. Troisi, H. Pein, A. M. Schaible, C. Weinigel, S. Rummler, H. Northoff, S. Laufer, T.J. Maier, O. Radmark, B. Samuelsson, A. Koeberle, L. Sautebin, O. Werz, Androgen-mediated sex bias impairs efficiency of leukotriene biosynthesis inhibitors in males, J. Clin. Investig. 127 (2017) 3167–3176.
[17] O. Werz, J. Gerstmeier, S. Libreros, X. De la Rosa, M. Werner, P.C. Norris, N. Chiang, C.N. Serhan, Human macrophages differentially produce specific resolvin or leukotriene signals that depend on bacterial pathogenicity, Nat. Commun. 9 (2018) 59.
[18] P.M. Jordan, J. Gerstmeier, S. Pace, R. Bilancia, Z. Rao, F. Borner, L. Miek, O. Gutierrez-Gutierrez, V. Arakandy, A. Rossi, A. Ialenti, C. Gonzalez-Estevez, B. Loffler, L. Tuchscherr, C.N. Serhan, O. Werz, Staphylococcus aureus-derived α-hemolysin evokes generation of specialized pro-resolving mediators promoting inflammation resolution, Cell Rep. 33 (2020), 108247.
[19] L. Fischer, D. Szellas, O. Radmark, D. Steinhilber, O. Werz, Phosphorylation- and stimulus-dependent inhibition of cellular 5-lipoxygenase activity by nonredox-type inhibitors, FASEB J. 17 (2003) 949–951.
[20] D. Albert, I. Zundorf, T. Dingermann, W.E. Muller, D. Steinhilber, O. Werz, Hyperforin is a dual inhibitor of cyclooxygenase-1 and 5-lipoxygenase, Biochem. Pharm. 64 (2002) 1767–1775.
[21] A. Koeberle, U. Siemoneit, U. Buhring, H. Northoff, S. Laufer, W. Albrecht, O. Werz, Licofelone suppresses prostaglandin E2 formation by interference with the

inducible microsomal prostaglandin E2 synthase-1, J. Pharm. Exp. Ther. 326 (2008) 975–982.
[22] G. Lauro, S. Terracciano, V. Cantone, D. Ruggiero, K. Fischer, S. Pace, O. Werz, I. Bruno, G. Bifulco, A combinatorial virtual screening approach driving the synthesis of 2,4-thiazolidinedione-based molecules as new dual mPGES-1/5-LO inhibitors, ChemMedChem 15 (2020) 481–489.
[23] U. Siemoneit, B. Hofmann, N. Kather, T. Lamkemeyer, J. Madlung, L. Franke, G. Schneider, J. Jauch, D. Poeckel, O. Werz, Identification and functional analysis of cyclooxygenase-1 as a molecular target of boswellic acids, Biochem. Pharm. 75 (2008) 503–513.
[24] G. Grynkiewicz, M. Poenie, R.Y. Tsien, A new generation of Ca2+ indicators with greatly improved fluorescence properties, J. Biol. Chem. 260 (1985) 3440–3450.
[25] P.D. Adams, P.V. Afonine, G. Bunkoczi, V.B. Chen, I.W. Davis, N. Echols, J. J. Headd, L.W. Hung, G.J. Kapral, R.W. Grosse-Kunstleve, A.J. McCoy, N. W. Moriarty, R. Oeffner, R.J. Read, D.C. Richardson, J.S. Richardson, T. C. Terwilliger, P.H. Zwart, PHENIX: a comprehensive Python-based system for macromolecular structure solution, Acta Crystallogr. D. Biol. Crystallogr. 66 (2010) 213–221.
[26] S. Kim, P.A. Thiessen, E.E. Bolton, J. Chen, G. Fu, A. Gindulyte, L. Han, J. He, S. He, B.A. Shoemaker, J. Wang, B. Yu, J. Zhang, S.H. Bryant, PubChem substance and compound databases, Nucleic Acids Res. 44 (2016) D1202–D1213.
[27] N.C. Gilbert, J. Gerstmeier, E.E. Schexnaydre, F. Borner, U. Garscha, D.B. Neau, O. Werz, M.E. Newcomer, Structural and mechanistic insights into 5-lipoxygenase inhibition by natural products, Nat. Chem. Biol. 16 (2020) 783–790.
[28] Z. Yang, K. Lasker, D. Schneidman-Duhovny, B. Webb, C.C. Huang, E.F. Pettersen, T.D. Goddard, E.C. Meng, A. Sali, T.E. Ferrin, UCSF Chimera, MODELLER, and IMP: an integrated modeling system, J. Struct. Biol. 179 (2012) 269–278.
[29] O. Trott, A.J. Olson, AutoDock Vina: improving the speed and accuracy of docking with a new scoring function, efficient optimization, and multithreading, J. Comput. Chem. 31 (2010) 455–461.
[30] A. Rossi, C. Pergola, S. Pace, O. Radmark, O. Werz, L. Sautebin, In vivo sex differences in leukotriene biosynthesis in zymosan-induced peritonitis, Pharm. Res. 87 (2014) 1–7.
[31] E. Romp, V. Arakandy, J. Fischer, C. Wolz, A. Siegmund, B. Löffler, L. Tuchscherr, O. Werz, U. Garscha, Exotoxins from Staphylococcus aureus activate 5-lipoxygenase and induce leukotriene biosynthesis, Cell Mol. Life Sci. 77 (2020) 3841–3858.
[32] M.E. Goldyne, G.F. Burrish, P. Poubelle, P. Borgeat, Arachidonic acid metabolism among human mononuclear leukocytes, Lipoxygenase-Relat. Pathw. J. Biol. Chem. 259 (1984) 8815–8819.
[33] M.P. Motwani, D.W. Gilroy, Macrophage development and polarization in chronic inflammation, Semin. Immunol. 27 (2015) 257–266.
[34] R. Cascao, B. Vidal, H. Raquel, A. Neves-Costa, N. Figueiredo, V. Gupta, J. E. Fonseca, L.F. Moita, Effective treatment of rat adjuvant-induced arthritis by celastrol, Autoimmun. Rev. 11 (2012) 856–862.
[35] H. Li, Y.Y. Zhang, H.W. Tan, Y.F. Jia, D. Li, Therapeutic effect of tripterine on adjuvant arthritis in rats, J. Ethnopharmacol. 118 (2008) 479–484.
[36] Z. Jia, C. Xu, J. Shen, T. Xia, J. Yang, Y. He, The natural compound celastrol inhibits necroptosis and alleviates ulcerative colitis in mice, Int. Immunopharmacol. 29 (2015) 552–559.
[37] M.E. Shaker, S.A. Ashamallah, M.E. Houssen, Celastrol ameliorates murine colitis via modulating oxidative stress, inflammatory cytokines and intestinal homeostasis, Chem. Biol. Interact. 210 (2014) 26–33.
[38] M. Alhouayek, H. Ameraoui, G.G. Muccioli, Bioactive lipids in inflammatory bowel diseases - from pathophysiological alterations to therapeutic opportunities, Biochim. Biophys. Acta Mol. Cell Biol. Lipids 2020 (1866), 158854.
[39] M. Perretti, L.V. Norling, Actions of SPM in regulating host responses in arthritis, Mol. Asp. Med. 58 (2017) 57–64.
[40] Z. Zeng, X. Lin, R. Zheng, H. Zhang, W. Zhang, Celastrol alleviates airway hyperresponsiveness and inhibits Th17 responses in obese asthmatic mice, Front. Pharm. 9 (2018) 49.
[41] J.Z. Haeggstrom, Leukotriene biosynthetic enzymes as therapeutic targets, J. Clin. Investig. 128 (2018) 2680–2690.
[42] X. Yu, Q. Zhao, X. Zhang, H. Zhang, Y. Liu, X. Wu, M. Li, X. Li, J. Zhang, X. Ruan, H. Zhang, Celastrol ameliorates inflammation through inhibition of NLRP3 inflammasome activation, Oncotarget 8 (2017) 67300–67314.
[43] J. Zhao, Y. Sun, P. Shi, J.N. Dong, L.G. Zuo, H.G. Wang, J.F. Gong, Y. Li, L.L. Gu, N. Li, J.S. Li, W.M. Zhu, Celastrol ameliorates experimental colitis in IL-10 deficient mice via the up-regulation of autophagy, Int. Immunopharmacol. 26 (2015) 221–228.
[44] J. Dalli, S. Ramon, P.C. Norris, R.A. Colas, C.N. Serhan, Novel proresolving and tissue-regenerative resolvin and protectin sulfido-conjugated pathways, FASEB J. 29 (2015) 2120–2136.
[45] V. Joshi, S.H. Venkatesha, C. Ramakrishnan, A.N. Nanjaraj Urs, V. Hiremath, K. D. Moudgil, D. Velmurugan, B.S. Vishwanath, Celastrol modulates inflammation through inhibition of the catalytic activity of mediators of arachidonic acid pathway: secretory phospholipase A2 group IIA, 5-lipoxygenase and cyclooxygenase-2, Pharm. Res. 113 (2016) 265–275.
[46] G.F. Pinna, M. Fiorucci, J.M. Reimund, N. Taquet, Y. Arondel, C.D. Muller, Celastrol inhibits pro-inflammatory cytokine secretion in Crohn's disease biopsies, Biochem. Biophys. Res. Commun. 322 (2004) 778–786.
[47] W. Xin, Q. Wang, D. Zhang, C. Wang, A new mechanism of inhibition of IL-1beta secretion by celastrol through the NLRP3 inflammasome pathway, Eur. J. Pharm. 814 (2017) 240–247.
[48] D. Luo, Y. Guo, Y. Cheng, J. Zhao, Y. Wang, J. Rong, Natural product celastrol suppressed macrophage M1 polarization against inflammation in diet-induced obese mice via regulating Nrf2/HO-1, MAP kinase and NF-kappaB pathways, Aging 9 (2017) 2069–2082.
[49] H. Meng, C.L. McClendon, Z. Dai, K. Li, X. Zhang, S. He, E. Shang, Y. Liu, L. Lai, Discovery of novel 15-lipoxygenase activators to shift the human arachidonic acid metabolic network toward inflammation resolution, J. Med. Chem. 59 (2016) 4202–4209.

Supplementary Fig. 1

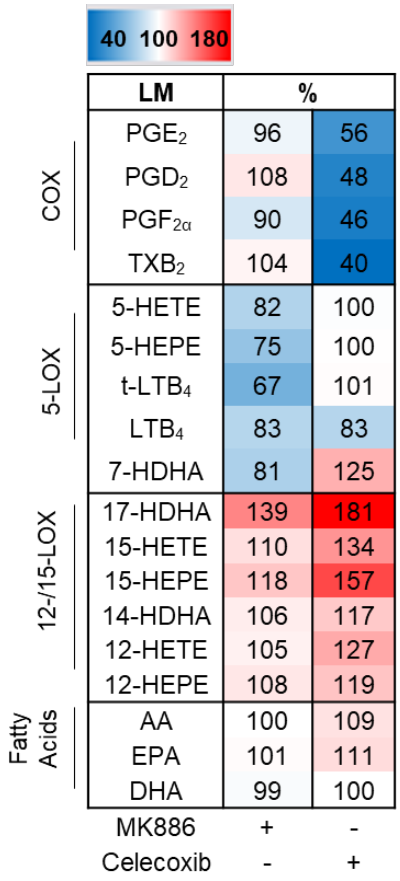

Fig. S1 Effect of MK886 and celecoxib on LM formation in M1 macrophages. Heatmap of the effect of MK886 (0.3 μM) and celecoxib (5 μM) pre-treatment on M1 MDM prior to stimulation with SACM. Data are expressed as. % of vehicle control treated SACM-stimulated M1-like MDM and represent the mean of n=3 independent experiments.

Supplementary Fig. 2

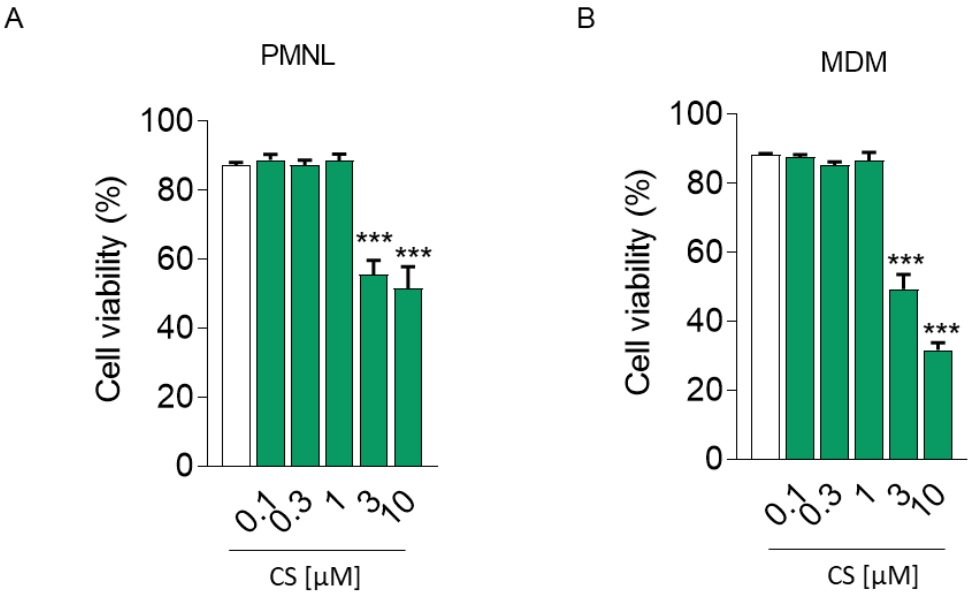

Fig. S2 Effect of CS on cell viability. Evaluation of cell viability after treatment with CS in A) Human PMNL ($2*10^6$ cells/mL) for 90 min and B) $M0_{GM\text{-}CSF}$ MDM for 180min. Cell viability was assessed by trypan blue staining by authomated cell counter. Data are shown as mean ± S.E.M. of n=3. For statistical analysis, ordinary one-way ANOVA has been performed. *p<0.05; **p< 0.01; ***p<0.001 vs vehicle treated cells.

Supplementary Fig. 3

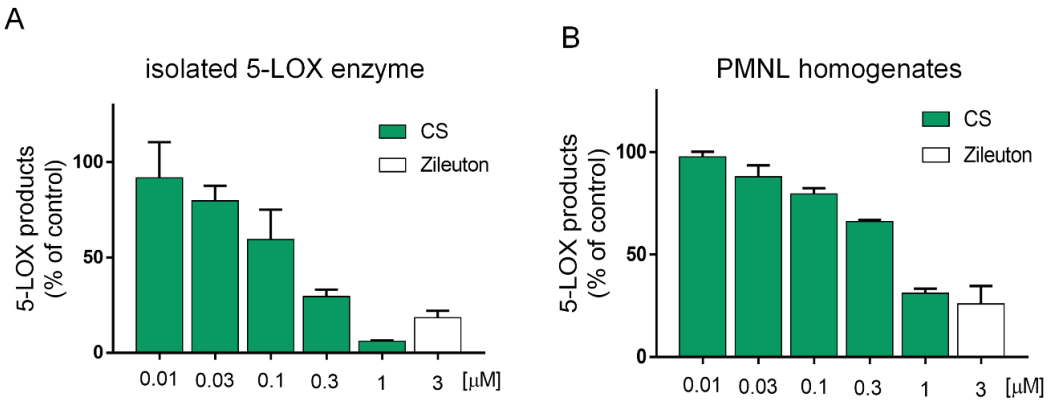

Fig. S3 Effect of CS and zileuton on 5-LOX activity. Inhibition of **A**) isolated human recombinant 5-LOX and **B**) 5-LOX in human PMNL homogenates by CS and zileuton at the indicated concentrations. Data are means ± S.E.M., n=3 independent experiments and expressed as % residual activity versus uninhibited control (DMSO = 100%).

Supplementary Fig. 4

A

0 350 9326

	LM	Vehicle	SACM	Fold
COX	PGE_2	45.4 ± 17.7	768 ± 301	17
	PGD_2	5.3 ± 1.6	91.2 ± 8.6	17
	$PGF_{2\alpha}$	27.8 ± 9.7	369 ± 84.4	13
	TXB_2	480 ± 141	15,457 ± 4,141	32
5-LOX	5-HETE	72.4 ± 32.0	3,091 ± 1,628	43
	5-HEPE	13.5 ± 6.5	806 ± 187	60
	t-LTB_4	62.7 ± 36.2	1,113 ± 322	18
	LTB_4	31.5 ± 17.8	7,218 ± 2,376	229
	7-HDHA	14.9 ± 1.6	307 ± 127	21
12-/15-LOX	17-HDHA	27.0 ± 10.5	5,275 ± 2,697	195
	15-HETE	46.0 ± 15.9	12,523 ± 5,888	272
	15-HEPE	5.4 ± 1.3	1,305 ± 571	242
	14-HDHA	7.3 ± 2.7	1,090 ± 555	149
	12-HETE	8.4 ± 2.6	1,246 ± 951	148
	12-HEPE	2.0 ± 0.6	18,498 ± 8,677	9326
	RvD5	0.9 ± 0.3	263 ± 154	305
Fatty Acids	AA	2,759 ± 950	32,739 ± 20,490	12
	EPA	486 ± 150	87,385 ± 31,148	180
	DHA	2,435 ± 1,148	39,914 ± 6,085	16

B

40 100 160

	LM	Vehicle	CS 1 µM	%
COX	PGE_2	757 ± 251	813 ± 169	107
	PGD_2	22.4 ± 6.5	24.3 ± 5.3	108
	$PGF_{2\alpha}$	43.3 ± 11.5	53.8 ± 6.9	124
	TXB_2	1,883 ± 760	2,063 ± 804	110
5-LOX	5-HETE	1,385 ± 706	893 ± 551	64
	5-HEPE	231 ± 139	134 ± 89.4	58
	t-LTB_4	222 ± 100	93.6 ± 42.8	42
	LTB_4	589 ± 383	254 ± 166	43
	7-HDHA	13.9 ± 3.2	15.8 ± 4.2	114
12-/15-LOX	17-HDHA	40.5 ± 10.5	51.0 ± 9.2	126
	15-HETE	87.1 ± 39.0	113 ± 44.1	129
	15-HEPE	12.2 ± 3.2	15.3 ± 2.5	125
	14-HDHA	10.3 ± 3.4	9.7 ± 3.0	94
	12-HETE	38.0 ± 20.9	34.6 ± 16.4	91
	12-HEPE	9.4 ± 5.6	8.1 ± 4.0	87
Fatty Acids	AA	8,724 ± 2,795	15,450 ± 3,511	177
	EPA	1,665 ± 576	2,514 ± 519	151
	DHA	6,412 ± 1,873	10,239 ± 1,980	160

Fig. S4 Celastrol (CS) modulates LM production in MDM A) Heatmap of M2 MDM stimulated with 1% SACM for 180 min. Fold change vs Vehicle (-); B) Heatmap of M1-like MDM treated with CS (1 µM) 180 min. Data (expressed as pg/2*106 cells) are shown as mean ± S.E.M., n=5 or n=7.

3.3 Manuscript III

Modulation of inflammation-related lipid mediator pathways by celastrol during human macrophage polarization

Kehong Zhang, Paul M. Jordan, Simona Pace, Robert K. Hofstetter, Markus Werner, Xinchun Chen, Oliver Werz (2022)

Journal of Inflammation Research, in press

Here, we studied the long-term effects of CS at a low, sub-cytotoxic concentration (0.2 μM) on LM profiles after manipulation of human MDM during polarization towards M1- and M2-like phenotypes. During M1-MDM polarization, CS significantly reduced gene and enzyme expression of COX-2 and mPGES-1, as well as M1 surface markers, and impeded phosphorylation of NF-κB and p38 MAPK. During M2-MDM polarization, CS decreased the capacity to generate large amounts of almost all LMs, assessed by LM metabololipidomics, including pro-inflammatory COX and 5-LOX products as well the formation of 12-/15-LOX products and SPM, but without affecting the release of fatty acid substrates. To summarize, CS not only favorably affects LOX activities in macrophages but also the expression of LM-biosynthetic enzymes during macrophage polarization which is linked to inflammation-related alterations of LM biosynthesis. The strong impairment of pro-inflammatory mediator levels by CS treatment may be favorable in view of the potential application of CS to treat inflammatory disorders.

Contribution (75%): Cell culture and performance of blood cell isolation, determination of cell viability, cell samples preparation for flow cytometry, SACM preparation, SDS-PAGE and Western blot, determination of LM formation by UPLC-MS/MS, qPCR analysis, analysis of data and preparation of graphs, statistical analysis, writing of the manuscript.

Manuskript III

Titel des Manuskriptes: Modulation of inflammation-related lipid mediator pathways by celastrol during human macrophage polarization

Autoren: Kehong Zhang, Paul M. Jordan, Simona Pace, Robert K. Hofstetter, Markus Werner, Xinchun Chen, Oliver Werz

Bibliographische Informationen In press

Der Kandidat / Die Kandidatin ist (bitte ankreuzen)

☒ Erstautor/-in, ☐ Ko-Erstautor/-in, ☐ Korresp. Autor/-in, ☐ Koautor/-in.

Anteile (in %) der Autoren / der Autorinnen an der Publikation (anzugeben ab 20%)

Autor/-in	Konzeptionell	Datenanalyse	Experimentell	Verfassen des Manuskriptes	Bereitstellung von Material
Kehong Zhang	20%	80%	80%	30%	20%
Oliver Werz	60%			50%	
Others	20%	20%	20%	20%	80%
Total	100%	100%	100%	100%	100%

Modulation of inflammation-related lipid mediator pathways by celastrol during human macrophage polarization

Kehong Zhang[a,b], Paul M. Jordan[a], Simona Pace[a], Robert K. Hofstetter[a], Markus Werner[a], Xinchun Chen[b], Oliver Werz[a,*]

[a]Department of Pharmaceutical/Medicinal Chemistry, Institute of Pharmacy, Friedrich Schiller University Jena, Philosophenweg 14, D-07743 Jena, Germany.

[b]Guangdong Provincial Key Laboratory of Regional Immunity and Diseases, Department of Pathogen Biology, Shenzhen University School of Medicine, Shenzhen 518000, China.

*** Corresponding author:** oliver.werz@uni-jena.de

Abstract

Background and purpose: Celastrol (CS) is a major active ingredient of the Chinese/Asian herb *Tripterygium wilfordii* that is frequently used as phytomedicine to treat inflammation and autoimmune diseases. We showed before that short-term exposure to CS (1 μM) favorably impacts the biosynthesis of inflammation-related lipid mediators (LM) in human polarized macrophages by modulating the activities of different lipoxygenases (LOXs). However, whether CS regulates the expression of LOXs and other related LM-biosynthetic enzymes during macrophage polarization is unknown. Here, we investigated how CS affects LM-biosynthetic enzyme expression on the protein level and studied concomitant LM signature profiles during polarization of human monocyte-derived macrophages (MDM) towards M1- and M2-like phenotypes.

Methods and Results: We used LM metabololipidomics to study long-term effects of CS on LM profile signatures after manipulation of human monocyte-derived macrophages (MDM) during polarization. Exposure of MDM to low concentrations of CS (ie, 0.2 μM) during polarization to an inflammatory M1 phenotype potently suppressed the formation of pro-inflammatory cyclooxygenase (COX)- and 5-LOX-derived LM, especially prostaglandin (PG)E_2. Notably, gene and enzyme expression of COX-2 and microsomal PGE_2 synthase (mPGES)-1 as well as M1 markers were strongly decreased by CS during M1-MDM polarization, along with impaired activation of nuclear factor-κB and p38 mitogen-activated protein kinase. During IL-4-induced M2 polarization, CS decreased the capacity of the resulting M2-MDM to generate pro-inflammatory COX and 5-LOX products as well but it reduced also the formation of 12/15-LOX products and specialized pro-resolving mediators, without affecting the levels of liberated fatty acid substrates.

Conclusions: Depending on the timing and concentration, CS not only favorably affects LOX activities in macrophages but also the expression of LM-biosynthetic enzymes during macrophage polarization connected to changes of inflammation-related LM which might be of relevance for potential application of CS to treat inflammatory disorders.

Keywords: Inflammation, macrophages, lipoxygenase, cyclooxygenase, lipid mediators, specialized pro-resolving mediators, celastrol.

Introduction

Inflammation is an essential immune response to pathogens, tissue injury and other harmful events, in order to remove the stimulus and to accomplish tissue repair and regeneration [1]. Prolonged inflammatory processes can lead to persistent inflammation and tissue damage, and ultimately to chronic diseases [1-4]. Numerous anti-inflammatory drugs, either steroidal or nonsteroidal, have long been applied to treat inflammatory disorders, however, the inevitable and various side effects are limiting their therapeutic use [3,5-9]. In this respect, the discovery of anti-inflammatory agents from natural sources with better tolerability is continuously popular and accepted for modern pharmaceutical therapies [10-13].

Aberrant biosynthesis of lipid mediators (LMs) is causative for many chronic inflammatory diseases [2,14-16]. LMs are generated from polyunsaturated fatty acids (PUFA) in complex networks via cyclooxygenases (COX), lipoxygenases (LOX) and cytochrome P450 enzymes as key players in conjunction with additional LM-biosynthetic enzymes [17-19]. These LMs include on one hand pro-inflammatory eicosanoids that initiate and maintain inflammation but also specialized pro-

resolving mediators (SPMs) promoting the resolution of inflammation and the return to homeostasis on the other [2,16,18]. Pro-inflammatory eicosanoids such as COX-derived prostaglandins (PGs) and 5-LOX-derived leukotrienes (LTs) are derived from arachidonic acid (AA) that is liberated from membrane phospholipids mainly by cytosolic phospholipase (cPL)A_2 upon cell stimulation [20]. Thus, 5-LOX and the inducible COX-2 isoform are major targets to treat pathological inflammation by suppressing the biosynthesis of pro-inflammatory LMs [21]. However, uncontrolled inflammation is now widely appreciated to be promoted also by a deficiency of SPMs including lipoxins (LX), maresins (MaR), protectins (PD), and resolvins (Rv) that all counter-regulate excessive and persistent inflammation and promote its resolution [22-24]. Therefore, pharmacological strategies capable of shifting from formation of pro-inflammatory PGs and LTs to inflammation-resolving SPMs may constitute novel and innovative approaches for intervention with chronic inflammatory diseases [24,25].

Plant-derived pentacyclic triterpenes from the lupane, oleanane and ursane groups possess substantial pharmacological relevance with multi-target properties such as anti-inflammatory, wound healing, anti-bacterial, anti-viral, hepatoprotective and anti-tumoral effects, combined with low toxicity [26-28]. Major representatives with marked anti-inflammatory features encompass betulin/betulinic acid, lupeol, boswellic acids, ursolic acid, glycyrrhetinic acid and oleanolic acid. The pentacyclic triterpenoid quinone methide celastrol (CS) is one major active component contained in the Chinese traditional medicinal plant *Tripterygium wilfordii* Hook F (TwHF) and has been examined for the treatment of various inflammation-associated diseases [29-32]. Like other pentacyclic triterpene acids, CS possesses anti-inflammatory, anti-tumor, anti-oxidant and immunomodulatory activities, and is now being increasingly recognized as a promising clinical candidate for the therapy of autoimmune disease, in particular rheumatoid arthritis (RA) [30,33,34].

The compound has been studied in-depth for interference with pro-inflammatory cytokines and chemokines, and modulation of cellular inflammatory responses [35-37]. But still, the exact mechanisms underlying the beneficial actions of CS in the treatment of inflammatory disease are not entirely clear. Compared to other pentacyclic triterpene acids, CS contains an α,β-unsaturated carbonyl as part of the quinone methide conferring it susceptible to conjugate addition due to the highly electrophilic carbon C-6 [38], and thus CS may differ in its pharmacological profile and target interactions.

With respect to interference with LM biosynthesis, CS is a multi-enzyme inhibitor targeting $sPLA_2$-IIA in addition to 5-LOX and COX-2, supporting its potential as anti-inflammatory drug [39,40]. Moreover, we recently reported that CS at 1 μM promotes SPM biosynthesis by activation of 15-LOX-1 as key enzyme during short-term (3 h) treatment in human monocyte-derived macrophages (MDM) [40]. In mice, CS impaired zymosan-induced LT formation along with elevated levels of SPM and other 12-/15-LOX-derived LM in peritoneal exudates, spleen and plasma *in vivo* [40]. But how CS impacts the LM networks on the protein expression level under long-term treatment has not been elucidated yet. Here we employed human MDM that were polarized towards M1- and M2-like subtypes in order to acquire phenotypic LM profiles [41], and we aimed at elucidating how CS affects LM-biosynthetic enzyme expression on the protein level and concomitant LM signature profiles during macrophage polarization. Our results show for the first time that CS considerably impacts the expression of LM-biosynthetic enzymes during macrophage polarization with implications for the respective LM signature profiles and thus for the occurrence of the macrophage phenotype.

Materials and Methods

Materials

Celastrol (CS; item number 70950) was supplied from Biomol GmbH (Hamburg, Germany). Deuterated and non-deuterated LM standards for ultra-performance liquid chromatography-tandem mass spectrometry (UPLC-MS-MS) were purchased from Cayman Chemicals (Ann Arbor, MI, USA). All other chemicals and reagents were obtained from Sigma-Aldrich (Steinheim, Germany), unless stated otherwise.

Isolation of cells from human blood

Human leukocyte concentrates from freshly withdrawn blood (16 IU heparin/mL) from healthy adult male and female volunteers were obtained from the Department of Transfusion Medicine at the University Hospital of Jena, Germany. The research was conducted in accordance with the Declaration of Helsinki. The research protocols have been approved by the local ethical committee and were performed in accordance with guidelines and regulations; informed consent was obtained. Peripheral blood mononuclear cells (PBMC) were separated by dextran sedimentation, followed by density gradient centrifugation on lymphocyte separation medium (C-44010, Promocell, Heidelberg, Germany). PBMC from the intermediate fraction were washed with PBS pH 5.9/0.9% NaCl (1:1, v/v) and resuspended in PBS pH 7.4 and 1 mM $CaCl_2$. PBMC were finally seeded in RPMI 1640 (Thermo Fisher Scientific, City Schwerte, Germany) containing 10% (v/v) heat-inactivated fetal calf serum (FCS), 2 mM L-glutamine, 100 U/mL penicillin, and 100 µg/mL streptomycin in cell culture flasks (Greiner Bio-one, Frickenhausen, Germany) for 1.5 h at 37 °C and 5% CO_2 for adherence of monocytes.

Differentiation and polarization of human MDM and incubation for LM formation

For differentiation of monocytes to macrophages, $M0_{GM\text{-}CSF}$ and $M0_{M\text{-}CSF}$ were generated by incubating freshly isolated blood monocytes with 20 ng/mL granulocyte macrophage-colony stimulating factor (GM-CSF) or M-CSF (Cell Guidance Systems Ltd., Cambridge, UK), respectively, in RPMI 1640 supplemented with 10% FCS, 2 mmol/L L-glutamine and 100 U/mL penicillin-streptomycin for 6 days. M1-MDM were obtained by incubation of $M0_{GM\text{-}CSF}$ with 100 ng/mL lipopolysaccharide (LPS) and 20 ng/mL interferon (IFN)γ (Peprotech, Hamburg, Germany) for 48 h, while M2-MDM were obtained by incubation of $M0_{M\text{-}CSF}$ with 20 ng/mL interleukin (IL)-4 (Peprotech) for 48 h. To assess effects of CS on LM pathways during macrophage polarization, $M0_{GM\text{-}CSF}$ or $M0_{M\text{-}CSF}$ (2×10^6/mL, each) were pre-treated with CS (0.2 µM) or DMSO (0.1%) as vehicle for 15 min before the addition of polarizing agents. Cell supernatants from treated M1-MDMs and M2-MDMs were carefully removed and cells were further incubated in 1 mL PBS containing 1 mM $CaCl_2$ and kept at 37 °C with or without 1% *Staphylococcus aureus* 6850-conditioned medium (SACM) for another 90 min to generate LM [42]. The reaction was stopped by transferring supernatants (1 mL) into 2 mL ice-cold MeOH, and deuterated LM standards (200 nM d8-5S-HETE, d4-LTB_4, d5-LXA_4, d5-RvD2, d4-PGE_2 and 10 µM d8-AA; Cayman Chemical/Biomol GmbH, Hamburg, Germany) were added. Then, samples were processed for LM analysis by solid phase extraction and UPLC-MS-MS as described below.

Lipid mediator metabololipidomics by UPLC-MS-MS

Samples were kept at −20 °C for at least 60 min to allow for protein precipitation. After centrifugation (1200 × g, 4 °C, 10 min), acidified H_2O (8 mL, final pH = 3.5) was added and samples were subjected to solid phase extraction (Sep-Pak® Vac 6cc 500 mg/6 mL C18; Waters, Milford, MA, USA). Briefly, columns were equilibrated with 6 mL methanol and 2 mL H_2O before sample loading, washed with 6 mL H_2O and 6 mL *n*-hexane, before eluting LMs with 6 mL methyl formate. The eluent was evaporated (TurboVap LV, Biotage, Uppsala, Sweden) and the residue resuspended in 100 µL methanol/water (50/50, v/v) for UPLC-MS-MS analysis using an Acquity™ UPLC (Waters, Milford, MA, USA) and a QTRAP 5500 Mass Spectrometer (ABSciex, Darmstadt, Germany) equipped with a Turbo V™ Source and electrospray ionization. LM were separated on an ACQUITY UPLC® BEH C18 column (1.7 µm, 2.1 mm × 100 mm; Waters, Eschborn, Germany) at 50 °C with a flow rate of 0.3 mL/min and a mobile phase consisting of methanol-water-acetic acid (starting at 42:58:0.01, *v*/*v*/*v*) that was ramped to 86:14:0.01 over 12.5 min and then to 98:2:0.01 for 3 min [43]. The QTRAP 5500 was operated in negative mode using scheduled multiple reaction monitoring (MRM) coupled with information-dependent acquisition. The scheduled MRM window was 60 s, optimized LM parameters were adopted [43], and the curtain gas pressure was set to 35 psi. The retention time and at least six diagnostic ions for each LM were confirmed by means of an external standard (Cayman Chemical/Biomol GmbH, Hamburg, Germany). Quantification was achieved by calibration curves for each LM. Linear calibration curves were obtained for each LM and gave r^2 values of 0.99 [43].

Determination of cell viability by MTT assay

$M0_{GM\text{-}CSF}$ or $M0_{M\text{-}CSF}$ (2×10^5/mL) in a 96-well plate were pre-incubated with 0.1% vehicle (DMSO), 0.2 µM CS or 1% Triton X-100 that was used as positive control, for 15 min. Then, 100 ng/mL LPS and 20 ng/mL IFNγ or 20 ng/mL IL-4 (for M1 and M2 polarization, respectively) were added. After 48 h, calcein-AM and 3-(4,5-dimethylthiazol-2-yl)-2,5-diphenyltetrazolium bromide (MTT, 5 mg/mL, 20 µL; Sigma-Aldrich, Munich, Germany) solution were added in the darkness for 2 – 3 h at 37 °C and 5% CO_2, and formazan product was solubilized with sodium dodecyl sulfate (SDS, 10% in 20 mM HCl). The absorbance was measured at 570 nm using a Multiskan Spectrum microplate reader (Thermo Fisher Scientific, Schwerte, Germany).

Analysis of LM-biosynthetic enzyme expression by SDS-PAGE and Western Blot

$M0_{GM\text{-}CSF}$ and $M0_{M\text{-}CSF}$ MDM (2×10^6/mL) were pre-treated with 0.2 µM CS or 0.1% DMSO as vehicle for 15 min prior to addition of 100 ng/mL LPS plus 20 ng/mL IFNγ or 20 ng/mL IL-4 (for M1- or M2-MDM polarization, respectively) or vehicle for 48 h. Then, cells were lysed as previously described [42] and the protein concentration was determined by DC-protein assay kit (Bio-Rad Laboratories GmbH, Munich, Germany). Lysates were mixed with 4×SDS loading buffer (50 mM Tris-HCl, pH 6.8, 2% (w/v) SDS, 10% (v/v) glycerol, 1% (v/v) β-mercaptoethanol, 12.5 mM EDTA, 0.02% (w/v) bromophenol blue) followed by heating at 95 °C for at least 5 min. Each sample was adjusted to the same amount of protein and separated on 8% (for $cPLA_2\alpha$ and COX-2), 10% (for 15-LOX-1, 15-LOX-2, LTA_4H, phospho-p38 MAPK, p38 MAPK, phospho-NF-κB p65, NF-κB p65), 16% (for COX-1, mPGES-1, 5-LOX and FLAP) SDS-PAGE gels and then blotted onto nitrocellulose membranes (Amersham Protran Supported 0.45 µm nitrocellulose,

GE Healthcare, Freiburg, Germany). The membranes were incubated with the following primary antibodies: rabbit polyclonal anti-cPLA$_2$α,1:1000 (2832S; Cell Signaling Technology); rabbit monoclonal anti-COX-2, 1:1000 (12282S; Cell Signaling Technology); mouse monoclonal anti-15-LOX-1, 1:500 (ab119774; Abcam, Cambridge, UK); rabbit polyclonal anti-15-LOX-2, 1:500 (ab23691; Abcam); rabbit monoclonal anti-LTA$_4$H, 1:1000 (ab133512; Abcam); rabbit polyclonal anti-COX-1, 1:1000 (4841S; Cell Signaling Technology); rabbit polyclonal anti-mPGES-1, 1:5000 (kindly provided by Dr. Per-Johan Jakobsson, Karolinska Institute, Stockholm, Sweden); rabbit polyclonal anti-5-LOX, 1:1000 (to a peptide corresponding to the C-terminal 12 amino acids of 5-LOX: CSPDRIPNSVAI; kindly provided by Dr. M. E. Newcomer, Louisiana State University, Baton Rouge, LA); rabbit polyclonal anti-FLAP, 1:1000 (ab85227; Abcam); rabbit monoclonal anti-p38 MAPK, 1:1000 (8690S; Cell Signaling); rabbit polyclonal anti-phospho-p38 MAPK (Thr180/Tyr182), 1:1000 (9211S; Cell Signaling); rabbit monoclonal anti-NF-κB p65 (C22B4), 1:1000 (4764S; Cell Signaling); mouse monoclonal anti-phospho-NF-κB p65 (Ser536), 1:1000 (13346S; Cell Signaling); mouse monoclonal anti-β-actin, 1:1000 (3700S; Cell Signaling); rabbit monoclonal anti-glyceraldehyde-3-phosphate dehydrogenase (GAPDH), 1:1000 (5174S; Cell Signaling). Immunoreactive bands were stained with IRDye 800CW Goat anti-Mouse IgG (H + L), 1:10,000 (926-32210, LI-COR Biosciences, Lincoln, NE), IRDye 800CW Goat anti-Rabbit IgG (H + L), 1:15,000 (926 32211, LI-COR Biosciences) and/or IRDye 680LT Goat anti-Mouse IgG (H + L), 1:40,000 (926-68020, LI-COR Biosciences), and visualized by an Odyssey infrared imager (LI-COR Biosciences, Lincoln, NE, USA). Data from densitometric analysis were background corrected.

Real time PCR

$M0_{GM\text{-}CSF}$ (10^6/mL) were pre-treated with 0.2 µM CS or 0.1% DMSO as vehicle for 15 min prior to exposure to 100 ng/mL LPS and 20 ng/mL IFNγ. After 0, 6, 24 or 48 h, total RNA was isolated from the cells using E.Z.N.A.® Total RNA Kit I (Omega Bio-tek, Inc. via VWR, Dresden, Germany) according to the manufacturer´s protocol and then quantified by NanoVue (GE Healthcare; Spekol, Analytic Jena, Germany). Reverse transcription reaction was performed with 0.5 to 1.5 µg RNA in a 20 µL reaction using High-Capacity cDNA Reverse Transcription Kit with RNase Inhibitor (Applied Biosystems™ via Thermo Fisher Scientific, Schwerte, Germany) according to the manufacturer's instructions. The qPCR reaction was performed in a qTOWER³ G touch Instrument (Analytik Jena) using the PerfeCTa™ SYBR® Green SuperMix, ROX™ kit (Quantabio via VWR, Dresden, Germany) containing optimized concentrations of $MgCl_2$, dNTPs, AccuStart Taq DNA Polymerase, SYBR Green I dye, ROX Reference Dye, and stabilizers. For qPCR, 25 µL reaction mix containing PerfeCTa SYBR Green SuperMix, ROX (2X), diluted cDNA template and 0.5 µM of forward and reverse primer (listed in **Table 1**) was used. Reaction mixes were prewarmed for 10 min at 95 °C, followed by 40 cycles of denaturation for 15 s at 95 °C, annealing for 30 s at 60 °C and extension for 30 s at 72 °C. Data were collected and processed with qPCRsoft 4.1 software (Analytik Jena). The $2^{-\Delta\Delta CT}$ method was used to calculate relative gene expression levels [44]. GAPDH was used as reference gene. As quality controls, negative control measurements, melting curves analysis and determination of qPCR efficiency by LinRegPCR 2021.1 software (developed by Dr. J. M. Ruijter, Dept. Medical Biology Amsterdam, Academic Medical Centre, University of Amsterdam) [45] were performed.

Flow Cytometry

$M0_{M\text{-}CSF}$ (2×10^6/mL) were treated with CS (0.2 µM) or vehicle (0.1% DMSO) for 48 h. Then, cells were stained in PBS pH 7.4 containing 0.5% bovine serum albumin, 2 mM EDTA and 0.1% sodium azide by Zombie Aqua™ Fixable Viability Kit (Biolegend, San Diego, CA, USA) for 5 min at 4 °C to determine cell viability. Non-specific antibody binding was blocked by using mouse serum (10 min at 4 °C) prior to staining by the following fluorochrome-labelled antibodies (20 min, 4 °C): FITC anti-human CD14 (clone M5E2, #555397, BD Biosciences, San Jose, CA, USA), APC-H7 anti-human CD80 (clone L307.4, #561134, BD Biosciences), PE-Cy7 anti-human CD54 (clone HA58, #353115, Biolegend)), PE anti-human CD163 (clone GHI/61, #556018, BD Biosciences), APC anti-human CD206 (clone 19.2, #550889, BD Biosciences) to determine M1 and M2 surface marker expression using LSRFortessa™ cell analyzer (BD Biosciences), and data were analyzed using FlowJo X Software (BD Biosciences).

Statistical Analysis

Results are expressed as mean ± S.E.M. of each independent experiment, where n represents the indicated numbers from separate donors performed on different days. Statistical analysis and graphs were made by using GraphPad Prism 9 software (San Diego, CA, USA). Paired t-test was used to analyze experiments for comparison of two groups; while one-way ANOVA or multiple paired t-tests were applied for multiple comparisons as indicated. A p-value ≤ 0.05 is a criterion for statistical significance.

Results

Impact of CS on MDM viability and expression of M1- and M2-phenotypic surface markers during polarization

Macrophages exhibit high plasticity where inflammatory M1-like cells strongly express COX-2 and 5-LOX generating mainly PGs/TX and LTs, while anti-inflammatory M2-like phenotypes express abundant 15-LOX-1 and produce substantial amounts of SPMs [41,43,46]. In order to study how CS affects these LM networks and connected LM formation during macrophage polarization, we employed human MDMs that were either polarized for 48 h towards M1- and M2-like phenotypes or left untreated for 48 h, in the presence and absence of CS, with subsequent stimulation by bacterial exotoxins (using SACM) to evoke several LM-biosynthetic pathways [42].

Since CS (at ≥ 3 µM) can be cytotoxic for innate immune cells [40], we first determined its impact on the viability of MDMs during polarization. MDMs, differentiated with GM-CSF ($M0_{GM\text{-}CSF}$) were polarized to M1-MDMs by LPS and IFNγ, while MDMs, differentiated with M-CSF ($M0_{M\text{-}CSF}$) were polarized to M2-MDMs by IL-4. MTT assays after 48 h of polarization showed that CS up to 0.3 µM caused only minor detrimental effects but at ≥ 1 µM CS, the viability of both M1- and M2-MDMs was significantly reduced; the EC_{50} values were determined at 3.5 µM and 2.7 µM for M1- and M2-MDM, respectively (**Fig. 1A,B**). Thus, we limited the concentration of CS to 0.2 µM for subsequent experiments, in order to exclude cytotoxicity as trigger for potential modulatory effects on LM networks.

We then assessed whether CS could affect macrophage polarization, as suggested by others before [37,47]. We studied the expression of CD54 and CD80 as markers for human M1-MDMs and CD163 and CD206 as markers for M2-MDMs [41] in the presence or absence of 0.2 µM CS. We found a

significant reduction of the two M1 markers CD54 and CD80 by CS after 48 h with minor impact on M2 markers, where only CD206 was slightly reduced but not CD163 (**Fig. 1C,D**). These data indicate that CS impairs the polarization towards pro-inflammatory M1-like macrophages, while marginally affecting M2-like markers.

Impact of CS on LM signature profiles in human M1-like MDM

In order to study how CS affects LM signature profiles of M1-like MDMs, we used $M0_{GM\text{-}CSF}$ that were pre-incubated (15 min) with 0.2 µM CS and then polarized for 48 h with LPS/IFNγ towards M1-MDMs or left unpolarized. Afterwards, LM biosynthesis was assessed in unstimulated or SACM-challenged MDMs upon incubation for another 90 min. In agreement with results from previous studies [40-43], polarization to M1-MDMs led to high amounts of COX products (PGE_2, PGD_2, $PGF_2\alpha$, TXB_2, 11-HEPE and 11-HETE), formed even in the absence SACM as stimulus, especially PGE_2 (**Fig. 2**, **Table 2**). Also, the capacity to generate 5-LOX products (LTB_4, t-LTB_4, 5-HETE, 5-HEPE) and to release the PUFAs AA, eicosapentaenoic acid (EPA) and docosahexaenoic acid (DHA) was strongly upregulated during polarization and further elevated by subsequent SACM-challenge (**Fig. 2**, **Table 2**). A similar pattern was observed for generation of 12/15-LOX products (**Fig. 2**), although the overall amounts of these LMs were comparably low (**Table 2**).

CS (0.2 µM) suppressed the strong formation of COX products in M1-MDMs by about 50% regardless of SACM-challenge, while in unpolarized MDMs, CS was without marked effects after 48 h incubation (**Fig. 2**, **Table 2A,B**). Most striking (> 60%) inhibition was evident for PGE_2 (**Table 2B**). Formation of 5-LOX products (LTB_4, t-LTB_4, 5-HETE, 5-HEPE) was less affected

by CS, with major effects in unpolarized/unstimulated cells and in SACM-activated M1-MDMs (**Fig. 2, Table 2B**). A similar pattern was found for modulation of 12/15-LOX products (14-HDHA, 12-HETE, 12-HEPE, 17-HDHA, 15-HETE and 15-HEPE) by CS, although it should be noted that unstimulated cells produced rather low amounts of several 12/15-LOX products (eg, 15-HEPE, 14-HDHA, 12-HEPE; **Table 2A,B**) due to minute protein levels of the 12- and 15-LOXs in M1-MDMs [41,43]. Suppression of 12/15-LOX products in SACM-activated M1-MDMs by CS was evident only for the substantially formed 15-HETE (**Table 2B**) that can be generated in M1-MDMs as 15(*R*)-HETE by COX enzymes [43]. Liberation of PUFA, regardless of the experimental conditions, was not significantly altered by CS (**Fig. 2, Table 2A,B**). Together, CS efficiently repressed the strong COX product formation acquired during M1 polarization, especially of PGE_2, with a tendency of reduced 5-LOX and 12/15-LOX product levels in M1-MDMs when elicited by SACM.

Impact of CS on LM profiles in anti-inflammatory M2-like MDM

We then assessed the effects of CS on LM formation in M2-like MDMs using $M0_{M\text{-}CSF}$ that were pre-incubated (15 min) with 0.2 µM CS, polarized for 48 h towards M2-MDMs or left untreated (= unpolarized), and LM biosynthesis was then assessed in unstimulated or SACM-challenged cells after 90 min incubation. Except TXB_2, only relatively low amounts of COX, 5-LOX and 12/15-LOX products were formed in unpolarized $M0_{M\text{-}CSF}$ or M2-MDMs (cultured for 48 h) that received no SACM (**Table 3, Fig. 3A**). However, challenge with SACM strikingly induced formation of essentially all LMs regardless of polarization. As reported before [40-43], M2-MDMs produced much higher amounts of 12/15-LOX products and SPMs compared to M1-MDMs, especially upon challenge with SACM (**Table 3B**).

In the presence of CS, unpolarized $M0_{M\text{-}CSF}$ or M2-MDMs (that generated low amounts of LMs) were hardly and inconsistently affected, without significant modulation of LM biosynthesis, albeit levels of free PUFAs were elevated (**Table 3A**, **Fig. 3**). However, in case of SACM stimulation, treatment of MDMs (unpolarized or M2 cells) with CS for 48 h suppressed the subsequent COX and 5-LOX product formation, most prominently for 5-LOX products in unpolarized $M0_{M\text{-}CSF}$. Also, a tendency for reduced 12/15-LOX product formation was obvious in SACM-challenged cells due to CS, and formation of the detectable SPM, that is, PDX, RvD5, MaR2 and RvE4 as well as their monohydroxylated precursors 17-HDHA, 14-HDHA and 15-HEPE were suppressed by CS (**Table 3B**). Note that despite the suppressive effects of CS on generation of essentially all COX/LOX products upon challenge with SACM, the levels of free PUFAs remained mainly unaffected by CS (**Fig. 3**). Taken together, incubation of $M0_{M\text{-}CSF}$ in the presence of CS with or without polarization agent IL-4 strongly suppresses the subsequent capacity to generate massive COX and 5-LOX products as well as SPMs elicited by SACM-challenge.

Effect of CS on the expression of LM-biosynthetic enzymes in human MDM

Since CS markedly affected LM pathways during MDMs culture and polarization with mainly suppressive outcome, it appeared reasonable that CS may compromise the expression level of the respective LM-biosynthetic enzymes during the incubations. Thus, we assessed the protein levels of the enzymes in M1- and M2-MDMs by Western Blot which are relevant for the biosynthesis of those LMs that were affected by CS, namely $cPLA_2$, 5-LOX, FLAP, LTA_4H, 15-LOX-1 (only in M2-MDMs), mPGES-1 (only in M1-MDMs), COX-1, COX-2, and 15-LOX-2. $M0_{GM\text{-}CSF}$ and $M0_{M\text{-}CSF}$ were pretreated (15 min) with 0.2 µM CS and then kept for 48 h with and without polarizing agents (LPS/IFNγ for M1; IL-4 for M2). In the absence of LPS/IFNγ, CS did not affect

protein levels of any of the LM-biosynthetic enzymes in $M0_{GM\text{-}CSF}$ within 48 h (**Fig. 4A,B**). However, the upregulated expression of COX-2 obtained during polarization of $M0_{GM\text{-}CSF}$ towards M1-MDMs, was significantly reduced by CS, with concomitant decrease of mPGES-1 protein, but without alteration of the levels other enzymes (ie, $cPLA_2$, 5-LOX, FLAP, LTA_4H, 15-LOX-2, COX-1) (**Fig. 4A,B**). In analogy to $M0_{GM\text{-}CSF}$ the protein levels after 48 h culture of $M0_{M\text{-}CSF}$ were not significantly affected by CS (**Fig. 4C,D**). When $M0_{M\text{-}CSF}$ were polarized towards M2-MDMs with IL-4 for 48 h, the presence of CS caused a tendency for reduced protein levels of most of the enzymes, except for LTA_4H, being most pronounced and significant for 15-LOX-1 and -2 (**Fig. 4C,D**). Conclusively, CS clearly impairs COX-2 and mPGES-1 protein during M1 polarization with minor inhibitory effects on $cPLA_2$ and 5-LOX but markedly on 15-LOX-1 and -2 during polarization towards M2, which fits well to the strong suppression of COX product formation, especially of PGE_2, in M1- and overall decreased LM formation in M2-MDMs after SACM-challenge, respectively.

Since COX-2 and mPGES-1 are known to be upregulated during M1 macrophage polarization [48] and because CS efficiently impaired COX-2 and mPGES-1 protein levels in M1-MDMs, we investigated if CS would affect these enzymes also on the mRNA level. Analysis by qPCR showed that CS downregulated both PTGS2 (COX-2) and PTGES (mPGES-1) during M1-MDM polarization, after 6 and 24 h (**Fig. 4E**). These data suggest that CS interferes with COX-2, and to a lesser extent with mPGES-1, at the transcription level, with respective consequences for COX-2/mPGES-1 protein and COX-2 product formation.

Effects of CS on the activation of NF-κB and p38 MAPK in human MDMs

LPS-stimulated phosphorylation (and thus activation) of NF-κB and p38 MAPK is crucial for COX-2 expression in macrophages [49,50]. Accordingly, the phosphorylation of NF-κB p65 was increased upon LPS/IFNγ-treatment of $M0_{GM\text{-}CSF}$ after 3 and 6 h. This was clearly reduced when 0.2 μM CS was included during the incubation (**Fig. 5A**). Phosphorylation of p38 MAPK was slightly elevated by LPS/IFNγ-treatment after 6 h (but not yet after 3 h), and again, CS impaired this stimulatory effect (**Fig. 5B**). Together, these data suggest that CS may block the phosphorylation of both NF-κB p65 and p38 MAPK during M1-polariaztion of human MDMs which may result in impaired expression of COX-2.

Discussion

Here we show that CS from anti-rheumatic *Tripterygium wilfordii* modulates the biosynthetic pathways of pro-inflammatory and anti-inflammatory LMs which are acquired during macrophage polarization. When human MDMs were polarized to the M1 phenotype, CS markedly suppressed the capacity for exotoxin-elicited formation of pro-inflammatory COX products, especially of PGE_2, and to a minor extent also of 5-LOX-derived LM such as LTB_4. Accordingly, CS markedly decreased the protein levels of COX-2 and mPGES-1 with moderate suppression of 5-LOX during M1-MDM polarization, in parallel to impaired expression of M1 phenotypic surface markers. Similarly, during polarization of MDMs towards the M2 phenotype, CS suppressed the capacity of exotoxin-challenged cells to generate COX and 5-LOX products but also SPM formation was considerably inhibited along with impaired 15-LOX-1 and -2 protein levels. Since pro-inflammatory PG and LT are typical features of M1 macrophages [41], lowering these LM by CS

confirms impaired M1 polarization. Thus, our data suggest mainly anti-inflammatory properties of CS by suppressing pro-inflammatory LM pathways in M1-like macrophages, but they imply also an impact of CS on inflammation resolution by impairing the acquired capacity for pronounced SPM generation in M2 macrophages by down-regulating 15-LOX-1/2.

CS was recently shown to promote a switch from LT biosynthesis to formation of SPM and other 12/15-LOX-derived LM in short-term (3 h) incubations when given to polarized MDMs that either were in a resting state or stimulated by SACM [40]. These effects were traced back to direct interference of CS with 5-LOX and 15-LOX-1. Also, after short-term (2.5 h) treatment of mice, CS given intraperitoneally impaired zymosan-induced LT formation and simultaneously elevated the levels of SPM and related 12-/15-LOX-derived LM in peritoneal exudates, spleen and plasma [40]. Under these short-term conditions, CS appears to act as direct enzyme modulator, inhibiting 5-LOX activity with reduced LTB_4 levels but promoting 15-LOX-1 activation yielding elevated SPM concentrations. Such LM class switch from pro-inflammatory to pro-resolving LOX-derived LM is considered as innovative pharmacological strategy for actively promoting the resolution of inflammation [23-25]. In the present study, where CS was evaluated in long-term incubations during macrophage polarization, the compound affected the protein level of the LM biosynthetic enzymes with consequent changes in the LM profiles upon subsequent cell stimulation. CS-containing *Tripterygium wilfordii* glycosides (TWG) also efficiently suppressed agonist-induced formation of 5-LOX products during short-term incubations of M1-MDMs and neutrophils while pronounced SPM formation and 12/15-LOX products were evident in M2-MDMs [51]. Note that in analogy to our present data with CS, during 48 h M1-MDM polarization these TWG decreased the capacity to generate 5-LOX and COX products and impaired COX-2 and mPGES-1 protein levels as well as M1 markers [51].

Our results suggest that the suppression of the COX-2 and mPGES-1 protein levels by CS during M1 polarization is due to inhibition of the NF-κB and, at least to some extent, of the p38 MAPK pathways. COX-2 and mPGES-1 are upregulated during M1 macrophage polarization [48] and NF-κB and p38 MAPK are known to be required for induction of COX-2 expression in macrophages by LPS [49,50], the agent used together with IFNγ to trigger M1-MDM polarization. Previous studies demonstrated that CS could control macrophage polarization through modulating the cross-talk among LPS-stimulated MAPKs (ie, p38 MAPK, ERK1/2, JNK) and nuclear translocation of NF-κB p65 and other transcription factor-related axes [37,52]. The α,β-unsaturated carbonyl of the quinone methide of CS confers its position C-6 highly electrophilic and thus susceptible for conjugation to cysteine thiols, whereby CS targets the early virus-encoded protein Tat [53] and proteostasis [38]. In fact, NF-κB contains redox-regulated cysteine residues and covalently modification of the thiol moieties (e.g. by S-nitrosylation at Cys-62 [54]) results in the inhibition of NF-κB DNA recognition and binding [55]. Possibly, CS binds these crucial thiols of the reactive cysteine residues in NF-κB thereby suppressing its signaling activity.Macrophage polarization towards functionally opposite phenotypes is eventually caused by the activation of different signaling pathways, transcription factors and cytokine secretion, which are of importance for the progression and resolution of inflammatory responses of various human diseases [56-58]. Canonically activated macrophages (M1-like) often exhibit antibacterial and antitumor functions, and are characterized by a high production of various pro-inflammatory cytokines as well as PGs and LTs [41,46,56]. On the other hand, alternatively activated macrophages (M2-like) are regarded as anti-inflammatory phenotypes involved in immunosuppression and tissue repair, producing anti-inflammatory cytokines and numerous SPMs [41,46,56,59]. Our current data suggest that CS may govern the balance of macrophage polarization suppressing the occurrence of a M1-like phenotype

since the characteristic upregulation of COX-2 and mPGES-1 as well as CD54 and CD80 were prevented by CS during M1 polarization. This is supported by findings in mice, where CS blocked M1 polarization in diet-induced obese animals [37], and when loaded in nanomicelles, reduced the expression of the M1 biomarkers TNF-α, IL-1β, IL-6, and inducible nitric oxide synthase [47]. In our hands, CS did not or hardly affect the M2-like markers CD163 and CD206, but impaired the expression levels of the 15-LOX-1 and 15-LOX-2 that are key enzymes in SPM biosynthesis [60,61], and where at least 15-LOX-1 protein is strongly upregulated in human M2-MDMs [41]. Similarly, in diet-induced obese mice, the expression of the M2 biomarkers arginase-1 and IL-10 were only marginally altered by CS, while M1 markers were strikingly impaired [47]. Another study demonstrated that CS protects against acute ischemic stroke-induced brain injury by promoting microglia/macrophage M2 polarization [62]. Our results show that M2 polarization in the presence of CS impaired the capacity to produce SPMs upon exotoxin challenge of M2-MDMs, which implies rather detrimental consequences for inflammation resolution. Moreover, CS significantly impaired the viability of M1- and M2-MDMs during long-term (48 h) incubations at concentrations ≥ 1 μM, which is in agreement with the well-known toxicity of CS [63] and thus further questions the pharmacotherapeutic safety of this natural product. It is interesting that a variety of nanotechnology-based CS formulations have been developed that were able to reduce the toxicity and/or improved bioavailability [64]. Future investigations of nanotechnology-based CS formulations in our experimental systems of macrophage polarization and LM biosynthesis might reveal if cytotoxicity and SPM-impairing effects may be circumvented. Indeed, drug delivery by nanofluids improved the efficacy of isoniazid [65] or of bromocriptine [66], and encapsulation of a cytotoxic indirubin derivative into polymer-based nanoparticles reduced its detrimental impact on monocyte viability [67].

Conclusions

Our data show that CS considerably impacts the expression of LM-biosynthetic enzymes during macrophage polarization with implications for the subsequent LM signature profiles produced by these cells after adequate challenge. In particular, CS mainly blocked the upregulation of the inducible COX-2 and mPGES-1 in inflammatory M1-MDMs along with strong suppression of the respective pro-inflammatory LM, namely PGE_2. Although CS hardly affected polarization to the M2 phenotype, it clearly impaired the capacity to produce SPMs along with reduced expression of 15-LOX-1 and -2. Therefore, despite the favorable anti-inflammatory properties of CS due to interference with pro-inflammatory LM pathways in M1-like macrophages, a detrimental impact on inflammation resolution due to the suppression of SPM generation should be considered in the overall judgment of the pharmacological profile of this natural product.

Data Sharing Statement

The datasets generated and analyzed in this study will be available by the corresponding author upon reasonable request.

Acknowledgments

The authors thank Anna König, Heidi Traber, Petra Wiecha, Katrin Fischer and Alrun Schumann for expert technical assistance.

Author Contributions

All authors significantly contributed to the reported work related to the conception, study design, execution, acquisition of data, analysis and interpretation; took part in drafting, revising or critically reviewing the article; gave final approval of the manuscript; have agreed on the journal to which the article has been submitted; agree to be accountable for all aspects of the work.

Funding

This work was supported by the Free State of Thuringia and the European Social Fund (2019 FGR 0095) and by the Deutsche Forschungsgemeinschaft (DFG), Collaborative Research Center SFB 1278 "PolyTarget" (project number 316213987, project A04) and - SFB 1127 "ChemBioSys" (project number 239748522, project A04).

Disclosure

The authors declare no conflicts of interest in this work

References

1. Medzhitov R. Origin and physiological roles of inflammation. *Nature*. Jul 24 2008;454(7203):428-35. doi:10.1038/nature07201
2. Serhan CN. Pro-resolving lipid mediators are leads for resolution physiology. *Nature*. Jun 5 2014;510(7503):92-101. doi:10.1038/nature13479
3. Tabas I, Glass CK. Anti-inflammatory therapy in chronic disease: challenges and opportunities. *Science*. Jan 11 2013;339(6116):166-72. doi:10.1126/science.1230720
4. Furman D, Campisi J, Verdin E, et al. Chronic inflammation in the etiology of disease across the life span. *Nat Med*. Dec 2019;25(12):1822-1832. doi:10.1038/s41591-019-0675-0

5. Mahesh G, Anil Kumar K, Reddanna P. Overview on the Discovery and Development of Anti-Inflammatory Drugs: Should the Focus Be on Synthesis or Degradation of PGE2? *J Inflamm Res*. 2021;14:253-263. doi:10.2147/JIR.S278514
6. Patil KR, Mahajan UB, Unger BS, et al. Animal Models of Inflammation for Screening of Anti-inflammatory Drugs: Implications for the Discovery and Development of Phytopharmaceuticals. *Int J Mol Sci*. Sep 5 2019;20(18)doi:10.3390/ijms20184367
7. Rainsford KD. Anti-inflammatory drugs in the 21st century. *Subcell Biochem*. 2007;42:3-27.
8. Sostres C, Gargallo CJ, Arroyo MT, Lanas A. Adverse effects of non-steroidal anti-inflammatory drugs (NSAIDs, aspirin and coxibs) on upper gastrointestinal tract. *Best Pract Res Clin Gastroenterol*. Apr 2010;24(2):121-32. doi:10.1016/j.bpg.2009.11.005
9. Peres MF, Ribeiro FV, Ruiz KG, Nociti FH, Jr., Sallum EA, Casati MZ. Steroidal and non-steroidal cyclooxygenase-2 inhibitor anti-inflammatory drugs as pre-emptive medication in patients undergoing periodontal surgery. *Braz Dent J*. 2012;23(6):621-8. doi:10.1590/s0103-64402012000600001
10. Kishore N, Kumar P, Shanker K, Verma AK. Human disorders associated with inflammation and the evolving role of natural products to overcome. *Eur J Med Chem*. Oct 1 2019;179:272-309. doi:10.1016/j.ejmech.2019.06.034
11. Koeberle A, Werz O. Multi-target approach for natural products in inflammation. *Drug Discov Today*. Dec 2014;19(12):1871-82. doi:10.1016/j.drudis.2014.08.006
12. Mishra BB, Tiwari VK. Natural products: an evolving role in future drug discovery. *Eur J Med Chem*. Oct 2011;46(10):4769-807. doi:10.1016/j.ejmech.2011.07.057
13. Furst R, Zundorf I. Plant-derived anti-inflammatory compounds: hopes and disappointments regarding the translation of preclinical knowledge into clinical progress. *Mediators Inflamm*. 2014;2014:146832. doi:10.1155/2014/146832
14. Bennett M, Gilroy DW. Lipid Mediators in Inflammation. *Microbiol Spectr*. Nov 2016;4(6)doi:10.1128/microbiolspec.MCHD-0035-2016
15. Chiurchiu V, Leuti A, Maccarrone M. Bioactive Lipids and Chronic Inflammation: Managing the Fire Within. *Front Immunol*. 2018;9:38. doi:10.3389/fimmu.2018.00038
16. Dennis EA, Norris PC. Eicosanoid storm in infection and inflammation. *Nat Rev Immunol*. Aug 2015;15(8):511-23. doi:10.1038/nri3859
17. Calder PC. Eicosanoids. *Essays Biochem*. Sep 23 2020;64(3):423-441. doi:10.1042/EBC20190083
18. Chiang N, Serhan CN. Specialized pro-resolving mediator network: an update on production and actions. *Essays Biochem*. Sep 23 2020;64(3):443-462. doi:10.1042/EBC20200018

19. Christie WW, Harwood JL. Oxidation of polyunsaturated fatty acids to produce lipid mediators. *Essays Biochem*. Sep 23 2020;64(3):401-421. doi:10.1042/EBC20190082
20. Leslie CC. Cytosolic phospholipase A(2): physiological function and role in disease. *J Lipid Res*. Aug 2015;56(8):1386-402. doi:10.1194/jlr.R057588
21. Sala A, Proschak E, Steinhilber D, Rovati GE. Two-pronged approach to anti-inflammatory therapy through the modulation of the arachidonic acid cascade. *Biochem Pharmacol*. Dec 2018;158:161-173. doi:10.1016/j.bcp.2018.10.007
22. Dalli J, Serhan CN. Identification and structure elucidation of the pro-resolving mediators provides novel leads for resolution pharmacology. *Br J Pharmacol*. Apr 2019;176(8):1024-1037. doi:10.1111/bph.14336
23. Serhan CN, Gupta SK, Perretti M, et al. The Atlas of Inflammation Resolution (AIR). *Mol Aspects Med*. Aug 2020;74:100894. doi:10.1016/j.mam.2020.100894
24. Serhan CN, Levy BD. Resolvins in inflammation: emergence of the pro-resolving superfamily of mediators. *J Clin Invest*. Jul 2 2018;128(7):2657-2669. doi:10.1172/JCI97943
25. Gilbert NC, Newcomer ME, Werz O. Untangling the web of 5-lipoxygenase-derived products from a molecular and structural perspective: the battle between pro- and anti-inflammatory lipid mediators. *Biochem Pharmacol*. Sep 3 2021:114759. doi:10.1016/j.bcp.2021.114759
26. Ghiulai R, Rosca OJ, Antal DS, et al. Tetracyclic and Pentacyclic Triterpenes with High Therapeutic Efficiency in Wound Healing Approaches. *Molecules*. Nov 26 2020;25(23)doi:10.3390/molecules25235557
27. Laszczyk MN. Pentacyclic triterpenes of the lupane, oleanane and ursane group as tools in cancer therapy. *Planta Med*. Dec 2009;75(15):1549-60. doi:10.1055/s-0029-1186102
28. Safayhi H, Sailer ER. Anti-inflammatory actions of pentacyclic triterpenes. *Planta Med*. Dec 1997;63(6):487-93. doi:10.1055/s-2006-957748
29. Salminen A, Lehtonen M, Paimela T, Kaarniranta K. Celastrol: Molecular targets of Thunder God Vine. *Biochem Biophys Res Commun*. Apr 9 2010;394(3):439-42. doi:10.1016/j.bbrc.2010.03.050
30. Cascao R, Fonseca JE, Moita LF. Celastrol: A Spectrum of Treatment Opportunities in Chronic Diseases. *Front Med (Lausanne)*. 2017;4:69. doi:10.3389/fmed.2017.00069
31. Chen SR, Dai Y, Zhao J, Lin L, Wang Y, Wang Y. A Mechanistic Overview of Triptolide and Celastrol, Natural Products from Tripterygium wilfordii Hook F. *Front Pharmacol*. 2018;9:104. doi:10.3389/fphar.2018.00104
32. Ng SW, Chan Y, Chellappan DK, et al. Molecular modulators of celastrol as the keystones for its diverse pharmacological activities. *Biomed Pharmacother*. Jan 2019;109:1785-1792. doi:10.1016/j.biopha.2018.11.051

33. Song X, Zhang Y, Dai E, Du H, Wang L. Mechanism of action of celastrol against rheumatoid arthritis: A network pharmacology analysis. *Int Immunopharmacol*. Sep 2019;74:105725. doi:10.1016/j.intimp.2019.105725
34. Venkatesha SH, Dudics S, Astry B, Moudgil KD. Control of autoimmune inflammation by celastrol, a natural triterpenoid. *Pathog Dis*. Aug 2016;74(6)doi:10.1093/femspd/ftw059
35. Kannaiyan R, Shanmugam MK, Sethi G. Molecular targets of celastrol derived from Thunder of God Vine: potential role in the treatment of inflammatory disorders and cancer. *Cancer Lett*. Apr 1 2011;303(1):9-20. doi:10.1016/j.canlet.2010.10.025
36. Lee JY, Lee BH, Kim ND, Lee JY. Celastrol blocks binding of lipopolysaccharides to a Toll-like receptor4/myeloid differentiation factor2 complex in a thiol-dependent manner. *J Ethnopharmacol*. Aug 22 2015;172:254-60. doi:10.1016/j.jep.2015.06.028
37. Luo D, Guo Y, Cheng Y, Zhao J, Wang Y, Rong J. Natural product celastrol suppressed macrophage M1 polarization against inflammation in diet-induced obese mice via regulating Nrf2/HO-1, MAP kinase and NF-kappaB pathways. *Aging (Albany NY)*. Oct 16 2017;9(10):2069-2082. doi:10.18632/aging.101302
38. Boridy S, Le PU, Petrecca K, Maysinger D. Celastrol targets proteostasis and acts synergistically with a heat-shock protein 90 inhibitor to kill human glioblastoma cells. *Cell Death Dis*. May 8 2014;5:e1216. doi:10.1038/cddis.2014.182
39. Joshi V, Venkatesha SH, Ramakrishnan C, et al. Celastrol modulates inflammation through inhibition of the catalytic activity of mediators of arachidonic acid pathway: Secretory phospholipase A2 group IIA, 5-lipoxygenase and cyclooxygenase-2. *Pharmacol Res*. Nov 2016;113(Pt A):265-275. doi:10.1016/j.phrs.2016.08.035
40. Pace S, Zhang K, Jordan PM, et al. Anti-inflammatory celastrol promotes a switch from leukotriene biosynthesis to formation of specialized pro-resolving lipid mediators. *Pharmacol Res*. May 2021;167:105556. doi:10.1016/j.phrs.2021.105556
41. Werz O, Gerstmeier J, Libreros S, et al. Human macrophages differentially produce specific resolvin or leukotriene signals that depend on bacterial pathogenicity. *Nat Commun*. Jan 4 2018;9(1):59. doi:10.1038/s41467-017-02538-5
42. Jordan PM, Gerstmeier J, Pace S, et al. Staphylococcus aureus-Derived alpha-Hemolysin Evokes Generation of Specialized Pro-resolving Mediators Promoting Inflammation Resolution. *Cell Rep*. Oct 13 2020;33(2):108247. doi:10.1016/j.celrep.2020.108247
43. Werner M, Jordan PM, Romp E, et al. Targeting biosynthetic networks of the proinflammatory and proresolving lipid metabolome. *FASEB J*. May 2019;33(5):6140-6153. doi:10.1096/fj.201802509R

44. Livak KJ, Schmittgen TD. Analysis of Relative Gene Expression Data Using Real-Time Quantitative PCR and the 2−ΔΔCT Method. *Methods*. 2001/12/01/ 2001;25(4):402-408. doi:https://doi.org/10.1006/meth.2001.1262
45. Ruijter JM, Ramakers C, Hoogaars WM, et al. Amplification efficiency: linking baseline and bias in the analysis of quantitative PCR data. *Nucleic Acids Res*. Apr 2009;37(6):e45. doi:10.1093/nar/gkp045
46. Dalli J, Serhan CN. Specific lipid mediator signatures of human phagocytes: microparticles stimulate macrophage efferocytosis and pro-resolving mediators. *Blood*. Oct 11 2012;120(15):e60-72. doi:10.1182/blood-2012-04-423525
47. Zhao J, Luo D, Zhang Z, et al. Celastrol-loaded PEG-PCL nanomicelles ameliorate inflammation, lipid accumulation, insulin resistance and gastrointestinal injury in diet-induced obese mice. *J Control Release*. Sep 28 2019;310:188-197. doi:10.1016/j.jconrel.2019.08.026
48. Mosca M, Polentarutti N, Mangano G, et al. Regulation of the microsomal prostaglandin E synthase-1 in polarized mononuclear phagocytes and its constitutive expression in neutrophils. *J Leukoc Biol*. Aug 2007;82(2):320-6. doi:10.1189/jlb.0906576
49. D'Acquisto F, Iuvone T, Rombola L, Sautebin L, Di Rosa M, Carnuccio R. Involvement of NF-kappaB in the regulation of cyclooxygenase-2 protein expression in LPS-stimulated J774 macrophages. *FEBS Lett*. Nov 24 1997;418(1-2):175-8. doi:10.1016/s0014-5793(97)01377-x
50. Takada Y, Aggarwal BB. Genetic deletion of the tumor necrosis factor receptor p60 or p80 sensitizes macrophages to lipopolysaccharide-induced nuclear factor-kappa B, mitogen-activated protein kinases, and apoptosis. *J Biol Chem*. Jun 27 2003;278(26):23390-7. doi:10.1074/jbc.M213237200
51. Zhang K, Pace S, Jordan PM, et al. Beneficial Modulation of Lipid Mediator Biosynthesis in Innate Immune Cells by Antirheumatic Tripterygium wilfordii Glycosides. *Biomolecules*. May 17 2021;11(5)doi:10.3390/biom11050746
52. Ma X, Xu L, Alberobello AT, et al. Celastrol Protects against Obesity and Metabolic Dysfunction through Activation of a HSF1-PGC1alpha Transcriptional Axis. *Cell Metab*. Oct 6 2015;22(4):695-708. doi:10.1016/j.cmet.2015.08.005
53. Narayan V, Ravindra KC, Chiaro C, et al. Celastrol inhibits Tat-mediated human immunodeficiency virus (HIV) transcription and replication. *J Mol Biol*. Jul 29 2011;410(5):972-83. doi:10.1016/j.jmb.2011.04.013
54. Marshall HE, Hess DT, Stamler JS. S-nitrosylation: physiological regulation of NF-kappaB. *Proc Natl Acad Sci U S A*. Jun 15 2004;101(24):8841-2. doi:10.1073/pnas.0403034101
55. Pande V, Sousa SF, Ramos MJ. Direct covalent modification as a strategy to inhibit nuclear factor-kappa B. *Curr Med Chem*. 2009;16(32):4261-73. doi:10.2174/092986709789578222

56. Murray PJ. Macrophage Polarization. *Annu Rev Physiol*. Feb 10 2017;79:541-566. doi:10.1146/annurev-physiol-022516-034339
57. Sica A, Mantovani A. Macrophage plasticity and polarization: in vivo veritas. *J Clin Invest*. Mar 2012;122(3):787-95. doi:10.1172/JCI59643
58. Martinez FO, Gordon S. The M1 and M2 paradigm of macrophage activation: time for reassessment. *F1000Prime Rep*. 2014;6:13. doi:10.12703/P6-13
59. Dalli J, Serhan C. Macrophage Proresolving Mediators-the When and Where. *Microbiol Spectr*. Jun 2016;4(3)doi:10.1128/microbiolspec.MCHD-0001-2014
60. Jordan PM, Werz O. Specialized pro-resolving mediators: biosynthesis and biological role in bacterial infections. *FEBS J*. Nov 6 2021;doi:10.1111/febs.16266
61. Perry SC, Kalyanaraman C, Tourdot BE, et al. 15-Lipoxygenase-1 biosynthesis of 7S,14S-diHDHA implicates 15-lipoxygenase-2 in biosynthesis of resolvin D5. *J Lipid Res*. Jul 2020;61(7):1087-1103. doi:10.1194/jlr.RA120000777
62. Jiang M, Liu X, Zhang D, et al. Celastrol treatment protects against acute ischemic stroke-induced brain injury by promoting an IL-33/ST2 axis-mediated microglia/macrophage M2 polarization. *J Neuroinflammation*. Mar 14 2018;15(1):78. doi:10.1186/s12974-018-1124-6
63. Hou W, Liu B, Xu H. Celastrol: Progresses in structure-modifications, structure-activity relationships, pharmacology and toxicology. *Eur J Med Chem*. Mar 1 2020;189:112081. doi:10.1016/j.ejmech.2020.112081
64. Wagh PR, Desai P, Prabhu S, Wang J. Nanotechnology-Based Celastrol Formulations and Their Therapeutic Applications. *Front Pharmacol*. 2021;12:673209. doi:10.3389/fphar.2021.673209
65. Zomorodbakhsh S, Abbasian Y, Naghinejad M, Sheikhpour M. The Effects Study of Isoniazid Conjugated Multi-Wall Carbon Nanotubes Nanofluid on Mycobacterium tuberculosis. *Int J Nanomedicine*. 2020;15:5901-5909. doi:10.2147/IJN.S251524
66. Kamazani FM, Sotoodehnejad Nematalahi F, Siadat SD, Pornour M, Sheikhpour M. A success targeted nano delivery to lung cancer cells with multi-walled carbon nanotubes conjugated to bromocriptine. *Sci Rep*. Dec 24 2021;11(1):24419. doi:10.1038/s41598-021-03031-2
67. Czapka A, Grune C, Schadel P, et al. Drug delivery of 6-bromoindirubin-3'-glycerol-oxime ether employing poly(D,L-lactide-co-glycolide)-based nanoencapsulation techniques with sustainable solvents. *J Nanobiotechnology*. Jan 4 2022;20(1):5. doi:10.1186/s12951-021-01179-7

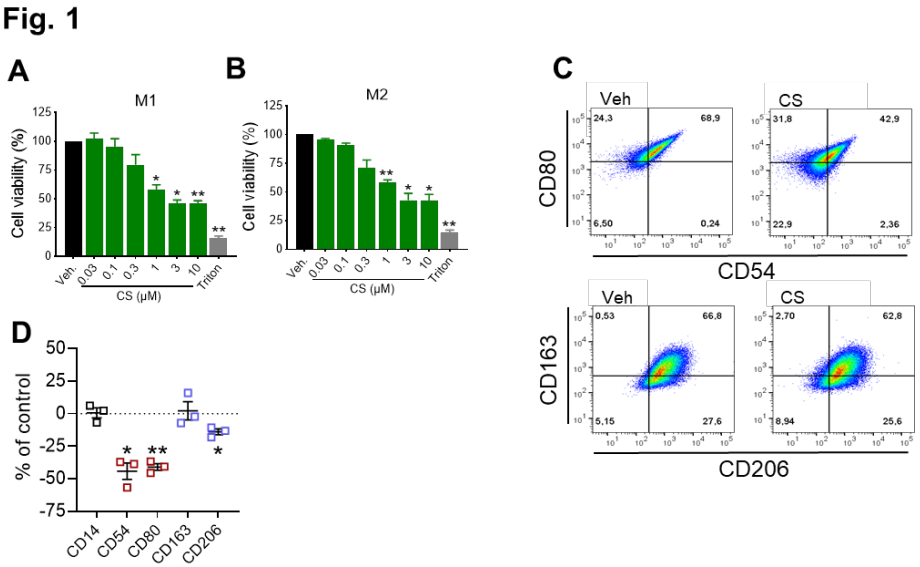

Fig. 1. Impact of celastrol (CS) on cell viability and polarization of human MDM. (**A,B**) Effects of CS on cell viability. $M0_{GM\text{-}CSF}$ (**A**) and $M0_{M\text{-}CSF}$ (**B**) were pre-treated with CS at the indicated concentrations, 0.1% DMSO as vehicle, or 1% Triton X-100 as positive control, for 15 min before adding the polarizing agents (LPS/IFNγ for M1-, IL-4 for M2-MDM). After 48 h, cell viability was assessed by MTT assay. Values are means + S.E.M., n = 3, expressed as percentage of vehicle control (= 100%); * $p < 0.05$, ** $p < 0.01$ vs. control group, one-way ANOVA for multiple comparisons with Dunnett's correction. (**C,D**) Effects of CS on the expression of macrophage phenotype surface markers. $M0_{M\text{-}CSF}$ were treated with 0.2 µM CS or 0.1% DMSO (as vehicle) for 48 h. (**C**) Expression of surface markers CD54 and CD80 (M1-like) as well as CD163 and CD206 (M2-like) among living $CD14^+$ cells was analyzed by flow cytometry; shown are representative pseudocolor dot plots of the M1-like and M2-like surface markers. (**D**) Mean fluorescence intensity (MFI) of each marker in (C) was determined. The change of the MFI from CS-treated MDM against the MFI of vehicle-treated cells was calculated and is given in % of control in scatter dot plots as single values and means + S.E.M., n = 3. * $p < 0.05$, ** $p < 0.01$ CS vs. control group, ratio paired t-test.

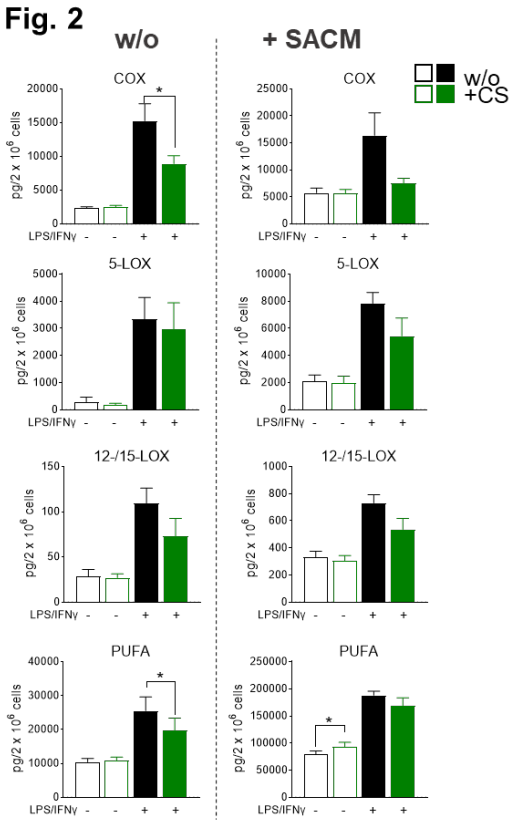

Fig. 2. Celastrol (CS) modulates LM pathways during polarization towards human M1-MDM. $M0_{GM\text{-}CSF}$ were pre-treated with 0.2 µM CS or 0.1% DMSO (as vehicle) for 15 min before adding the polarizing agents LPS/IFNγ or vehicle. After 48 h, cells were incubated in 1 mL PBS pH 7.4 plus 1 mM $CaCl_2$ without or with 1% *S. aureus*-conditioned medium (SACM) for 90 min. Produced LM were analyzed in cell supernatants by UPLC-MS-MS. The sum of COX products (PGE_2, PGD_2, $PGF_{2\alpha}$, TXB_2), 5-LOX products (LTB_4, t-LTB_4, 5-HETE, 5-HEPE), 12/15-LOX products (17-HDHA, 15-HETE, 15-HEPE, 14-HDHA, 12-HETE, 12-HEPE), and PUFA (AA, EPA, DHA) are shown as pg/2 × 10^6 cells of CS-treated and vehicle-treated cells, in the resting state or upon challenge with SACM. Data are means + S.E.M., n = 4 and were log-transformed for statistical analysis, * $p < 0.05$, CS vs. control group, one-way ANOVA for multiple comparisons with Sidak's correction.

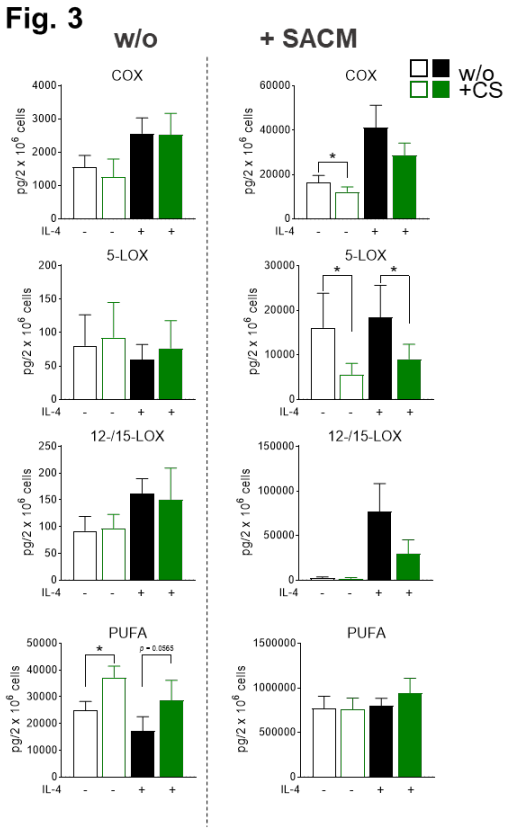

Fig. 3. Celastrol (CS) modulates LM pathways during polarization towards human M2-MDM. $M0_{M\text{-}CSF}$ were pre-treated with 0.2 µM CS or 0.1% DMSO (as vehicle) for 15 min before adding the polarizing agent IL-4 or vehicle. After 48 h, cells were incubated in 1 mL PBS pH 7.4 plus 1 mM $CaCl_2$ without or with 1% *S. aureus*-conditioned medium (SACM) for 90 min. Produced LM were analyzed in cell supernatants by UPLC-MS-MS. The sum of COX products (PGE_2, PGD_2, $PGF_{2\alpha}$, TXB_2), 5-LOX products (LTB_4, t-LTB_4, 5-HETE, 5-HEPE), 12/15-LOX products (17-HDHA, 15-HETE, 15-HEPE, 14-HDHA, 12-HETE, 12-HEPE), and PUFA (AA, EPA, DHA) are shown as pg/2 × 10^6 cells of CS-treated and vehicle-treated cells, in the resting state or upon challenge with SACM. Data are means + S.E.M., n = 4 and were log-transformed for statistical analysis, * $p < 0.05$, CS vs. control group, one-way ANOVA for multiple comparisons. with Sidak's correction.

Fig. 4

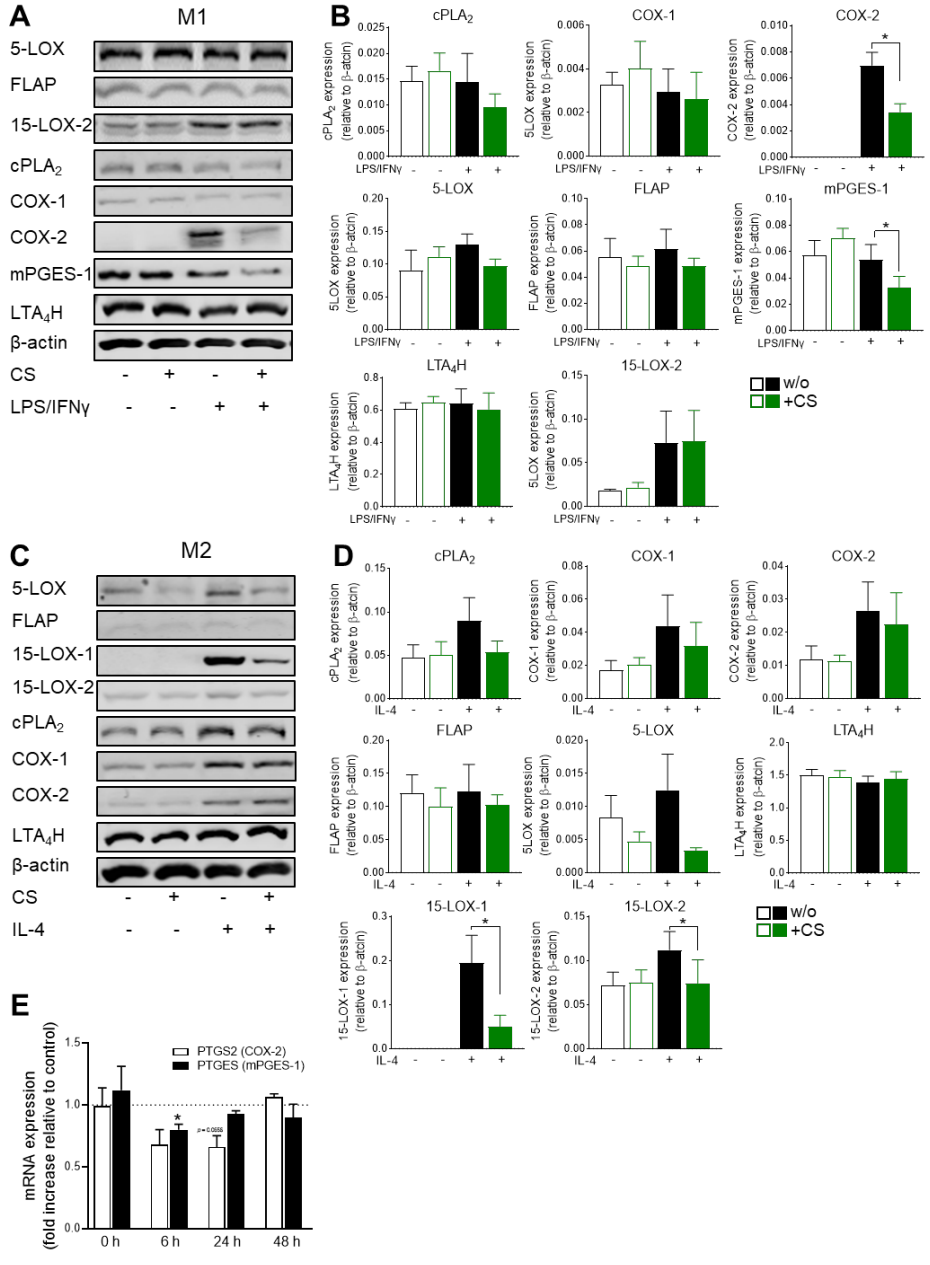
A
M1
5-LOX
FLAP
15-LOX-2
cPLA2
COX-1
COX-2
mPGES-1
LTA4H
β-actin
CS
LPS/IFNγ
B
cPLA2
COX-1
COX-2
5-LOX
FLAP
mPGES-1
LTA4H
15-LOX-2
w/o
+CS
C
M2
5-LOX
FLAP
15-LOX-1
15-LOX-2
cPLA2
COX-1
COX-2
LTA4H
β-actin
CS
IL-4
D
cPLA2
COX-1
COX-2
FLAP
5-LOX
LTA4H
15-LOX-1
15-LOX-2
w/o
+CS
E
PTGS2 (COX-2)
PTGES (mPGES-1)
mRNA expression (fold increase relative to control)
0 h
6 h
24 h
48 h

Fig. 4. Celastrol (CS) modulates the expression of LM-biosynthetic enzymes during polarization of human MDM. (**A, B**) $M0_{GM\text{-}CSF}$ and (**C, D**) $M0_{M\text{-}CSF}$ were pre-treated with 0.2 µM CS or 0.1% DMSO (as vehicle) for 15 min before adding the polarizing agents LPS/IFNγ or IL-4, respectively, or vehicle. After 48 h, cells were harvested, lysates were prepared, and proteins were analyzed by SDS-PAGE and Western blotting. Immunoreactive protein bands of LM-biosynthetic enzymes are shown for (**A**) M1-MDM and (**C**) M2-MDM. Immunoreactive bands of LM-biosynthetic enzymes were analysed by densitometry for proteins derived from (B) M1-MDM and (D) M2-MDM, normalized to β-actin. Data are shown as means + S.E.M. from n = 4 separate donors. Densitometric ratios were used for statistical analysis. * $p < 0.05$, CS vs. control group, one-way ANOVA for multiple comparisons with Sidak's correction. (**E**) Effects of CS on PTGS2 and PTGES mRNA levels during polarization towards human M1-MDM. $M0_{GM\text{-}CSF}$ were pretreated with 0.2 µM CS or 0.1% DMSO (as vehicle) for 15 min and polarized for 0, 6, 24 and 48 h towards M1-MDM using LPS/IFNγ. RNA was isolated, transformed in cDNA by reverse transcription and amplified by qPCR for quantification. Data are expressed as fold increase to DMSO control for n = 3 separate donors. Statistics: * = expression ratio is significantly different from 1, $p < 0.05$, CS vs. control group; multiple paired t- test with Holm-Sidak correction.

Fig. 5

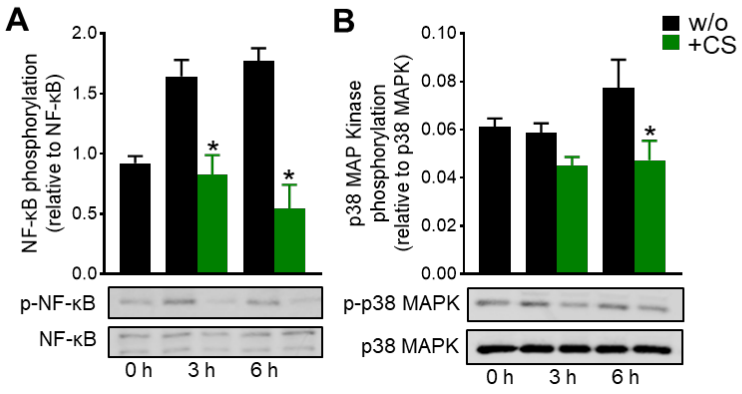

Fig. 5. Effects of celastrol (CS) on the activation of NF-κB and p38 MAPK in human M1-MDM. $M0_{GM\text{-}CSF}$ were pretreated for 15 min with 0.2 µM CS or 0.1% DMSO (as vehicle) prior to polarization to M1-MDM using LPS/IFNγ for 3 or 6 h. Protein phosphorylation of (**A**) NF-κB p65 and (**B**) p38 MAPK was analyzed by SDS-PAGE and Western blotting using phospho-specific antibodies of cell lysates; the respective unphosphorylated proteins were used for normalization. Representative Western blots of n=3 independent experiments are shown; data are means + SEM. Densitometric ratios were used for statistical analysis. * $p < 0.05$, CS-treated vs. DMSO-treated, one-way ANOVA for multiple comparisons with Sidak's correction.

Table 1. Prime sequences for qPCR assays

Target genes		Sequence (5'-3')
PTGS2	Forward Primer	TGCCTGATGATTGCCCGACT
	Rervese Primer	TGAAAGCTGGCCCTCGCTTA
PTGES	Forward Primer	AGTATTGCAGGAGCGACCCC
	Rervese Primer	GCATCCAGGCGACAAAAGGG
GAPDH	Forward Primer	TTTGCGTCGCCAGCCGAG
	Rervese Primer	TTCTCAGCCTTGACGGTGCC

Table 2. Effects of celastrol (CS) on LM pathways during human M1-MDM polarization.

A w/o — % vs. control: 0 100 201

LM	LPS/IFNγ (-)			LPS/IFNγ (+)		
	Veh.	CS	%	Veh.	CS	%
PGD_2	27.5 ± 8.7	26.7 ± 4.3	97	110 ± 20.5	75.6 ± 13.7	69
PGE_2	94.1 ± 10.5	83.6 ± 10.9	89	11262 ± 1937	6190 ± 1018	55
$PGF_{2\alpha}$	165 ± 28.0	169 ± 11.3	102	422 ± 67.7	278 ± 13.7	66
TXB_2	2038 ± 195	2194 ± 239	108	3484 ± 618	2382 ± 214	68
11-HEPE	0.5 ± 0.1	0.5 ± 0.1	95	5.9 ± 1.2	3.6 ± 0.7	61
11-HETE	7.7 ± 1.7	7.5 ± 1.1	98	109 ± 13.1	62.2 ± 12.8	57
$t\text{-}LTB_4$	81.1 ± 49.3	41.3 ± 18.2	51	845 ± 118	749 ± 219	89
LTB_4	114 ± 80.4	59.5 ± 34.1	52	1487 ± 425	1228 ± 413	83
5-HEPE	19.7 ± 10.7	11.9 ± 4.9	60	197 ± 49.7	203 ± 81.0	103
5-HETE	79.7 ± 34.8	55.7 ± 17.1	70	810 ± 220	781.3 ± 291	96
7-HDHA	7.3 ± 2.0	6.4 ± 1.9	87	23.2 ± 7.0	20 ± 6.6	85
17-HDHA	2.5 ± 1.3	5.1 ± 1.3	201	11.6 ± 3.1	5.4 ± 2.4	46
15-HEPE	1.1 ± 0.3	1.3 ± 0.3	117	3.5 ± 0.7	3.1 ± 1.0	87
15-HETE	14.9 ± 2.4	13.3 ± 2.3	90	79.4 ± 10.4	54.6 ± 14.1	69
14-HDHA	0.7 ± 0.4	0.4 ± 0.2	52	2.3 ± 1.3	0.8 ± 0.3	34
12-HEPE	0.6 ± 0.2	0.6 ± 0.2	100	2.0 ± 0.4	1.6 ± 0.5	78
12-HETE	9.0 ± 5.5	6.4 ± 0.5	71	10.8 ± 2.0	7.6 ± 2.5	70
4-HDHA	2.0 ± 0.5	1.5 ± 0.4	78	3.8 ± 0.8	3.2 ± 0.6	84
18-HEPE	6.4 ± 1.3	5.4 ± 1.0	85	8.1 ± 0.5	6.7 ± 1.7	82
9-HODE	137 ± 22.2	132 ± 16.1	96	166 ± 21.9	133 ± 9.2	80
13-HODE	204 ± 38.5	206 ± 30.9	101	253 ± 38.3	192 ± 10.3	76
RvD5	n.d.	n.d.	n.d	n.d.	n.d.	n.d
AA	6940 ± 675	7095 ± 645	102	18773 ± 3175	14351 ± 2817	76
EPA	905 ± 92.3	990 ± 93.9	109	2167 ± 319	1718 ± 322	79
DHA	2602 ± 273	2776 ± 348	107	4595 ± 942	3602 ± 665	78

B + SACM — % vs. control: 0 100 201

LM	LPS/IFNγ (-)			LPS/IFNγ (+)		
	Veh.	CS	%	Veh.	CS	%
PGD_2	40.8 ± 2.4	36.0 ± 4.0	88	105 ± 15.9	61.1 ± 2.8	58
PGE_2	267 ± 40.0	236 ± 20.5	88	11309 ± 3111	4414 ± 697	39
$PGF_{2\alpha}$	450 ± 111	440 ± 80.7	98	388 ± 95.1	218 ± 10.0	56
TXB_2	5001 ± 787	4926 ± 676	99	4597 ± 1035	2851 ± 311	62
11-HEPE	11.8 ± 3.2	11.9 ± 3.3	101	23.6 ± 6.6	14.9 ± 1.5	63
11-HETE	140 ± 16.3	134 ± 9.4	96	592 ± 79.2	318 ± 40.8	54
$t\text{-}LTB_4$	296 ± 68.0	283 ± 75.9	95	1193 ± 75.6	775 ± 190	65
LTB_4	669 ± 276	616 ± 258	92	2619 ± 361	1775 ± 478	68
5-HEPE	257 ± 52.7	235 ± 33.8	92	718 ± 85.6	533 ± 125	74
5-HETE	894 ± 127	841 ± 190	94	3327 ± 348	2358 ± 590	71
7-HDHA	31.6 ± 1.2	35.3 ± 7.5	112	79.0 ± 6.9	60.6 ± 11.2	77
17-HDHA	71.5 ± 10.8	58.1 ± 10.9	81	92.6 ± 8.9	99.1 ± 11.7	107
15-HEPE	13.1 ± 1.1	12.2 ± 1.4	93	12.6 ± 1.2	14.6 ± 1.4	117
15-HETE	190 ± 20.0	174 ± 21.5	92	520 ± 56.8	331 ± 61.2	64
14-HDHA	9.2 ± 2.3	10.3 ± 2.4	113	19.1 ± 1.5	18.7 ± 0.5	98
12-HEPE	6.3 ± 0.8	6.4 ± 0.4	102	9.5 ± 2.2	9.4 ± 1.7	98
12-HETE	44.0 ± 8.9	41.8 ± 7.9	95	77.8 ± 13.9	63.5 ± 12.3	82
4-HDHA	14.1 ± 2.0	14.3 ± 1.4	102	22.2 ± 1.9	22.0 ± 2.3	99
18-HEPE	22.2 ± 2.8	19.0 ± 2.2	86	17.9 ± 1.6	15.8 ± 2.0	88
9-HODE	199 ± 7.1	168 ± 13.0	85	256 ± 32.4	226 ± 27.0	88
13-HODE	243 ± 20.9	206 ± 17.4	85	342 ± 53.4	292 ± 39.3	86
RvD5	4.8 ± 0.8	5.8 ± 1.4	119	9.6 ± 0.9	7.0 ± 1.3	73
AA	49528 ± 4386	56911 ± 5904	115	110116 ± 5337	97293 ± 11106	88
EPA	9625 ± 1034	12429 ± 1570	129	17833 ± 1239	16860 ± 1564	95
DHA	19817 ± 2038	23170 ± 2457	117	60363 ± 2442	54893 ± 2246	91

Table 3. Effects of celastrol (CS) on LM pathways during human M2-MDM polarization.

A w/o

% vs. control: 0 100 247

LM	IL-4 (-)			IL-4 (+)		
	Veh.	CS	%	Veh.	CS	%
PGD_2	16.2 ± 2.1	16.3 ± 3.3	100	28.7 ± 4.8	26.8 ± 5.9	94
PGE_2	92.5 ± 51.6	74.3 ± 41.5	80	137 ± 61.0	135 ± 65.8	98
$PGF_{2\alpha}$	66.4 ± 18.9	51.7 ± 20.7	78	72.6 ± 20.4	69.1 ± 20.8	95
TXB_2	1368 ± 294	1116 ± 477	82	2329 ± 407	2287 ± 567	98
11-HEPE	1.0 ± 0.5	1.2 ± 0.6	118	1.4 ± 0.3	1.1 ± 0.5	80
11-HETE	11.9 ± 5.8	12.0 ± 6.6	101	14.4 ± 5.4	19.0 ± 8.8	132
t-LTB_4	12.9 ± 8.7	11.7 ± 8.3	91	8.2 ± 3.5	8.6 ± 4.9	105
LTB_4	21.7 ± 16.9	17.5 ± 14.6	81	9.0 ± 6.4	10.5 ± 7.9	117
5-HEPE	11.6 ± 6.9	13.8 ± 6.4	119	10.2 ± 3.5	12.9 ± 6.4	126
5-HETE	34.5 ± 13.8	49.8 ± 23.4	144	31.9 ± 10.0	44.5 ± 22.1	139
7-HDHA	9.4 ± 0.5	23.1 ± 7.9	247	25.2 ± 8.4	17.1 ± 2.9	68
17-HDHA	18.1 ± 3.5	20.0 ± 6.9	111	38.8 ± 8.8	44.1 ± 15.1	114
15-HEPE	4.5 ± 1.4	3.8 ± 1.1	83	12.1 ± 3.9	7.8 ± 2.8	65
15-HETE	55.1 ± 18.4	57.1 ± 15.7	104	87.7 ± 14.0	76.8 ± 30.9	88
14-HDHA	3.1 ± 0.9	2.7 ± 0.4	85	7.3 ± 3.0	6.5 ± 4.0	90
12-HEPE	1.3 ± 0.3	1.9 ± 0.6	142	3.3 ± 0.7	2.8 ± 0.7	86
12-HETE	10.3 ± 3.2	11.7 ± 3.8	114	13.5 ± 1.7	12.7 ± 5.9	94
4-HDHA	5.7 ± 0.6	6.2 ± 0.8	109	6.1 ± 0.5	6.5 ± 1.1	106
18-HEPE	8.1 ± 2.9	7.3 ± 2.3	90	9.2 ± 2.4	7.8 ± 3.3	85
9-HODE	87.8 ± 40.8	110 ± 28.9	125	115 ± 37.0	121 ± 56.0	105
13-HODE	112.6 ± 56.1	141.5 ± 44.4	126	149 ± 55.2	177 ± 91.8	119
PDX	n.d.	n.d.	n.d.	n.d.	n.d.	n.d.
RvD5	n.d.	n.d.	n.d.	n.d.	n.d.	n.d.
MaR2	n.d.	n.d.	n.d.	n.d.	n.d.	n.d.
RvE4	n.d.	n.d.	n.d.	n.d.	n.d.	n.d.
AA	16737 ± 2299	23393 ± 3204	140	11367 ± 3956	17709 ± 5424	156
EPA	2107 ± 332	3412 ± 844	162	1378 ± 472	2567 ± 851	186
DHA	6176 ± 796	10458 ± 651	169	4499 ± 1010	8397 ± 1251	187

B + SACM

% vs. control: 0 100 247

LM	IL-4 (-)			IL-4 (+)		
	Veh.	CS	%	Veh.	CS	%
PGD_2	345 ± 104	274 ± 75.7	79	849 ± 229	453 ± 101	53
PGE_2	1142 ± 274	814 ± 142	71	2440 ± 339	1716 ± 232	70
$PGF_{2\alpha}$	677 ± 113	433 ± 67.0	64	824 ± 173	544 ± 88.7	66
TXB_2	14145 ± 2892	10672 ± 2017	75	37119 ± 9532	25916 ± 5290	70
11-HEPE	46.4 ± 16.1	19.6 ± 3.3	42	198 ± 62.0	85.0 ± 26.4	43
11-HETE	622 ± 181	354 ± 64.6	57	2610 ± 720	1273 ± 381	49
t-LTB_4	1531 ± 772	568 ± 293	37	2286 ± 1130	896 ± 345	39
LTB_4	2703 ± 951	753 ± 257	28	6694 ± 3100	1430 ± 476	21
5-HEPE	2324 ± 1430	512 ± 226	22	1484 ± 499	1031 ± 504	69
5-HETE	9563 ± 4715	3773 ± 1796	39	7956 ± 2554	5681 ± 2200	71
7-HDHA	62.9 ± 9.6	46.4 ± 4.8	74	566 ± 193	215 ± 57.8	38
17-HDHA	431 ± 150	428 ± 153	99	14993 ± 5607	4812 ± 2165	32
15-HEPE	99.3 ± 42.9	63.6 ± 25.6	64	9182 ± 4386	2027 ± 1101	22
15-HETE	1782 ± 826	1347 ± 661	76	36279 ± 13339	19208 ± 10538	53
14-HDHA	18.6 ± 5.1	16.7 ± 2.8	90	4168 ± 1873	851 ± 501	20
12-HEPE	25.6 ± 7.8	13.6 ± 4.9	53	1821 ± 873	400 ± 220	22
12-HETE	188 ± 63.9	105 ± 39.3	56	10642 ± 5535	2089 ± 1426	20
4-HDHA	40.4 ± 3.4	33.7 ± 1.3	83	73.9 ± 13.9	42.2 ± 3.8	57
18-HEPE	53.0 ± 14.1	28.0 ± 3.0	53	194 ± 59.1	86.6 ± 25.1	45
9-HODE	157 ± 29.3	130 ± 29.9	83	263 ± 26.2	186 ± 8.3	71
13-HODE	190 ± 37.2	160 ± 34.8	84	2275 ± 876	598 ± 205	26
PDX	n.d.	n.d.	n.d.	205 ± 87.5	41.9 ± 20.1	20
RvD5	5.7 ± 1.0	4.5 ± 1.2	78	2143 ± 931	331 ± 139	15
MaR2	n.d.	n.d.	n.d.	89.7 ± 40.0	14.2 ± 4.7	16
RvE4	20.0 ± 10.7	n.d.	n.d.	590 ± 369	53.6 ± 26.8	9
AA	644949 ± 173254	500628 ± 87037	78	539612 ± 56101	667516 ± 132276	124
EPA	119181 ± 32375	95981 ± 25042	81	102144 ± 14530	98053 ± 19004	96
DHA	142616 ± 21950	162353 ± 26174	114	157759 ± 27198	175629 ± 27256	111

4 Discussion

The host defense response against invading pathogens and tissue damage is generally divided into two phases of inflammation: initiation and resolution [5]. The concept of resolution has been expanded to provide a highly coordinated, active process that contributes to pathogen clearance and can be mediated by various biomolecules such as cytokines, chemokines, and lipid mediators including eicosanoids and SPM [5]. Human macrophages as major innate immune cells play essential roles in both initiation and resolution phases of inflammation producing LM families that are specific for different macrophage subtypes [203,204]. Because of the promising therapeutic effects of TwHF extracts and its bioactive ingredient CS they are emerging as interesting drugs for treatment of inflammation [126]. This thesis describes the specific modulation of inflammation-related LM by TWG and CS, which might explain their potential to be amenable for therapeutic intervention with inflammation-based diseases.

4.1 Inhibition of *Tripterygium wilfordii* glycosides in human macrophages

Previous clinical trials revealed that TwHF-based therapy is of potential value for anti-RA therapy due to its prominent anti-inflammatory and immunosuppressive effects [6,205]. However, several crucial gaps in the knowledge of the modes of action remain to explain its therapeutic effects on the premise of safety assurance. This thesis focuses on the important and emerging aspects of LM modulation and highlights the major challenges and strategies for using the LM metabololipidomics approach to gain new insights into an unresolved question – how TWG beneficially regulates the biosynthesis of the LM network in innate immune cells. The data show that TWG suppresses 5-LOX products and thromboxane formation in polarized M1-MDM, but enhances the production of 12-/15-LOX in polarized M2-MDM. During macrophage polarization, TWG reduces both 5-LOX and COX product formation in M1-MDM, and intriguingly, induces 12-/15-LOX in M2-MDM. Our data disclose the crucial roles of TWG in the regulation of the biosynthesis of LM in human macrophages (**manuscript I**), which might help to explain its wide and successful application in RA treatment.

In our study, TWG was clearly shown to act as a direct 5-LOX inhibitor in cell-free assay

and also suppressed 5-LOX-derived LM products in M1-MDM and PMNL for both short- and long-time treatment. 5-LOX and its product LT are powerful mediators in inflammation processes which usually causes pain, fibrosis, and bone erosion, thus targeting 5-LOX activity was retained to be a satisfactory approach for treating rheumatoid inflammation [28,206]. Likewise, both treatments with 5-LOX inhibitors and knockdown of 5-LOX using shRNA exerted similar effects in attenuating TNF-α-induced inflammation in human synovial fibroblasts [207]. It has been demonstrated that LTB_4 is highly expressed in RA patients and synovial fluid from RA patients compared to levels seen in healthy donors [208,209]. Many studies have implicated that blockade of LTB_4 receptors such as BLT1 and 2, markedly suppresses arthritic features in cell lines and animal models [210,211]. In addition, Li et al. reported the IC_{50} value of 5-LOX inhibition by using TW extract to be 22 µg/ml, while in our experimental setting, it is more potent at 2.9 µg/ml, which could be explained by different conditions of 5-LOX assay and applied TwHF extract due to different extraction methods [212]. Therefore, our finding that TWG suppressed LT formation in M1-MDM and PMNL may reasonably contribute to the amelioration of RA.

In short-term polarized M1-MDM, TWG selectively blocked TXB_2 formation but with opposite upregulation of other COX-derived prostanoids (PGD_2, $PGF_{2\alpha}$, and PGE_2). Studies have shown that serum and urine TXA_2 levels are significantly higher in RA patients than in healthy individuals [213,214], and TXB_2 are also detected in the synovial fluid of RA patients [215]. This could be one reason for the beneficial effects of TWG for RA treatment. We confirmed that TWG does not directly inhibit the TXAS which converts PGH_2 towards TXA_2 (rapidly hydrolyzed to TXB_2) using a cell-free assay, indicating TXAS inhibition may require an intact cellular environment.

While during M1-MDM polarization in a long-term setting, TWG strongly diminished all COX-derived products seemingly due to suppression of COX-2 expression. Of note, TWG reduced the capacities to generate PGE_2 which is consistent with a previous study that described that two TwHF extracts suppressed the up-regulation of COX-2 without affecting COX-1 expression and thereby blocking PGE_2 production in various human cells [134]. Dysregulated PGE_2 synthesis or degradation is known to be associated with a wide range of pathological conditions, and leads to the classic signs of inflammation such as redness, swelling and pain [27]. Our results also revealed that TWG significantly reduced COX-2 on the protein level and slightly impaired the mPGES-1 enzyme activity and expression. mPGES-1 as a major terminal synthase in PGE_2 formation, relates to numerous inflammatory diseases [216]. Thus, mPGES-1 inhibitors are promising agents in the prevention of inflammation including RA [217,218]. This suggests that TWG may be beneficial for treatment RA by inhibition of PGE_2 through impairment of mPGES-1 enzyme expression.

In-depth research on the mechanism of the anti-inflammatory and anti-rheumatic mechanism of TWG in vivo is the limitation of this study, which together with development of reduced toxicity helps the clinical application of TWG in the therapy of diseases. In

IL-1β-stimulated RA synovial fibroblasts, TwHF extract inhibited COX-2 protein and mRNA expression similarly to dexamethasone, also inhibited PGE_2 production in a concentration-dependent manner, possibly via inhibition of NF-$\varkappa$B activity [219]. Different immune cell-based experiments further confirmed the alternative modes of action of TwHF extract, that is, inhibition of expression of proinflammatory genes such as those for IL-1, and IL-17-inducible MMP-3 and MMP-13 through interfering with AP-1 and NF-$\varkappa$B activities but not with p38 and c-Jun N-terminal kinase (JNK) MAPK pathway [135]. Of interest, another study showed TWG decreases the pro-inflammatory cytokines such as IL-6, IL-1β, and TNF-α, but induces the upregulation of anti-inflammatory cytokine IL-37 associated with extracellular signal-regulated kinase ERK1/2 and p38 MAPK signal pathways [220]. Apart from the fact that TwHF can suppress numerous proinflammatory cytokines (e.g., TNF-α, IL-1β, IL-6, IL-8, and IFN-γ) in different T cell subsets and macrophages [221], it also reduced T/B cell proliferation and synovial fibroblast growth as well as induce T cell apoptosis [146,147]. All these processes are crucial for the development and propagation of RA. Future studies on how TWG modulates LM production in co-culture systems like human macrophages and synovial cell lines or testing the anti-inflammatory and anti-rheumatic effects by using a combination of conventional DMARD may sustain the direct link to the favorable impact on RA.

We hypothesized that TWG, promoting a switch from pro-inflammatory LT and PG towards pro-resolving SPM, is a possibility or new strategy for RA treatment. It is known that LT and PG play important roles in numerous excessive inflammatory responses, including synovitis, arthritis, and airway inflammation [222,223]. Nevertheless, current innovative therapeutic strategies favor SPM and resolution which promotes tissue restoration and regeneration and extends our knowledge in regulating host responses in arthritis [224,225]. Several studies have proved the importance of SPM and their cognate GPCRs in autoimmune disorders including inflammatory arthritis. For instance, RvD5 and RvE2 were found to be significantly correlated with arthritis disease activity [224,226], and LXA_4, RvD1, RvE1 were expressed at lower levels in RA patients [227]. Also, metabololipidomics profiling in arthritic joints revealed 17R-RvD1 increased levels of protective SPM while the protective actions disappeared in RvD1 receptor-deficient ALX/Fpr2/3$^{-/-}$ (Fpr2/3; ortholog to human FPR2 (formyl peptide receptor)/ ALX (lipoxin A_4 receptpr)) mice [228]. In line with these studies, our experiments with short-time exposure of M2-MDM to TWG revealed striking production of 12-/15-LOX products and SPM; while during long time treatment by TWG in M2-MDM, it did not impair the ability to form 12-/15-LOX products even existing the reduced capacities to generate 5-LOX products and partial COX products. Further understanding of how TWG directly links to some GPCRs could be of great interest.

TWG contains many different bioactive ingredients and which of them accounts for the increased production of 12-/15-LOX products and SPM remains to be investigated. CS as one major component (calculated to be 0.158% in TWG using RP-HPLC analysis in the current study), may positively correlate to our another LM experiments showing that

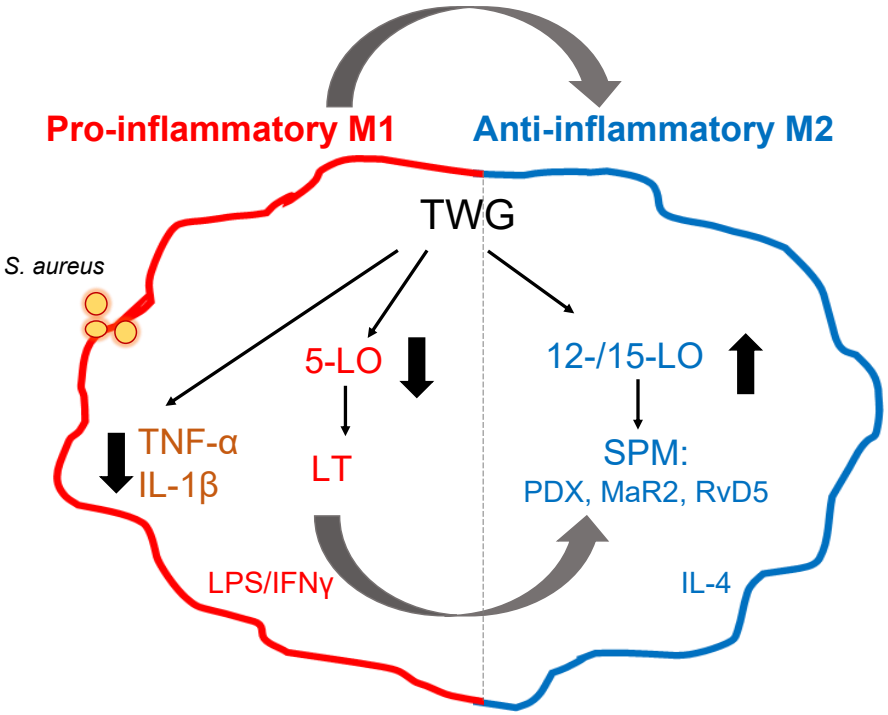

Figure 4.1: Schematics of *Tripterygium wilfordii* glycosides on lipid mediator network in human macrophages.

massive formation of 12-/15-LOX in M2-MDM due to short time incubation with CS [229]. Another major constituent of TwHF is TP, a diterpene triepoxide that was also found to downregulate COX-2 and iNOS in human RA synovial fibroblasts [230]. How TP exerts therapeutic effects in RA through whole complex LM networks (in particular SPM) requires further investigations.

In summary, we evaluated the pharmacological potential of TWG on the modulation of LM formation in activated human macrophages with implications related to the use of TwHF in inflammatory arthritis. Our investigations suggest that TWG is detrimental to LT and PG and facilitates the production of SPM, opening up new perspectives for the treatment of RA.

4.2 Inhibition of celastrol in polarized human macrophages

We show that CS from TwHF modulates inflammation-related LM biosynthesis in vitro and in vivo (**manuscript II**). Importantly, on the one hand, CS strikingly suppressed 5-LOX products in pro-inflammatory M1-MDM and PMNL as well as directly inhibited 5-LOX

without affecting other related LM biosynthetic enzymes in cell-free assays. On the other hand, CS significantly induced 12-/15-LOX activity and SPM formation in anti-inflammatory M2-MDM and in vivo in a model of acute inflammation. Such an LM profile induced by a small molecule like CS offers an alternate strategy for intervention with inflammatory disorders.

The broad spectrum of the pharmacological properties of CS makes this compound an attractive therapeutic option in a variety of inflammation-related diseases [8,231]. CS shows anti-RA effects in CIA or AIA mice [185,232]. CS also ameliorates murine colitis and colitis-related colorectal cancer in mice via suppression of the inflammatory response [154,233]. In terms of molecular perspective, CS attenuates the release of IL-1β and IL-18 from macrophages through a process mediated by the NLRP3 inflammasome [177]. Since NLRP3 inflammasome activation contributes to the pathogenesis of RA [234], CS was subsequently found to exert anti-RA effects by suppressing NLRP3 inflammasome activation through 1) inhibiting ROS-NF-$\varkappa$B-NLRP3 axis [235] or 2) inhibiting K63 deubiquitination of NLRP3 [236].

Of note, aberrant LM formation with upregulation of pro-inflammatory PG, TX, LT, and downregulation of SPM plays crucial roles connected to arthritis and colitis as common inflammatory diseases models [224,237]. Over the past few decades, 5-LOX-derived LT are known to contribute to numerous inflammatory disorders, for review see [238-240]. Regarding the dual role of 5-LOX in the formation of pro-inflammatory LT and pro-resolving LX and other SPM [5], we questioned if there is a feasible way to exclusively limit LT formation without lower pro-resolving mediators of the 5-LOX pathway? Recently, studies with synthetic small molecules such as ginkgolic acid, benzenesulfonamide-derivatives, and 3-O-acetyl-11-keto-β-boswellic acid (AKBA) reported to be potential 5-LOX inhibitors support our hypothesis that inhibition of LT formation can trigger SPM generation, calling for consideration as a promising pharmacological strategy for anti-inflammatory therapy [241-243]. Interestingly, we found a similar LM pattern induced by CS that effectively suppressed LT in M1-MDM but induced massive formation of SPM in M2-MDM. This is in consistent with previous findings that macrophage phenotypes are associated with different LM production, pro-inflammatory M1 are usually generating more PG and LT but few SPM, while anti-inflammatory M2 appear to induce substantial SPM [244,245]. Thus, a shift from LT formation towards SPM by CS treatment may explain why CS ameliorates many inflammatory diseases.

In addition, CS showed quite potent inhibitory activity for human recombinant 5-LOX and 5-LOX in PMNL homogenates with IC_{50} values in the range of 0.19-0.49 μM, compared with somewhat different findings by Joshi et al. (IC_{50} = 5 μM) possibly due to different concentrations of AA that were used [178]. Also, CS exhibited potent inhibitory activity on cellular 5-LOX in both intact M1-MDM and PMNL at 1 μM, but with higher efficiency in PMNL. This could be explained by CS having better accessibility for 5-LOX in the cytosol of PMNL than 5-LOX in the nucleosol of M1-MDM [246].

Macrophage populations may possess diverse phenotypes in the body [247], and we assume that the co-existence of polarized M1 and M2 are in balance in our experimental context. We wondered if the complex LM production regulated by CS treatment is likewise dynamically balanced with decreased 5-LOX formation but increased SPM? However, how CS modulates macrophage polarization and phenotypes is poorly understood. Here are only two studies that mentioned the relationship between CS and M1 and M2 macrophage subtypes. One is that CS exhibited anti-obesity effects via suppressing pro-inflammatory M1 macrophage polarization via regulating Nrf2/HO-1, MAP kinase, and NF-$\varkappa$B pathways [248]. Another study showed that CS treatment reduces ischemic stroke-induced brain damage through 1) increasing both inflammatory cytokines like IL-1β, IL-6, and TNF-α, as well as the anti-inflammatory cytokine such as IL-33 and IL-10, in patients and animal models; and 2) decreasing inflammatory cytokine expression via an IL-33/ST2 axis-mediated M2 microglia/macrophage polarization in cell models [249]. In M2-MDM, we found that CS 1) induced the activation of 15-LOX-1 but did not affected 5-LOX, and 2) induced 12-/15-LOX-derived LM and SPM but decreased 5-LOX-derived LM, in line with our hypothesis.

SPM promotes the resolution of inflammation in an active process, and its biosynthesis and activities on phagocytes showing beneficial effects in animal models of diseases has been previously proved, for review see [250-252]. For instance, RvD1 and its metabolic precursor 17-HpDHA were shown to reduce tissue damage and pain more efficiently than steroids in a murine model of arthritis [253]. LXA_4 and its analogs improved DSS-induced colitis in mice [254,255]. Hence, the SPM induced by CS treatment may counteract inflammatory diseases. However, the mechanism underlying how CS induces the pro-resolving mediators is still not clear. On this theme, it would be exciting to see how CS impacts the phenotype of murine peritoneal macrophages in zymosan-induce mice models alongside the LM class switch.

Recently, the pentacyclic triterpene acid AKBA was shown to bind at an allosteric site of 5-LOX between the C2-like and the catalytic domain which not only mediates inhibition of LT formation but also changes the enzyme's regiospecificity to convert AA to 12- and 15-LOX products [243]. Our docking experiments clearly support the binding of CS at the same 5-LOX allosteric site as the one for AKBA. It is tempting to speculate that the pentacyclic triterpenoid CS, like the pentacyclic triterpene acid AKBA, would activate both 5-LOX and 15-LOX-1. Even though they have a different chemical structure, small chemicals that engage with an allosteric site to activate 15-LOX have recently been described [256]. Further docking on 15-LOX-1 by AKBA and CS is ongoing.

Besides, CS showed a similar LM pattern as compared to TWG, that is, suppression of pro-inflammatory LM but SPM induction in a short-term manner which may imply its contribution to the antirheumatic properties [257]. In fact, CS was restricted in further application mostly due to its cytotoxicity [9,164], thus we carefully checked its effect on the viability of PMNL and MDM in all short-term experiments. We were also interested to see

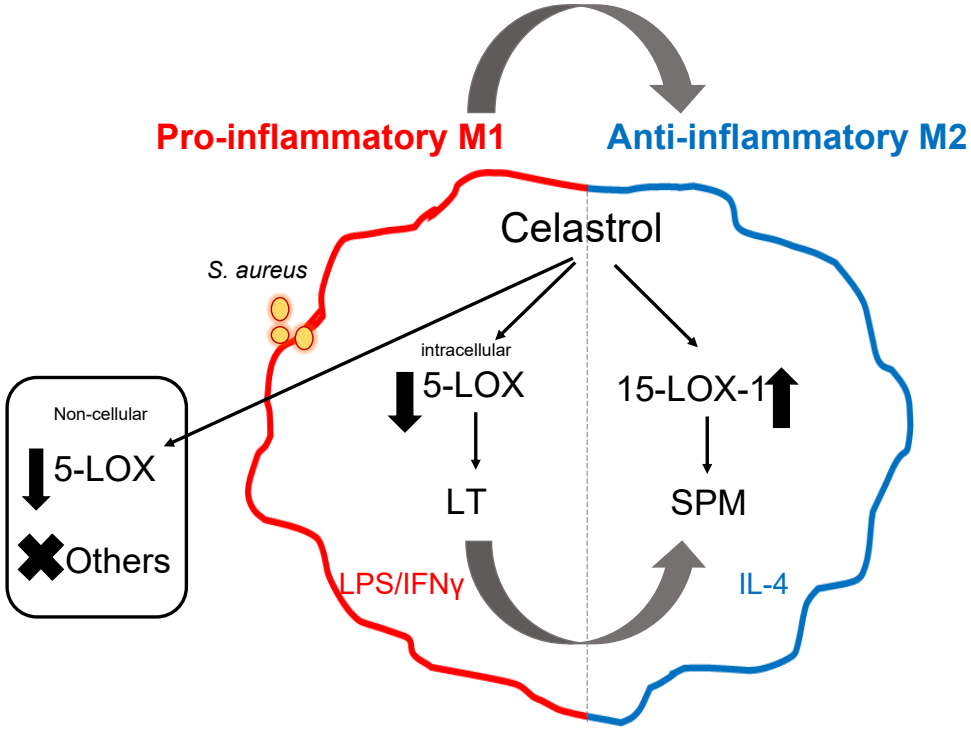

Figure 4.2: Manipulation of lipid mediator biosynthesis by short-time exposure of celastrol in polarized human macrophages.

how CS affects the LM network after long-term exposure during macrophage polarization, which will be discussed in the next section. Overall, our studies revealed 5-LOX as a high-affinity target for CS that can be effectively inhibited in vitro at sub-micromolar IC_{50} values and also in vivo with great effectiveness. CS noticeably evoked the production of 12-/15-LOX-derived LM and SPM by activation of 15-LOX-1 in M2-MDM. Intriguingly, CS promoted the LM class switch from pro-inflammatory LT to inflammation-resolving SPM also in vivo in a mouse model of acute inflammation. Our findings imply that small compounds like CS could be used to turn on the button of resolution of inflammation by boosting endogenous SPM production in inflammatory disorders.

4.3 Inhibition of celastrol during human macrophages polarization

We studied how CS modulates LM biosynthesis pathways during human macrophage polarization (**manuscript III**). For MDM polarized to M1 phenotype, CS strikingly impaired the capacity for exotoxin-induced formation of pro-inflammatory COX products, particularly

of PGE_2, and also slightly hampered 5-LOX-derived LM such as LTB_4. CS strongly reduced both mRNA and protein levels of COX-2 and mPEGS-1, but to a minor extent affected 5-LOX expression during M1 polarization, along with diminished M1 phenotypic surface markers. The inhibition of the COX-2 pathway by CS was further found to be associated with phosphorylation of both NF-$\varkappa$B and p38 MAPK. During M2-MDM polarization, CS not only inhibited pro-inflammatory COX and 5-LOX products but also reduced 12-/15-LOX activities and SPM generation upon challenge with exotoxin. This is in parallel with the marked reduction of 15-LOX protein expression. But CS did not affect fatty acid release. Taken together, CS mainly impaired pro-inflammatory LM pathways in M1-MDM which may contribute to its anti-inflammatory properties, while the unfavorable impact of CS in downregulation of pro-resolving SPM in M2-MDM cannot be ignored and needs to be further investigated.

In a previous study, our group reported that CS promotes a switch from LT biosynthesis to formation of SPM in a short-term (3 h) incubation in polarized human MDMs and also in mice (2.5 h) [229]. Such LM class switch is considered as a novel pharmacological strategy for promoting the resolution of inflammation [5]. In the present study, CS was found to impair pro-inflammatory LM and its biosynthetic enzymes in long-term incubations (48 h) during MDM polarization. Since CS is one major component from TWG, our data are also in compliance with our previous study where TWG reduced the capacities of MDM to produce 5-LOX and COX products and impairment of COX-2 and mPEGS-1 enzyme expression as well as M1 surface marker [257].

During M1 polarization, CS clearly showed inhibition of COX-derived LM products, especially PGE_2, and also impaired both mRNA and protein levels of COX-2 and mPEGS-1, which may be due to the inhibition of NF-$\varkappa$B and to some extent of the p38 MAPK. In vitro data have revealed that low concentrations (0.05–1 μM) of CS inhibit the production of NO and PEG_2, accompanied by a decrease in iNOS and COX-2 protein expression, and inhibit TNF and IL-6 release, and suppress the activity of NF-$\varkappa$B and AP-1 in LPS-stimulated macrophages [258,259]. In CD biopsies, CS suppressed the production of pro-inflammatory cytokines by inhibiting the nuclear translocation of NF-$\varkappa$B and the phosphorylation of p38 kinase [167]. CS is a potent inhibitor of the I$\varkappa$B kinase/NF-$\varkappa$B (IKK/NF-$\varkappa$B) signaling and it has been used for hundreds of years as an ingredient of Thunder God Vine [260]. CS not only suppressed IKKβ activity but also exerted anti-inflammatory and anti-tumor activities [258]. Other studies demonstrated that CS could control macrophage polarization through modulating the cross-talk among LPS-stimulated MAPKs (ie, p38 MAPK, ERK1/2, JNK) and nuclear translocation of NF-$\varkappa$B p65 and other transcription factor-related axes [248,261]. In addition, p38 MAPK activation by cell stress was found to induce LT formation in leukocytes [262]. This contradicts our findings that CS increased the capacity to generate 5-LOX products upon SACM challenge while p38 MAPK activation is slightly inhibited during M1 polarization.

Inhibition of PG biosynthesis can impede the class switch of lipid mediators and may

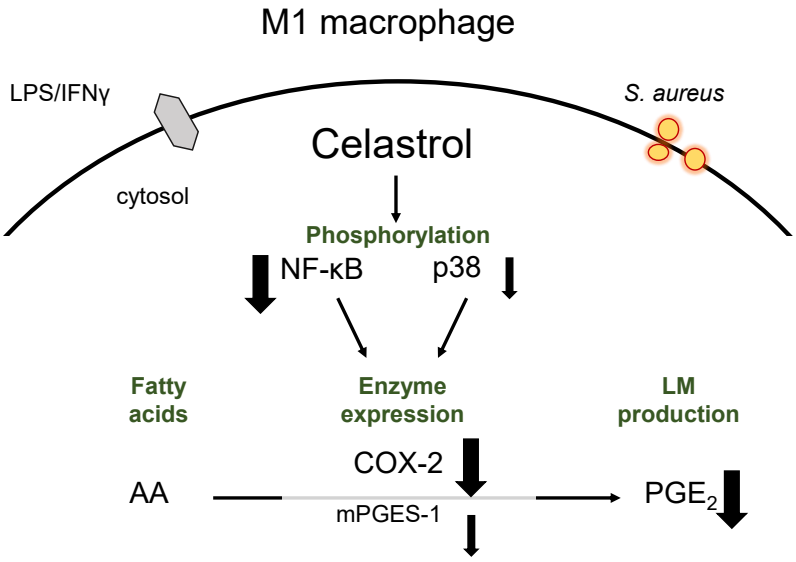

Figure 4.3: Proposed mechanism of celastrol inhibition in affecting COX-2 pathways during M1 macrophages polarization.

delay resolution [12,263], this may explain why SPM were generated in large amounts in M2-MDM but were downregulated after long time incubation of CS in the current study. CS impaired protein levels of 15-LOX-1 and 15-LOX-2 that are key enzymes in SPM biosynthesis [186], alongside hardly affected M2-MDM surface marker expression, indicating long-term treatment of CS may be detrimental for resolution of inflammation through two possibilities of macrophage subtype phenotypic interfering – 1) negatively regulated M0 macrophages polarize towards to M2 phenotype; or 2) inhibition of the repolarizing process from M1 to M2 subtypes. Likewise, CS exhibited anti-obesity effects via suppressing pro-inflammatory M1 macrophage polarization [248]. In contrast, CS treatment protects against acute ischemic stroke-induced brain injury by promoting an IL-33/ST2 axis-mediated microglia/macrophage M2 polarization [249]. CS-loaded nanomicelles were also reported to reduce the expression of macrophage M1 biomarkers (e.g., IL-6, IL-1β, TNF-α, iNOS) in a dose-dependent manner and marginally increased the expression of macrophage M2 biomarkers (e.g., arginase-1 (Arg-1), IL-10) [264].

In addition, TwHF extracts and TP caused inhibitory effect on PGE_2 formation in a variety of human cells by blocking the up-regulation of COX-2 [134]. Ethyl acetate extracts of TwHF inhibited PGE_2 production by downregulating the expression of the COX-2 gene at the

inflammatory site without interfering with COX-1 production in the non-inflammed organs [133]. Mechanistic studies of TwHF revealed no impact on the activation of extracellular signal-regulated kinase, p38 MAPK, and JNK. Instead, TwHF partially inhibited the DNA binding capacity of cytokine-stimulated AP-1 and NF-$\varkappa$B transcription factors [135]. TP, a principal bioactive component of TwHF, was recently revealed to dysregulate glucose uptake via inhibition of the IKKβ-NF-$\varkappa$B pathway by p53 activation in cardiomyocytes [265]. Other studies reported that TP and its analogs (5*R*)-5-hydroxytriptolide (LLDT-8) and tripchlorolide (T4) inhibit NF-$\varkappa$B activation and JNK phosphorylation but not ERK1/2 and p38 phosphorylation in an LPS-triggered macrophage cell line (RAW 264.7) and microglial cells, suggesting that NF-$\varkappa$B and JNK were probably crucial targets for TwHF extracts [266,267].

Severe systemic toxicity of CS, resulting in a narrow therapeutic window, has been extensively reported [9,164]. Thus, the present study applied low concentration of CS (0.2 μM) that caused no cytotoxicity under the applied incubation conditions. Further investigation on nanotechnology-based and co-therapy of CS may further reduce the toxicity and improve bioavailability and may provide more evidence for the pharmacological therapy using this natural product.

In conclusion, our results revealed that CS affected polarization to M1 phenotypes via inhibition of pro-inflammatory COX-2 expression, COX-derived LM, especially PGE_2, through inhibition of inducible mPEGS-1. CS hardly affected polarization to the M2 phenotype but has a detrimental impact on the capacity to generate SPM which might be due to blocking 15-LOX-1 and 15-LOX-2 expression. These studies reveal complex LM network modulation by CS in a long-term manner, calling for consideration of the application of this natural product to treat inflammatory diseases.

5 References

1. Medzhitov, R. Origin and physiological roles of inflammation. *Nature* 2008, 454, 428-435.
2. Nathan, C. Points of control in inflammation. *Nature* 2002, 420, 846-852.
3. Chiurchiu, V.; Leuti, A.; Maccarrone, M. Bioactive lipids and chronic inflammation: Managing the fire within. *Front Immunol* 2018, 9, 38.
4. Serhan, C.N.; Brain, S.D.; Buckley, C.D.; Gilroy, D.W.; Haslett, C.; O'Neill, L.A.; Perretti, M.; Rossi, A.G.; Wallace, J.L. Resolution of inflammation: State of the art, definitions and terms. *FASEB J* 2007, 21, 325-332.
5. Serhan, C.N. Pro-resolving lipid mediators are leads for resolution physiology. *Nature* 2014, 510, 92-101.
6. Zhang, Y.; Mao, X.; Li, W.; Chen, W.; Wang, X.; Ma, Z.; Lin, N. Tripterygium wilfordii: An inspiring resource for rheumatoid arthritis treatment. *Med Res Rev* 2021, 41, 1337-1374.
7. Xu, X.; Li, Q.J.; Xia, S.; Wang, M.M.; Ji, W. Tripterygium glycosides for treating late-onset rheumatoid arthritis: A systematic review and meta-analysis. *Altern Ther Health Med* 2016, 22, 32-39.
8. Venkatesha, S.H.; Dudics, S.; Astry, B.; Moudgil, K.D. Control of autoimmune inflammation by celastrol, a natural triterpenoid. *Pathog Dis* 2016, 74.
9. Chen, S.R.; Dai, Y.; Zhao, J.; Lin, L.; Wang, Y.; Wang, Y. A mechanistic overview of triptolide and celastrol, natural products from tripterygium wilfordii hook f. *Front Pharmacol* 2018, 9, 104.
10. Serhan, C.N.; Savill, J. Resolution of inflammation: The beginning programs the end. *Nat Immunol* 2005, 6, 1191-1197.
11. Gilroy, D.W.; Lawrence, T.; Perretti, M.; Rossi, A.G. Inflammatory resolution: New opportunities for drug discovery. *Nat Rev Drug Discov* 2004, 3, 401-416.
12. Levy, B.D.; Clish, C.B.; Schmidt, B.; Gronert, K.; Serhan, C.N. Lipid mediator class switching during acute inflammation: Signals in resolution. *Nat Immunol* 2001, 2, 612-619.
13. Serhan, C.N. Resolution phase of inflammation: Novel endogenous anti-inflammatory

and proresolving lipid mediators and pathways. *Annu Rev Immunol* 2007, 25, 101-137.

14. Fullerton, J.N.; Gilroy, D.W. Resolution of inflammation: A new therapeutic frontier. *Nat Rev Drug Discov* 2016, 15, 551-567.
15. Dalli, J. Does promoting resolution instead of inhibiting inflammation represent the new paradigm in treating infections? *Mol Aspects Med* 2017, 58, 12-20.
16. Hansen, T.V.; Vik, A.; Serhan, C.N. The protectin family of specialized pro-resolving mediators: Potent immunoresolvents enabling innovative approaches to target obesity and diabetes. *Front Pharmacol* 2018, 9, 1582.
17. Malmsten, C.L. Prostaglandins, thromboxanes, and leukotrienes in inflammation. *Am J Med* 1986, 80, 11-17.
18. Moreno, J.J. Differential effects of arachidonic and eicosapentaenoic acid-derived eicosanoids on polymorphonuclear transmigration across endothelial cell cultures. *J Pharmacol Exp Ther* 2009, 331, 1111-1117.
19. Bergstroem, S.; Samuelsson, B. Prostaglandins. *Annu Rev Biochem* 1965, 34, 101-108.
20. Simmons, D.L.; Botting, R.M.; Hla, T. Cyclooxygenase isozymes: The biology of prostaglandin synthesis and inhibition. *Pharmacol Rev* 2004, 56, 387-437.
21. Smith, W.L.; Urade, Y.; Jakobsson, P.J. Enzymes of the cyclooxygenase pathways of prostanoid biosynthesis. *Chem Rev* 2011, 111, 5821-5865.
22. Dubois, R.N.; Abramson, S.B.; Crofford, L.; Gupta, R.A.; Simon, L.S.; Van De Putte, L.B.; Lipsky, P.E. Cyclooxygenase in biology and disease. *FASEB J* 1998, 12, 1063-1073.
23. Smyth, E.M.; Grosser, T.; Wang, M.; Yu, Y.; FitzGerald, G.A. Prostanoids in health and disease. *J Lipid Res* 2009, 50 Suppl, S423-428.
24. Zarghi, A.; Arfaei, S. Selective cox-2 inhibitors: A review of their structure-activity relationships. *Iran J Pharm Res* 2011, 10, 655-683.
25. Wang, D.; Wang, M.; Cheng, Y.; Fitzgerald, G.A. Cardiovascular hazard and non-steroidal anti-inflammatory drugs. *Curr Opin Pharmacol* 2005, 5, 204-210.
26. Trelle, S.; Reichenbach, S.; Wandel, S.; Hildebrand, P.; Tschannen, B.; Villiger, P.M.; Egger, M.; Juni, P. Cardiovascular safety of non-steroidal anti-inflammatory drugs: Network meta-analysis. *BMJ* 2011, 342, c7086.
27. Funk, C.D. Prostaglandins and leukotrienes: Advances in eicosanoid biology. *Science* 2001, 294, 1871-1875.
28. Radmark, O.; Werz, O.; Steinhilber, D.; Samuelsson, B. 5-lipoxygenase, a key enzyme for leukotriene biosynthesis in health and disease. *Biochim Biophys Acta* 2015, 1851, 331-339.
29. Chiang, N.; Arita, M.; Serhan, C.N. Anti-inflammatory circuitry: Lipoxin, aspirin-triggered lipoxins and their receptor alx. *Prostaglandins Leukot Essent Fatty Acids*

2005, 73, 163-177.

30. Wan, M.; Tang, X.; Stsiapanava, A.; Haeggstrom, J.Z. Biosynthesis of leukotriene b4. *Semin Immunol* 2017, 33, 3-15.
31. Bell, R.L.; Harris, R.R. The enzymology and pharmacology of 5-lipoxygenase and 5-lipoxygenase activating protein. *Clin Rev Allergy Immunol* 1999, 17, 91-109.
32. Duroudier, N.P.; Tulah, A.S.; Sayers, I. Leukotriene pathway genetics and pharmacogenetics in allergy. *Allergy* 2009, 64, 823-839.
33. Segal, B.H.; Kuhns, D.B.; Ding, L.; Gallin, J.I.; Holland, S.M. Thioglycollate peritonitis in mice lacking c5, 5-lipoxygenase, or p47(phox): Complement, leukotrienes, and reactive oxidants in acute inflammation. *J Leukoc Biol* 2002, 71, 410-416.
34. Joshi, Y.B.; Pratico, D. The 5-lipoxygenase pathway: Oxidative and inflammatory contributions to the alzheimer's disease phenotype. *Front Cell Neurosci* 2014, 8, 436.
35. Cheon, E.C.; Strouch, M.J.; Krantz, S.B.; Heiferman, M.J.; Bentrem, D.J. Genetic deletion of 5-lipoxygenase increases tumor-infiltrating macrophages in apc(delta468) mice. *J Gastrointest Surg* 2012, 16, 389-393.
36. Wenzel, S.E. The role of leukotrienes in asthma. *Prostaglandins Leukot Essent Fatty Acids* 2003, 69, 145-155.
37. Poff, C.D.; Balazy, M. Drugs that target lipoxygenases and leukotrienes as emerging therapies for asthma and cancer. *Curr Drug Targets Inflamm Allergy* 2004, 3, 19-33.
38. Pettersen, D.; Davidsson, O.; Whatling, C. Recent advances for flap inhibitors. *Bioorg Med Chem Lett* 2015, 25, 2607-2612.
39. Calder, P.C. Omega-3 polyunsaturated fatty acids and inflammatory processes: Nutrition or pharmacology? *Br J Clin Pharmacol* 2013, 75, 645-662.
40. Ryan, A.; Godson, C. Lipoxins: Regulators of resolution. *Curr Opin Pharmacol* 2010, 10, 166-172.
41. Ghasemi Fard, S.; Cameron-Smith, D.; Sinclair, A.J. N - 3 docosapentaenoic acid: The iceberg n - 3 fatty acid. *Curr Opin Clin Nutr Metab Care* 2021, 24, 134-138.
42. Barnig, C.; Cernadas, M.; Dutile, S.; Liu, X.; Perrella, M.A.; Kazani, S.; Wechsler, M.E.; Israel, E.; Levy, B.D. Lipoxin a4 regulates natural killer cell and type 2 innate lymphoid cell activation in asthma. *Sci Transl Med* 2013, 5, 174ra126.
43. Kazani, S.; Planaguma, A.; Ono, E.; Bonini, M.; Zahid, M.; Marigowda, G.; Wechsler, M.E.; Levy, B.D.; Israel, E. Exhaled breath condensate eicosanoid levels associate with asthma and its severity. *J Allergy Clin Immunol* 2013, 132, 547-553.
44. Serhan, C.N.; Jain, A.; Marleau, S.; Clish, C.; Kantarci, A.; Behbehani, B.; Colgan, S.P.; Stahl, G.L.; Merched, A.; Petasis, N.A., et al. Reduced inflammation and tissue damage in transgenic rabbits overexpressing 15-lipoxygenase and endogenous anti-

inflammatory lipid mediators. *J Immunol* 2003, 171, 6856-6865.

45. Bannenberg, G.L.; Aliberti, J.; Hong, S.; Sher, A.; Serhan, C. Exogenous pathogen and plant 15-lipoxygenase initiate endogenous lipoxin a4 biosynthesis. *J Exp Med* 2004, 199, 515-523.
46. Chandrasekharan, J.A.; Sharma-Walia, N. Lipoxins: Nature's way to resolve inflammation. *J Inflamm Res* 2015, 8, 181-192.
47. Godson, C.; Mitchell, S.; Harvey, K.; Petasis, N.A.; Hogg, N.; Brady, H.R. Cutting edge: Lipoxins rapidly stimulate nonphlogistic phagocytosis of apoptotic neutrophils by monocyte-derived macrophages. *J Immunol* 2000, 164, 1663-1667.
48. Bafica, A.; Scanga, C.A.; Serhan, C.; Machado, F.; White, S.; Sher, A.; Aliberti, J. Host control of mycobacterium tuberculosis is regulated by 5-lipoxygenase-dependent lipoxin production. *J Clin Invest* 2005, 115, 1601-1606.
49. Wang, X.; Zhu, M.; Hjorth, E.; Cortes-Toro, V.; Eyjolfsdottir, H.; Graff, C.; Nennesmo, I.; Palmblad, J.; Eriksdotter, M.; Sambamurti, K., et al. Resolution of inflammation is altered in alzheimer's disease. *Alzheimers Dement* 2015, 11, 40-50 e41-42.
50. Zhu, M.; Wang, X.; Hjorth, E.; Colas, R.A.; Schroeder, L.; Granholm, A.C.; Serhan, C.N.; Schultzberg, M. Pro-resolving lipid mediators improve neuronal survival and increase abeta42 phagocytosis. *Mol Neurobiol* 2016, 53, 2733-2749.
51. Nielsen, M.M.; Lambertsen, K.L.; Clausen, B.H.; Meyer, M.; Bhandari, D.R.; Larsen, S.T.; Poulsen, S.S.; Spengler, B.; Janfelt, C.; Hansen, H.S. Mass spectrometry imaging of biomarker lipids for phagocytosis and signalling during focal cerebral ischaemia. *Sci Rep* 2016, 6, 39571.
52. Serhan, C.N.; Yang, R.; Martinod, K.; Kasuga, K.; Pillai, P.S.; Porter, T.F.; Oh, S.F.; Spite, M. Maresins: Novel macrophage mediators with potent antiinflammatory and proresolving actions. *J Exp Med* 2009, 206, 15-23.
53. Dalli, J.; Zhu, M.; Vlasenko, N.A.; Deng, B.; Haeggstrom, J.Z.; Petasis, N.A.; Serhan, C.N. The novel 13s,14s-epoxy-maresin is converted by human macrophages to maresin 1 (mar1), inhibits leukotriene a4 hydrolase (lta4h), and shifts macrophage phenotype. *FASEB J* 2013, 27, 2573-2583.
54. Deng, B.; Wang, C.W.; Arnardottir, H.H.; Li, Y.; Cheng, C.Y.; Dalli, J.; Serhan, C.N. Maresin biosynthesis and identification of maresin 2, a new anti-inflammatory and pro-resolving mediator from human macrophages. *PLoS One* 2014, 9, e102362.
55. Saito-Sasaki, N.; Sawada, Y.; Mashima, E.; Yamaguchi, T.; Ohmori, S.; Yoshioka, H.; Haruyama, S.; Okada, E.; Nakamura, M. Maresin-1 suppresses imiquimod-induced skin inflammation by regulating il-23 receptor expression. *Sci Rep* 2018, 8, 5522.
56. Cezar, T.L.C.; Martinez, R.M.; Rocha, C.D.; Melo, C.P.B.; Vale, D.L.; Borghi, S.M.; Fattori, V.; Vignoli, J.A.; Camilios-Neto, D.; Baracat, M.M., et al. Treatment with

maresin 1, a docosahexaenoic acid-derived pro-resolution lipid, protects skin from inflammation and oxidative stress caused by uvb irradiation. *Sci Rep* 2019, 9, 3062.

57. Serhan, C.N.; Dalli, J.; Karamnov, S.; Choi, A.; Park, C.K.; Xu, Z.Z.; Ji, R.R.; Zhu, M.; Petasis, N.A. Macrophage proresolving mediator maresin 1 stimulates tissue regeneration and controls pain. *FASEB J* 2012, 26, 1755-1765.
58. Francos-Quijorna, I.; Santos-Nogueira, E.; Gronert, K.; Sullivan, A.B.; Kopp, M.A.; Brommer, B.; David, S.; Schwab, J.M.; Lopez-Vales, R. Maresin 1 promotes inflammatory resolution, neuroprotection, and functional neurological recovery after spinal cord injury. *J Neurosci* 2017, 37, 11731-11743.
59. Yang, T.; Xu, G.; Newton, P.T.; Chagin, A.S.; Mkrtchian, S.; Carlstrom, M.; Zhang, X.M.; Harris, R.A.; Cooter, M.; Berger, M., et al. Maresin 1 attenuates neuroinflammation in a mouse model of perioperative neurocognitive disorders. *Br J Anaesth* 2019, 122, 350-360.
60. Serhan, C.N.; Hong, S.; Gronert, K.; Colgan, S.P.; Devchand, P.R.; Mirick, G.; Moussignac, R.L. Resolvins: A family of bioactive products of omega-3 fatty acid transformation circuits initiated by aspirin treatment that counter proinflammation signals. *J Exp Med* 2002, 196, 1025-1037.
61. Serhan, C.N.; Levy, B.D. Resolvins in inflammation: Emergence of the pro-resolving superfamily of mediators. *J Clin Invest* 2018, 128, 2657-2669.
62. Li, C.; Wu, X.; Liu, S.; Shen, D.; Zhu, J.; Liu, K. Role of resolvins in the inflammatory resolution of neurological diseases. *Front Pharmacol* 2020, 11, 612.
63. Titos, E.; Rius, B.; Gonzalez-Periz, A.; Lopez-Vicario, C.; Moran-Salvador, E.; Martinez-Clemente, M.; Arroyo, V.; Claria, J. Resolvin d1 and its precursor docosahexaenoic acid promote resolution of adipose tissue inflammation by eliciting macrophage polarization toward an m2-like phenotype. *J Immunol* 2011, 187, 5408-5418.
64. Recchiuti, A. Resolvin d1 and its gpcrs in resolution circuits of inflammation. *Prostaglandins Other Lipid Mediat* 2013, 107, 64-76.
65. Serhan, C.N.; Dalli, J.; Colas, R.A.; Winkler, J.W.; Chiang, N. Protectins and maresins: New pro-resolving families of mediators in acute inflammation and resolution bioactive metabolome. *Biochim Biophys Acta* 2015, 1851, 397-413.
66. Serhan, C.N.; Gotlinger, K.; Hong, S.; Lu, Y.; Siegelman, J.; Baer, T.; Yang, R.; Colgan, S.P.; Petasis, N.A. Anti-inflammatory actions of neuroprotectin d1/protectin d1 and its natural stereoisomers: Assignments of dihydroxy-containing docosatrienes. *J Immunol* 2006, 176, 1848-1859.
67. Berg, R.W.V.; Davidsson, J.; Lidin, E.; Angeria, M.; Risling, M.; Gunther, M. Brain tissue saving effects by single-dose intralesional administration of neuroprotectin d1 on experimental focal penetrating brain injury in rats. *J Clin Neurosci* 2019, 64,

227-233.

68. Serhan, C.N.; Fredman, G.; Yang, R.; Karamnov, S.; Belayev, L.S.; Bazan, N.G.; Zhu, M.; Winkler, J.W.; Petasis, N.A. Novel proresolving aspirin-triggered dha pathway. *Chem Biol* 2011, 18, 976-987.

69. Bazan, N.G.; Eady, T.N.; Khoutorova, L.; Atkins, K.D.; Hong, S.; Lu, Y.; Zhang, C.; Jun, B.; Obenaus, A.; Fredman, G., et al. Novel aspirin-triggered neuroprotectin d1 attenuates cerebral ischemic injury after experimental stroke. *Exp Neurol* 2012, 236, 122-130.

70. Chiang, N.; Serhan, C.N. Specialized pro-resolving mediator network: An update on production and actions. *Essays Biochem* 2020, 64, 443-462.

71. Serhan, C.N.; Chiang, N.; Dalli, J. New pro-resolving n-3 mediators bridge resolution of infectious inflammation to tissue regeneration. *Mol Aspects Med* 2018, 64, 1-17.

72. Norris, P.C.; Libreros, S.; Serhan, C.N. Resolution metabolomes activated by hypoxic environment. *Sci Adv* 2019, 5, eaax4895.

73. Arita, M.; Bianchini, F.; Aliberti, J.; Sher, A.; Chiang, N.; Hong, S.; Yang, R.; Petasis, N.A.; Serhan, C.N. Stereochemical assignment, antiinflammatory properties, and receptor for the omega-3 lipid mediator resolvin e1. *J Exp Med* 2005, 201, 713-722.

74. Tjonahen, E.; Oh, S.F.; Siegelman, J.; Elangovan, S.; Percarpio, K.B.; Hong, S.; Arita, M.; Serhan, C.N. Resolvin e2: Identification and anti-inflammatory actions: Pivotal role of human 5-lipoxygenase in resolvin e series biosynthesis. *Chem Biol* 2006, 13, 1193-1202.

75. Quiros, M.; Feier, D.; Birkl, D.; Agarwal, R.; Zhou, D.W.; Garcia, A.J.; Parkos, C.A.; Nusrat, A. Resolvin e1 is a pro-repair molecule that promotes intestinal epithelial wound healing. *Proc Natl Acad Sci U S A* 2020, 117, 9477-9482.

76. Oh, S.F.; Dona, M.; Fredman, G.; Krishnamoorthy, S.; Irimia, D.; Serhan, C.N. Resolvin e2 formation and impact in inflammation resolution. *J Immunol* 2012, 188, 4527-4534.

77. Isobe, Y.; Arita, M.; Matsueda, S.; Iwamoto, R.; Fujihara, T.; Nakanishi, H.; Taguchi, R.; Masuda, K.; Sasaki, K.; Urabe, D., et al. Identification and structure determination of novel anti-inflammatory mediator resolvin e3, 17,18-dihydroxyeicosapentaenoic acid. *J Biol Chem* 2012, 287, 10525-10534.

78. Deyama, S.; Shimoda, K.; Ikeda, H.; Fukuda, H.; Shuto, S.; Minami, M. Resolvin e3 attenuates lipopolysaccharide-induced depression-like behavior in mice. *J Pharmacol Sci* 2018, 138, 86-88.

79. Sato, M.; Aoki-Saito, H.; Fukuda, H.; Ikeda, H.; Koga, Y.; Yatomi, M.; Tsurumaki, H.; Maeno, T.; Saito, T.; Nakakura, T., et al. Resolvin e3 attenuates allergic airway inflammation via the interleukin-23-interleukin-17a pathway. *FASEB J* 2019, 33, 12750-12759.

80. Dalli, J.; Colas, R.A.; Serhan, C.N. Novel n-3 immunoresolvents: Structures and actions. *Sci Rep* 2013, 3, 1940.

81. Dalli, J.; Chiang, N.; Serhan, C.N. Elucidation of novel 13-series resolvins that increase with atorvastatin and clear infections. *Nat Med* 2015, 21, 1071-1075.

82. Colas, R.A.; Souza, P.R.; Walker, M.E.; Burton, M.; Zaslona, Z.; Curtis, A.M.; Marques, R.M.; Dalli, J. Impaired production and diurnal regulation of vascular rvdn-3 dpa increase systemic inflammation and cardiovascular disease. *Circ Res* 2018, 122, 855-863.

83. Walker, M.E.; Souza, P.R.; Colas, R.A.; Dalli, J. 13-series resolvins mediate the leukocyte-platelet actions of atorvastatin and pravastatin in inflammatory arthritis. *FASEB J* 2017, 31, 3636-3648.

84. Flak, M.B.; Colas, R.A.; Munoz-Atienza, E.; Curtis, M.A.; Dalli, J.; Pitzalis, C. Inflammatory arthritis disrupts gut resolution mechanisms, promoting barrier breakdown by porphyromonas gingivalis. *JCI Insight* 2019, 4.

85. Gobbetti, T.; Dalli, J.; Colas, R.A.; Federici Canova, D.; Aursnes, M.; Bonnet, D.; Alric, L.; Vergnolle, N.; Deraison, C.; Hansen, T.V., et al. Protectin d1n-3 dpa and resolvin d5n-3 dpa are effectors of intestinal protection. *Proc Natl Acad Sci U S A* 2017, 114, 3963-3968.

86. Frigerio, F.; Pasqualini, G.; Craparotta, I.; Marchini, S.; van Vliet, E.A.; Foerch, P.; Vandenplas, C.; Leclercq, K.; Aronica, E.; Porcu, L., et al. N-3 docosapentaenoic acid-derived protectin d1 promotes resolution of neuroinflammation and arrests epileptogenesis. *Brain* 2018, 141, 3130-3143.

87. Janeway, C.A., Jr.; Medzhitov, R. Innate immune recognition. *Annu Rev Immunol* 2002, 20, 197-216.

88. van Furth, R.; Cohn, Z.A. The origin and kinetics of mononuclear phagocytes. *J Exp Med* 1968, 128, 415-435.

89. Auffray, C.; Sieweke, M.H.; Geissmann, F. Blood monocytes: Development, heterogeneity, and relationship with dendritic cells. *Annu Rev Immunol* 2009, 27, 669-692.

90. Swirski, F.K.; Nahrendorf, M.; Etzrodt, M.; Wildgruber, M.; Cortez-Retamozo, V.; Panizzi, P.; Figueiredo, J.L.; Kohler, R.H.; Chudnovskiy, A.; Waterman, P., et al. Identification of splenic reservoir monocytes and their deployment to inflammatory sites. *Science* 2009, 325, 612-616.

91. Van Furth, R.; Diesselhoff-den Dulk, M.C.; Mattie, H. Quantitative study on the production and kinetics of mononuclear phagocytes during an acute inflammatory reaction. *J Exp Med* 1973, 138, 1314-1330.

92. Serbina, N.V.; Jia, T.; Hohl, T.M.; Pamer, E.G. Monocyte-mediated defense against microbial pathogens. *Annu Rev Immunol* 2008, 26, 421-452.

93. Jakubzick, C.; Gautier, E.L.; Gibbings, S.L.; Sojka, D.K.; Schlitzer, A.; Johnson, T.E.; Ivanov, S.; Duan, Q.; Bala, S.; Condon, T., et al. Minimal differentiation of classical monocytes as they survey steady-state tissues and transport antigen to lymph nodes. *Immunity* 2013, 39, 599-610.

94. Passlick, B.; Flieger, D.; Ziegler-Heitbrock, H.W. Identification and characterization of a novel monocyte subpopulation in human peripheral blood. *Blood* 1989, 74, 2527-2534.

95. Geissmann, F.; Jung, S.; Littman, D.R. Blood monocytes consist of two principal subsets with distinct migratory properties. *Immunity* 2003, 19, 71-82.

96. Tacke, F.; Randolph, G.J. Migratory fate and differentiation of blood monocyte subsets. *Immunobiology* 2006, 211, 609-618.

97. Weber, C.; Belge, K.U.; von Hundelshausen, P.; Draude, G.; Steppich, B.; Mack, M.; Frankenberger, M.; Weber, K.S.; Ziegler-Heitbrock, H.W. Differential chemokine receptor expression and function in human monocyte subpopulations. *J Leukoc Biol* 2000, 67, 699-704.

98. Sallusto, F.; Lanzavecchia, A. Efficient presentation of soluble antigen by cultured human dendritic cells is maintained by granulocyte/macrophage colony-stimulating factor plus interleukin 4 and downregulated by tumor necrosis factor alpha. *J Exp Med* 1994, 179, 1109-1118.

99. Grage-Griebenow, E.; Zawatzky, R.; Kahlert, H.; Brade, L.; Flad, H.; Ernst, M. Identification of a novel dendritic cell-like subset of cd64(+) / cd16(+) blood monocytes. *Eur J Immunol* 2001, 31, 48-56.

100. Sunderkotter, C.; Nikolic, T.; Dillon, M.J.; Van Rooijen, N.; Stehling, M.; Drevets, D.A.; Leenen, P.J. Subpopulations of mouse blood monocytes differ in maturation stage and inflammatory response. *J Immunol* 2004, 172, 4410-4417.

101. Gordon, S.; Taylor, P.R. Monocyte and macrophage heterogeneity. *Nat Rev Immunol* 2005, 5, 953-964.

102. Gordon, S. The role of the macrophage in immune regulation. *Res Immunol* 1998, 149, 685-688.

103. Yona, S.; Kim, K.W.; Wolf, Y.; Mildner, A.; Varol, D.; Breker, M.; Strauss-Ayali, D.; Viukov, S.; Guilliams, M.; Misharin, A., et al. Fate mapping reveals origins and dynamics of monocytes and tissue macrophages under homeostasis. *Immunity* 2013, 38, 79-91.

104. Epelman, S.; Lavine, K.J.; Randolph, G.J. Origin and functions of tissue macrophages. *Immunity* 2014, 41, 21-35.

105. Saradna, A.; Do, D.C.; Kumar, S.; Fu, Q.L.; Gao, P. Macrophage polarization and allergic asthma. *Transl Res* 2018, 191, 1-14.

106. Arora, S.; Dev, K.; Agarwal, B.; Das, P.; Syed, M.A. Macrophages: Their role, activation and polarization in pulmonary diseases. *Immunobiology* 2018, 223, 383-396.

107. Robbe, P.; Draijer, C.; Borg, T.R.; Luinge, M.; Timens, W.; Wouters, I.M.; Melgert, B.N.; Hylkema, M.N. Distinct macrophage phenotypes in allergic and nonallergic lung inflammation. *Am J Physiol Lung Cell Mol Physiol* 2015, 308, L358-367.

108. Dalli, J.; Serhan, C.N. Specific lipid mediator signatures of human phagocytes: Microparticles stimulate macrophage efferocytosis and pro-resolving mediators. *Blood* 2012, 120, e60-72.

109. Gordon, S. Alternative activation of macrophages. *Nat Rev Immunol* 2003, 3, 23-35.

110. Dewhurst, J.A.; Lea, S.; Hardaker, E.; Dungwa, J.V.; Ravi, A.K.; Singh, D. Characterisation of lung macrophage subpopulations in copd patients and controls. *Sci Rep* 2017, 7, 7143.

111. Abdelaziz, M.H.; Abdelwahab, S.F.; Wan, J.; Cai, W.; Huixuan, W.; Jianjun, C.; Kumar, K.D.; Vasudevan, A.; Sadek, A.; Su, Z., et al. Alternatively activated macrophages; a double-edged sword in allergic asthma. *J Transl Med* 2020, 18, 58.

112. Novak, M.L.; Koh, T.J. Macrophage phenotypes during tissue repair. J Leukoc Biol 2013, 93, 875-881.

113. Witherel, C.E.; Graney, P.L.; Freytes, D.O.; Weingarten, M.S.; Spiller, K.L. Response of human macrophages to wound matrices in vitro. *Wound Repair Regen* 2016, 24, 514-524.

114. Kubota, T.; Inoue, M.; Kubota, N.; Takamoto, I.; Mineyama, T.; Iwayama, K.; Tokuyama, K.; Moroi, M.; Ueki, K.; Yamauchi, T., et al. Downregulation of macrophage irs2 by hyperinsulinemia impairs il-4-indeuced m2a-subtype macrophage activation in obesity. *Nat Commun* 2018, 9, 4863.

115. Mirza, R.; Koh, T.J. Dysregulation of monocyte/macrophage phenotype in wounds of diabetic mice. *Cytokine* 2011, 56, 256-264.

116. Klinkert, K.; Whelan, D.; Clover, A.J.P.; Leblond, A.L.; Kumar, A.H.S.; Caplice, N.M. Selective m2 macrophage depletion leads to prolonged inflammation in surgical wounds. *Eur Surg Res* 2017, 58, 109-120.

117. Burn, G.L.; Foti, A.; Marsman, G.; Patel, D.F.; Zychlinsky, A. The neutrophil. *Immunity* 2021, 54, 1377-1391.

118. Park, S.A.; Hyun, Y.M. Neutrophil extravasation cascade: What can we learn from two-photon intravital imaging? *Immune Netw* 2016, 16, 317-321.

119. Yang, F.; Feng, C.; Zhang, X.; Lu, J.; Zhao, Y. The diverse biological functions of neutrophils, beyond the defense against infections. *Inflammation* 2017, 40, 311-323.

120. Tamassia, N.; Bianchetto-Aguilera, F.; Arruda-Silva, F.; Gardiman, E.; Gasperini, S.;

Calzetti, F.; Cassatella, M.A. Cytokine production by human neutrophils: Revisiting the "dark side of the moon". *Eur J Clin Invest* 2018, 48 Suppl 2, e12952.

121. Qian, C.; Cao, X. Dendritic cells in the regulation of immunity and inflammation. *Semin Immunol* 2018, 35, 3-11.

122. Mukai, K.; Tsai, M.; Saito, H.; Galli, S.J. Mast cells as sources of cytokines, chemokines, and growth factors. *Immunol Rev* 2018, 282, 121-150.

123. Vivier, E.; Tomasello, E.; Baratin, M.; Walzer, T.; Ugolini, S. Functions of natural killer cells. *Nat Immunol* 2008, 9, 503-510.

124. Iype, J.; Fux, M. Basophils orchestrating eosinophils' chemotaxis and function in allergic inflammation. *Cells* 2021, 10.

125. Luo, D.; Zuo, Z.; Zhao, H.; Tan, Y.; Xiao, C. Immunoregulatory effects of tripterygium wilfordii hook f and its extracts in clinical practice. *Front Med* 2019, 13, 556-563.

126. Song, C.Y.; Xu, Y.G.; Lu, Y.Q. Use of tripterygium wilfordii hook f for immune-mediated inflammatory diseases: Progress and future prospects. *J Zhejiang Univ Sci B* 2020, 21, 280-290.

127. Tao, X.; Lipsky, P.E. The chinese anti-inflammatory and immunosuppressive herbal remedy tripterygium wilfordii hook f. *Rheum Dis Clin North Am* 2000, 26, 29-50, viii.

128. Qin, W.Z.; Lin, J. Advance of the research on tripterygium wilfordii hook f. To a new height. *Chin J Integr Med* 2005, 11, 87-88.

129. Tao, X.; Cai, J.J.; Lipsky, P.E. The identity of immunosuppressive components of the ethyl acetate extract and chloroform methanol extract (t2) of tripterygium wilfordii hook. F. *J Pharmacol Exp Ther* 1995, 272, 1305-1312.

130. Lipsky, P.E.; Tao, X.L. A potential new treatment for rheumatoid arthritis: Thunder god vine. *Semin Arthritis Rheum* 1997, 26, 713-723.

131. Canter, P.H.; Lee, H.S.; Ernst, E. A systematic review of randomised clinical trials of tripterygium wilfordii for rheumatoid arthritis. *Phytomedicine* 2006, 13, 371-377.

132. Lin, N.; Zhang, Y.Q.; Jiang, Q.; Liu, W.; Liu, J.; Huang, Q.C.; Wu, K.Y.; Tu, S.H.; Zhou, Z.S.; Chen, W.H., et al. Clinical practice guideline for tripterygium glycosides/tripterygium wilfordii tablets in the treatment of rheumatoid arthritis. *Front Pharmacol* 2020, 11, 608703.

133. Tao, X.; Ma, L.; Mao, Y.; Lipsky, P.E. Suppression of carrageenan-induced inflammation in vivo by an extract of the chinese herbal remedy tripterygium wilfordii hook f. *Inflamm Res* 1999, 48, 139-148.

134. Tao, X.; Schulze-Koops, H.; Ma, L.; Cai, J.; Mao, Y.; Lipsky, P.E. Effects of tripterygium wilfordii hook f extracts on induction of cyclooxygenase 2 activity and prostaglandin e2 production. *Arthritis Rheum* 1998, 41, 130-138.

135. Sylvester, J.; Liacini, A.; Li, W.Q.; Dehnade, F.; Zafarullah, M. Tripterygium wilfordii hook f extract suppresses proinflammatory cytokine-induced expression of matrix metalloproteinase genes in articular chondrocytes by inhibiting activating protein-1 and nuclear factor-kappab activities. *Mol Pharmacol* 2001, 59, 1196-1205.

136. Brinker, A.M.; Ma, J.; Lipsky, P.E.; Raskin, I. Medicinal chemistry and pharmacology of genus tripterygium (celastraceae). *Phytochemistry* 2007, 68, 732-766.

137. Luk, J.M.; Lai, W.; Tam, P.; Koo, M.W. Suppression of cytokine production and cell adhesion molecule expression in human monocytic cell line thp-1 by tripterygium wilfordii polysaccharide moiety. *Life Sci* 2000, 67, 155-163.

138. Chang, D.M.; Kuo, S.Y.; Lai, J.H.; Chang, M.L. Effects of anti-rheumatic herbal medicines on cellular adhesion molecules. *Ann Rheum Dis* 1999, 58, 366-371.

139. Abdin, A.A.; Hasby, E.A. Modulatory effect of celastrol on th1/th2 cytokines profile, tlr2 and cd3+ t-lymphocyte expression in a relapsing-remitting model of multiple sclerosis in rats. *Eur J Pharmacol* 2014, 742, 102-112.

140. Zhou, Y.; Hong, Y.; Huang, H. Triptolide attenuates inflammatory response in membranous glomerulo-nephritis rat via downregulation of nf-kappab signaling pathway. *Kidney Blood Press Res* 2016, 41, 901-910.

141. Qiu, D.; Kao, P.N. Immunosuppressive and anti-inflammatory mechanisms of triptolide, the principal active diterpenoid from the chinese medicinal herb tripterygium wilfordii hook. F. *Drugs R D* 2003, 4, 1-18.

142. Wang, H.L.; Jiang, Q.; Feng, X.H.; Zhang, H.D.; Ge, L.; Luo, C.G.; Gong, X.; Li, B. Tripterygium wilfordii hook f versus conventional synthetic disease-modifying anti-rheumatic drugs as monotherapy for rheumatoid arthritis: A systematic review and network meta-analysis. *BMC Complement Altern Med* 2016, 16, 215.

143. Zhou, Y.Y.; Xia, X.; Peng, W.K.; Wang, Q.H.; Peng, J.H.; Li, Y.L.; Wu, J.X.; Zhang, J.Y.; Zhao, Y.; Chen, X.M., et al. The effectiveness and safety of tripterygium wilfordii hook. F extracts in rheumatoid arthritis: A systematic review and meta-analysis. *Front Pharmacol* 2018, 9, 356.

144. Zheng, W.; Mei, Y.; Chen, C.; Cai, L.; Chen, H. The effectiveness and safety of tripterygium wilfordii glycosides combined with disease-modifying anti-rheumatic drugs in the treatment of rheumatoid arthritis: A systematic review and meta-analysis of 40 randomized controlled trials. *Phytother Res* 2021, 35, 2902-2924.

145. Jiang, M.; Zha, Q.; Zhang, C.; Lu, C.; Yan, X.; Zhu, W.; Liu, W.; Tu, S.; Hou, L.; Wang, C., et al. Predicting and verifying outcome of tripterygium wilfordii hook f. Based therapy in rheumatoid arthritis: From open to double-blinded randomized trial. *Sci Rep* 2015, 5, 9700.

146. Li, X.W.; Weir, M.R. Radix tripterygium wilfordii–a chinese herbal medicine with

potent immunosuppressive properties. *Transplantation* 1990, 50, 82-86.

147. Ho, L.J.; Chang, D.M.; Chang, M.L.; Kuo, S.Y.; Lai, J.H. Mechanism of immunosuppression of the antirheumatic herb twhf in human t cells. *J Rheumatol* 1999, 26, 14-24.

148. Bai, J.P.; Shi, Y.L. Inhibition of ca(2+) channels in mouse spermatogenic cells by male antifertility compounds from tripterygium wilfordii hook. F. *Contraception* 2002, 65, 441-445.

149. Horiuch, M.; Murakami, C.; Fukamiya, N.; Yu, D.; Chen, T.H.; Bastow, K.F.; Zhang, D.C.; Takaishi, Y.; Imakura, Y.; Lee, K.H. Tripfordines a-c, sesquiterpene pyridine alkaloids from tripterygium wilfordii, and structure anti-hiv activity relationships of tripterygium alkaloids. *J Nat Prod* 2006, 69, 1271-1274.

150. Liu, L.; Zhao, H.; Sun, X.; Zheng, Q.; Luo, Y.; Ru, Y.; Zhang, Y.; Chen, X.; Zhu, B.; Yin, C., et al. Efficacy and safety of tripterygium wilfordii hook f for chronic urticaria: A systematic review and meta-analysis. *BMC Complement Altern Med* 2018, 18, 243.

151. Tao, X.; Davis, L.S.; Lipsky, P.E. Effect of an extract of the chinese herbal remedy tripterygium wilfordii hook f on human immune responsiveness. *Arthritis Rheum* 1991, 34, 1274-1281.

152. Asano, K.; Matsuishi, J.; Yu, Y.; Kasahara, T.; Hisamitsu, T. Suppressive effects of tripterygium wilfordii hook f., a traditional chinese medicine, on collagen arthritis in mice. *Immunopharmacology* 1998, 39, 117-126.

153. Ru, Y.; Luo, Y.; Zhou, Y.; Kuai, L.; Sun, X.; Xing, M.; Liu, L.; Lu, Y.; Hong, S.; Chen, X., et al. Adverse events associated with treatment of tripterygium wilfordii hook f: A quantitative evidence synthesis. *Front Pharmacol* 2019, 10, 1250.

154. Shaker, M.E.; Ashamallah, S.A.; Houssen, M.E. Celastrol ameliorates murine colitis via modulating oxidative stress, inflammatory cytokines and intestinal homeostasis. *Chem Biol Interact* 2014, 210, 26-33.

155. Chen, X.; Zhao, Y.; Luo, W.; Chen, S.; Lin, F.; Zhang, X.; Fan, S.; Shen, X.; Wang, Y.; Liang, G. Celastrol induces ros-mediated apoptosis via directly targeting peroxiredoxin-2 in gastric cancer cells. *Theranostics* 2020, 10, 10290-10308.

156. Lu, Y.; Liu, Y.; Zhou, J.; Li, D.; Gao, W. Biosynthesis, total synthesis, structural modifications, bioactivity, and mechanism of action of the quinone-methide triterpenoid celastrol. *Med Res Rev* 2021, 41, 1022-1060.

157. Gunatilaka, A.A. Triterpenoid quinonemethides and related compounds (celastroloids). *Progress Chem Org Nat Prod* 1996, 1-123.

158. Hernandes, C.; Pereira, A.M.S.; Severino, P. Compounds from celastraceae targeting cancer pathways and their potential application in head and neck squamous cell carcinoma: A review. *Curr Genomics* 2017, 18, 60-74.

159. de la Torre, M.C.; Sierra. Comments on recent achievements in biomimetic organic synthesis. *Angew Chem* 2004, 43, 160-181.

160. Camelio, A.M.; Johnson, T.C.; Siegel, D. Total synthesis of celastrol, development of a platform to access celastroid natural products. *J Am Chem Soc* 2015, 137, 11864-11867.

161. Song, J.; Shi, F.; Zhang, Z.; Zhu, F.; Xue, J.; Tan, X.; Zhang, L.; Jia, X. Formulation and evaluation of celastrol-loaded liposomes. *Molecules* 2011, 16, 7880-7892.

162. Figueiredo, S.A.C.; Salvador, J.A.R.; Cortes, R.; Cascante, M. Design, synthesis and biological evaluation of novel c-29 carbamate celastrol derivatives as potent and selective cytotoxic compounds. *Eur J Med Chem* 2017, 139, 836-848.

163. Shan, W.G.; Wang, H.G.; Chen, Y.; Wu, R.; Wen, Y.T.; Zhang, L.W.; Ying, Y.M.; Wang, J.W.; Zhan, Z.J. Synthesis of 3- and 29-substituted celastrol derivatives and structure-activity relationship studies of their cytotoxic activities. *Bioorg Med Chem Lett* 2017, 27, 3450-3453.

164. Hou, W.; Liu, B.; Xu, H. Celastrol: Progresses in structure-modifications, structure-activity relationships, pharmacology and toxicology. *Eur J Med Chem* 2020, 189, 112081.

165. Wong, K.F.; Yuan, Y.; Luk, J.M. Tripterygium wilfordii bioactive compounds as anti-cancer and anti-inflammatory agents. *Clin Exp Pharmacol Physiol* 2012, 39, 311-320.

166. Zhao, J.; Sun, Y.; Shi, P.; Dong, J.N.; Zuo, L.G.; Wang, H.G.; Gong, J.F.; Li, Y.; Gu, L.L.; Li, N., et al. Celastrol ameliorates experimental colitis in il-10 deficient mice via the up-regulation of autophagy. *Int Immunopharmacol* 2015, 26, 221-228.

167. Pinna, G.F.; Fiorucci, M.; Reimund, J.M.; Taquet, N.; Arondel, Y.; Muller, C.D. Celastrol inhibits pro-inflammatory cytokine secretion in crohn's disease biopsies. *Biochem Biophys Res Commun* 2004, 322, 778-786.

168. Wang, R.; Gu, X.; Dai, W.; Ye, J.; Lu, F.; Chai, Y.; Fan, G.; Gonzalez, F.J.; Duan, G.; Qi, Y. A lipidomics investigation into the intervention of celastrol in experimental colitis. *Mol Biosyst* 2016, 12, 1436-1444.

169. Peroni, D.G.; Nuzzi, G.; Trambusti, I.; Di Cicco, M.E.; Comberiati, P. Microbiome composition and its impact on the development of allergic diseases. *Front Immunol* 2020, 11, 700.

170. Kim, D.Y.; Park, J.W.; Jeoung, D.; Ro, J.Y. Celastrol suppresses allergen-induced airway inflammation in a mouse allergic asthma model. *Eur J Pharmacol* 2009, 612, 98-105.

171. Kim, Y.; Kim, K.; Lee, H.; Han, S.; Lee, Y.S.; Choe, J.; Kim, Y.M.; Hahn, J.H.; Ro, J.Y.; Jeoung, D. Celastrol binds to erk and inhibits fcepsilonri signaling to exert an anti-allergic effect. *Eur J Pharmacol* 2009, 612, 131-142.

172. Akhmetshina, A.; Dees, C.; Busch, N.; Beer, J.; Sarter, K.; Zwerina, J.; Zimmer, A.; Distler, O.; Schett, G.; Distler, J.H. The cannabinoid receptor cb2 exerts antifibrotic

effects in experimental dermal fibrosis. *Arthritis Rheum* 2009, 60, 1129-1136.

173. Jiang, X.; Chen, S.; Zhang, Q.; Yi, C.; He, J.; Ye, X.; Liu, M.; Lu, W. Celastrol is a novel selective agonist of cannabinoid receptor 2 with anti-inflammatory and anti-fibrotic activity in a mouse model of systemic sclerosis. *Phytomedicine* 2020, 67, 153160.

174. Tang, M.; Cao, X.; Zhang, K.; Li, Y.; Zheng, Q.Y.; Li, G.Q.; He, Q.H.; Li, S.J.; Xu, G.L.; Zhang, K.Q. Celastrol alleviates renal fibrosis by upregulating cannabinoid receptor 2 expression. *Cell Death Dis* 2018, 9, 601.

175. Li, G.; Liu, D.; Zhang, Y.; Qian, Y.; Zhang, H.; Guo, S.; Sunagawa, M.; Hisamitsu, T.; Liu, Y. Celastrol inhibits lipopolysaccharide-stimulated rheumatoid fibroblast-like synoviocyte invasion through suppression of tlr4/nf-kappab-mediated matrix metalloproteinase-9 expression. *PLoS One* 2013, 8, e68905.

176. Wu, M.; Chen, W.; Yu, X.; Ding, D.; Zhang, W.; Hua, H.; Xu, M.; Meng, X.; Zhang, X.; Zhang, Y., et al. Celastrol aggravates lps-induced inflammation and injuries of liver and kidney in mice. *Am J Transl Res* 2018, 10, 2078-2086.

177. Xin, W.; Wang, Q.; Zhang, D.; Wang, C. A new mechanism of inhibition of il-1beta secretion by celastrol through the nlrp3 inflammasome pathway. *Eur J Pharmacol* 2017, 814, 240-247.

178. Joshi, V.; Venkatesha, S.H.; Ramakrishnan, C.; Nanjaraj Urs, A.N.; Hiremath, V.; Moudgil, K.D.; Velmurugan, D.; Vishwanath, B.S. Celastrol modulates inflammation through inhibition of the catalytic activity of mediators of arachidonic acid pathway: Secretory phospholipase a2 group iia, 5-lipoxygenase and cyclooxygenase-2. *Pharmacol Res* 2016, 113, 265-275.

179. Hu, M.; Luo, Q.; Alitongbieke, G.; Chong, S.; Xu, C.; Xie, L.; Chen, X.; Zhang, D.; Zhou, Y.; Wang, Z., et al. Celastrol-induced nur77 interaction with traf2 alleviates inflammation by promoting mitochondrial ubiquitination and autophagy. *Mol Cell* 2017, 66, 141-153 e146.

180. Muller-Ladner, U.; Kriegsmann, J.; Franklin, B.N.; Matsumoto, S.; Geiler, T.; Gay, R.E.; Gay, S. Synovial fibroblasts of patients with rheumatoid arthritis attach to and invade normal human cartilage when engrafted into scid mice. *Am J Pathol* 1996, 149, 1607-1615.

181. Xu, Z.; Wu, G.; Wei, X.; Chen, X.; Wang, Y.; Chen, L. Celastrol induced DNA damage, cell cycle arrest, and apoptosis in human rheumatoid fibroblast-like synovial cells. *Am J Chin Med* 2013, 41, 615-628.

182. de Seabra Rodrigues Dias, I.R.; Mok, S.W.F.; Gordillo-Martinez, F.; Khan, I.; Hsiao, W.W.L.; Law, B.Y.K.; Wong, V.K.W.; Liu, L. The calcium-induced regulation in the molecular and transcriptional circuitry of human inflammatory response and autoimmunity. *Front Pharmacol* 2017, 8, 962.

183. Wong, V.K.W.; Qiu, C.; Xu, S.W.; Law, B.Y.K.; Zeng, W.; Wang, H.; Michelangeli, F.; Dias, I.; Qu, Y.Q.; Chan, T.W., et al. Ca(2+) signalling plays a role in celastrol-mediated suppression of synovial fibroblasts of rheumatoid arthritis patients and experimental arthritis in rats. *Br J Pharmacol* 2019, 176, 2922-2944.

184. Cascao, R.; Vidal, B.; Raquel, H.; Neves-Costa, A.; Figueiredo, N.; Gupta, V.; Fonseca, J.E.; Moita, L.F. Effective treatment of rat adjuvant-induced arthritis by celastrol. *Autoimmun Rev* 2012, 11, 856-862.

185. Gao, Q.; Qin, H.; Zhu, L.; Li, D.; Hao, X. Celastrol attenuates collagen-induced arthritis via inhibiting oxidative stress in rats. *Int Immunopharmacol* 2020, 84, 106527.

186. Perry, S.C.; Kalyanaraman, C.; Tourdot, B.E.; Conrad, W.S.; Akinkugbe, O.; Freedman, J.C.; Holinstat, M.; Jacobson, M.P.; Holman, T.R. 15-lipoxygenase-1 biosynthesis of 7s,14s-dihdha implicates 15-lipoxygenase-2 in biosynthesis of resolvin d5. *J Lipid Res* 2020, 61, 1087-1103.

187. Wang, C.; Shi, C.; Yang, X.; Yang, M.; Sun, H.; Wang, C. Celastrol suppresses obesity process via increasing antioxidant capacity and improving lipid metabolism. *Eur J Pharmacol* 2014, 744, 52-58.

188. Liu, J.; Lee, J.; Salazar Hernandez, M.A.; Mazitschek, R.; Ozcan, U. Treatment of obesity with celastrol. *Cell* 2015, 161, 999-1011.

189. Peng, B.; Xu, L.; Cao, F.; Wei, T.; Yang, C.; Uzan, G.; Zhang, D. Hsp90 inhibitor, celastrol, arrests human monocytic leukemia cell u937 at g0/g1 in thiol-containing agents reversible way. *Mol Cancer* 2010, 9, 79.

190. Zhu, Y.; Liu, X.; Zhao, P.; Zhao, H.; Gao, W.; Wang, L. Celastrol suppresses glioma vasculogenic mimicry formation and angiogenesis by blocking the pi3k/akt/mtor signaling pathway. *Front Pharmacol* 2020, 11, 25.

191. Chen, Y.; Ou, Y.; Tao, Y.; Liu, H.; Yin, H.; Zhong, S.; Yu, H.; Zhao, Z.; He, B. Effect and mechanisms of celastrol on the apoptosis of hos osteosarcoma cells. *Oncol Rep* 2018, 40, 2260-2268.

192. Yang, H.S.; Kim, J.Y.; Lee, J.H.; Lee, B.W.; Park, K.H.; Shim, K.H.; Lee, M.K.; Seo, K.I. Celastrol isolated from tripterygium regelii induces apoptosis through both caspase-dependent and -independent pathways in human breast cancer cells. *Food Chem Toxicol* 2011, 49, 527-532.

193. Moreira, H.; Szyjka, A.; Paliszkiewicz, K.; Barg, E. Prooxidative activity of celastrol induces apoptosis, DNA damage, and cell cycle arrest in drug-resistant human colon cancer cells. *Oxid Med Cell Longev* 2019, 2019, 6793957.

194. Allison, A.C.; Cacabelos, R.; Lombardi, V.R.; Alvarez, X.A.; Vigo, C. Celastrol, a potent antioxidant and anti-inflammatory drug, as a possible treatment for alzheimer's disease. *Prog Neuropsychopharmacol Biol Psychiatry* 2001, 25, 1341-1357.

195. Youn, G.S.; Kwon, D.J.; Ju, S.M.; Rhim, H.; Bae, Y.S.; Choi, S.Y.; Park, J. Celastrol ameliorates hiv-1 tat-induced inflammatory responses via nf-kappab and ap-1 inhibition and heme oxygenase-1 induction in astrocytes. *Toxicol Appl Pharmacol* 2014, 280, 42-52.

196. Ryu, Y.B.; Park, S.J.; Kim, Y.M.; Lee, J.Y.; Seo, W.D.; Chang, J.S.; Park, K.H.; Rho, M.C.; Lee, W.S. Sars-cov 3clpro inhibitory effects of quinone-methide triterpenes from tripterygium regelii. *Bioorg Med Chem Lett* 2010, 20, 1873-1876.

197. Yu, J.S.; Tseng, C.K.; Lin, C.K.; Hsu, Y.C.; Wu, Y.H.; Hsieh, C.L.; Lee, J.C. Celastrol inhibits dengue virus replication via up-regulating type i interferon and downstream interferon-stimulated responses. *Antiviral Res* 2017, 137, 49-57.

198. Sun, H.; Liu, X.; Xiong, Q.; Shikano, S.; Li, M. Chronic inhibition of cardiac kir2.1 and herg potassium channels by celastrol with dual effects on both ion conductivity and protein trafficking. *J Biol Chem* 2006, 281, 5877-5884.

199. Bai, J.P.; Shi, Y.L.; Fang, X.; Shi, Q.X. Effects of demethylzeylasteral and celastrol on spermatogenic cell ca2+ channels and progesterone-induced sperm acrosome reaction. *Eur J Pharmacol* 2003, 464, 9-15.

200. Kusy, S.; Ghosn, E.E.; Herzenberg, L.A.; Contag, C.H. Development of b cells and erythrocytes is specifically impaired by the drug celastrol in mice. *PLoS One* 2012, 7, e35733.

201. Zheng, L.; Fu, Y.; Zhuang, L.; Gai, R.; Ma, J.; Lou, J.; Zhu, H.; He, Q.; Yang, B. Simultaneous nf-kappab inhibition and e-cadherin upregulation mediate mutually synergistic anticancer activity of celastrol and saha in vitro and in vivo. *Int J Cancer* 2014, 135, 1721-1732.

202. Guo, L.; Luo, S.; Du, Z.; Zhou, M.; Li, P.; Fu, Y.; Sun, X.; Huang, Y.; Zhang, Z. Targeted delivery of celastrol to mesangial cells is effective against mesangioproliferative glomerulonephritis. *Nat Commun* 2017, 8, 878.

203. Dalli, J.; Serhan, C. Macrophage proresolving mediators-the when and where. *Microbiol Spectr* 2016, 4.

204. Watanabe, S.; Alexander, M.; Misharin, A.V.; Budinger, G.R.S. The role of macrophages in the resolution of inflammation. *J Clin Invest* 2019, 129, 2619-2628.

205. Bao, J.; Dai, S.M. A chinese herb tripterygium wilfordii hook f in the treatment of rheumatoid arthritis: Mechanism, efficacy, and safety. *Rheumatol Int* 2011, 31, 1123-1129.

206. Gheorghe, K.R.; Korotkova, M.; Catrina, A.I.; Backman, L.; af Klint, E.; Claesson, H.E.; Radmark, O.; Jakobsson, P.J. Expression of 5-lipoxygenase and 15-lipoxygenase in rheumatoid arthritis synovium and effects of intraarticular glucocorticoids. *Arthritis Res Ther* 2009, 11, R83.

207. Lin, H.C.; Lin, T.H.; Wu, M.Y.; Chiu, Y.C.; Tang, C.H.; Hour, M.J.; Liou, H.C.; Tu, H.J.; Yang, R.S.; Fu, W.M. 5-lipoxygenase inhibitors attenuate tnf-alpha-induced inflammation in human synovial fibroblasts. *PLoS One* 2014, 9, e107890.

208. Ahmadzadeh, N.; Shingu, M.; Nobunaga, M.; Tawara, T. Relationship between leukotriene b4 and immunological parameters in rheumatoid synovial fluids. *Inflammation* 1991, 15, 497-503.

209. Gursel, T.; Firat, S.; Ercan, Z.S. Increased serum leukotriene b4 level in the active stage of rheumatoid arthritis in children. *Prostaglandins Leukot Essent Fatty Acids* 1997, 56, 205-207.

210. Mathis, S.P.; Jala, V.R.; Lee, D.M.; Haribabu, B. Nonredundant roles for leukotriene b4 receptors blt1 and blt2 in inflammatory arthritis. *J Immunol* 2010, 185, 3049-3056.

211. Miyabe, Y.; Miyabe, C.; Luster, A.D. Ltb4 and blt1 in inflammatory arthritis. *Semin Immunol* 2017, 33, 52-57.

212. Li, R.W.; David Lin, G.; Myers, S.P.; Leach, D.N. Anti-inflammatory activity of chinese medicinal vine plants. *J Ethnopharmacol* 2003, 85, 61-67.

213. Ferrante, E.; Vazzana, N.; Santilli, F.; Di Cicco, M.; Lauriti, C.; Di Battista, L.; Ciabattoni, G.; Di Matteo, L.; Davi, G. Determinants of thromboxane biosynthesis in rheumatoid arthritis: Role of rage and oxidant stress. *Free Radic Biol Med* 2010, 49, 857-864.

214. Wang, M.J.; Huang, Y.; Huang, R.Y.; Chen, X.M.; Zhou, Y.Y.; Yu, W.L.; Chu, Y.L.; Huang, Q.C. Determination of role of thromboxane a2 in rheumatoid arthritis. *Discov Med* 2015, 19, 23-32.

215. Trang, L.E.; Granstrom, E.; Lovgren, O. Levels of prostaglandins f2 alpha and e2 and thromboxane b2 in joint fluid in rheumatoid arthritis. *Scand J Rheumatol* 1977, 6, 151-154.

216. Sampey, A.V.; Monrad, S.; Crofford, L.J. Microsomal prostaglandin e synthase-1: The inducible synthase for prostaglandin e2. *Arthritis Res Ther* 2005, 7, 114-117.

217. Bahia, M.S.; Katare, Y.K.; Silakari, O.; Vyas, B.; Silakari, P. Inhibitors of microsomal prostaglandin e2 synthase-1 enzyme as emerging anti-inflammatory candidates. *Med Res Rev* 2014, 34, 825-855.

218. Koeberle, A.; Werz, O. Perspective of microsomal prostaglandin e2 synthase-1 as drug target in inflammation-related disorders. *Biochem Pharmacol* 2015, 98, 1-15.

219. Maekawa, K.; Yoshikawa, N.; Du, J.; Nishida, S.; Kitasato, H.; Okamoto, K.; Tanaka, H.; Mizushima, Y.; Kawai, S. The molecular mechanism of inhibition of interleukin-1beta-induced cyclooxygenase-2 expression in human synovial cells by tripterygium wilfordii hook f extract. *Inflamm Res* 1999, 48, 575-581.

220. Wang, S.; Li, R.; He, S.; He, L.; Zhao, H.; Deng, X.; Chen, Z. Tripterygium wilfordii glycosides upregulate the new anti-inflammatory cytokine il-37 through erk1/2 and

p38 mapk signal pathways. *Evid Based Complement Alternat Med* 2017, 2017, 9148523.

221. Pandya, J.M.; Lundell, A.C.; Hallstrom, M.; Andersson, K.; Nordstrom, I.; Rudin, A. Circulating t helper and t regulatory subsets in untreated early rheumatoid arthritis and healthy control subjects. *J Leukoc Biol* 2016, 100, 823-833.

222. Di Gennaro, A.; Haeggstrom, J.Z. The leukotrienes: Immune-modulating lipid mediators of disease. *Adv Immunol* 2012, 116, 51-92.

223. Korotkova, M.; Jakobsson, P.J. Persisting eicosanoid pathways in rheumatic diseases. Nat Rev Rheumatol 2014, 10, 229-241.

224. Barden, A.E.; Moghaddami, M.; Mas, E.; Phillips, M.; Cleland, L.G.; Mori, T.A. Specialised pro-resolving mediators of inflammation in inflammatory arthritis. *Prostaglandins Leukot Essent Fatty Acids* 2016, 107, 24-29.

225. Perretti, M.; Norling, L.V. Actions of spm in regulating host responses in arthritis. *Mol Aspects Med* 2017, 58, 57-64.

226. Yamada, H.; Saegusa, J.; Sendo, S.; Ueda, Y.; Okano, T.; Shinohara, M.; Morinobu, A. Effect of resolvin d5 on t cell differentiation and osteoclastogenesis analyzed by lipid mediator profiling in the experimental arthritis. *Sci Rep* 2021, 11, 17312.

227. Ozgul Ozdemir, R.B.; Soysal Gunduz, O.; Ozdemir, A.T.; Akgul, O. Low levels of pro-resolving lipid mediators lipoxin-a4, resolvin-d1 and resolvin-e1 in patients with rheumatoid arthritis. *Immunol Lett* 2020, 227, 34-40.

228. Norling, L.V.; Headland, S.E.; Dalli, J.; Arnardottir, H.H.; Haworth, O.; Jones, H.R.; Irimia, D.; Serhan, C.N.; Perretti, M. Proresolving and cartilage-protective actions of resolvin d1 in inflammatory arthritis. *JCI Insight* 2016, 1, e85922.

229. Pace, S.; Zhang, K.; Jordan, P.M.; Bilancia, R.; Wang, W.; Borner, F.; Hofstetter, R.K.; Potenza, M.; Kretzer, C.; Gerstmeier, J., et al. Anti-inflammatory celastrol promotes a switch from leukotriene biosynthesis to formation of specialized pro-resolving lipid mediators. *Pharmacol Res* 2021, 167, 105556.

230. Yao, H.; Zhou, J.; Li, D.; Wu, N.; Bader, A.; Hoxtermann, S.; Altmeyer, P.; Brockmeyer, N.H. Fk506 enhances triptolide-induced down-regulation of cyclooxygenase-2, inducible nitric oxide synthase as well as their products pge2 and no in tnf-alpha-stimulated synovial fibroblasts from rheumatoid arthritic patients. *Eur J Med Res* 2005, 10, 110-116.

231. Venkatesha, S.H.; Moudgil, K.D. Celastrol and its role in controlling chronic diseases. *Adv Exp Med Biol* 2016, 928, 267-289.

232. Cascao, R.; Vidal, B.; Carvalho, T.; Lopes, I.P.; Romao, V.C.; Goncalves, J.; Moita, L.F.; Fonseca, J.E. Celastrol efficacy by oral administration in the adjuvant-induced arthritis model. *Front Med* (Lausanne) 2020, 7, 455.

233. Lin, L.; Sun, Y.; Wang, D.; Zheng, S.; Zhang, J.; Zheng, C. Celastrol ameliorates

ulcerative colitis-related colorectal cancer in mice via suppressing inflammatory responses and epithelial-mesenchymal transition. *Front Pharmacol* 2015, 6, 320.

234. Guo, C.; Fu, R.; Wang, S.; Huang, Y.; Li, X.; Zhou, M.; Zhao, J.; Yang, N. Nlrp3 inflammasome activation contributes to the pathogenesis of rheumatoid arthritis. *Clin Exp Immunol* 2018, 194, 231-243.

235. Jing, M.; Yang, J.; Zhang, L.; Liu, J.; Xu, S.; Wang, M.; Zhang, L.; Sun, Y.; Yan, W.; Hou, G., et al. Celastrol inhibits rheumatoid arthritis through the ros-nf-kappab-nlrp3 inflammasome axis. *Int Immunopharmacol* 2021, 98, 107879.

236. Yan, C.Y.; Ouyang, S.H.; Wang, X.; Wu, Y.P.; Sun, W.Y.; Duan, W.J.; Liang, L.; Luo, X.; Kurihara, H.; Li, Y.F., et al. Celastrol ameliorates propionibacterium acnes/lps-induced liver damage and msu-induced gouty arthritis via inhibiting k63 deubiquitination of nlrp3. *Phytomedicine* 2021, 80, 153398.

237. Alhouayek, M.; Ameraoui, H.; Muccioli, G.G. Bioactive lipids in inflammatory bowel diseases - from pathophysiological alterations to therapeutic opportunities. *Biochim Biophys Acta Mol Cell Biol Lipids* 2021, 1866, 158854.

238. Steinhilber, D. 5-lipoxygenase: A target for antiinflammatory drugs revisited. *Curr Med Chem* 1999, 6, 71-85.

239. Sharma, J.N.; Mohammed, L.A. The role of leukotrienes in the pathophysiology of inflammatory disorders: Is there a case for revisiting leukotrienes as therapeutic targets? *Inflammopharmacology* 2006, 14, 10-16.

240. Meshram, D.; Bhardwaj, K.; Rathod, C.; Mahady, G.B.; Soni, K.K. The role of leukotrienes inhibitors in the management of chronic inflammatory diseases. *Recent Pat Inflamm Allergy Drug Discov* 2020, 14, 15-31.

241. Cheung, S.Y.; Werner, M.; Esposito, L.; Troisi, F.; Cantone, V.; Liening, S.; Konig, S.; Gerstmeier, J.; Koeberle, A.; Bilancia, R., et al. Discovery of a benzenesulfonamide-based dual inhibitor of microsomal prostaglandin e2 synthase-1 and 5-lipoxygenase that favorably modulates lipid mediator biosynthesis in inflammation. *Eur J Med Chem* 2018, 156, 815-830.

242. Gerstmeier, J.; Seegers, J.; Witt, F.; Waltenberger, B.; Temml, V.; Rollinger, J.M.; Stuppner, H.; Koeberle, A.; Schuster, D.; Werz, O. Ginkgolic acid is a multi-target inhibitor of key enzymes in pro-inflammatory lipid mediator biosynthesis. *Front Pharmacol* 2019, 10, 797.

243. Gilbert, N.C.; Gerstmeier, J.; Schexnaydre, E.E.; Borner, F.; Garscha, U.; Neau, D.B.; Werz, O.; Newcomer, M.E. Structural and mechanistic insights into 5-lipoxygenase inhibition by natural products. *Nat Chem Biol* 2020, 16, 783-790.

244. Werz, O.; Gerstmeier, J.; Libreros, S.; De la Rosa, X.; Werner, M.; Norris, P.C.; Chiang, N.; Serhan, C.N. Human macrophages differentially produce specific resolvin or

leukotriene signals that depend on bacterial pathogenicity. *Nat Commun* 2018, 9, 59.

245. Werner, M.; Jordan, P.M.; Romp, E.; Czapka, A.; Rao, Z.; Kretzer, C.; Koeberle, A.; Garscha, U.; Pace, S.; Claesson, H.E., et al. Targeting biosynthetic networks of the proinflammatory and proresolving lipid metabolome. *FASEB J* 2019, 33, 6140-6153.
246. Gerstmeier, J.; Weinigel, C.; Rummler, S.; Radmark, O.; Werz, O.; Garscha, U. Time-resolved in situ assembly of the leukotriene-synthetic 5-lipoxygenase/5-lipoxygenase-activating protein complex in blood leukocytes. *FASEB J* 2016, 30, 276-285.
247. Motwani, M.P.; Gilroy, D.W. Macrophage development and polarization in chronic inflammation. *Semin Immunol* 2015, 27, 257-266.
248. Luo, D.; Guo, Y.; Cheng, Y.; Zhao, J.; Wang, Y.; Rong, J. Natural product celastrol suppressed macrophage m1 polarization against inflammation in diet-induced obese mice via regulating nrf2/ho-1, map kinase and nf-kappab pathways. *Aging* 2017, 9, 2069-2082.
249. Jiang, M.; Liu, X.; Zhang, D.; Wang, Y.; Hu, X.; Xu, F.; Jin, M.; Cao, F.; Xu, L. Celastrol treatment protects against acute ischemic stroke-induced brain injury by promoting an il-33/st2 axis-mediated microglia/macrophage m2 polarization. *J Neuroinflammation* 2018, 15, 78.
250. Serhan, C.N.; Chiang, N.; Dalli, J.; Levy, B.D. Lipid mediators in the resolution of inflammation. *Cold Spring Harb Perspect Biol* 2014, 7, a016311.
251. Serhan, C.N.; Chiang, N.; Dalli, J. The resolution code of acute inflammation: Novel pro-resolving lipid mediators in resolution. *Semin Immunol* 2015, 27, 200-215.
252. Serhan, C.N. Treating inflammation and infection in the 21st century: New hints from decoding resolution mediators and mechanisms. *FASEB J* 2017, 31, 1273-1288.
253. Lima-Garcia, J.F.; Dutra, R.C.; da Silva, K.; Motta, E.M.; Campos, M.M.; Calixto, J.B. The precursor of resolvin d series and aspirin-triggered resolvin d1 display anti-hyperalgesic properties in adjuvant-induced arthritis in rats. *Br J Pharmacol* 2011, 164, 278-293.
254. Gewirtz, A.T.; Collier-Hyams, L.S.; Young, A.N.; Kucharzik, T.; Guilford, W.J.; Parkinson, J.F.; Williams, I.R.; Neish, A.S.; Madara, J.L. Lipoxin a4 analogs attenuate induction of intestinal epithelial proinflammatory gene expression and reduce the severity of dextran sodium sulfate-induced colitis. *J Immunol* 2002, 168, 5260-5267.
255. Agis, E.R.; Savas, B.; Melli, M. Impact of colonic mucosal lipoxin a4 synthesis capacity on healing in rats with dextran sodium sulfate-induced colitis. *Prostaglandins Other Lipid Mediat* 2015, 121, 63-69.
256. Meng, H.; McClendon, C.L.; Dai, Z.; Li, K.; Zhang, X.; He, S.; Shang, E.; Liu, Y.; Lai, L. Discovery of novel 15-lipoxygenase activators to shift the human arachidonic acid metabolic network toward inflammation resolution. *J Med Chem* 2016, 59, 4202-4209.

257. Zhang, K.; Pace, S.; Jordan, P.M.; Peltner, L.K.; Weber, A.; Fischer, D.; Hofstetter, R.K.; Chen, X.; Werz, O. Beneficial modulation of lipid mediator biosynthesis in innate immune cells by antirheumatic tripterygium wilfordii glycosides. *Biomolecules* 2021, 11.

258. Lee, J.H.; Koo, T.H.; Yoon, H.; Jung, H.S.; Jin, H.Z.; Lee, K.; Hong, Y.S.; Lee, J.J. Inhibition of nf-kappa b activation through targeting i kappa b kinase by celastrol, a quinone methide triterpenoid. *Biochem Pharmacol* 2006, 72, 1311-1321.

259. Kim, D.H.; Shin, E.K.; Kim, Y.H.; Lee, B.W.; Jun, J.G.; Park, J.H.; Kim, J.K. Suppression of inflammatory responses by celastrol, a quinone methide triterpenoid isolated from celastrus regelii. *Eur J Clin Invest* 2009, 39, 819-827.

260. Salminen, A.; Lehtonen, M.; Paimela, T.; Kaarniranta, K. Celastrol: Molecular targets of thunder god vine. *Biochem Biophys Res Commun* 2010, 394, 439-442.

261. Ma, X.; Xu, L.; Alberobello, A.T.; Gavrilova, O.; Bagattin, A.; Skarulis, M.; Liu, J.; Finkel, T.; Mueller, E. Celastrol protects against obesity and metabolic dysfunction through activation of a hsf1-pgc1alpha transcriptional axis. *Cell Metab* 2015, 22, 695-708.

262. Werz, O.; Klemm, J.; Radmark, O.; Samuelsson, B. P38 map kinase mediates stress-induced leukotriene synthesis in a human b-lymphocyte cell line. *J Leukoc Biol* 2001, 70, 830-838.

263. Bandeira-Melo, C.; Serra, M.F.; Diaz, B.L.; Cordeiro, R.S.; Silva, P.M.; Lenzi, H.L.; Bakhle, Y.S.; Serhan, C.N.; Martins, M.A. Cyclooxygenase-2-derived prostaglandin e2 and lipoxin a4 accelerate resolution of allergic edema in angiostrongylus costaricensis-infected rats: Relationship with concurrent eosinophilia. *J Immunol* 2000, 164, 1029-1036.

264. Zhao, J.; Luo, D.; Zhang, Z.; Fan, N.; Wang, Y.; Nie, H.; Rong, J. Celastrol-loaded peg-pcl nanomicelles ameliorate inflammation, lipid accumulation, insulin resistance and gastrointestinal injury in diet-induced obese mice. *J Control Release* 2019, 310, 188-197.

265. Xi, Y.; Zhang, Y.; Pan, J.; Chen, S.; Lu, S.; Shen, F.; Huang, Z. Triptolide dysregulates glucose uptake via inhibition of ikkbeta-nf-kappab pathway by p53 activation in cardiomyocytes. *Toxicol Lett* 2020, 318, 1-11.

266. Zhou, R.; Zheng, S.X.; Tang, W.; He, P.L.; Li, X.Y.; Yang, Y.F.; Li, Y.C.; Geng, J.G.; Zuo, J.P. Inhibition of inducible nitric-oxide synthase expression by (5r)-5-hydroxytriptolide in interferon-gamma- and bacterial lipopolysaccharide-stimulated macrophages. *J Pharmacol Exp Ther* 2006, 316, 121-128.

267. Pan, X.D.; Chen, X.C.; Zhu, Y.G.; Chen, L.M.; Zhang, J.; Huang, T.W.; Ye, Q.Y.; Huang, H.P. Tripchlorolide protects neuronal cells from microglia-mediated beta-amyloid

neurotoxicity through inhibiting nf-kappab and jnk signaling. *Glia* 2009, 57, 1227-1238.

6 Appendices

6.1 Acknowledgements

This doctoral thesis would not have been accomplished without the help and support of the kind people around me. Thus, I would like to extend my sincere thanks to all of them.

Foremost, I would like to express my deepest gratitude to my supervisor, Prof. Dr. Oliver Werz, who opened the door of his group for me with challenging research projects in the field of lipid-mediated inflammation. He imparted his knowledge and expertise in the projects, motivating me to be a better researcher not only during my PhD stage but also from this time forth.

I would like to thank my second supervisor, Prof. Dr. Xinchun Chen who brought me into the joint Jena-Shenzhen joint PhD program. I am really grateful for his constant support and help throughout my doctoral studies.

Special thanks to Prof. Dr. Robert Fürst from Goethe University Frankfurt for the kind agreement to review my dissertation.

Next, I highly appreciated Dr. Simona Pace as my advisor and mentor for her inspiring guidance, valuable discussion, and encouragement. She always has creative ideas and was also critical to my data process at the beginning step which helps me a lot. She is such an intelligent person and willing to share knowledge with me but not only on academic topics. I am very pleased to work together with her.

I would like to thank all my colleagues in the Prof. Dr. Werz group who willingly helped me out with their abilities. Thanks to Paul, Robert, Laura, Friedemann, Markus, Katharina, Elena, Lukas, and others for their support and great patience at all times. Also, thanks to my compatriots Rao, Wenfei and Yuping for supporting and accompanying me with a feeling of relief in the lab. Special thanks to the secretary Theresa, our lab manager Nadja, Uwe and the technicians Alrun, Heidi, Petra, Katrin in our group. All academic and social activities make me feel we are a big family and I really have a wonderful time in Jena.

I would like to acknowledge the financial support of Shenzhen University and the Graduate Academy of Jena.

Thanks to my collaborative partners from the Nanocare4skin project. Their productive work and professional presentation, thrilling discussion impressed me to move forward in

the research work.

Thanks to my noteworthy friends in Jena for enjoying life together, the priceless time with them will not be forgotten.

In the end, I would like to thank my lovely parents and younger sister for always supporting my study abroad journey. A known saying of "what doesn't kill you makes you stronger" often used by my mother is useful to me over the years when I've felt sad and restless. I love you forever (Wo ai ni men). Now I am looking forward to a new start!

6.2 List of publications

1. **K. Zhang**, P. M. Jordan, S. Pace, R. K. Hofstetter, M. Werner, X. Chen, O. Werz. Celastrol suppresses human macrophage M1 polarization via reduction of pro-inflammatory lipid mediators (2022). *Journal of inflammatory research.* In press.
2. **K. Zhang***, S. Pace*, P. M. Jordan, L. K. Peltner, A. Weber, D. Fischer, R. K. Hofstetter, X. Chen, O. Werz. Beneficial Modulation of Lipid Mediator Biosynthesis in Innate Immune Cells by Antirheumatic *Tripterygium wilfordii* Glycosides. *Biomolecules.* 2021(11)746
3. S. Pace*, **K. Zhang***, P. M. Jordan , R. Bilancia, W. Wang, F. Börner, R. K. Hofstetter, M. Potenza, C. Kretzer, J. Gerstmeier, D. Fischer, S. Lorkowski, N. C. Gilbert, M. E. Newcomer, A. Rossi, X. Chen, O. Werz. Anti-inflammatory celastrol promotes a switch from leukotriene biosynthesis to formation of specialized pro-resolving lipid mediators. *Pharmacological Research.* 2021 (167)105556
4. **K. Zhang**, Y. Ning, F. Kong, X. Chen, Y. Cai. Genome instability in the pathogenesis of tuberculosis. *Genome Instability & Disease.* 2021 (1-8).
5. S. Mo*, X. Liu*, **K. Zhang**, W. Wang, Y. Cai, Q. Ouyang, C. Zhu, D. Lin, H. Wan, D. Li, Z. Wen, X. Chen. Flunarizine suppresses *Mycobacterium tuberculosis* growth via calmodulin-dependent phagosome maturation. *Journal of Leukocyte Biology.* 2021 (1-9).
6. W. Wang*, Y. Ning*, Y. Wang*, S.Pace, S. A. Barth, C. Menge, **K. Zhang**, Y. Dai, Y. Cai, X. Chen, O. Werz. Sulfasalazine facilitates *Mycobacterium tuberculosis* clearance by human macrophages concomitant to repression of the upregulated cyclooxygenase-2 pathway. *Frontiers in immunology* (2022). In revision.
7. Q. Ouyang, **K. Zhang**, D. Lin, C. G. Feng, Y. Cai, X. Chen. Bazedoxifene Suppresses Intracellular *Mycobacterium tuberculosis* Growth by Enhancing Autophagy, *mSphere.* 2020 (5) e00124-20.
8. **K. Zhang**, X. Wang, J. Tu, H. Rong, O. Werz, X. Chen. The interplay between depression and tuberculosis. *Journal of leukocyte biology.* 2019 (106)749-757.
9. Z. Yu, W. Wang, C. Zhu, **K. Zhang**, X. Chen, J. Chen. The Polymorphism rs17525495 of LTA4H Is Associated with Susceptibility of Crohn's Disease instead of Intestinal Tuberculosis in a Chinese Han Population. *BioMed Research International.* 2019 (1-7).

6.3 Author contribution statement

Manuscript I

Kurzreferenz [Zhang et al (2021), *Biomolecules*]

Beitrag des Doktoranden / der Doktorandin

Beitrag des Doktoranden / der Doktorandin zu Abbildungen, die experimentelle Daten wiedergeben (nur für Originalartikel):

Abbildungen	1-5	100%	Eigenanteil
Tabellenkästen	1-3	100%	Eigenanteil
Abbildungen	6 & S1	0%	Eigenanteil, ausschließlich basierend auf Daten von Koautoren

Manuscript II

Kurzreferenz [Pace et al (2021), *Pharmacol. Res.*]

Beitrag des Doktoranden / der Doktorandin

Beitrag des Doktoranden / der Doktorandin zu Abbildungen, die experimentelle Daten wiedergeben (nur für Originalartikel):

Abbildungen	1A, 1C, 2A-2D, 3A, 4D, 4E; S1-S4	100%	Eigenanteil
Abbildungen	1B, 1D, 3B, 3E, 4B, 4C	60%	Experimentell, Datenanalyse, Visualisierung
Abbildungen	2E-2H, 3C, 3D, 4A	0%	Eigenanteil, ausschließlich basierend auf Daten von Koautoren

Manuscript III

Kurzreferenz [Zhang et al (2022), *J. Inflamm. Res.*]

Beitrag des Doktoranden / der Doktorandin

Beitrag des Doktoranden / der Doktorandin zu Abbildungen, die experimentelle Daten wiedergeben (nur für Originalartikel):

Abbildungen	1A, 1B, 2-5	100%	Eigenanteil
Tabellenkästen	1-3	100%	Eigenanteil
Abbildungen	1C, 1D	0%	Eigenanteil, ausschließlich basierend auf Daten von Koautoren

6.4 Eigenständigkeitserklärung

Hiermit erkläre ich, dass mir die Promotionsordnung der Fakultät für Biowissenschaften der Friedrich-Schiller-Universität Jena bekannt ist, ich die Dissertation selbst angefertigt habe und alle von mir benutzten Hilfsmittel, persönlichen Mitteilungen und Quellen in meiner Arbeit angegeben sind.

Ich versichere, dass ich die Hilfe eines Promotionsberaters nicht in Anspruch genommen habe und dass Dritte weder unmittelbar noch mittelbar geldwerte Leistungen von mir für Arbeiten erhalten haben, die im Zusammenhang mit dem Inhalt der vorgelegten Dissertation stehen.

Die vorliegende Dissertation wurde von mir bei keiner bisherigen Prüfungsarbeit für eine staatliche oder andere wissenschaftliche Prüfung eingereicht. Weiterhin versichere ich, dass ich die gleiche, eine in wesentlichen Teilen ähnliche oder eine andere Abhandlung nicht bei einer anderen Universität als Dissertation eingereicht habe.